To the Graduate Council:

I am submitting herewith a dissertation written by Terron Lee Miller, entitled "Application of Diffusion Models in the Design of Monitoring Surveys for Air Quality Assessment." I recommend that it be accepted in partial fulfillment of the requirements for the degree of Doctor of Philosophy, with a major in Civil Engineering.

Kenneth E. Noll, Major Professor

We have read this dissertation
and recommend its acceptance:

Accepted for the Council:

Vice Chancellor
Graduate Studies and Research

.M544
cop. 2

APPLICATION OF DIFFUSION MODELS IN THE DESIGN OF MONITORING SURVEYS FOR AIR QUALITY ASSESSMENT

A Dissertation

Presented for the

Doctor of Philosophy

Degree

The University of Tennessee

Terron Lee Miller

December 1975

1269156

ACKNOWLEDGEMENTS

This dissertation was written after preparing manuals for the Federal Highway Administration on Highway Air Quality Monitoring (see references 3 and 4) and conducting research on highway air pollution dispersion sponsored by the Tennessee Department of Transportation (see references 59 and 62). Thanks go to these two organizations for the support provided resulting in this document. Special thanks are expressed to Dr. Kenneth E. Noll (major professor) whose guidance and perspective were invaluable. Appreciation is also expressed to Ronnie Miller for graphics, Carolyn Snow for typing the report, and to my wife, Joyce, whose understanding and encouragement has made my achievements possible.

ABSTRACT

The purpose of this investigation was to develop a methodology for designing air pollution monitoring surveys using diffusion models and sampling statistics to provide cost effective surveys which meet specific sampling objectives. A survey was designed for validating highway line source dispersion models and conducted in Nashville, Tennessee. The survey included real-time measurements of ambient concentrations of carbon monoxide, wind speed and direction, traffic volumes, vehicle speeds, and truck mix. Correlation and regression analyses of measured pollution levels compared to those predicted by the models showed that the models tended to overpredict concentrations under parallel wind conditions and underestimate concentrations for perpendicular and oblique wind conditions. Two empirical models were developed which were independent of atmospheric stability conditions. These models show promise as predictive tools, but require testing at other sites.

TABLE OF CONTENTS

CHAPTER	PAGE
INTRODUCTION.	1
Perspective.	1
Objective.	1
Organization and Statement of Originality.	2
I. OVERVIEW OF SURVEY DESIGN	4
Introduction	4
The Role of Monitoring and Modeling in Air Quality Assessment.	5
Setting Objectives and the Initial Air Monitoring Survey Planning Process	8
Systematic Methods for Selecting Air Monitoring Sites to Meet Survey Objectives	10
Introduction.	10
Defining Micro-, Meso-, and Macroscale Air Pollution Regimes.	11
Selecting Monitoring Sites Near Sources - Micro-scale Monitoring	14
Selecting Sites for General Area Wide Background Studies in Urban Areas	15
Air Monitoring Network Specifications.	16
Selecting Air Monitoring Station Equipment	18
Cost of Air Monitoring	23
Summary.	26

CHAPTER PAGE

II. LITERATURE REVIEW. 29

Introduction. 29

Air Monitoring Site Selection 30

Introduction 30

Station Siting Criteria. 30

Network Siting Criteria. 38

Evaluation of Meteorological Data 47

Introduction 47

Mesoscale Meteorological Analysis. 48

Method of Analyzing Historical Meteorological Data. 51

Microscale Meteorological Analysis 54

Available Sources of Meteorological Data 58

Applicable Sampling Statistics. 59

Determine How Many Samples are Needed. 59

Sample Sizes and Confidence Intervals for the Mean. 59

Sample Sizes and Confidence Intervals for Extremes. 60

Sampling from Finite Populations 63

Atmospheric Diffusion Models. 64

Nongaussian Atmospheric Diffusion Models 64

Gaussian Plume Models. 70

Plume Rise. 99

CHAPTER PAGE

Introduction. 99
Momentum Sources. 99
Buoyant Plumes. 100
A Nomographic Solution for Plume Rise 102
General Solutions of Point Source Diffusion Models. 104
Introduction. 104
Graphical Solutions 104
Nomographic Solutions 106
III. DESIGNING AIR MONITORING SURVEYS. 112
Introduction. 112
Defining Micro-, Meso-, and Macroscale Air Pollution Regimes. 116
Locating Monitoring Stations Near Highway Line Sources. 118
Selecting Sites for Monitoring Area Wide Background Concentrations 136
Applying Diffusion Models to Selecting Air Monitoring Sites Near Point Sources. 147
IV. A SURVEY DESIGN FOR LINE SOURCE MODEL VALIDATION. 174
Introduction 174
General Description of Models. 175
EPA Model 175
California Model. 175

CHAPTER PAGE

Major Differences in the Models. 176
Model Assumptions. 176
Model Input Parameters 179
EPA and California Model Equations. 180
EPA Model. 180
California Model 181
Experimental Procedure. 184
Data Presentation 187
EPA and California Models. 187
Empirical Models 190
Discussion of Results 194
Introduction 194
Experimental Error 197
Performance of the EPA and California Models 198
Performance of the Empirical Model 199
Conclusions 203
LIST OF REFERENCES 204
VITA 210

LIST OF TABLES

TABLE		PAGE
I.	Sampling Location Guidelines for Areas of Estimated Maximum Pollutant Concentration.	33
II.	Recommended Criteria for Siting Monitoring Stations . . .	39
III.	Air Quality Surveillance System Requirements.	46
IV.	Meteorological Frequency Table.	56
V.	Pasquill's Atmospheric Stability Categories	77
VI.	Correction Factor for Multiple Stack.	114
VII.	Table of Probabilities Associated with Values as Extreme as Observed Values of z in the Normal Distribution . .	164
VIII.	Statistical Data Summary: EPA Model - Site 10.	188
IX.	Statistical Data Summary: California Model - Site 10 . .	189

LIST OF FIGURES

FIGURE		PAGE
1.	Interaction of Modeling and Monitoring to Assess the Air Quality Impact of a Project.	6
2.	The Planning and Management Process for an Air Quality Survey	9
3.	Background Air Quality Definition	13
4.	Hardware Components of an Air Quality Monitoring Station.	20
5.	Achievable Spatial Resolution and Capital Costs for Conducting an Air Quality Survey with Various Numbers of Monitoring Sites and Three Levels of Equipment Sophistication	25
6.	Achievable Temporal Resolution and Operating Costs for an Air Quality Survey of Various Durations for Three Levels of Equipment Sophistication	27
7.	Simplified Schematic of Dual Air Monitoring System Monitor No. 1 is the Pedestrian Exposure Station and Monitor No. 2 is the Background Exposure Station	36
8.	Inferred Spatial Distribution of Vehicular Air Pollutant Concentration (Carbon Monoxide, Lead, etc.) in an Urban Area	37
9.	Proposed Siting Plan for the St. Louis Regional Air Measurement Network.	44
10.	Paradise Steam Plant Air Monitoring Network	45

FIGURE PAGE

11. Analyzing Historical Meteorological Data for a Mesoscale Study. 50
12. Seasonal Wind Roses 52
13. Example of a Mesoscale Streamline Analysis. 53
14. Example of an Air Trajectory Generated from Eight Hourly Observations of Wind Speed and Direction 55
15. Confidence Intervals for the Mean of a Group of Random Samples. 61
16. Design of a Sampling Program for Quality Control. 62
17. Number of Samples Required to Determine the Geometric Mean Within ± 10 Percent with 95 Percent Confidence for Various Population Sizes 65
18. Number of Samples Required to Determine the Geometric Mean Within ± 20 Percent with 95 Percent Confidence for Various Population Sizes 66
19. Area-Source "Box" Diffusion Model 68
20. Dispersion of the Plume from a Point Source 71
21. Standard Normal Curve 74
22. Coordinate System Showing Gaussian Distributions in the Horizontal and Vertical. 74
23. Coordinate System of Real Source and Imaginary Source 75
24. Horizontal Diffusion Coefficient Versus Travel Distance 78

FIGURE PAGE

25. Vertical Diffusion Coefficient Versus Travel Distance for Pasquill's Turbulence Types. 78

26. Rural Plume Half-Depth, R_z, vs. Distance Downwind 79

27. Rural Plume Half-Width, R_y, vs. Distance Downwind 80

28. Urban Plume Half-Depth, R_z, vs. Distance Downwind 81

29. Urban Plume Half-Width, R_y, vs. Distance Downwind 82

30. Horizontal Gaussian Standard Deviation of Plume Distribution as a Function of Downwind Distance from the Source 84

31. Vertical Gaussian Standard Deviation of Plume Distribution as a Function of Downwind Distance from the Source . . . 85

32. Cross Section Revealing Surface of Constant Ambient Concentration for an Infinitely Long Line Source on the y-axis 86

33. A Line Source Curve Around a Receptor at P. 87

34. Ground Level Concentration Ratio, A, Downwind from Highway Line Source Parallel Wind At-Grade Section for all Stability Classes. 89

35. Illustration of how EPA "Hiway" Model Simulates a Line Source with Multiple Point Sources 91

36. Horizontal Dispersion Parameters. 92

37. Vertical Dispersion Parameters. 93

38. Comparison of σ_z Values Used in the EPA and California Models 94

39. Determining the Extent of the Area Source 95

FIGURE PAGE

40. The Effect on Ground Level Pollutant Concentration of Increasing the Size of the Urban Area Source for Various Mixing Depth. 97

41. Buoyant Plume Rise, Δh, Versus G and Mean Wind Speed, $\bar{u}$, for Neutral and Stable Atmospheric Stability. 103

42. $\chi u/Q$ With Distance for Various Heights of Emission (H) and Limits to Vertical Dispersion (L), B Stability. 105

43. Isopleths of $\chi u/Q$ for a Ground-Level Source, C Stability 107

44. Isopleths of $\chi u/Q$ for a Source 100 Meters High, C Stability 108

45. Distance of Maximum Concentration and Maximum $\chi u/Q$ as a Function of Stability (Curves) and Effective Height (Meters) of Emission (Numbers). 109

46. Plume Centerline 1-hr Average Surface Concentration, x, Versus Downwind Distance, r, Effective Stack Height, h_e, Effluent Emission Rate, Q, and Mean Wind Speed, $\bar{u}$. 110

47. Distance, X_{max}, Versus Stack Height, h_s, and h_d, for Inversion Breakup Dispersion. 111

48. Decrease in Ground Level Ambient Air Pollution Concentration at Increasing Distance Downwind From Highway Edge. 120

49. Isopleth Concentration Lines Downwind of a Highway Line Source. 121

FIGURE PAGE

50. Optimum Locations of Air Sampling Sites Determined for Crosswind Conditions According to the California Model. 123

51. Relative Concentration Versus Normal Distance From an At-Grade Highway for All Wind Directions and Stabilities Calculated From the California Model. 125

52. Percentage of Mixing Cell Concentration Where Background Concentrations can Effectively be Measured 128

53. Maximum Distance From Project Corridor that a Mesoscale Background Station Should be Located vs. Distance to Nearest Major Pollution Source 130

54. Acceptable Height of a Mesoscale Monitoring Station if Ground Level Concentrations are to be Measured 132

55. Study Area Divided into Grid Squares According to Land Use. 139

56. Average Emission Flux Values for Each Grid Square near Project Corridor 139

57. Hypothetic Profiles of Typical Seasonal, Daily, and Hourly Fluctuations in CO and O_3 Concentrations. . . . 145

58. Identifying Potential Zones Where C_{max} May Occur. 151

59. Graphical Method for Determining X_{10} Versus Distance Downwind to X_{max} 157

60. Illustrating the Number of Sites Needed to Maximize Coverage Between 1-10 km for D Stability 158

FIGURE PAGE

61. Y_{10} Versus Distance Downwind for Six Stabilities. 160

62. Illustration of the Coverage Area of a Single Station Downwind of a Point Source 161

63. Single Station Coverage Ratios, CR_S, Versus Distance Downwind for Six Stability Classes 165

64. Coverage Ratio Required to Observe C_{max}, n times, with 99% Confidence, versus the Number of Occurrences, N, of Meteorological Phenomena Causing C_{max}. 167

65. Dependence of the Maximun Concentration on Averaging Time 169

66. The Probability Required to Successfully Monitor C_{max} Twice if the Appropriate Meteorological Event Occurs N Times. 170

67. Dispersion From Virtual Image (EPA Model) and Mixing Cell (California Model) 177

68. Comparison of σ_z Values Used in the EPA and California Models 178

69. Gallatin Road Location Site 10. 185

70. Statistical Data Summary Diagram, California Site 10. . . . 191

71. Statistical Data Summary Diagram, EPA Site 10 192

72. Statistical Data Summary Diagram, EMP-1 Site 10 195

73. Statistical Data Summary Diagram, EMP-2 Site 10 196

74. Nondimentionalized Pollutant Concentration Versus Normal Distance Downwind of the Road as Calculated Using EPA and California Models for Stabilities B & E Under Perpendicular Wind Conditions. 200

FIGURE PAGE

75. Nondimentionalized Pollutant Concentrations Versus Normal Distance From the Road Edge as Calculated Using the EPA and California Models for Stabilities B & E Under Oblique (45°) Wind Conditions. 201

76. Nondimentionalized Pollutant Concentration Versus Normal Distance for the Road as Calculated Using the EPA and California Models for Stabilities B & E. 202

INTRODUCTION

Perspective

Due primarily to federal legislation within the last ten years (i.e., Amendments to the Clear Air Act of 1963 (1) and the National Environmental Policy Act (2)) air pollution monitoring activities in the United States have accelerated at a high level. Because air quality is a dynamic and complex environmental phenomena exhibiting large spatial and temporal variations, monitoring surveys designed to resolve these variations are necessarily complex. The demands of NEPA (2) have made air quality survey design even more complex, requiring adequate planning to assure that prescribed objectives can be attained in the shortest possible time and at the least cost. Comprehensive survey design and management is also required to minimize costs because the actual monitoring is expensive and time consuming requiring skilled personnel and sophisticated analytical equipment.

Objective

To design complex surveys requires expertise which is continually developing. The objective of this dissertation is to review and establish the current state-of-the-art of air monitoring survey design, and develop new concepts (particularly in regards to site selection) based on an engineering design approach (an approach currently lacking in many surveys). The design approach presented makes use of available atmospheric diffusion models, analysis of historical meteorological records, and applies probability and statistics to evaluate the ability of various survey designs to meet stated objectives. Important elements

of survey design include the selection of number and location of sites, the duration of the study, and the sampling schedules employed. Each of these elements is considered in the design approach.

Furthermore, a basic premise of the design approach presented herein is that air quality measurements can best be used to suppliment, and verify air quality predictions from mathematical models. This is because the spatial and temporal variations of air pollution concentration which occur in the environment are too complex to resolve by monitoring alone (the numbers of stations required approaches infinity). For this reason the site selection methods presented are designed to provide good data for model validation. Validated models can then be used to determine spatial variations in pollution levels, estimating concentrations even at sites where monitoring was not performed. This provides much more air quality information than can be derived from monitoring alone.

Organization and Statement of Originality

The dissertation is separated into five major sections each of which is a chapter.

Chapter I presents an overview of survey design.

Chapter II contains a literature review of subject areas pertinent to understanding the design methods presented in subsequent chapters. Topics covered in Chapter II include a review of current site selection criteria, a summary of atmospheric diffusion models used to describe ambient air pollution concentrations downwind of sources, methods of analyzing historical meteorological records, a summary of models describing plume rise from point sources, general solutions to the

diffusion models for point sources, and statistical methods for determining the numbers of samples required.

Chapter III presents the major original contribution of the dissertation (i.e., the application of diffusion models to the selection of air monitoring sites). Site selection techniques for monitoring near line, area, and point sources is presented. Also discussed are the numbers of samples, sampling schedules, and the duration of study required to meet specific objectives.

Chapter IV contains more original work describing an application of survey design for the purpose of validating a line source diffusion model. The results of correlation and regression analyses of field data compared to model predictions are presented in this chapter.

CHAPTER I

OVERVIEW OF SURVEY DESIGN

Introduction

In recent years, ambient air monitoring has become an important part of many environmental impact statements to satisfy the requirements of the National Environmental Policy Act (2). This has served to make air quality surveys more complex, requiring comprehensive planning to assure that prescribed objectives can be attained in the shortest possible time and at the least cost.

Adequate planning and good survey designs and management is required because monitoring is an expensive and time consuming undertaking requiring skilled personnel and sophisticated analytical equipment. This chapter discusses the role of air monitoring in environmental quality assessment, the planning and management process, the selection process for air monitoring sites and air monitoring equipment, and the cost of air quality surveys.

A well designed air quality survey will address the following items in the order listed (3,4):

1. Set the objectives of the air monitoring investigation.
2. Determine the physical parameters to be measured.
3. Set the network specifications including the location of air monitoring stations; the duration of the study and sampling schedules; and the air sampling method to be used.
4. Set the specifications for the individual stations in the network including the equipment needed to conduct the study, the method and frequency for equipment calibration, and the data recording methods.

5. Determine the type of data analysis to be performed and method of data reporting.

It should be recognized that these steps are interdependent and that a properly designed survey would consider each step in terms of the effect on the other parts of the survey design.

The Role of Monitoring and Modeling in Air Quality Assessment

In order to determine the environmental impact of a new or existing project, provide routine source surveillance or operate an intermittent air pollution control program, it is necessary to estimate air pollution concentrations either by monitoring or modeling or by a combination of these methods. The interrelationship between monitoring and modeling which can lead to an optimum design of an air quality survey is illustrated schematically in Figure 1.

As shown in the figure, the purpose of mathematical models is to quantitatively combine the effects of source strength and meteorology to describe the resulting ambient air pollution concentrations. Source strength is affected by a number of variables including the size of the source, variable emission rates, and the efficiency of air pollution control equipment employed. Meteorology is affected by wind speed and direction, atmospheric stability, inversion height, and terrain features. Useful mathematical models must be able to account for all these parameters.

Air pollution models vary in complexity from simple microscale dispersion models, to sophisticated mesoscale, multi-source models

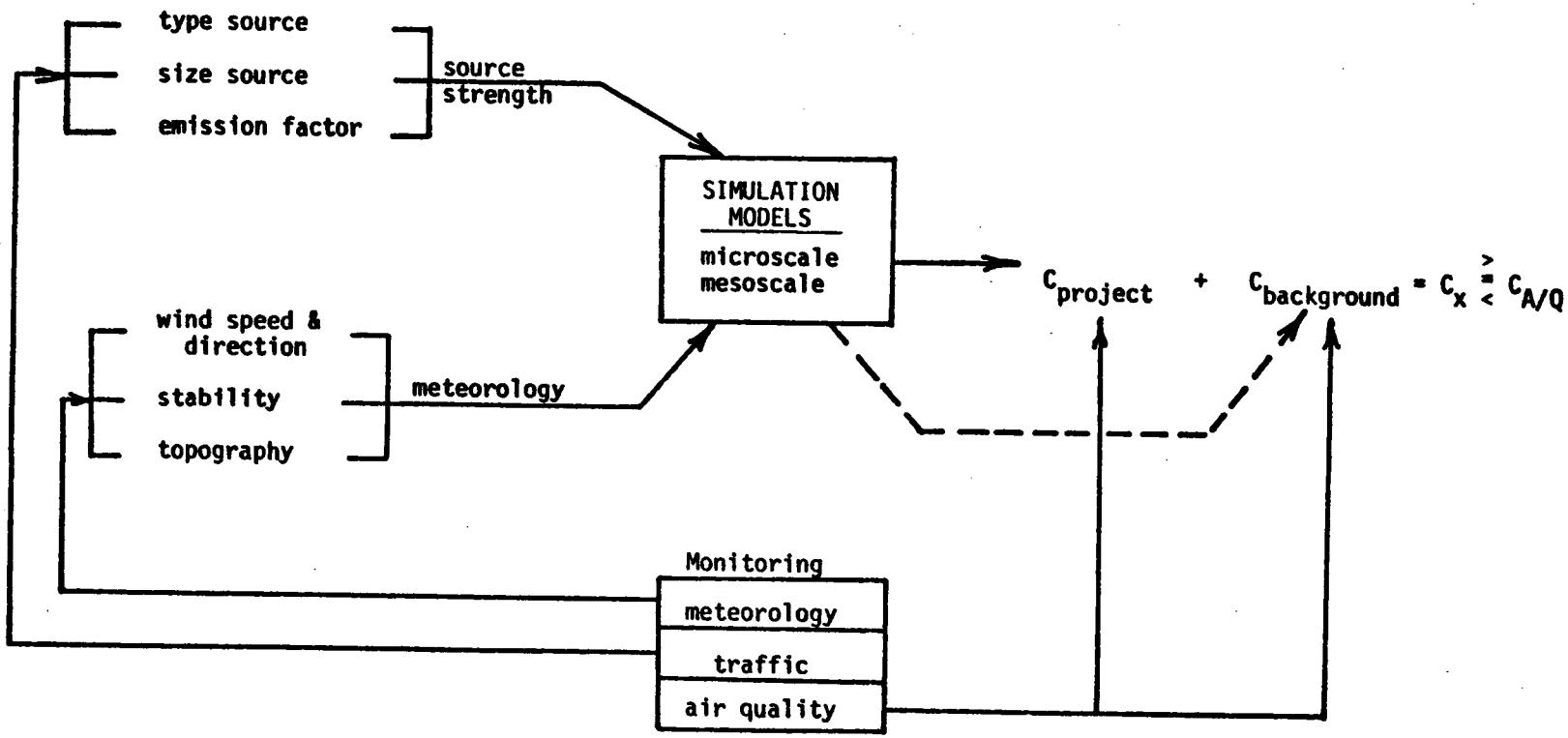

Figure 1. Interaction of Modeling and Monitoring to Assess the Air Quality Impact of a Project.

describing transport, dispersion, and photochemical reactions of pollutants.

Microscale models are used to estimate the ambient pollution levels near a single source or project, $C_{project}$. Mesoscale models are used to estimate the area wide impact of a proposed source or project, or the background concentrations, $C_{background}$, due to other sources.

Ambient air pollution concentrations occurring downwind of a source consist of two components; pollution contributed directly by the source, and background. In most analyses, these components should be determined separately. The total air quality impact, represented in Figure 1 by the concentration C_x, is equal to the sum of the background plus the concentration contributed by the project under study. Whenever other major sources are nearby, their contribution of pollution must also be added to the project contribution. The objective of the air quality report is to determine the value of C_x as accurately as possible and to compare that concentration to the NAAQS (National Ambient Air Quality Standards (5)).

The role of monitoring is to measure ambient pollution concentrations, meteorological parameters, and/or source strength parameters. Air monitoring at carefully selected sites provides a direct measurement of background concentrations. Measurements of meteorological or source strength parameters can be used to verify model input data or validate air pollution dispersion models. Validating microscale models requires source strength, meteorology, and both microscale and mesoscale (background) air pollution concentration measurements. Validating mesoscale models requires that source strength, meteorology, and air pollution measurements all be representative of area wide conditions.

Setting Objectives and the Initial Air Monitoring Survey Planning Process

Figure 2 provides an overview of the important decision points required in the initial phases of planning a survey. In general, the broad objectives of any air quality monitoring study are to determine the extent of the existing air pollution problem, and to validate any mathematical models or assumptions used to estimate the future impact of a new source or change in emissions from an existing source on air quality. More specific objectives may include such things as (3,4):

- checking for compliance with ambient air quality standards at critical locations,
- determining when and where the worst case background pollutant concentrations presently occur within the impact area,
- validating or calibrating a mesoscale model to allow an accurate prediction of future background concentrations, and
- validating or calibrating a microscale model to allow an accurate estimate of the air quality impact of a proposed facility or change in emissions from an existing facility.

Consideration should also be given to the potential exposure of people to air pollutants. If sensitive receptors, such as children, the elderly, or the sick, are to be exposed to additional pollutant concentrations after the completion of a proposed project, it may be important to document the present levels of exposure of sensitive populations so that the future levels of exposure can be more accurately estimated.

Once the objectives of the air quality study are set, it is possible to develop and implement a field monitoring program which will fulfill the objectives. Working within the constraints of money, manpower, and time, priorities can be set in terms of the objectives

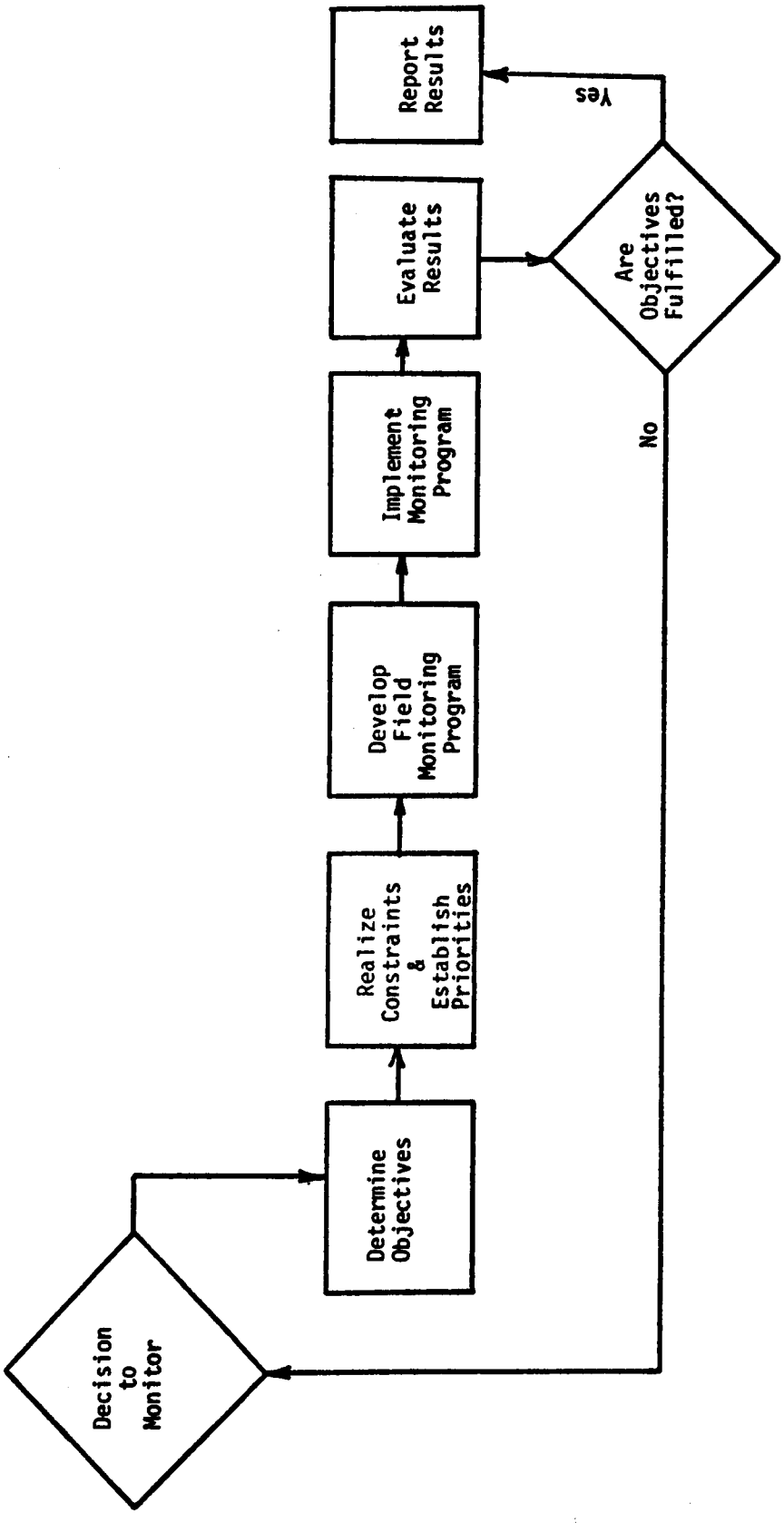

Figure 2. The Planning and Management Process for an Air Quality Survey.

which can realistically be met and the extent of the air quality study which can be afforded. If available resources are severely limited, an air quality monitoring study may not be advisable at all because a poorly planned, poorly financed, and hurriedly conducted air sampling survey will not provide data which can be easily evaluated in terms of the survey objectives.

Systematic Methods for Selecting Air Monitoring Sites to Meet Survey Objectives

Introduction

Choosing the "right" location for the "right" monitoring objective requires insight into the nature of air pollution emissions, transport, and dispersion from different types of sources. Because many variables must be considered, site selection is one of the most complex and critical elements in the design of an air quality monitoring survey. If the wrong sites are chosen or if a critical site is missed, no amount of accurate data will allow the objective of the study to be fully realized. Variables to be considered regarding the transport and dispersion of pollutants include: relative locations of pollution sources (inside and outside the study area), sensitive receptors, the effects of topography, source size and configuration, and meteorology. Each site chosen should fulfill a specific objective, such as (3,4):

- determining area wide "background" concentrations
- measuring the ambient concentrations within the microscale influence of a nearby source
- determining the mean, minimum, and maximum pollution concentrations near sensitive receptors.

The total number of monitoring sites which should be used in a study will depend on the diversity of the land use patterns, meteorological regimes, source configuration, and location of sensitive receptors. This number will be limited by the number of technically suitable sites available, the constraints of money and manpower available and the level of statistical significance or confidence desired in the results.

Defining Micro-, Meso-, and Macroscale Air Pollution Regimes

Before air monitoring sites can be effectively selected an understanding of the spatial distribution of pollution concentration is important. It is useful to define three separate air pollution regimes, the microscale regime, the mesoscale regime, and the macroscale regime as follows (3,4):

- Microscale: The microscale air pollution regime represents a relatively small air mass exhibiting large variations in ground level air pollution concentrations. This phenomena usually occurs very near sources of air pollution when the rate of increasing atmospheric dispersion with downwind distance is very great.

- Mesoscale: The mesoscale regime represents a "community size" air mass exhibiting fairly homogeneous ground level air pollution concentrations such as the ambient concentrations which result within urban areas from the emission of relatively small quantities of air pollutants from a large number of ground level sources (i.e., automobiles, residential and commercial space heating furnaces, and even numerous small industrial sources). These "local background" concentrations can vary considerably at different locations within an urban area.

- Macroscale: A macroscale regime is represented by "regional background" air pollution concentrations, which can be fairly homogeneous over linear distances from tens to hundreds of kilometers. Large variations in pollutant concentration indicate the presence of mesoscale and microscale air pollution regimes which are superimposed upon the regional background air pollution concentration regime.

The combined effects of the three pollution regimes on ambient pollution levels are illustrated in Figure 3 for highway sources of carbon monoxide (CO). Shown in the figure are the location of local streets, arterials, and a major high-capacity freeway route for a hypothetical urban area. On the right side of the figure, a plot of the CO concentrations which might be observed at ground level for winds blowing "across town" as illustrated. Initially, the air mass contains CO at only the regional background concentrations, but as the air mass passes over numerous city streets where automobiles are being operated the CO levels increase. In the case of city streets where emission sources are numerous, but diffuse, the horizontal distribution of concentrations will reflect a rather smooth profile of slightly increasing concentrations at greater distance from the upwind edge of the urban area source. This smooth horizontal concentration profile represents changes in pollution levels within the mesoscale regime, and is defined as the local background concentration.

At major arterial streets, with high traffic volumes, a peak in the concentrations above the background level will occur. The influence of this line source is significant within a horizontal distance of roughly 100 meters from the edge of the highway. Throughout this distance, atmospheric dispersion of the pollutants occurs. At distances beyond 100 meters only a small additional contribution to the local background concentration is observed.

A similar but greater air pollution concentration anomaly occurs at the location of a high capacity freeway due to the higher pollutant emission rate. As in the case of the arterial street, the ground level

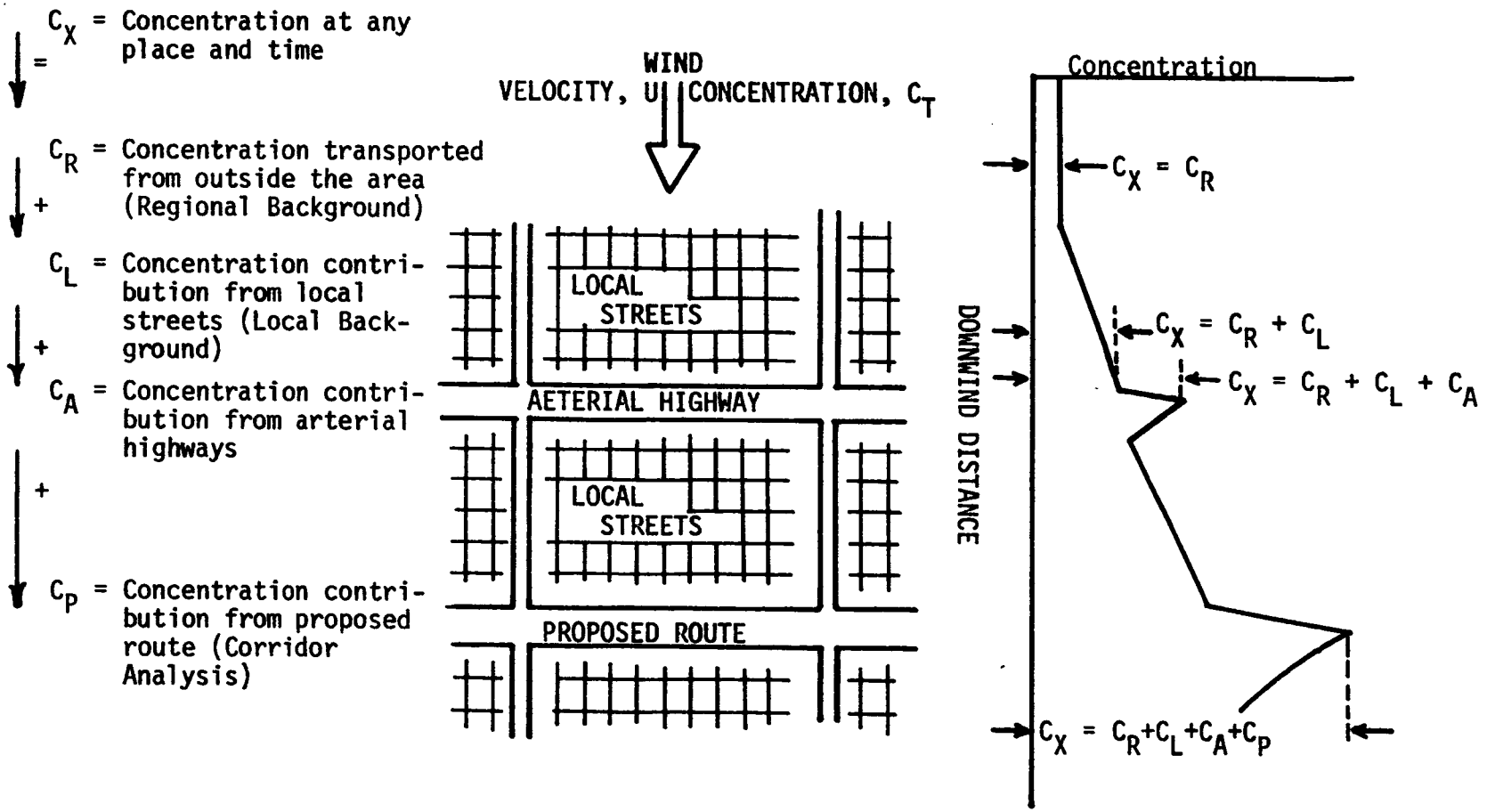

Figure 3. Background Air Quality Definition.

pollution concentration returns to near local background downwind from the freeway. This geographical area near major streets and freeways where the ambient pollution levels are above the local background concentrations defines the microscale regime of the pollution concentration distribution. This same elevation in concentration occurs near large point sources of pollution.

Pollution levels in the proximity of major sources consist of three component parts, the microscale concentration (contributed directly by the nearby source), the mesoscale concentration (the local background concentration due to area wide sources of pollutant emissions), and the macroscale concentration (the regional background concentration due to distance pollution sources). Frequently the macroscale pollution concentration is so low that this term can be ignored, leaving only two components to any ground level observation--the local background air pollution concentration plus the microscale concentration due to a nearby source. Air monitoring sites located outside the microscale regime measure only mesoscale and macroscale concentrations (background). Sampling sites located within the microscale regime measure the concentration due to the combined microscale, mesoscale, and macroscale regimes.

Selecting Monitoring Sites Near Sources - Microscale Monitoring

Whenever air quality near a specific air pollution source is to be monitored, mathematical dispersion models should be employed to assist in determining optimum air sampling sites. Numerous point and line source models are available (6-10) which can be used to calculate where the maximum ground level concentrations are expected to occur. Models can also be used to determine ground level concentration profiles

at various distances from the source in order to determine the extent of the impact area. A detailed discussion of how models can be used to locate sampling sites near major sources is described in Chapter III.

Selecting Sites for General Area Wide Background Studies in Urban Areas

The number and location of sites where background air pollution levels should be monitored will depend on the variety of homogeneous areas within the vicinity of the proposed source. Homogeneous areas can be selected on the basis of land use patterns, common meteorological regimes, and sensitive receptor areas. Types of homogeneous areas which may require monitoring are outlined below (8):

A. Land Use Patterns

1. Forested areas
2. Agricultural areas
3. Urban areas
4. Industrial areas

B. Meteorological Regimes

1. Effects of topography
2. Localized drainage winds
3. Prevailing wind directions
4. Wind speeds which produce maximum concentrations

C. Sensitive Receptor Areas

1. Schools
2. Hospitals
3. Parks for children's activities
4. Convalescent homes
5. Residential areas

These features should be considered and may be plotted on a map of the area. Ideally, samples should be taken within each of the different homogeneous sections. However, if manpower and/or equipment limitations restrict the number of sampling sites, the sites to be air monitored

should be selected on a priority basis. Three locations have particular priority (3,4). (See Figure 1, page 6.)

- where the maximum project concentrations, $C_{P_{max}}$, is expected,
- where maximum background, $C_{B_{max}}$, is expected,
- where high air pollution concentrations are expected at sensitive receptors.

Locating monitoring stations near sensitive receptors is as important as measuring the maximum background concentration. Some data is needed to assure that levels at sensitive receptors will be lower than levels at maximum background sites, especially if levels are expected to be near the NAAQS, or if controversy is anticipated.

Air Monitoring Network Specifications

The sum total of all air monitoring stations, meteorological stations, calibration equipment, and data acquisition equipment required to meet the total objective of an air quality survey represent the air monitoring network.

In order to understand the interrelationships between all of the component parts of the network and allow decisions to be made about the number and type of each piece of equipment and the interdependence of the equipment in meeting the survey objectives, a set of specifications for the network must be developed early in the planning process.

Air monitoring network specifications should include the number of sites to be monitored, air pollution and meteorological measurements required at each site, the duration of the study, and manpower requirements. Network specifications should be determined in light of known limitations of physical, engineering, economic, and human factors as

well as limitations due to completion deadlines or time delays in equipment procurement. Time, manpower, and budget constraints may significantly affect the feasibility of utilizing specific techniques or equipment to conduct the study.

Considering all of the stated sampling requirements and available resources, the types of air quality and meteorological monitoring equipment to be employed can be identified including the total number of samplers and analyzers for each type of measurement to be performed. To accomplish this, available sampling methods should be evaluated. For example, the number of continuous analyzers versus semi-automatic samplers versus manual sampling methods should be investigated. Obviously, the needed mobility of air sampling equipment should be considered and such factors as the high capital costs of continuous analyzers versus the high operating costs of semi-automatic or manual methods should be optimized for cost effectiveness where possible.

The calibration system to be used to insure accurate data from all the analyzers should be considered next. Each station can be equipped with calibration hardware, or calibration procedures can be utilized where either portable instruments are calibrated at a central laboratory, or permanent instruments are calibrated with a portable calibration device. The choice of needed calibration equipment will depend on the number of stations, distance separating the stations, and the frequency at which calibrations are performed. A typical integrated calibration system might consist of sophisticated dynamic calibration apparatus located at a central laboratory for performing periodic primary calibrations, with several portable calibrators or span gas bottles used for frequent on-site single-point calibration checks.

Once the air monitoring and calibration specifications have been fixed, the requirements of the data acquisition system can be evaluated. The data rates and data quantities generated by the monitoring network should be determined as a whole in order to calculate the data handling capacity needed for the overall sampling network. Data recording equipment which is ideal for a single monitoring station may be too expensive for use at numerous monitoring stations. Frequently it is less expensive to replace a variety of special devices with a central general-purpose control element, even though the speed and flexibility requirements of the system do not require it. Data telemetry and central data processing systems may represent the most efficient approach for monitoring networks with many remote sampling stations employing continuous air pollution analyzers. Conversely, for single station applications, strip chart recorders with manual data reduction may represent the most cost effective data collection method.

Selecting Air Monitoring Station Equipment

The network design will necessarily limit the number of air monitoring stations to be employed and set the functional sampling objectives of each station. At this point, air monitoring station specifications can be developed for each monitoring site in the network. Station specifications include the setting of sampling objectives for each station and the selecting of compatible hardware components for each station resulting in an integrated air monitoring sampling station design.

There are nine discrete component elements of air monitoring station design: the sampling probe and tubing, sample preconditioning, sample collectors, continuous air pollution analyzers, calibration equipment, flow control and flow meters, air movers, data acquisition equipment, and equipment shelters. (See Figure 4.)

The sequence of selection of station equipment should be arranged so that primary components are chosen before supportive or supplementary hardware. For example, equipment shelters should be designed after the total amount of equipment to be housed in the shelter has been determined; thus, the shelter will be properly sized, with adequate electrical wiring, plumbing, instrument mounting, and storage space as required by hardware components.

The first step in hardware selection is to choose air samplers and air pollution analyzers. Similar instruments can be compared on a cost basis, or by using manufacturers' instrument operations specifications. Instrument selection can be assisted by consulting the technical literature for reports on instrument performance tests or by obtaining personal recommendations from experts in the air monitoring instrumentation field. An extensive compilation of air monitoring instrument hardware specifications has been prepared by Lawrence Berkeley Laboratory (11) which may be especially useful for selecting instrument hardware. Also, the EPA has published Unacceptable Methods of Measurement for Criteria Pollutants (12) which should be consulted before selecting analyzers.

Second, calibration equipment should be selected which is compatible with the air monitoring instruments. The critical criteria is that calibration equipment must produce pollutant gas concentrations at

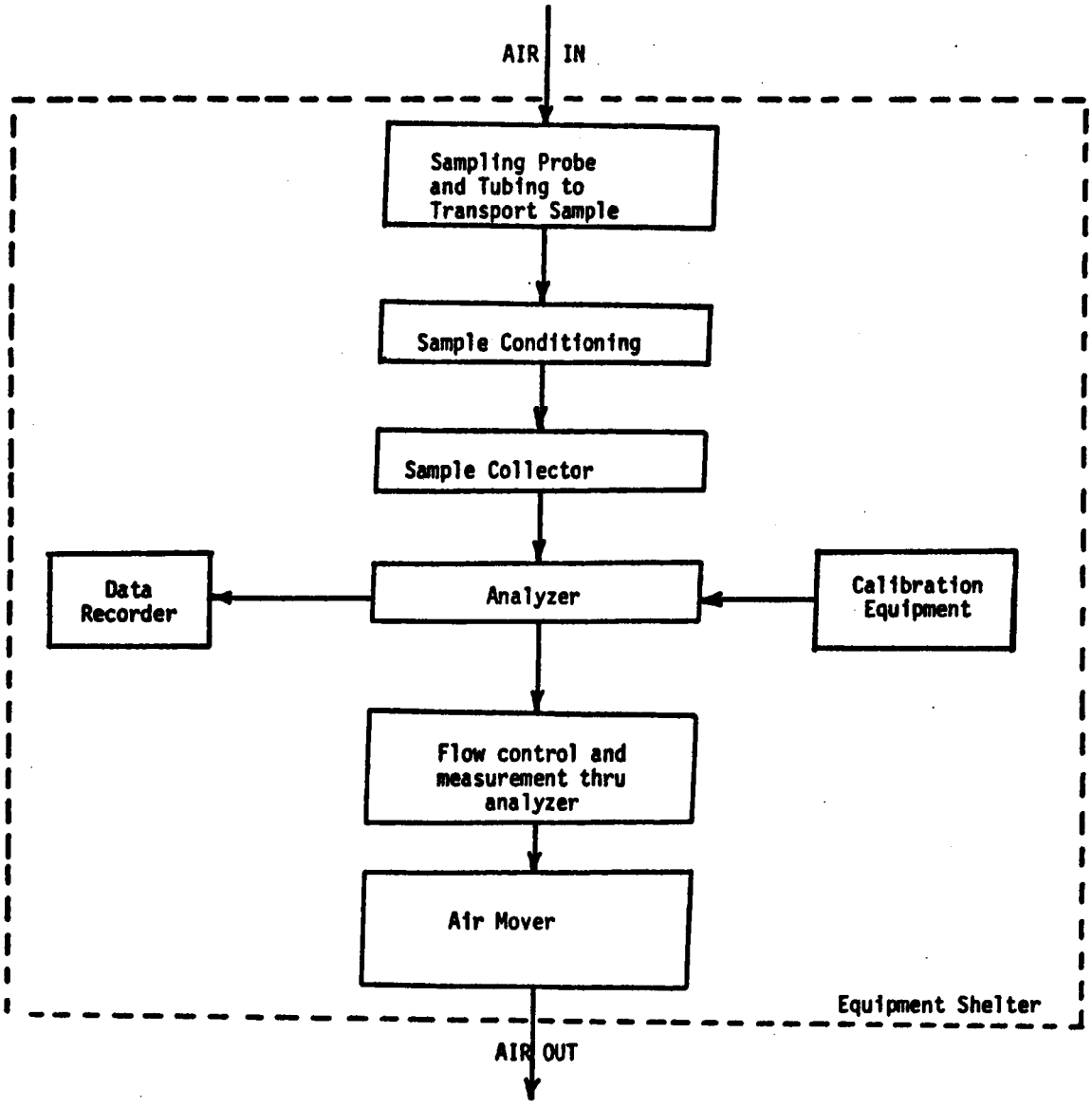

Figure 4. Hardware Components of an Air Quality Monitoring Station.

desired levels and in sufficiently large quantities to calibrate the monitoring equipment. Problems can arise if the monitoring instrument employs a high sample flow rate while the calibration device generates a low flow rate. Another common problem occurs when the pollutant gas concentration from the calibrator is too high to calibrate the monitoring instrument in the desired operating range.

Third, data acquisition equipment should be compatible with the air monitoring hardware previously selected. Voltage output ranges from monitoring equipment must match the voltage input ranges of the data acquisition equipment. The data acquisition system must be properly sized in order to accommodate the total data output from all air monitoring equipment. When monitoring stations are operated over long periods unattended, the data system must provide enough storage capacity to handle all the output data generated by the sensor. Data acquisition systems should also provide methods by which instrument calibration and maintenance information can be stored along with data from the air pollution and meteorological sensors.

Fourth, sample preconditioning devices should be selected according to the requirements of the air pollution analyzers employed. The installation of sample preconditioning equipment in the sampling lines may cause difficulties if the plumbing requirements are not anticipated before designing the sampling probe hardware. Since sample preconditioner plumbing requirements may affect the sampling probe or manifold design, the selection of preconditioning equipment should precede the sample handling system design.

Fifth, the entire sample handling system, which consists of the sampling probe and tubing, flow meters, flow controllers, and air mover equipment, should be designed as an integral unit with compatible components. The selection of the sampling probe and the sample tubing depends on the type of sampling to be conducted, the type of air pollutants to be measured, and the sample volume flow rates required by air samplers operated within the station. The important design criteria is that the tubing be sized to handle the air sample flow rates required by the instruments and that the materials of construction not affect the air sample before analysis. Flow meters should be employed on all sampling lines where the flow rate required periodic monitoring. Flow meters should be chosen according to both the flow rate to be measured and the materials of construction of the meter. Flow controlling devices and air movers should be properly matched to provide a continuous regulated sample flow rate through all "legs" of the sample handling system.

Sixth, the size of shelter needed depends on the total amount of equipment to be housed. An inventory of all equipment requirements such as space, electrical power needs, environmental control requirements, plumbing needs, and vibration effects can be used to insure an adequate shelter size, with adequate electrical wiring, plumbing, instrument mounts, and storage space as needed. Station mobility requirements must also be considered in light of the quantity of monitoring to be conducted and the supportive equipment required for remote or mobile station monitoring.

Cost of Air Monitoring

The cost of purchasing and operating an air monitoring network will depend on the level of temporal and spatial resolution of air quality measurements desired. The requirements for good spatial resolution differ from the requirements for good temporal resolution. Good spatial resolution can only be obtained by sampling at numerous locations, while good temporal resolution can only be obtained by sampling over short intervals for a long duration. Achieving both spatial and temporal resolution requires monitoring at many sites, for a long duration. This becomes so expensive that most projects either "trade off" temporal resolution for spatial, or spatial resolution for temporal. Usually both types of studies must be conducted simultaneously; thus characteristics of both types must be incorporated into the air sampling program design. In most cases, the goal of the survey design is to achieve "acceptable" temporal and spatial resolution at the lowest cost. "Good" resolution is very expensive to obtain and is required only for research or where unique or complex air quality problems exist.

The concept of a study designed to achieve good temporal or good spatial resolution is best illustrated by the extreme case. For example, an air quality study design providing good spatial resolution might consist of 20 to 30 semi-automatic air samplers located at an equal number of different sites; all samplers would be operated simultaneously. Ideally, this program would be conducted so that measurements are taken under all wind directions and with all possible sources acting. The resulting data would show where the highest and lowest air pollution concentrations occur, and under what conditions (i.e., wind direction,

season of year, etc.). A study designed to provide good temporal resolution might consist of a single station using a continuous air sampling method. This station would be operated 24 hours a day, with averages each hour for an entire year. The results would provide the most probable and "worst case" diurnal profiles of pollution levels, the seasonal fluctuations and frequency of occurrence of worst case one hour, eight hour and daily average air pollution concentrations. This type of study would provide the maximum amount of information regarding the temporal distribution of air pollution concentrations, illustrating when, how frequently, and how long adverse conditions occur at one location.

The approximate capital cost of the equipment required to conduct an air quality study is shown in Figure 5. The relative cost of using static air samplers, is compared to the cost using semi-automatic or continuous air samplers. These curves allow one to determine either the approximate number of stations and the type of equipment which can be purchased, or the least cost number of sites and type of equipment that will fulfill the monitoring objective.

The three types of equipment indicated in Figure 5 represent three distinctly different levels of sophistication. The approximate 1975 cost of a single static, semi-automatic or continuous air sampler is $50, $500, $5,000, respectively. These estimates represent the purchase price of the equipment only. The cose of shelters to house continuous monitoring equipment must be added. In most cases, these estimates are conservatively high.

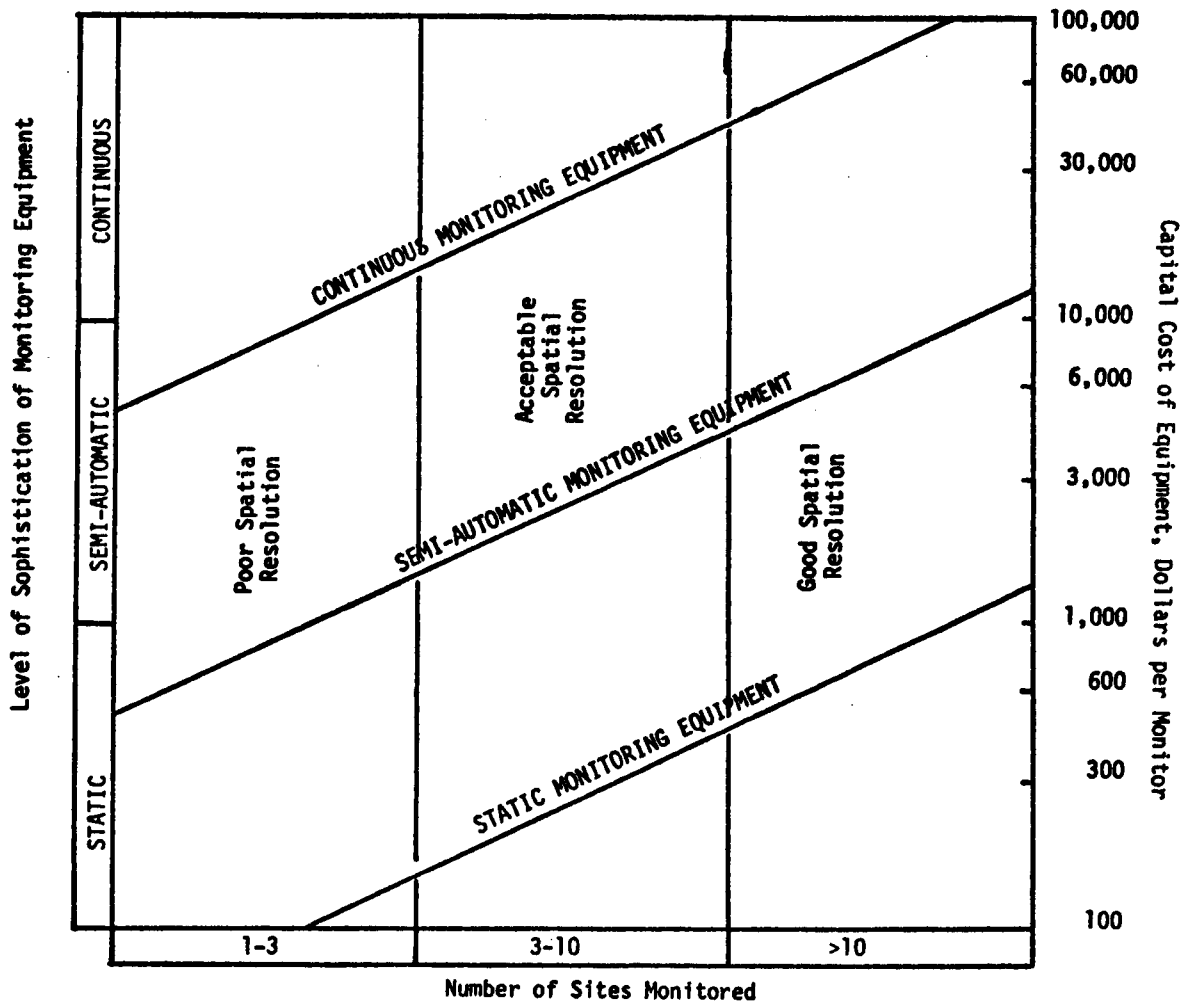

Figure 5. Achievable Spatial Resolution and Capital Costs for Conducting an Air Quality Survey with Various Numbers of Monitoring Sites and Three Levels of Equipment Sophistication.

The costs of operating stations for different durations is illustrated in Figure 6. These estimates assume that the operating cost for a continuous station is $25,000 per year. The cost of operating a semi-automatic station is approximately $2,500 per year and a static station is $250 per year. In order to consider the additional expenses encountered with short term projects, (i.e., a few days) the cost per day is assumed to be four times the cost per day for a year round station.

The estimates are for total costs to operate and reduce the data from a single station. Where appropriate, the cost estimates include the costs of operating and maintaining the monitoring equipment (including utilities, spare parts, chemical reagents, technician costs, etc.), calibration of the monitoring equipment, operation and maintenance of data recorders, and data reduction and logging. One of the assumptions upon which the cost estimates are based is that a continuous sampling station requires a considerable amount of "technician's time" each day, while a semi-automatic station requires no more than a single short visit each day, and a static air sampler will be visited only once per month. However, semi-automatic equipment operating on short sampling intervals may require considerably more of the technician's time. In such a case, the cost curve may approach that of a continuous station because a major portion of the cost of operating an air monitoring station is manpower.

Summary

The proper development of a cost effective air quality survey involves not only air quality monitoring, but also meteorological monitoring,

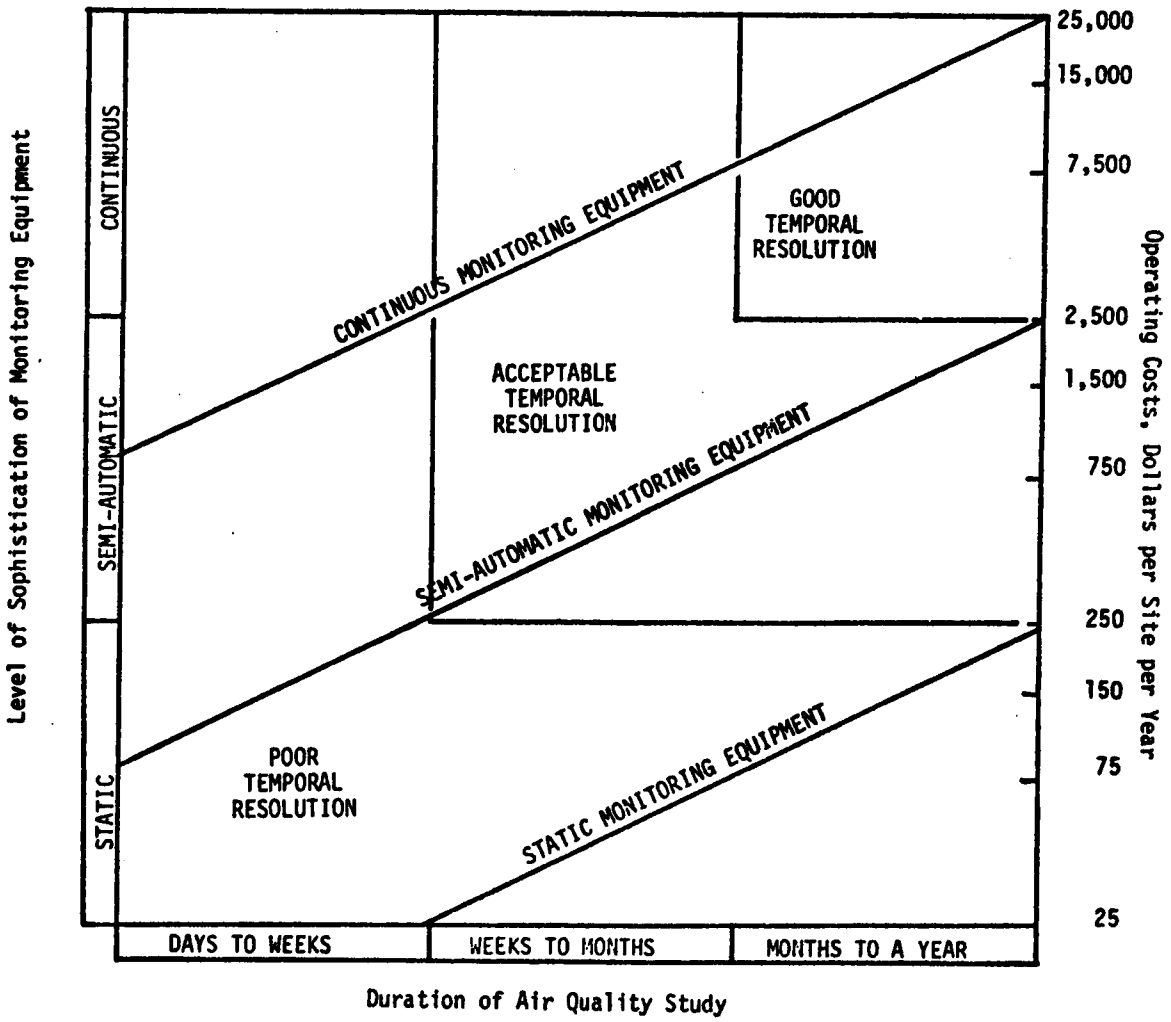

Figure 6. Achievable Temporal Resolution and Operating Costs for an Air Quality Survey of Various Durations for Three Levels of Equipment Sophistication.

calibration, and data acquisition systems. Failure to recognize this fact at the outset results in a system design based on many practical compromises that may fail to meet the sampling objectives. The engineering design of a cost effective system should reflect both the realities of current air quality monitoring system technology and the ultimate application for which the measurement system is intended.

CHAPTER II

LITERATURE REVIEW

Introduction

One of the most critical elements of air monitoring survey design is the location of sampling sites. Criteria for site selection has not been well defined in the literature, consisting mostly of subjective, general recommendations. Quoting from a 1971 EPA guideline document on air quality surveillance network, AP-98 (13): "Experience and technical judgement are essential for determining the number and location of sampling sites because adequate mathematical models or other methods have not been formulated.

It is the objective of this dissertation to present methods of applying available mathematical dispersion models to assist in site selection decisions. Before proceeding with a discussion of site selection methods using diffusion models, however, it is first necessary to review current air pollution literature on the subject and present information required to understand the survey design methods presented in Chapter III. This chapter reviews the literature addressing the following six subjects: air monitoring site selection, meteorological data evaluation, sampling statistics, atmospheric diffusion models, plume rise from point sources, and general solutions to the diffusion models. Each of these subjects are addressed in separate sections of this chapter.

Air Monitoring Site Selection

Introduction

It has been generally recognized that the choice of monitoring site depends on the objective of the monitoring to be performed. EPA (13) recognizes the following as principal objective for monitoring:

1. To judge compliance with and/or progress made toward meeting ambient air quality standards.

2. To activate emergency control procedures to prevent air pollution episodes.

3. To observe pollution trends throughout the region including the nonurban areas. (Information on the nonurban areas is needed to evaluate whether air quality in the cleaner portions of a region is deteriorating significantly and to gain knowledge about background levels.)

4. To provide a data base for application in evaluation of effects; urban, land use, and transportation planning; development and evaluation of abatement strategies; and development and validation of diffusion models.

In order to accomplish these objectives, criteria for air monitoring network sites and individual monitoring stations is required.

Station Siting Criteria

Most of the criteria which have been published regarding the location of an individual sampler or a continuous monitoring station is aimed at insuring a representative sample without undue influence from the immediate surroundings. Again quoting from AP-98 (13): "No definitive information is available concerning how air quality measurements are affected by the nearness of buildings, height from ground, and the like. There are, however, general quidelines that should be considered in site selection:"

1. Uniformity in height above ground level is desirable for the entire network within the region. Some exceptions may include canyons, high-rise apartments, and sites for special-purpose samplers.

2. Constraints to airflow from any direction should be avoided by placing inlet probes at least three meters from buildings or other obstructions. Inlet probes should be placed to avoid influence of convection currents.

3. The surrounding area should be free from stacks, chimneys, or other local emission points.

4. An elevation of three to six meters is suggested as the most suitable for representative sampling, especially in residential areas. Placement above three meters prevents most reintrainment of particulates, as well as the direct influence of automobile exhaust.

Pooler (14), in reference to sites chosen for the St. Louis Regional Air Pollution Study (RAPS), the objective of which is the development and validation of regional air quality simulation models, emphasizes the need for a representative site. "Ideally, sites chosen for the RAPS program should each be representative of a 1 Km^2 area of downtown St. Louis." However, because of the inhomogeneities of emissions throughout the study area, Pooler has restated his criteria to "avoidance of domination of a site by one or more local sources." He recommends that a site should be 1 km or more from a major traffic artery, it should not be in the lee of a building where downwash of effluents from that building or its immediate neighbors might occur, it should not be located within a local topographic depression, and busy parking lots are poor sampling locations.

Most authors recognize the need for accessibility and availability of utilities for each site which often eleminates many potential locations. Based on his experience with vandalism and theft at Chicago monitoring stations, Harrison (15) places the highest priority on security

stating: "Experience in urban areas leads one quickly to the unfortunate realization that the first criteria for placement for a sensor for any purpose is security."

The Highway Research Board (16) has published EPA recommendations which are more definitive in describing acceptable sampling locations. Table I lists specific guidelines for locating air monitoring instruments in areas of estimated maximum pollutant concentration as given by EPA (16).

> Sampling station guidelines are different for defining average CO concentration for one hour and eight hours because people would not ordinarily be exposed to CO concentrations that occur in a downtown area having high traffic density for a period of eight hours. When only a single sampling site is established to satisfy the minimum air quality surveillance requirement of the implementation plan, a site should be chosen that meets the guidelines for eight hour averaging time. Distance from the street is specified in the sampling location guidelines for CO because of the strong dependence on nearness to the street and CO concentration. For the same reason, height from the ground of the air inlet is more restrictive than for the other pollutants. It is desirable, however, to sample as close as possible to the breathing zone within practical considerations; sampling height limitations are specified accordingly for those pollutants. There are no well established meteorological dispersion models currently available for selecting areas of expected maximum concentration for the secondary pollutants. Selection of high concentration areas described in Table I, for those pollutants is based on available information on reaction kinetics of atmospheric photochemical reactions involving hydrocarbons, nitrogen oxides, and oxidants; atmospheric data on diurnal variation in pollutant concentration; distribution of primary mobile sources of pollution; and meteorological factors. A minimum distance away from major traffic arteries and parking areas is specified for the oxidant monitoring site because NO emissions from motor vehicles consume atmospheric ozone. NO_2 is considered to be both a primary stationary-source pollutant and a secondary pollutant, and air monitoring stations for this pollutant should be located consistent with the respective station location guidelines. Differences in horizontal and vertical clearance distance are based on increased probability of reaction between reactive gases and vertical surfaces.

The need for nationally standarized criteria for locating monitoring stations has been suggested in two papers by Ott (17,18). His study of

TABLE I

Sampling Location Guidelines for Areas of Estimated Maximum Pollutant Concentration (16)

Pollutant Category	Pollutant	Station Location	Position of Air Inlet		
			Height[a] (ft)	Vertical[b] (ft)	Horizontal[c] (ft)
Primary stationary source	SO_2 NO_2 Particulate matter	Determined from atmospheric diffusion model, historical data, emission density, or other information and representative of population exposure	<50	>3	>5
Primary mobile source	CO[d]	Representing area having high traffic density, slowly moving traffic, obstructions to air flow (tall buildings), and pedestrian population such as major downtown traffic intersection (<20 ft. from street curb)	<15	>3	>3
	CO[e]	Representing area having high traffic density in residential area such as major thoroughfare in center city or suburban area (<50 ft from street curb)	<15	>3	>3
Secondary	O_3	Representing residential area downwind of downtown area (5 to 15 miles from downtown and >300 ft from major traffic arteries or parking areas)[f]	<50	>3	>5

TABLE I. (continued)

Pollutant Category	Pollutant	Station Location	Position of Air Inlet		
			Height[a] (ft)	Vertical[b] (ft)	Horizontal[c] (ft)
	NO_2	Representing residential area downwind of downtown area (<5 miles from downtown)[f]	<50	>3	>5

[a] From ground.

[b] Clearance above supporting structure.

[c] Clearance beyond supporting structure; not applicable where air inlet is located above supporting structure.

[d] 1-hour averaging time.

[e] 8-hour averaging time.

[f] Downwind of prevailing daytime wind direction during oxidant season.

carbon monoxide concentrations in San Jose (17) indicates that air monitoring stations located near city streets "give drastically different results when moved only a block or two." This raises serious implications regarding the representativeness of these measurements to air quality in a large physical area surrounding the station. Because of the complex nature of the spatial variations in urban CO concentrations Ott (18) suggests a "dual monitoring system" consisting of a "background exposure station" located outside the range of influence of nearby traffic (greater than 100 meters from the curb) and a "pedestrial exposure station" with a sampling probe above the sidewalk, 0.5 meters away (horizontally) from the curb and 3 $\pm$ 0.5 meters above the sidewalk. (See Figure 7.)

In the dual monitoring approach, according to Ott, the pedestrian exposure station provides a measure of the exposure of individuals on downtown streets. The background exposure station measures concentrations occurring over a large physical area of the city. The horizontal CO concentration profile described by Ott is illustrated pictorial in Figure 8.

Ott goes on to say that few of today's air monitoring sites could be classified into either of the above two categories. He states (18): "My examination of many existing sites reveals that too many fall between categories--for example, too far from the curb to give an estimate of pedestrian exposure and too close to the street to avoid serious influence from traffic. In my view, such sites give ambiguous measurements. . . ." "It may not be possible to determine if an urban area is or is not in compliance with an air quality standard, as presently

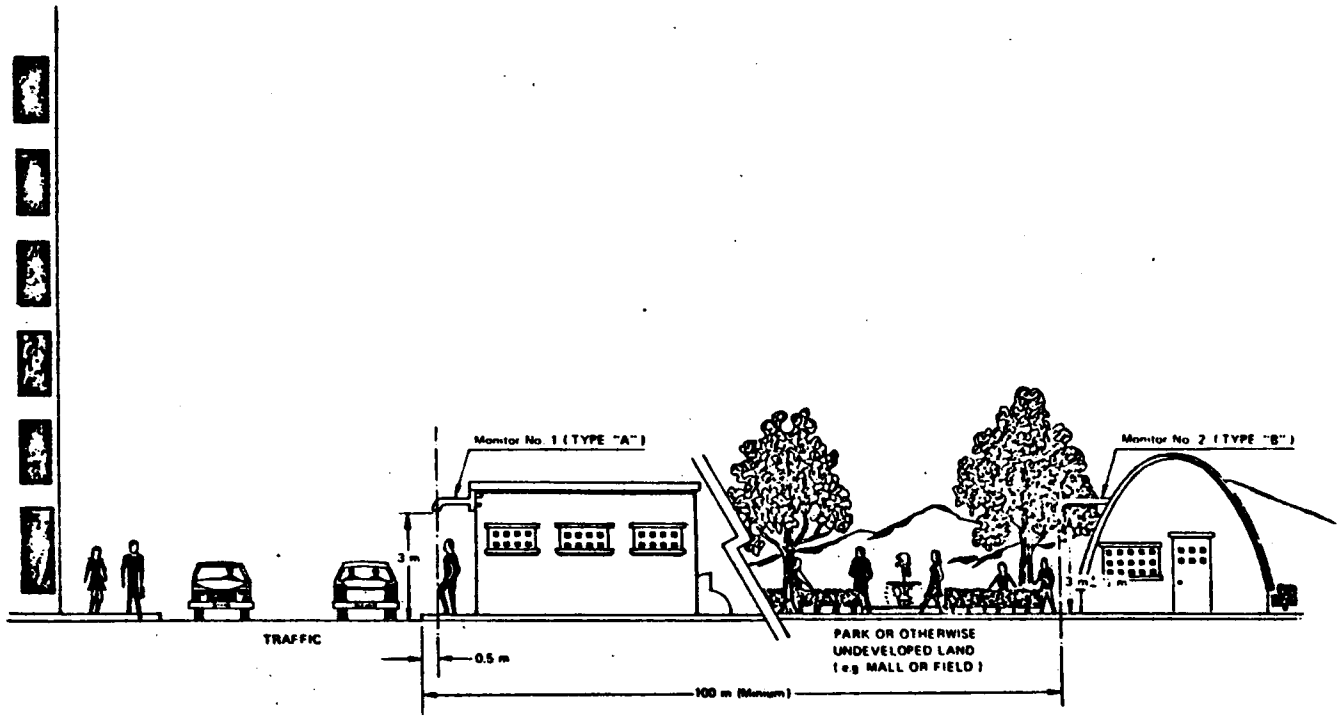

Figure 7. Simplified Schematic of Dual Air Monitoring System Monitor No. 1 is the Pedestrian Exposure Station and Monitor No. 2 is the Background Exposure Station.

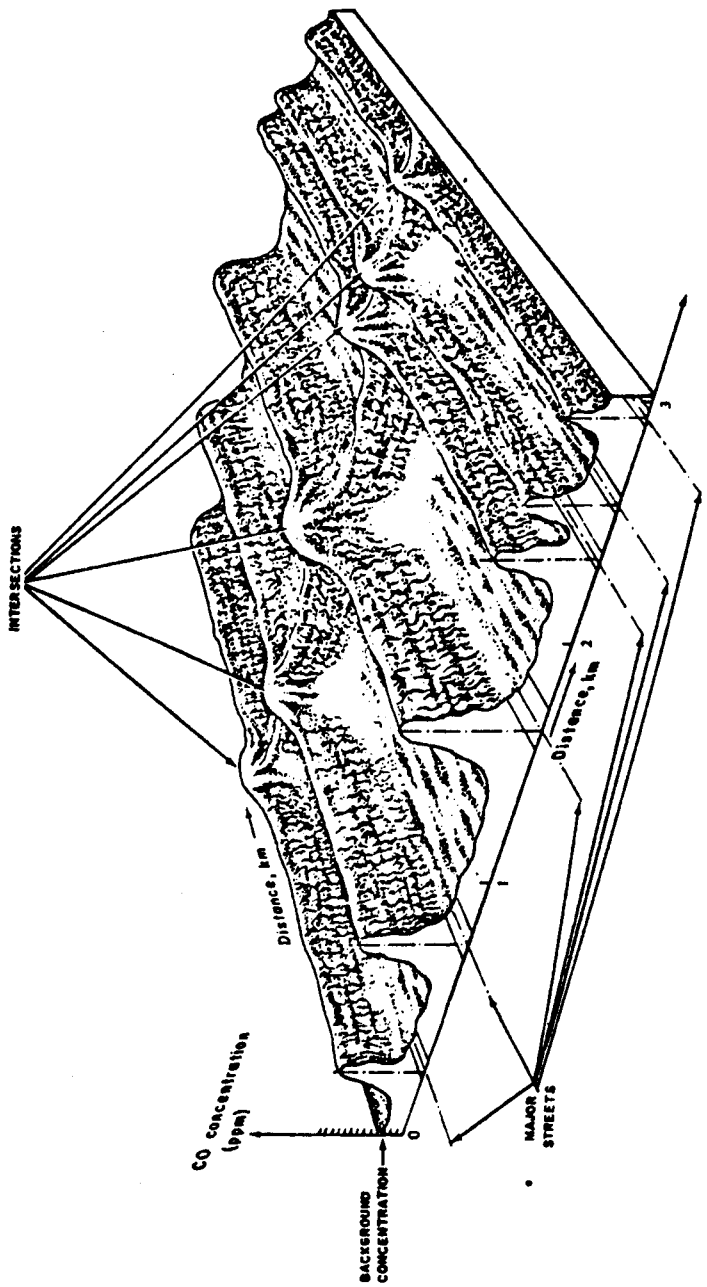

Figure 8. Inferred Spatial Distribution of Vehicular Air Pollutant Concentration (Carbon Monoxide, Lead, etc.) in an Urban Area.

defined, using data from existing air monitoring stations (17)." As a solution Ott (18) recommends adoption of six standard classifications of criteria for siting monitoring stations. (See Table II.)

Network Siting Criteria

In general, available information in the literature recognizes that the design of an air monitoring network involves a trade-off between what is considered desirable from a strictly technical point of view and what is feasible with the available resources. An ideal network will usually require more resources than are available. The objective is to design the least cost monitoring network still capable of meeting the major surveillance requirements. Network design should attempt to maximize the effectiveness of a minimally adequate network by careful selection of sampling sites, sampling schedules, and use of both semi-automatic and automatic (continuous) monitoring instruments.

According to EPA (13),

> Knowledge of the existing pollution levels and patterns within the region is essential in network design. The areas of highest pollution levels must be defined, together with geographical and temporal variations in the ambient levels. Isopleth maps of ambient concentrations derived from past sampling efforts and/or from diffusion modeling are the best tools for determining the number of stations needed and for suggesting the station locations. Additionally, information on meteorology, topography, population distribution, present and projected land uses, and pollution sources is extremely helpful in network design. . . . Information on emission densities and/or land use can be used together with wind-rose data to pinpoint areas of expected higher concentrations. Topographical maps provide additional information on wind flow and pollution dispersion characteristics. Maps of population distribution are essential in locating key stations for monitoring during episodes.

The following are guidelines suggested by EPA (13) as important network site selection criteria:

TABLE II

Recommended Criteria for Siting
Monitoring Stations (18)

Station Type	Description
TYPE A	Downtown Pedestrian Exposure Station. Locate station in the central business district (CBD) of the urban area on a congested, downtown street surrounded by buildings (i.e., a "canyon" type street) and having many pedestrians. Average daily travel (ADT) on the street must exceed 10,000 vehicles/day, with average speeds less than 15 miles/hour. Monitoring probe is to be located 1/2 meter from the curb at a height of 3 ± 1/2 meters.
TYPE B	Downtown Background Exposure Station. Locate station in the central business district (CBD) of the urban area but not close to any major streets. Specifically, no street with average daily travel (ADT) exceeding 500 vehicles/day can be less than 100 meters from the monitoring station. Typical locations are parks, malls, or landscaped areas having no traffic. Probe height is to be 3 ± 1/2 meters above the ground surface.
TYPE C	Residential Population Exposure Station. Locate station in the midst of a residential or suburban area but not in the central business district (CBD). Station must not be less than 100 meters from any street having a traffic voluem in excess of 500 vehicles/day. Station probe height must be 3 ± 1/2 meters.
TYPE D	Mesoscale Meteorological Station. Locate station in the urban area at appropriate height to gather meteorological data and air quality data at upper elevations. The purpose of this station is not to monitor human exposure but to gather trend data and meteorological data at various heights. Typical locations are tall buildings and broadcasting towers. The height of the probe, along with the nature of the station location, must be carefully specified along with the data.
TYPE E	Nonurban Background Station. Locate station in a remote, nonurban area having no traffic and no industrial activity. The purpose of this station is to monitor for trend analyses, for nondegradation assessments, and for large-scale geographical surveys. The location or height must not be changed during the period over which the trend is examined. The height of the probe must be specified along with the data. A suitable height is 3 ± 1/2 meters.

TABLE II. (continued)

Station Type	Description
TYPE F	Specialized Source Survey Station. Locate station very near a particular air pollution source under scrutiny. The purpose of the station is to determine the impact on air quality, at specified locations, of a particular emission source of interest. Station probe height should be 3 ± 1/2 meters unless special considerations of the survey require a nonuniform height.

1. The priority area is the zone of highest pollutant concentration within the region. One or more stations are to be located in this area.

2. Close attention should be given to densely populated areas within the region, especially when they are in the vicinity of heavy pollution.

3. For assessing the quality of air entering the region, stations must also be situated on the periphery of the region. Meteorological factors such as frequencies of wind direction are of primary importance in locating these stations.

4. For determining the effects of future development on the environment, sampling should be undertaken in areas of projected growth.

5. A major objective of surveillance is evaluation of the progress made in attaining the desired air quality. For this purpose, sampling stations should be strategically situated to facilitate evaluation of the implemented control tactics.

6. Some information of air quality should be available to represent all portions of the region.

> The air quality surveillance network should consist of stations that are situated primarily to document the highest pollution levels in the region, to measure population exposure, to measure the pollution generated by specific classes of sources, and to record the nonurban levels of pollution. Many stations will be capable of meeting more than one of these criteria. . . . Common sites, although not necessarily ideal for each pollutant, may be selected to provide adequate coverage for the pollutants of concern. Each pollutant, however, should be considered individually during the design phase to pinpoint pockets of high pollution that otherwise might be overlooked.

Pooler (14) has described the criteria used to select the air monitoring network for the Regional Air Pollution Study (RAPS) in St. Louis. According to Pooler sites chosen were based on the "conflicting requirement of extended regional coverage vs close spacing of sites to achieve desired spatial resolution." The basic objective of RAPS is mesoscale model validation in a complex urban area. Pooler states:

> This objective leads directly to the requirement that there be generated an extensive base of air quality measurements against which calculated values may be compared. Extensive spatial coverage is necessary to include the entire metropolitan area, and

simultaneous measurements should be made at all sites for a long enough interval of time to include all the varying large-scale weather situations that might reasonably be expected to occur. Measurements should be continuous, but with a time resolution short enough to be compatible with the resolution available from models. . . .

Since the network is for the purpose of model development, the resources to be put into the network must be balanced against resources required for other components in a total modeling effort, namely, the requirements for emission data, and the requirements for studies of the atmospheric processes of dispersion and transformations. . . .

The relationship between input resources and the value of data to be obtained is generally nonlinear, and thus there exist no simple formulations by which an optimum mix of fixed network measurements, special measurements, analytic studies, and the duration of each measurement and study may be derived. However, there are minima, which, if not met result in substantial losses of value in the output. One minimum we agreed on was the number of sites for such a network. We were originally thinking in terms of 40 to 50 sites, but when we began estimating costs, we were forced to consider what minimum number could serve our purposes, and arrived at the number 25. Our reasoning was quite subjective, but can be demonstrated by trying to place pins on a map, subject to the general criteria to be discussed below. . . .

Given the magnitude of the network and the measurements to be made, a schematic network layout can be devised, subject to several general criteria. First, if we are to model the influence of emissions from an urban area on air quality, we should know what the concentrations are in the air approaching the area, i.e., at least one station should be in an upwind sector regardless of the wind direction. Since upwind-downwind comparisons can be made of air quality as well as radiation parameters, each upwind site should have a downwind conterpart. This criterion can be met by having four rural sites at approximately 90° azimuth spacing, with the alignments along the most frequent wind directions, namely, west-northwest to east-southeast, and south to north.

The second general criterion is that the site spacing should depend on both concentrations and their spatial gradients, with the minimum spacing where the concentrations and gradients are highest. . . . Calculations of annual SO_2 and particulate patterns indicate the highest concentrations and gradients occur generally within about 10 km of the Arch, and, therefore, for these pollutants the network should be concentrated within this area. For primary pollutants from mobile sources, the patterns should more closely resemble patterns of vehicle emissions with a maximum in the downtown area, but generally more spread out than the calculated SO_2 and particulate patterns. Secondary mobile source pollutants should show more seasonal influence, since the higher solar intensities and air temperatures in summer will aid in their formation. We guess at this time that the maximum of O_3 will probably occur beyond

> the most distant sites, since it takes a number of hours for the O_3 maximum to develop. There should be occasions when the NO_2 maximum occurs within the bounds of the network, and, considering the summer wind patterns, should most frequently be found.
>
> Taking these various factors into account, a general station siting plan consisting of a central station surrounded by loosely arrayed rings of stations at increasing radial spacings appears to be a suitable arrangement. . . . The center of this array should be somewhat north of the downtown area of St. Louis, with the closest spacing of sites being about 4 km. The spacing should increase to 10 to 15 km at the outermost sites, excluding the four rural sites. . . . The general locations of these sites are shown by Figure [9].

An air monitoring network employed by the Tennessee Valley Authority (TVA) for evaluating the maximum SO_2 concentration occurring downwind of the Paradise Steam Plant has been described by Montogomery, et al. (19). This network employed 14 digital recording SO_2 instruments located within the 22-1/2 degree prevailing downwind sector within 17 km of the plant. Instruments were located on radial arcs, with the largest number in the expected area of maximum ground level SO_2 concentrations (i.e., within 4 and 5 km). There were also several other SO_2 instruments located in the peripheral areas around the steam plant. (See Figure 10.) This monitoring network was used to determine the types of meteorological conditions which produced the highest ground level SO_2 concentrations and the distances downwind of the plant where they occurred.

Regarding the number of stations required by a network, rules and regulations published by EPA in August 1971, in the Federal Register (20), state implementation plans must include provisions for surveillance of ambient air quality. These surveillance requirements include the minimum number of stations required to monitor criteria pollutants as a function of the region population. These minimum requirements are reproduced in Table III. Additional general criteria on the number of stations

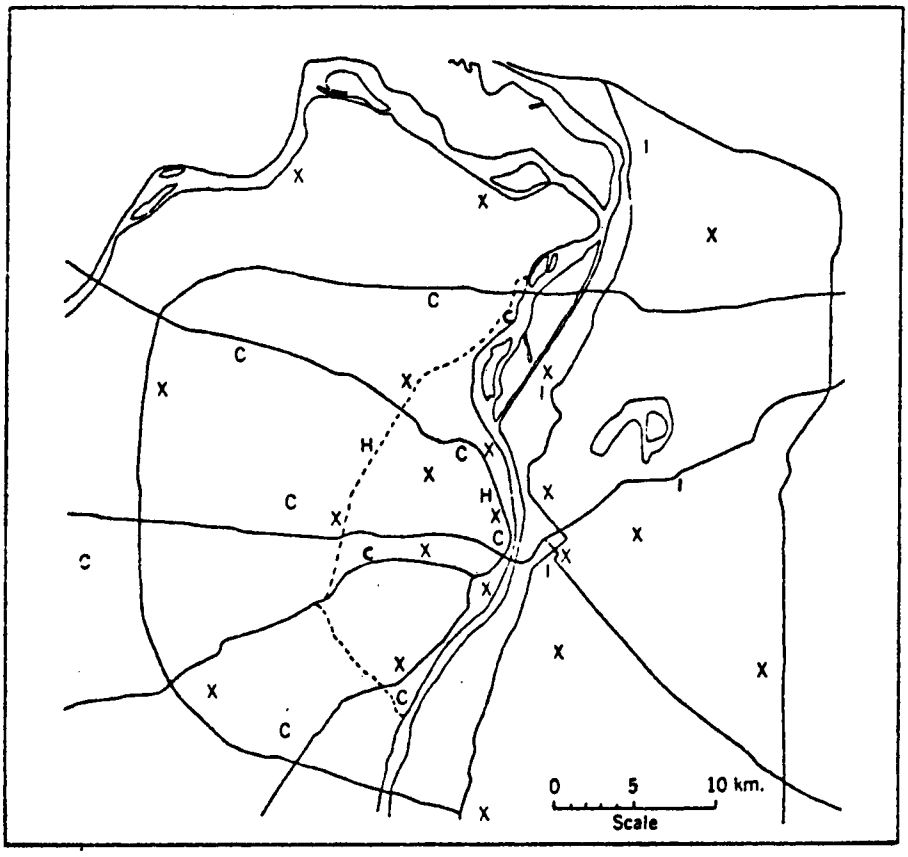

Figure 9. Proposed siting plan for the St. Louis Regional Air Measurement Network. Sites in existing networks indicated by letters: C, St. Louis City-County; H, CHESS; I, III, EPA. Crosses indicate the general locations of proposed sites. Four rural sites at distances of about 40 km from center of the network not shown.

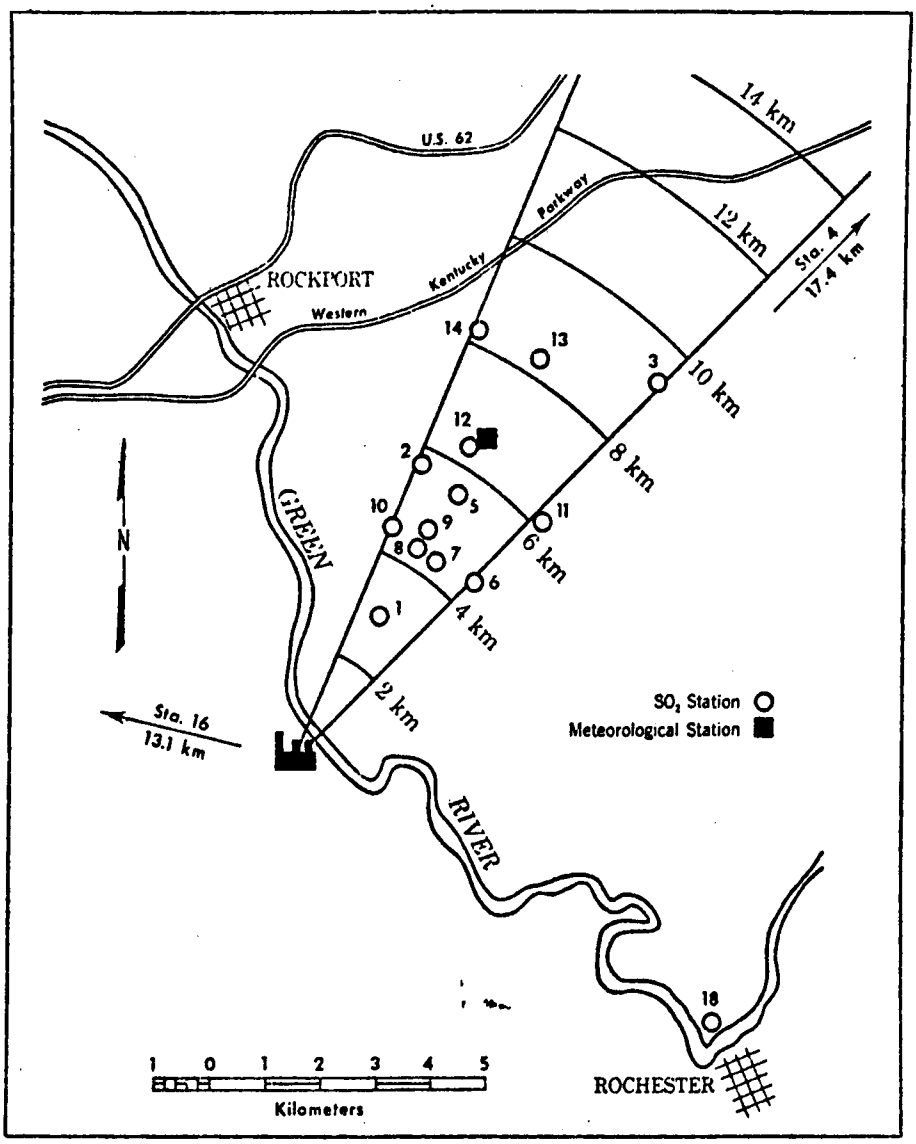

Figure 10. Paradise Steam Plant Air Monitoring Network.

TABLE III

Air Quality Surveillance System Requirements (Ref. 20)

Classification of region	Pollutant	Measurement method	Minimum frequency of sampling	Region population	Minimum number of air quality monitoring sites[h]
I	Suspended particulates	High volume sampler	One 24-hour sample every 6 days[a]	Less than 100,000	4.
				100,000–1,000,000	4+0.6 per 100,000 population.[c]
				1,000,001–5,000,000	7.5+0.25 per 100,000 population.
				Above 5,000,000	12+0.16 per 100,000 population.[c]
		Tape sampler	One sample every 2 hours		One per 250,000 population. up to eight sites.
	Sulfur dioxide	Pararosaniline or equivalent[d]	One 24-hour sample every 6 days (gas bubbler).[a]	Less than 100,000	3.
				100,000–1,000,000	2.5+0.5 per 100,000 population.[c]
				1,000,001–5,000,000	5+0.15 per 100,000 population.[c]
				Above 5,000,000	11+0.05 per 100,000 population.[c]
			Continuous	Less than 100,000	1.
				100,000–5,000,000	1+0.15 per 100,000 population.[c]
				Above 5,000,000	6+0.05 per 100,000 population.[c]
	Carbon monoxide	Nondispersive infrared or equivalent.[e]	Continuous	Less than 100,000	1.
				100,000–5,000,000	1+1.15 per 100,000 population.[c]
				Above 5,000,000	6+0.05 per 100,000 population.[c]
	Photochemical oxidants	Gas phase chemiluminescence or equivalent.[f]	Continuous	Less than 100,000	1.
				100,000–5,000,000	1+0.15 per 100,000 population.[c]
				Above 5,000,000	6+0.05 per 100,000 population.[c]
	Nitrogen dioxide	24-hour sampling method (Jacobs-Hochheiser method).	One 24-hour sample every 14 days (gas bubbler).[b]	Less than 100,000	3.
				100,000–1,000,000	4+0.6 per 100,000 population.[c]
				Above 1,000,000	10.
II	Suspended particulates	High volume sampler	One 24-hour sample every 6 days		3.
		Tape sampler	One sample every 2 hours		1.
	Sulfur dioxide	Pararosaniline or equivalent[d]	One 24-hour sample every 6 days (gas bubbler).[a]		3.
			Continuous		1.
III[g]	Suspended particulates	High volume sampler	One 24-hour sample every 6 days[a]		1.
	Sulfur dioxide	Pararosaniline or equivalent[d]	One 24-hour sample every 6 days (gas bubbler).[a]		1.

[a] Equivalent to 61 random samples per year.
[b] Equivalent to 26 random samples per year.
[c] Total population of a region. When required number of samplers includes a fraction, round-off to nearest whole number.
[d] Equivalent methods are (1) Gas Chromatographic Separation—Flame Photometric Detection (provided Teflon is used throughout the instrument system in parts exposed to the air stream), (2) Flame Photometric Detection (provided interfering sulfur compounds present in significant quantities are removed), (3) Coulometric Detection (provided oxidizing and reducing interferences such as O_2, NO_2, and H_2S are removed), and (4) the automated Pararosaniline Procedure.
[e] Equivalent method is Gas Chromatographic Separation—Catalytic Conversion—Flame Ionization Detection.
[f] Equivalent methods are (1) Potassium Iodide Colorimetric Detection (provided a correction is made for SO_2 and NO_2), (2) UV Photometric Detection of Ozone (provided compensation is made for interfering substances), and (3) Chemiluminescence Methods differing from that of the reference method.
[g] It is assumed that the Federal motor vehicle emission standards will achieve and maintain the national standards for carbon monoxide, nitrogen dioxide, and photochemical oxidants; therefore, no monitoring sites are required for these pollutants.
[h] In interstate regions, the number of sites required should be prorated to each State on a population basis.
[i] All measurement methods, except the Tape Sampler method, are described in the national primary and secondary ambient air quality standards published in the FEDERAL REGISTER on Apr. 30, 1971 (36 F.R. 8186). Other methods together with those specified under footnotes (d), (e), and (f) will be considered equivalent if they meet the following performance specifications:

required are available through EPA (13). Some authors have even addressed the problem of optimizing the number of stations required applying principles of operations research (21,22). These methods, while showing promise, are still in the early stages of development.

Evaluation of Meteorological Data

Introduction

Historical meteorological data, primarily measurements of wind speed and direction, are very useful in analyzing the typical and worst case conditions affecting air pollution transport and dispersion. Historical wind speed and direction data can be used to determine where air pollutants are likely to be transported, how these conditions change with time, and the frequency of occurrence of adverse dispersion conditions (i.e., low wind speeds and stable atmospheric conditions) within a study area. A summary of when and where air pollution concentrations are expected to be high is an important input to the design of an air monitoring survey.

In most cases, meteorological data will be used to perform either one, or both, of two different levels of analysis: (1) a mesoscale meteorological analysis (i.e., an evaluation of the area wide air movements that affect background air pollution levels within a study area), and (2) a microscale meteorological analysis (i.e., an evaluation of local air movements, especially ground level air movements that affect the dispersion of air pollutants near a proposed monitoring site).

Mesoscale Meteorological Analysis

A thorough mesoscale meteorological data analysis will include an evaluation of (3,4):

- prevailing surface wind patterns throughout the study area for different seasons of the year,
- when, how often, and for what duration low wind speeds and stable atmospheric conditions occur,
- meteorological conditions which transport air pollutants into the study area, resulting in high background air pollution concentrations,
- meteorological conditions which transport air pollutants generated by the proposed project away from the study area,
- the effects of large scale terrain features on the area wide movement of air, and
- possible sites where additional meteorological data may be needed and where mesoscale air quality measurements should be made.

In order to evaluate each of these things, area wide sources of air pollution and important terrain features, as well as the mesoscale meteorology of the study area must be identified. Most of a mesoscale meteorological analysis is probably best performed using a map large enough to show the study area plus the surrounding topographic and land use features. In most cases, the map should include at least 100 sq. kilometers of surrounding land area. Raised relief maps are especially useful in identifying significant mesoscale terrain features. Beaton, Ranzieri, and Skog (23) recommend the use of a topographic map to identify the following conditions:

- channeling effects of winds in canyons and valleys,
- areas of drainage winds,
- general wind flow around hills and mountains for different inversion bases,

- areas where a surface inversion may exist due to cool air drainage, and
- areas of limited dispersion due to valley walls.

Existing and future major point, line, and area sources of air pollution emissions should be included on the map. Since high local background concentrations usually occur downwind of major pollution sources, the map can be used to determine the direction from which the wind would transport air pollution into the study area. Adverse conditions for transporting pollutants out of the study area can also be identified. Historical meteorological data can be evaluated to determine the frequency of occurrence of winds from these directions, the wind speed, and what seasons of the year and times of day adverse conditions usually occur. An air pollution transport analysis of this type should begin with the largest and closest air pollution source and continue until all major sources are evaluated. For a comprehensive analysis, sophisticated mathematical models may be used (24,25).

A basic six step methodology is recommended by Noll and Miller (3) for performing a mesoscale analysis on historical meteorological data. This methodology, outlined in Figure 11, consists of the following steps:

1. Collect all available information including historical meteorological data, topographic data, demographic data, present and future land use data, present and future transportation plans, and available air pollution source emission inventory data.
2. Display as much of this information as possible on a topographic map; especially major transportation routes, major point sources of air pollution, land use characteristics, and terrain features.
3. Prepare wind rose from historical meteorological data and plot on the map. (Plot at the location of meteorological station when possible.)

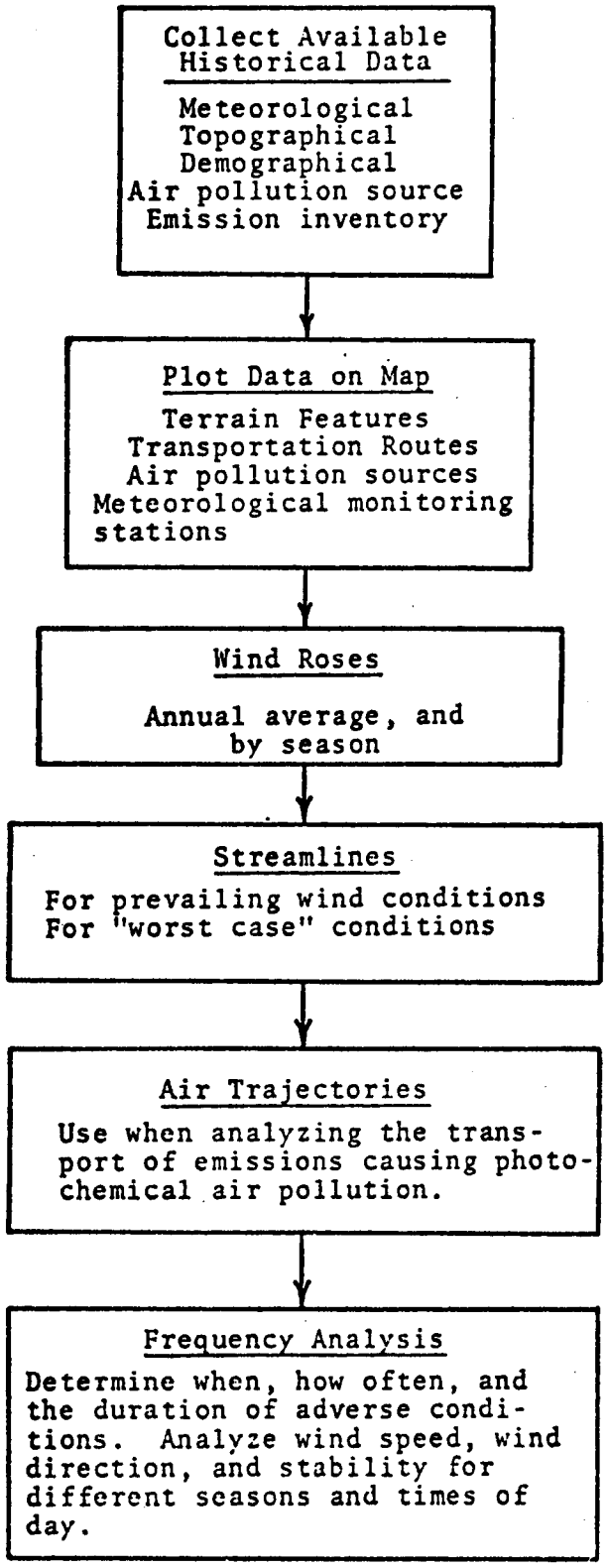

Figure 11. Analyzing Historical Meteorological Data for a Mesoscale Study.

4. Determine probable wind flow streamlines for the most probable and "worst case" wind directions. Plot streamlines for different wind conditions on transparent map overlays.

5. Determine air trajectories which transport air pollutants into and out of the study area. (Air trajectories are most applicable for determining the potential for high concentrations of photochemical pollutants). Plot air trajectories for different conditions on transparent map overlays.

6. Once adverse meteorological conditions for the transport of air pollutants either into or out of the study area have been identified, then a frequency analysis should be performed on the historical meteorological data to determine when (season and time of day), how often, and for what durations adverse conditions occur. The frequency analysis should include the occurrence of various wind speeds, wind directions, and atmospheric stabilities, for different seasons of the year and times of the day.

Method of Analyzing Historical Meteorological Data

Methods of analyzing historical meteorological data for the purposes mentioned above include wind roses, streamlines, air trajectories, and frequency analysis. Wind roses are commonly used to display historical data from a single measuring station by illustrating the frequency of occurrence of winds from each of 16 wind directions. Sometimes, the frequency of occurrence of various wind speed ranges is also illustrated. (See Figure 12.) Streamlines, which are especially applicable when terrain features influence the general flow of air, are frequently used to illustrate both microscale and mesoscale air flow patterns under various prevailing meteorological conditions. Streamlines are especially useful for illustrating the mesoscale effects of channeling or different types of drainage and valley winds. (See Figure 13.) Air trajectories, which are used to evaluate the area wide movement of a single "air parcel" as it is transported under changing conditions of wind speed

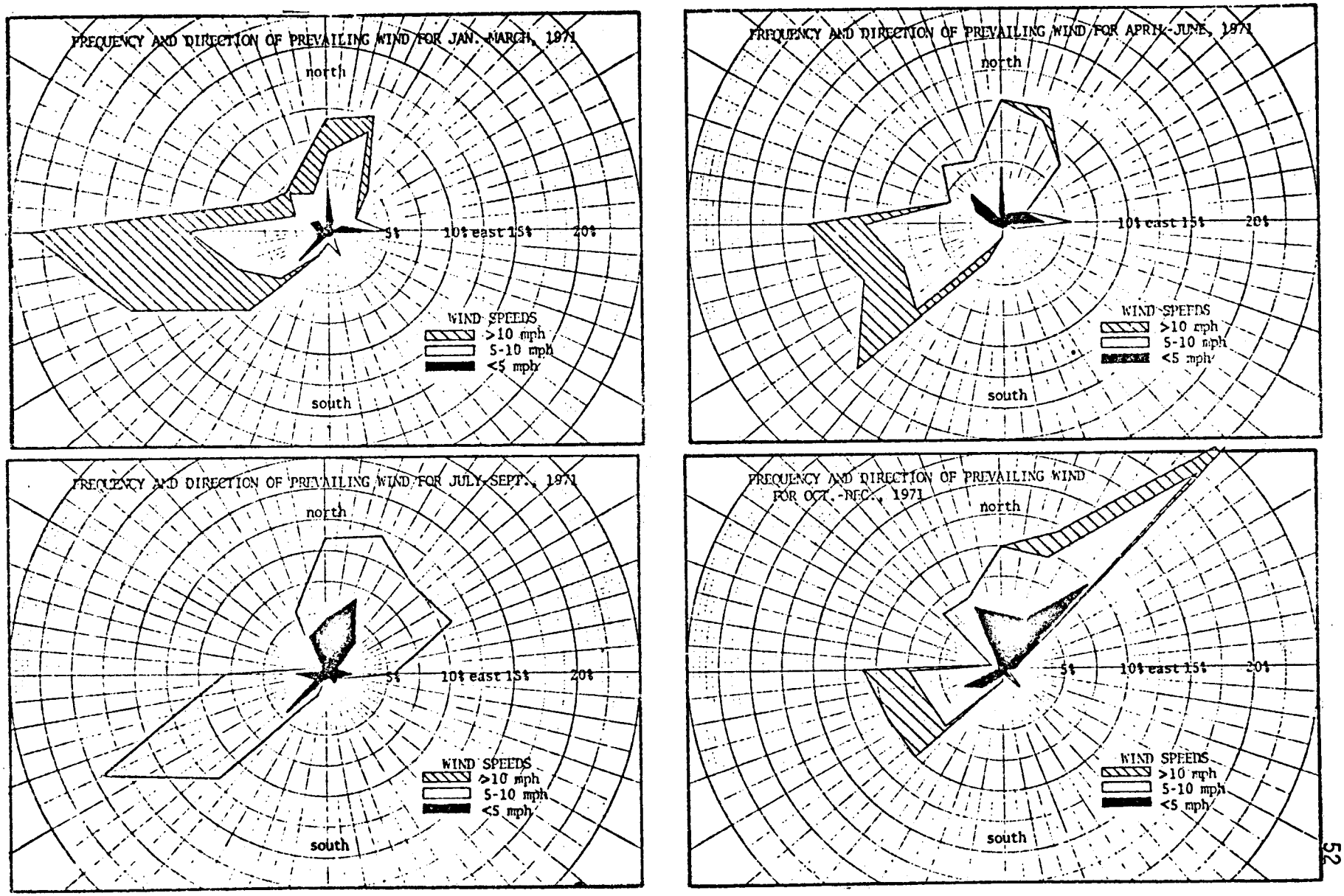

Figure 12. Seasonal Wind Roses (26).

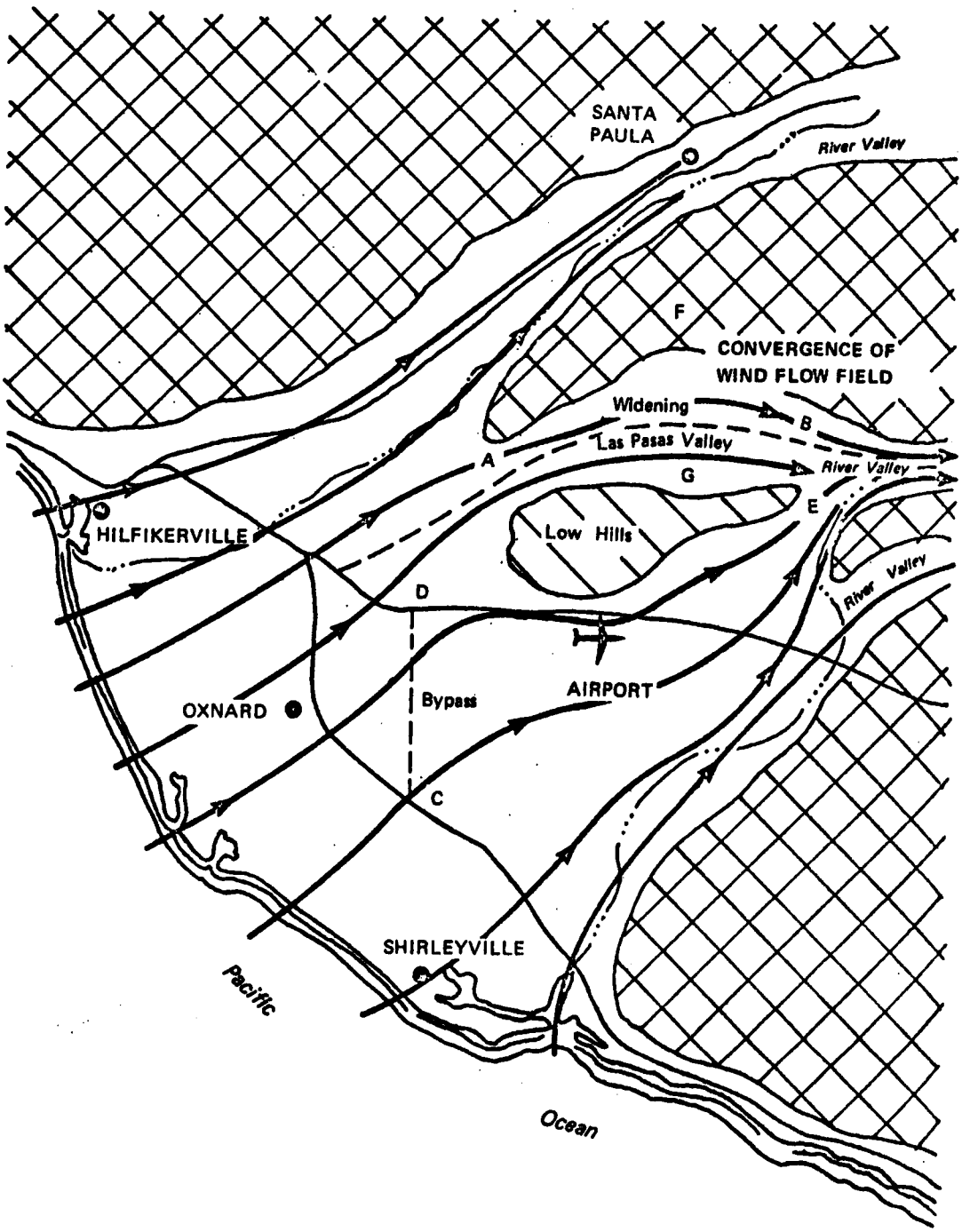

Figure 13. Example of a Mesoscale Streamline Analysis. (From Beaton (23).)

and direction, are most applicable for "back-tracking" air pollutants from a final location and time to their original location. (See Figure 14.) Air trajectories are less applicable to microscale analysis than to mesoscale analysis.

A frequency analysis is performed in order to determine when and how often meteorological conditions occur which are adverse to the transport and dispersion of air pollutants. A comprehensive evaluation includes an analysis of wind speed, wind direction, atmospheric stability, time of day, and season of year. A frequency analysis of mixing depths can also be performed when historical data are available. Using a tabular presentation of the results from a comprehensive frequency analysis (See Table IV), the frequency of occurrence of adverse meteorological conditions can be determined for each hour of day and season of the year.

Microscale Meteorological Analysis

The objective of the microscale evaluation is to study how the microscale terrain configuration influences the movement of air and to determine how air pollutants might be transported in the immediate vicinity of a proposed monitoring station.

A microscale meteorological analysis is probably best performed using a map including nearby sources, streets, points of intersection of existing streets, land use characteristics adjacent to the monitoring station, nearby sensitive receptors, and microscale terrain features (hills, trees, buildings, etc.). The map should be of a large enough scale to identify these microscale terrain features. A microscale meteorological analysis can then be performed to attempt to identify

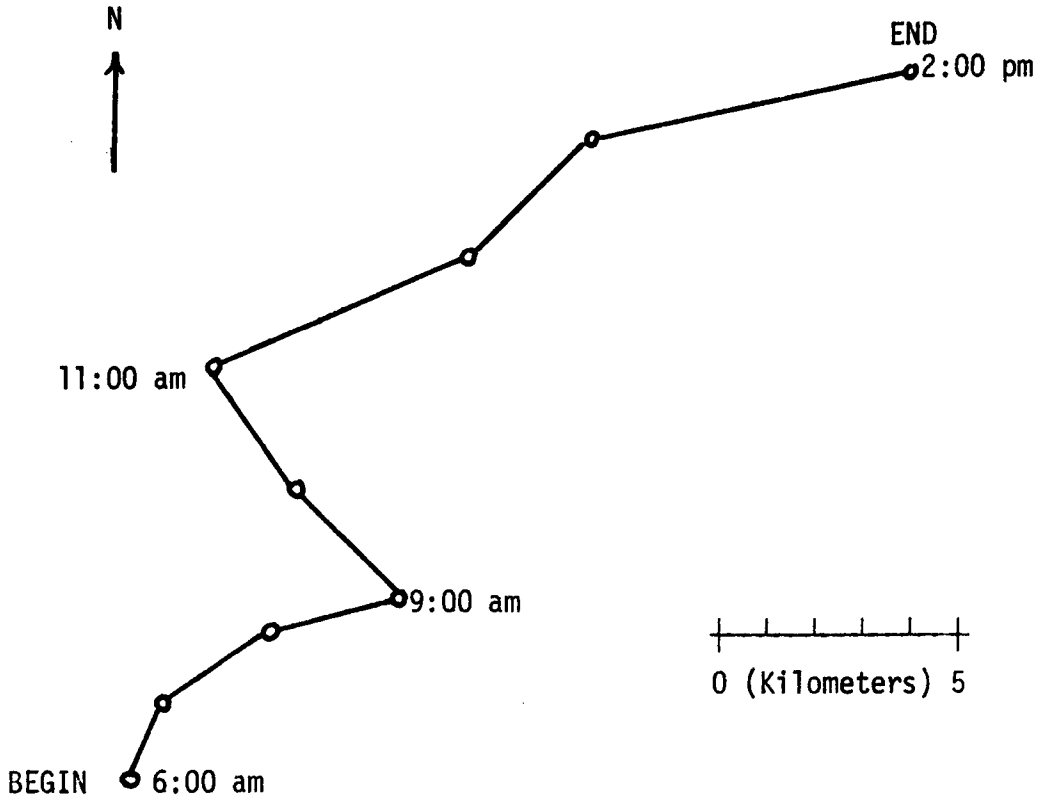

Figure 14. Example of an Air Trajectory Generated from Eight Hourly Observations of Wind Speed and Direction.

TABLE IV

Meteorological Frequency Table.
(by season, wind direction, wind speed, stability, and time of day)
Compiled from Five Years Record.

Station		Airport																	
Season		January, February, March																	
Wind Dir.		Northwest																	
Wind Speed		<2 m/s					2-3.5 m/s						4-6 m/s				>6 m/s		
Stability		A	B	D	E	F	A	B	C	D	E	F	B	C	D	E	C	D	TOTAL
TIME	1:00			.01	.04	.06					.03	.07							.21
	2:00			.01	.04	.06					.03	.07				.01			.22
	3:00			.01	.06	.07					.05	.08				.03			.30
	4:00			.02	.05	.10					.07	.05				.04			.33
	5:00			.03	.04	.12				.01	.08	.04			.03	.08			.43
	6:00			.01	.05	.15				.01	.12	.02			.02	.07			.45
	7:00			.02	.05	.08				.02	.10	.08			.03	.04		.04	.46
	8:00			.04	.04					.05	.04	.04			.03	.02		.15	.41
	9:00			.08					.02	.06					.05			.20	.41
	10:00			.08					.04	.08				.03	.06			.18	.47
	11:00		.04	.06				.06	.04	.05			.02	.03	.03		.15	.11	.59
	12:00		.05	.01				.06	.06	.02			.01	.03	.02		.08	.05	.39
	13:00	.21	.08				.10	.08	.04	.03			.02	.04	.02		.20		.82
	14:00	.25	.08				.10	.17	.08	.03			.02	.05	.03		.22		1.03
	15:00	.30	.10	.03			.08	.12	.12	.02			.01	.03	.02		.10	.05	.98
	16:00	.15	.09	.06			.12	.08	.05	.01			.02	.06	.02		.18	.06	.91
	17:00		.06	.07				.06	.04	.04			.01	.03	.02		.05	.16	.54
	18:00			.05					.04	.05				.03	.06		.02	.15	.40
	19:00			.01					.01	.08					.06			.10	.26
	20:00			.01					.01	.03	.03				.03			.13	.24
	21:00			.01						.03	.05				.02			.07	.18
	22:00									.02	.04	.04			.03			.05	.18
	23:00		.01	.00						.01	.03	.02			.02				.09
	24:00		.02	.03						.03	.03	.09							.20

TABLE IV (continued)

Station	Airport																	
Season	January, February, March																	
Wind Dir.	Northwest																	
Wind Speed	<2 m/s					2-3.5 m/s						4-6 m/s				>6 m/s		
Stability	A	B	D	E	F	A	B	C	D	E	F	B	C	D	E	C	D	TOTAL
TOTAL Stability	.91	.50	.62	.40	.67	.40	.67	.55	.68	.70	.60	.11	.30	.60	.29	1.0	1.5	
TOTAL Wind Speed	3.1							3.6					1.3			2.5		
TOTAL Wind Dir.	10.5%																	

potential problem areas for the transport and dispersion of air pollutants near the monitoring station.

A thorough microscale meteorological data analysis will include an evaluation of (3):

- the effects of local terrain features and highway design configuration in disrupting the flow of air near the station,
- sensitive receptors located near the station,
- when, how often, and for what duration low wind speeds and stable atmospheric conditions occur, and
- some determination of the representativeness of meteorological data collected at the site compared to area wide air movements.

Available Sources of Meteorological Data

Meteorological measurements of wind speed, wind direction, temperature, humidity, barometric pressure, ceiling height, visibility, precipitation, and some other parameters are recorded routinely each hour at over 300 NOAA Class A weather stations, military bases, and navy vessels, and disseminated by teletype for weather forecasting. In addition to being used for forecasting purposes, the raw data are permanently stored and made available by NOAA on request. This data can be obtained directly from the weather station taking the measurements or through the National Weather Records Center, Asheville, North Carolina. Raw data are available in log form, punch cards, magnetic tape, and, in some cases, as analog traces. Sometimes, only climatological summaries are needed. Several standard climatological summaries prepared by NOAA are available on request from the National Weather Records Center. A publication entitled Selective Guide to Climatic Data Sources (27) is an invaluable source of data summary information.

Applicable Sampling Statistics

Determine How Many Samples are Needed

Statistical methods for determining the number of samples needed to accurately define the mean and maximum pollution concentrations occurring during a year have been presented in the literature by several authors (28,29,30). In general, these methods assume that the samples collected are representative of the total population, which is either normally or lognormally distributed, and that each sample is chosen randomly.

Sample Sizes and Confidence Intervals for the Mean

Saltzman (30) assumes that the population to be sampled is infinite and applies the statistical t_{n-1} distribution to determine the confidence intervals of the mean.

$$\text{Confidence Interval} = \bar{X} \pm t_{n-1}\, S/n \qquad (1)$$

where

$\bar{X}$ = mean value of the samples,

S = standard deviation of the samples,

n = number of samples, and

t_{n-1} = a tabulated statistic for various confidence coefficients and degrees of freedom.

For more than 150 samples, t_{n-1} has a value close to that of the normal distribution statistic, ($z = 1.96$ for the 95% confidence interval, and 2.576 for 99%). In order to eliminate the use of tables, Saltzman has presented nomographic solutions to the above equation.

The nomograph illustrated in Figure 15 permits simple application to lognormal as well as normal populations.

Example: The standard geometric deviation of a lognormal distribution is 1.5. How many samples should be collected to establish the geometric mean within $\pm$ 5 percent with 95 percent confidence? How many for 99 percent confidence? Answer: Draw a straight line through 1.05 on the left side of the left scale and 1.5 on the left side of the center scale. The intersections on the two right scales are 250 and 440, signifying that if groups of 250 samples are collected, the geometric mean of 95 percent of the groups would be within the interval of the true geometric mean multiplied or divided by 1.05. Also, if groups of 440 samples are collected, the same agreement would be obtained for 99 percent of the groups (30).

Figure 15 can be applied simply and conveniently to determine the number of samples required for any desired degree of accuracy in the mean or in the geometric mean. Conversely the confidence intervals of the mean from a group of samples already collected may be determined.

Sample Sizes and Confidence Intervals for Extremes

Another important problem is the design of a sampling program to determine conformity with a specified air quality standard. For a given proportion, p, in the population exceeding a specified concentration, the probability of finding c or fewer samples exceeding the same concentration in a total number n of samples is given by:

$$\text{Probability } (m \leq c) = \sum_{m=0}^{c} \frac{n!}{m!(n-m)!} p^m (1-p)^{n-m} \qquad (2)$$

m = number of positive samples, assumed to have all integral values from 0 to c.

This calculation can be performed using a second nomogram presented by Saltzman (30). (See Figure 16.)

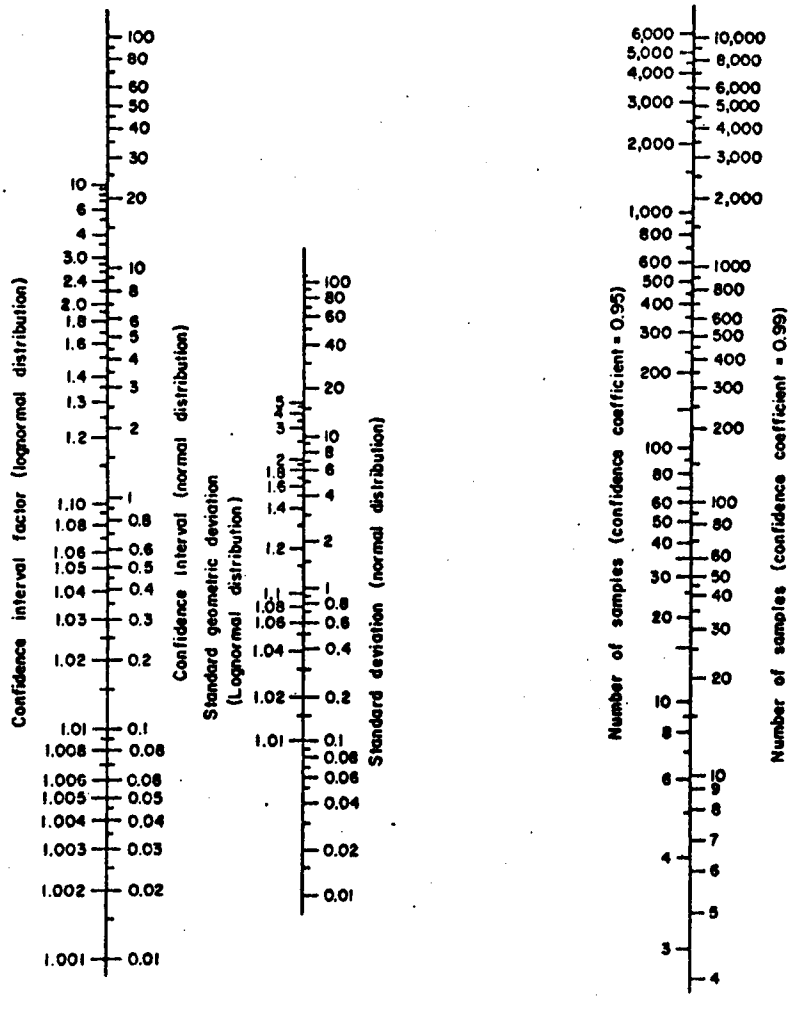

Figure 15. Confidence intervals for the mean of a group of random samples.

For a normal distribution, use numbers on right sides of center and left scales. A straight line connects related values of the confidence interval (above and below the mean), the standard deviation, and the number of samples (n) in the group for either 0.95 or 0.99 confidence coefficients (calculated from the t_{n-1} distributions). If desired, the numbers on both the standard deviation scale and on the confidence interval scale may be multiplied by the same factor (e.g., 0.1, 0.01, 0.001, etc.).

For a lognormal distribution, use numbers on left sides of center and left scale. A straight line connects related values of the confidence interval factor (with which to multiply or divide the geometric mean), the standard geometric deviation, and the same scales for number of samples in the group (30).

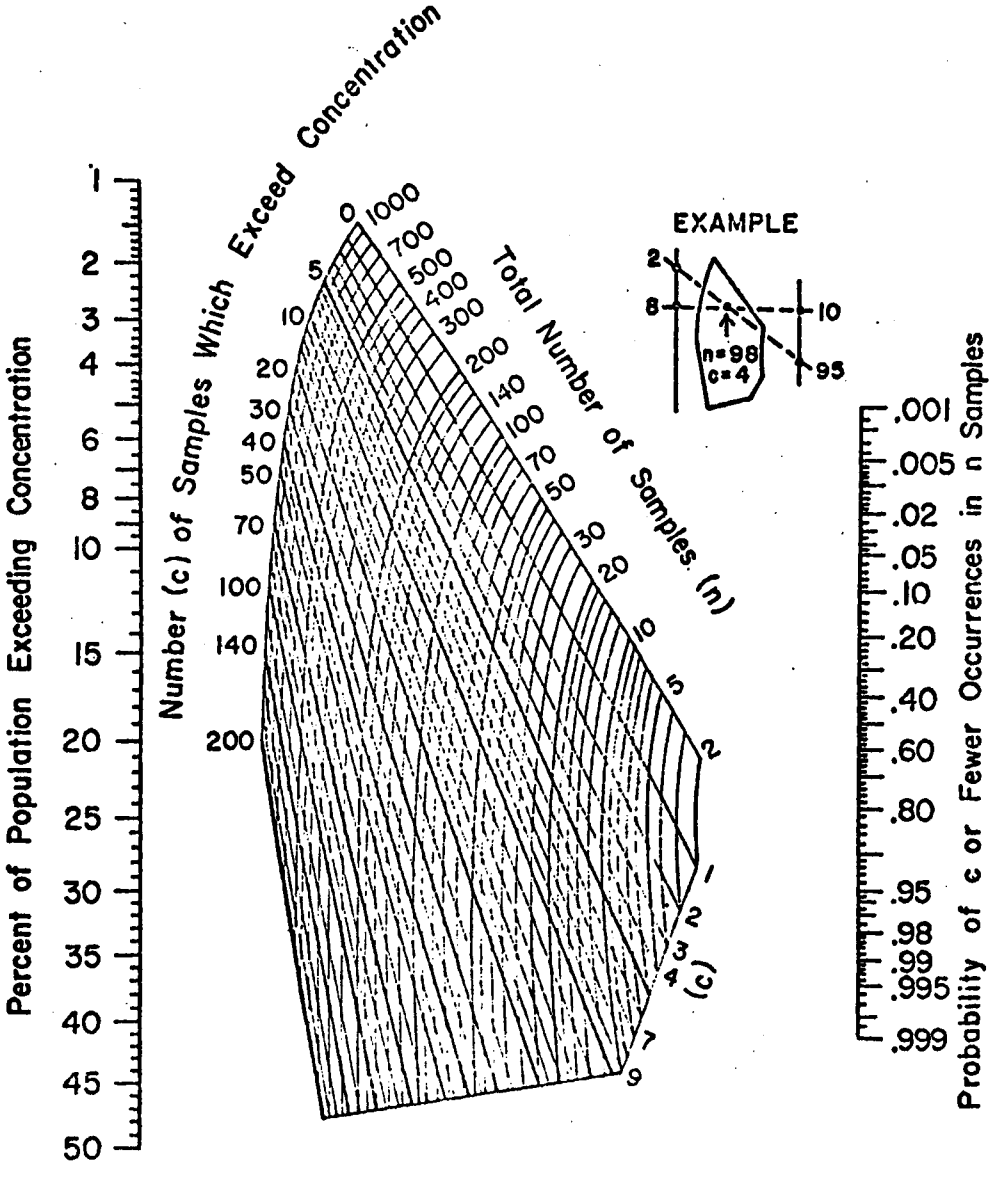

Figure 16. Design of a sampling program for quality control. Related variables are connected with a straight line. For proportions below 1%, divide numbers on left scale by a convenient integer (such as 19), and multiply numbers on n scale by the same integer. For proportions above 50%, the nomogram may be used by regarding the left scale and the c scale as representing the numbers of samples equal to or less than the critical concentration.

This chart also may be used to estimate the confidence intervals for proportions in the population by drawing lines through point [(c-1/2), n]; in this case the right scale represents probability that the true proportion is greater than the value intercepted on the left scale (30).

Example: Design a sampling program so that the probability of acceptance is >0.95 if actually < 2 percent of the population exceeds the critical value, but is <0.10 if actually > 8 percent do. Answer: (See illustration on the upper right of Figure 16). Draw a line connecting 2 percent on the left scale with 0.95 on the right scale and another one connecting 8 percent with 9.10. Their intersection in the center area gives values c = 4, n = 98. Thus, 98 samples should be collected and no more than four are allowed to exceed the critical concentrations.

It should be noted, however, that this calculation is based upon a random sampling program. If the peak values are known to occur at certain specified times, the procedure may be modified to collect most samples during those periods to provide greater assurance that such peaks are not occurring, or to determine the proportion with greater accuracy. For example, for peak oxidant sampling, the day may be divided into an eight hour period and a 16 hour period, such as 9 a.m. to 5 p.m. and 5 p.m. to 9 a.m. Only a few samples need be collected during the later period. Thus, considerable analytical work can be saved with almost no increase in confidence intervals. The proportions in each interval may be weighted by the length of the interval, and combined to give the proportion in the entire day (30).

Sampling from Finite Populations

The methods presented by Saltzman assume that samples are collected from an infinite population. Hale (28) has presented similar methods which assume that the population from which samples are taken is finite. In general, the number of samples required according to Hale's methods are less than for Saltzman's. For a lognormal distribution, the number of samples, n, required to determine tolerance and confidence interval given by Hale's equation is:

$$n = \frac{NZ^2 \ln^2 S_g}{N \ln^2(P+1) + Z^2 \ln^2 Sg} \quad (3)$$

where

N = population size (i.e., total number of possible samples)

Z = normal deviate corresponding to the upper percentage point for a specified level of confidence. For a 95% level Z = 1.96.

S_g = standard geometric deviation of samples

P = fraction of the geometric mean by which it can differ from the true geometric mean with specified probability.

Using this equation Figures 17 and 18 have been prepared. These figures can be used to determine the number of samples needed as a function of the standard geometric deviation and the size of the population being sampled. Figure 17 should be used to determine the geometric mean within $\pm$ 10% (at 95% confidence) and Figure 18 should be used for a $\pm$ 20% tolerance (at 95% confidence).

Atmospheric Diffusion Models

Nongaussian Atmospheric Diffusion Models

Box Model. About the simplest form of dispersion model is the "box" model sometimes used to estimate air pollution concentrations due to an area source. The "box" itself represents the three dimensional volume within which air pollutants are assumed to be thoroughly mixed. The box is usually defined as having unit width and oriented so that its length S lies in the direction of the mean wind, U. Pollutants are assumed to be emitted at a constant rate per unit time per unit area,

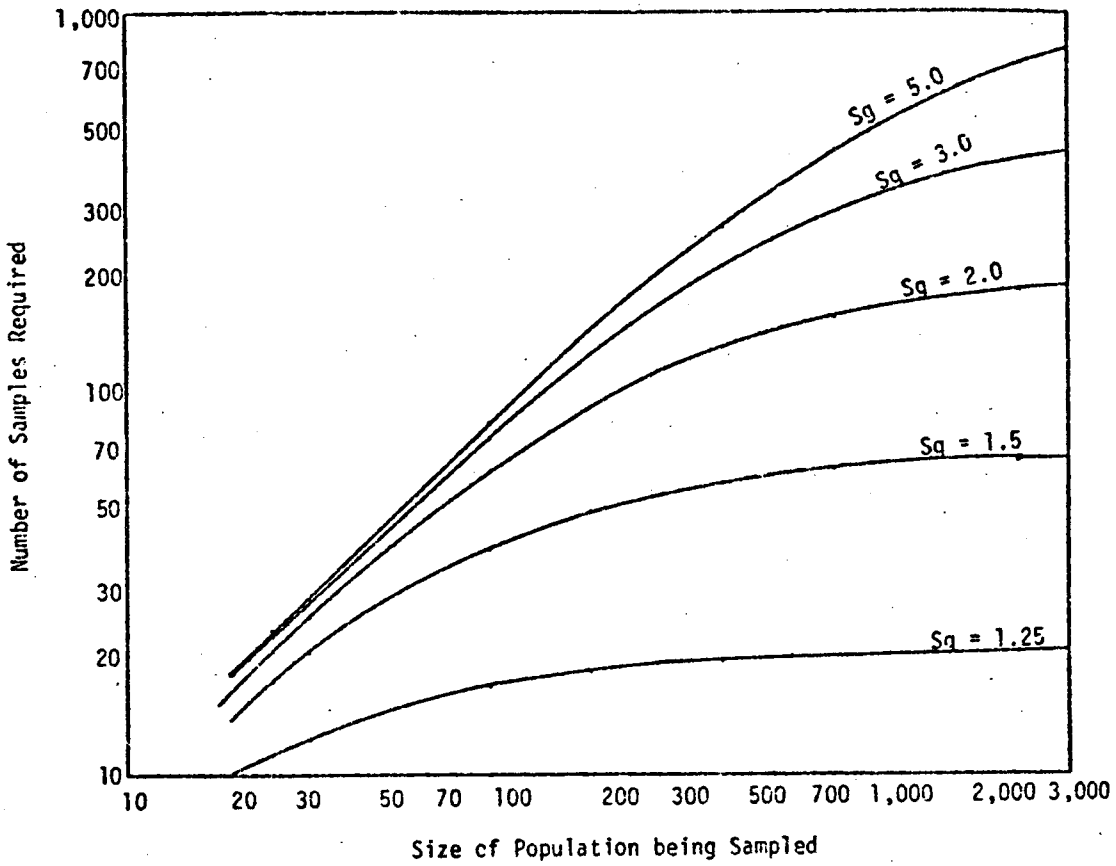

Figure 17. Number of Samples Required to Determine the Geometric Mean Within + 10 Percent with 95% Confidence for Various Population Sizes. (Z = 1.96 & P = 0.10.)

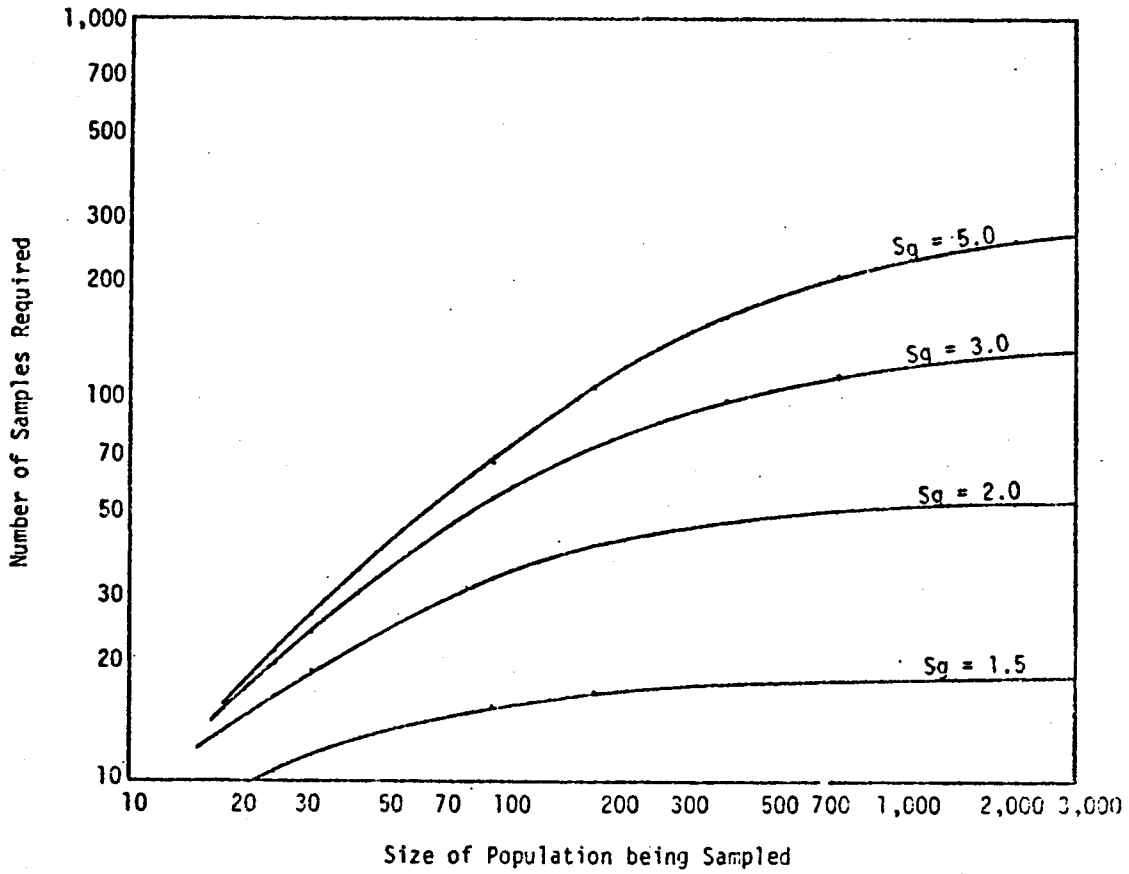

Figure 18. Number of Samples Required to Determine the Geometric Mean Within ± 20 Percent with 95% Confidence for Various Population Sizes. (Z = 1.96 & P = 0.20.)

$Q(gm/m^2\text{-sec})$. Z equals the height of the box, to which pollutants are dispersed. (See Figure 19.) QS is equal to the emission rate per unit width, which when divided by the ventilation rate, UZ, is equal to the equilibrium concentration, C_e, at a point S distant from the upwind edge of the area source.

$$C_e = \frac{QS}{UZ} \tag{4}$$

Box models can be used to obtain rough order-of-magnitude estimates of ambient pollution levels, however, the simplifying assumptions of the model (uniform mixing to a constant level, Z) lead to results which do not simulate true atmospheric conditions accurately (31). Special application of the box model is an elevated inversion above a point source in a valley. Then,

$$C = \frac{Q}{HWU} \tag{5}$$

where

W = the width of the valley, and

H = the mixing height.

K-Theory. Some atmospheric dispersion models have been developed which are theoretically based on diffusion theory. According to Fick's law, the rate of diffusion of a substance in solution (i.e., a pollutant in air), q, from a high concentration to a lower concentration is proportional to the concentration gradient: (in the X-direction)

$$\frac{dq}{dt} = K \frac{\partial^2 q}{\partial x^2} \tag{6}$$

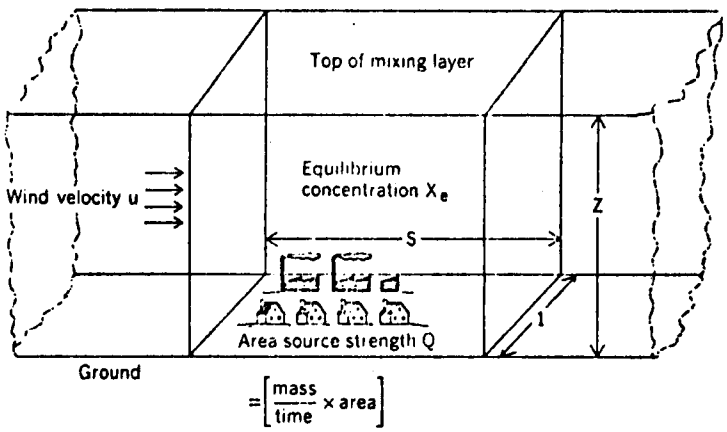

Figure 19. Area-Source "Box" Diffusion Model (31).

where K is constant and equal to the diffusivity or diffusion coefficient (32). For atmospheric diffusion the equation may be written for three dimensions:

$$\frac{dq}{dt} = \frac{\partial}{\partial x}\left(K_x \frac{\partial q}{\partial x}\right) + \frac{\partial}{\partial y}\left(K_y \frac{\partial q}{\partial y}\right) + \frac{\partial}{\partial z}\left(K_z \frac{\partial q}{\partial z}\right) \qquad (7)$$

K values are assumed to be determined solely by atmospheric properties such that the rates of diffusion of heat, K_h, turbulent momentum, K_m, and pollutants K_p in the atmosphere are related. According to Hanna (33), during adiabatic conditions $K_h \simeq K_m \simeq K_p$. During unstable conditions $K_p \simeq 3K_m$.

The most satisfactory application of K-theory has been to the case of crosswind dispersion from an infinite continuous line source. For a mean wind $\bar{u}$ on the X-axis, it is a reasonable assumption that:

$$\bar{u} \frac{\partial q}{\partial x} >> \frac{\partial}{\partial x}\left(K_x \frac{\partial q}{\partial x}\right); \qquad (8)$$

for which a solution has been given by Somers (33).

$$\frac{q}{Q} \simeq \frac{1}{(2\pi K_z \times \bar{u})^{1/2}} \exp\left(-\frac{\bar{u} z^2}{4K_z x}\right). \qquad (9)$$

According to Hanna (33), K_z can be calculated as a function of the friction wind speed, u_*, and height, Z

$$K_z = .4\, u_* Z \qquad 0 < Z < 100m \qquad (10)$$

$$K_z = (40m)(u_*) \qquad 100m < Z < 100m \qquad (11)$$

In practice K values are seldom determined from heat flux or turbulence flux measurements due to the difficulty of making these measurements. Rather, they are determined empirically from observed pollutant diffusion data. Also, the assumption that pollutant diffusion is Fickian (constant K) cannot be valid because of the known variations of mean wind shear and heat flux with time and space. Hence, though the basic equations are founded in diffusion theory, K-theory is at best semi-empirical. According to Bibbero (31), K-theory is "useful in practice but not in principle."

Gaussian Plume Models

Point sources. The most widely employed method of modeling air pollution dispersion is the use of Gaussian plume equations. These equations can be derived from a simple dimensional analysis plus the basic Gaussian distribution function. Air pollutants emitted at a constant rate, Q(gm/sec), from a smoke-stack are commonly referred to as a "point source" where pollutants are released into the atmosphere at a "point" in space located at the top of the stack. The material is then transported by the wind away from the source at a rate equal to the wind speed, U(m/sec), at the point of release. Hence, the pollutants are distributed in the downwind direction, X, with a mass density equal to $\frac{Q}{U}$ (gm/m). (See Figure 20.) Thus, for a conservative pollutant (no chemical reactions or fallout), the mass of pollutant contained in any volume of the plume with incremental length, ΔX, is equal at all distances downwind. However, the concentration C(gm/m^3) within the plume decreases with increasing distance downwind because atmospheric turbulence tends to disperse the material in the horizontal (y-direction)

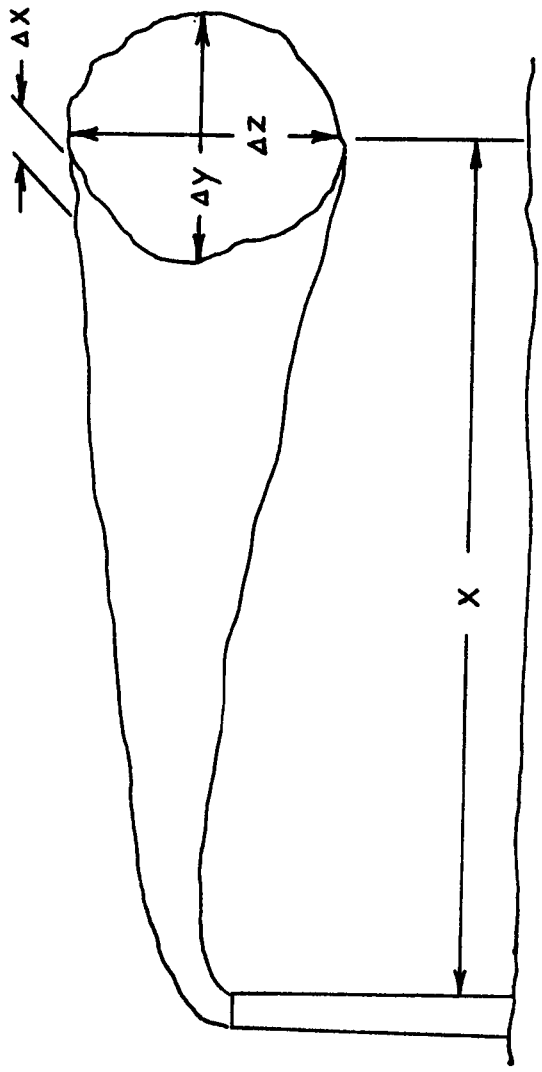

Figure 20. Dispersion of the Plume from a Point Source. (X = downwind distance, Δx = incremental distance, Δy = plume width, and Δz = plume height.)

and vertical (Z-direction) such that the plume "spreads" about its centerline. The average concentration of pollutant within the plume at a point, X, downwind is then inversely proportional to the amount of spreading of the plume (Δz and Δy) and the transport wind speed, U:

$$C \propto \frac{Q}{U\ \Delta z\ \Delta y} \tag{12}$$

From observations it has been found that the concentration within the plume is not uniform, but highest near the center and decreasing toward the outer edges of the plume. Both experimental results and theory (6) indicate that the concentration profile within a plume follows a "bell shaped" normal or Gaussian distribution curve (See Figure 21) where the peak of the curve (the population mean) describes C near the plume centerline and a point $\pm$ 3 standard deviations from the mean approximates the outer edge of the plume. The Gaussian distribution function for an x mean equal to zero, and standard deviation, σ is:

$$Y = \frac{1}{\sigma(2\pi)^{1/2}} \exp\left(-\frac{x^2}{2\sigma^2}\right) \tag{13}$$

In practice, σ equals the distance from the plume centerline to where the concentration is 0.6066 of the centerline concentration. The Gaussian function for both the Y and Z directions can then be used to replace $\Delta y = \sigma_y(2\pi)^{1/2}$ and $\Delta z = \sigma_z(2\pi)^{1/2}$, yielding,

$$C = \frac{Q}{2\pi\ U\ \sigma_y\ \sigma_y} \exp -\frac{1}{2}\left[\left(\frac{y}{\sigma_y}\right)^2 + \left(\frac{z}{\sigma_z}\right)^2\right] \tag{14}$$

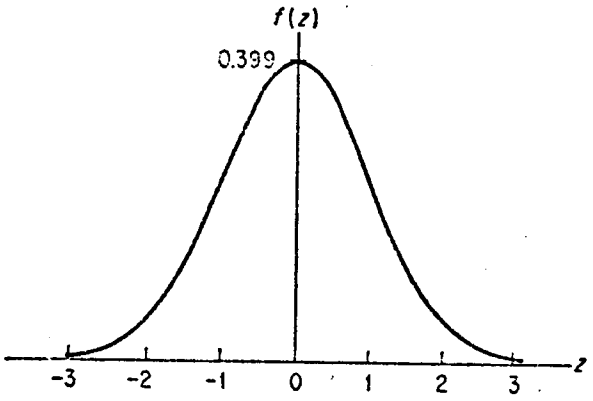

Figure 21. Standard Normal Curve.

where y and z equal the distance from the plume centerline. The most common convention is to use the coordinate system illustrated in Figure 22 such that Equation (14) is written:

$$C(x,y,z,H) = \frac{Q}{2\pi U \sigma_y \sigma_z} \exp -\frac{1}{2}\left[\left(\frac{y}{\sigma_y}\right)^2 + \left(\frac{H_e - Z}{\sigma_z}\right)^2 \right] \qquad (15)$$

Where H_e = the effective stack height. Further, beyond the point, x, where the plume first touches the ground the plume is assumed to be "reflected" because the earth's surface is a barrier to further dispersion. If the pollutant is not deposited or absorbed, then ground-level concentrations downwind of the touchdown point are underestimated by Equation (15). To account for "reflection" of the plume a mirror image source is assumed to exist, located symmetrically (with respect to the ground) to the actual source. (See Figure 23.) The final form of the Gaussian plume equation for a continuous point source is then,

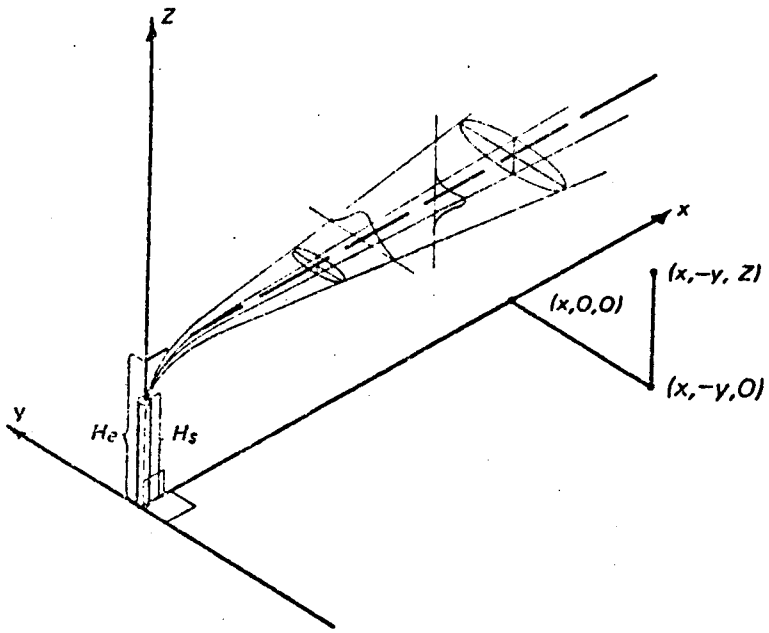

Figure 22. Coordinate System Showing Gaussian Distributions in the Horizontal and Vertical.

$$C(x,y,z,H) = \frac{Q}{2\pi\, U\, \sigma_y\, \sigma_z} \exp -\frac{1}{2}\left(\frac{y}{\sigma_y}\right)^2 \left[\exp\left(-\frac{1}{2}\left(\frac{z-H}{\sigma_z}\right)^2\right) + \exp\left(-\frac{1}{2}\left(\frac{z+H}{\sigma_y}\right)^2\right) \right] \quad (16)$$

Diffusion coefficients σ_y and σ_z. The determination of σ_y and σ_z for Equation (16) is a crucial step in predicting ambient pollution levels using the Gaussian model. Various authors (i.e., Smith (35), Pasquill (36), Brookhaven (37), Briggs (38), and TVA (39)) have summarized the results of dispersion studies and presented empirical values for σ_y and σ_z for use in Gaussian models. Each of these studies point

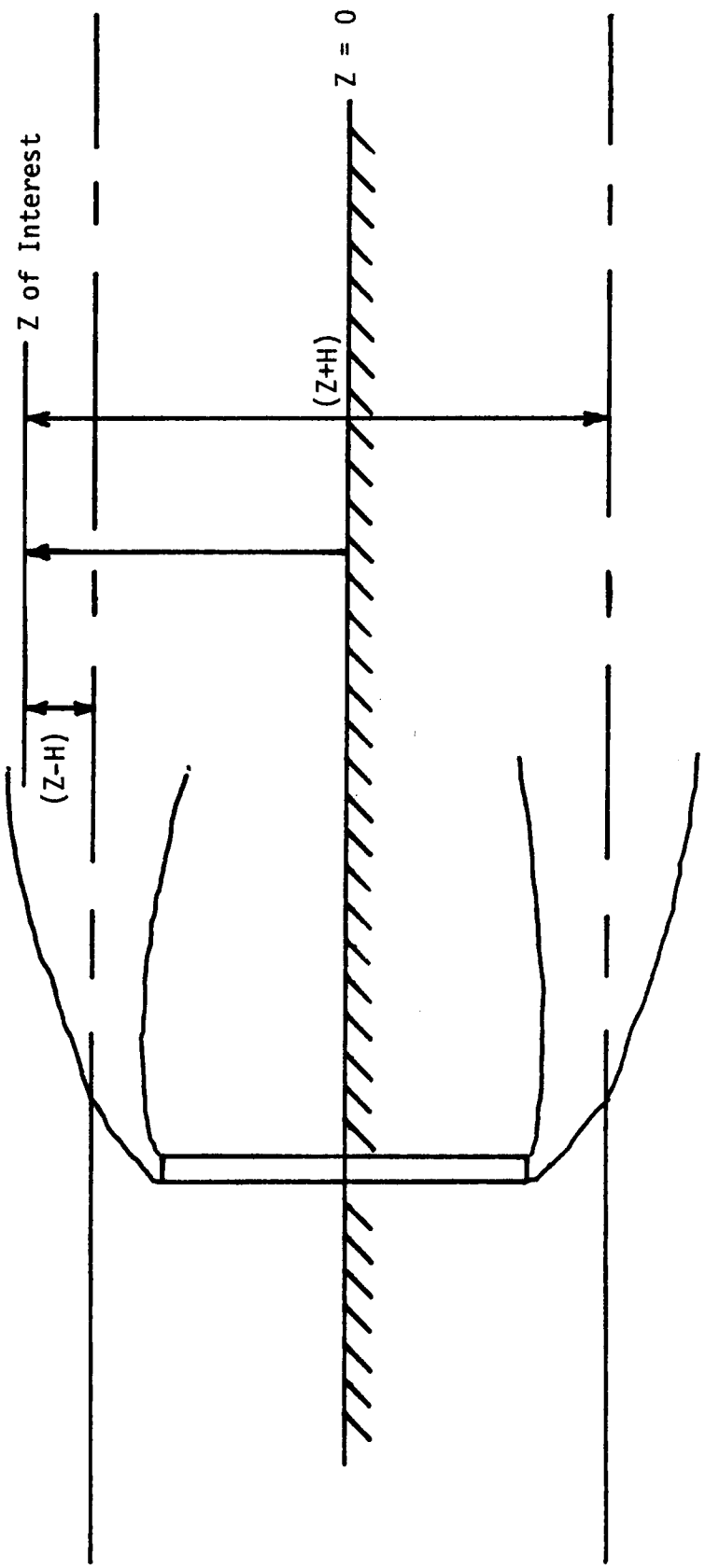

Figure 23. Coordinate System of Real Source and Imaginary Source.

out the dependence of diffusion rates on the turbulent condition of the atmosphere, which varies both temporally and spatially. Temporal variations due to changing insolation, vertical temperature structure and wind speeds result in different values of σ_y and σ_z during different times of day, etc. For this reason empirical values for σ_y and σ_z have been categorized by Pasquill (36) and others according to defined atmospheric stability classes. (See Table V.) Pasquill's diffusion coefficients can then be determined using Figures 24 and 25 according to the stability class and downwind distance.

Spatial variations in atmospheric turbulence occur due to the effects of wind shear with height and surface roughness. In general, turbulence intensity is greater near the earth's surface than at elevated heights (100's of meters) and it is generally greater over rough terrain (hills, buildings, etc.) than over smooth (grassland or desert). Not surprisingly, different diffusion coefficients may be needed for modeling very tall stacks or diffusion in downtown areas, because Pasquill's curves are based on ground source data with smooth terrain.

Briggs (38) suggests that different values of σ_y and σ_z be used for urban and rural terrain because diffusion is more rapid in urban surroundings due to the mechanical turbulence produced by wind flow over buildings and the convective turbulence generated by loss of building heat. Diffusion coefficients suggested by Briggs are given in Figures 26-29.

TVA (39) and Hanford (40) have published the results of diffusion studies on tall stacks which indicate that for stable conditions the use

TABLE V

Pasquill's Atmospheric
Stability Categories

Key to Stability Categories					
Surface wind speed (m/sec)	Insolation			Night	
	Strong	Moderate	Slight	Thinly overcast or ≥ 4/8 low cloud	≤ 3/8
<2	A	A-B	B	--	--
2-3	A-B	B	C	E	F
3-5	B	B-C	C	D	E
5-6	C	C-D	D	D	D
>6	C	D	D	D	D

(for A-B take average of values for A and B etc.)

Strong insolation corresponds to sunny midday in midsummer in England, slight insolation to similar conditions in midwinter. Night refers to the period from one hour before sunset to one hour after dawn. The neutral category D should also be used, regardless of wind speed, for overcast conditions during the hour preceding or following night as defined above.

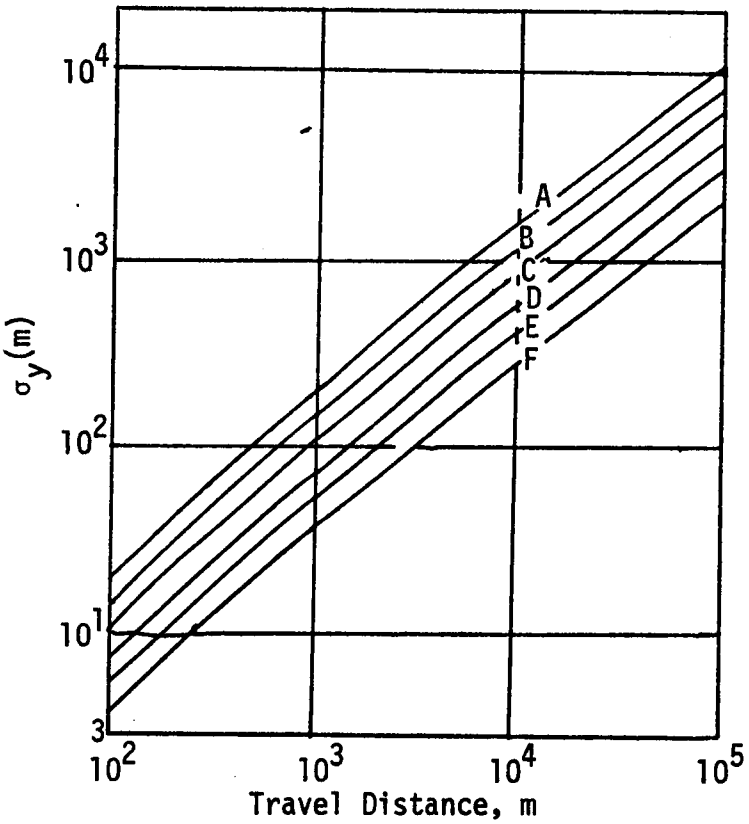

Figure 24. Horizontal Diffusion Coefficient Versus Travel Distance.

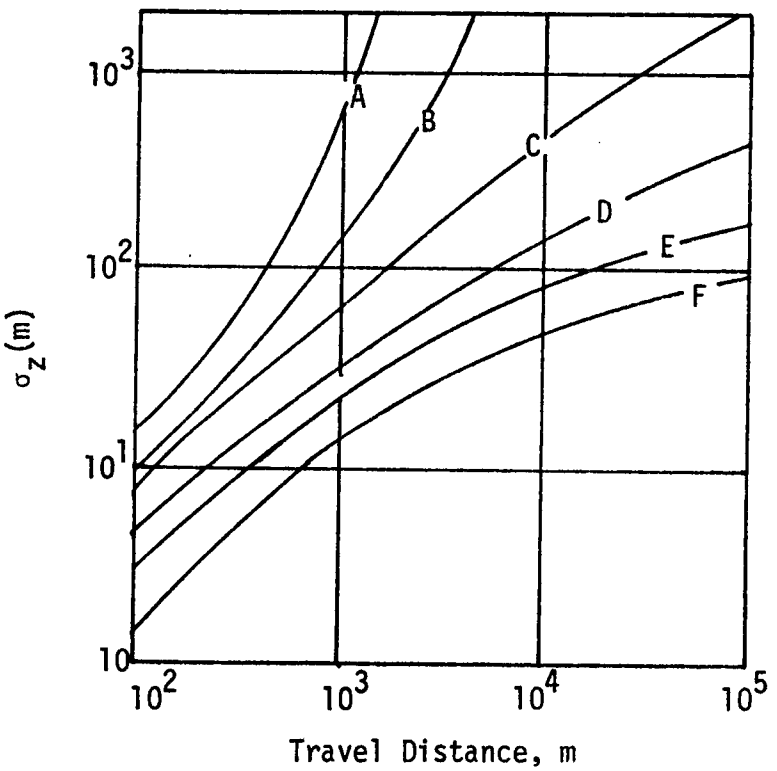

Figure 25. Vertical Diffusion Coefficient Versus Travel Distance for Pasquill's Turbulence Types.

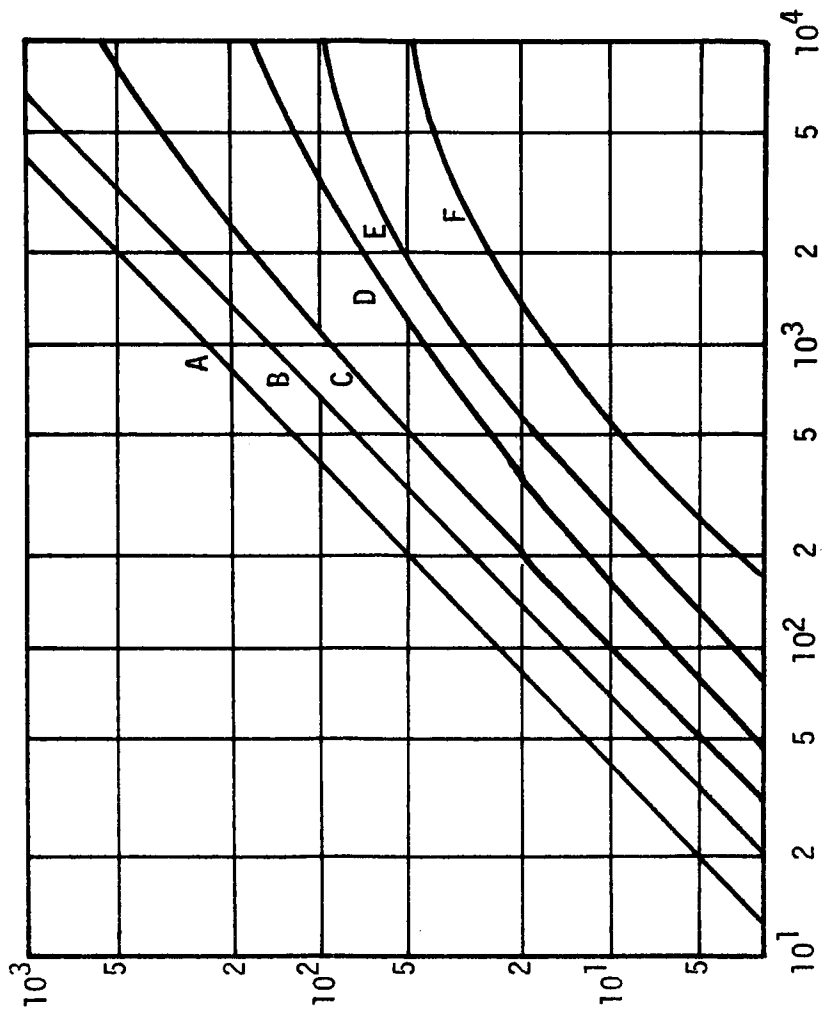

Figure 26. Rural Plume Half-Depth, R_z, vs. Distance Downwind. (From Briggs (38).)

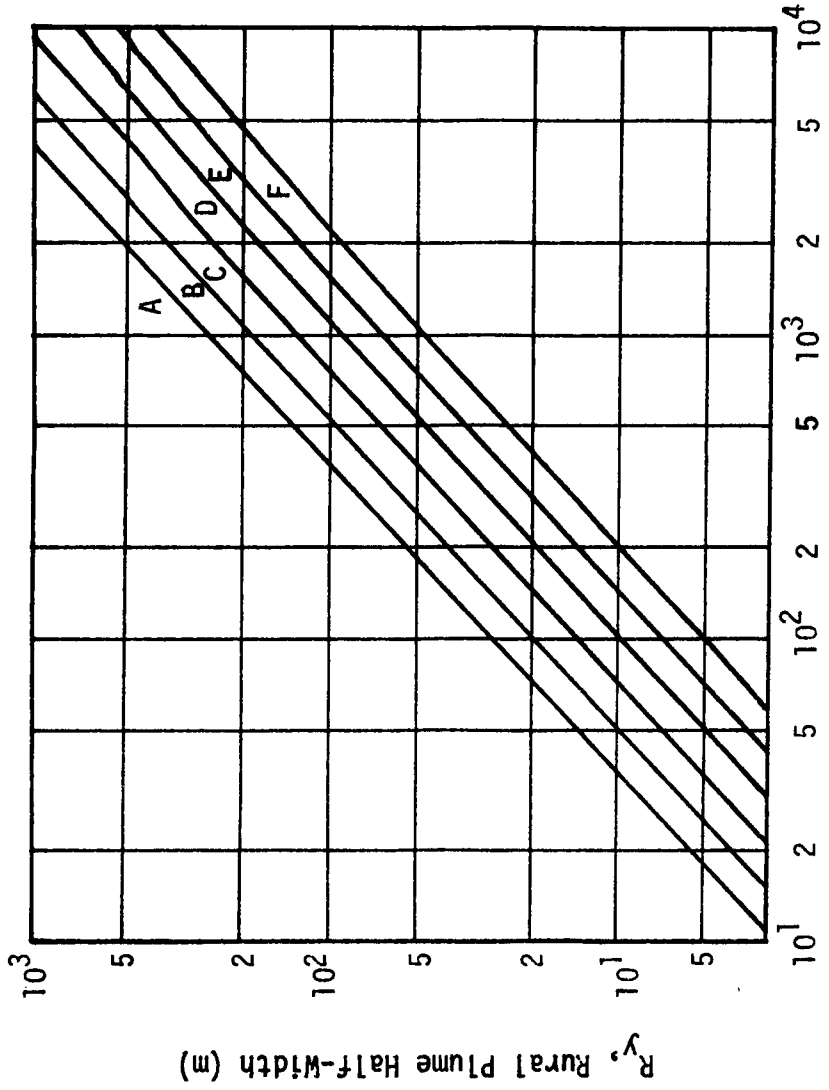

Figure 27. Rural Plume Half-Width, R_y, vs. Distance Downwind. (From Briggs (38).)

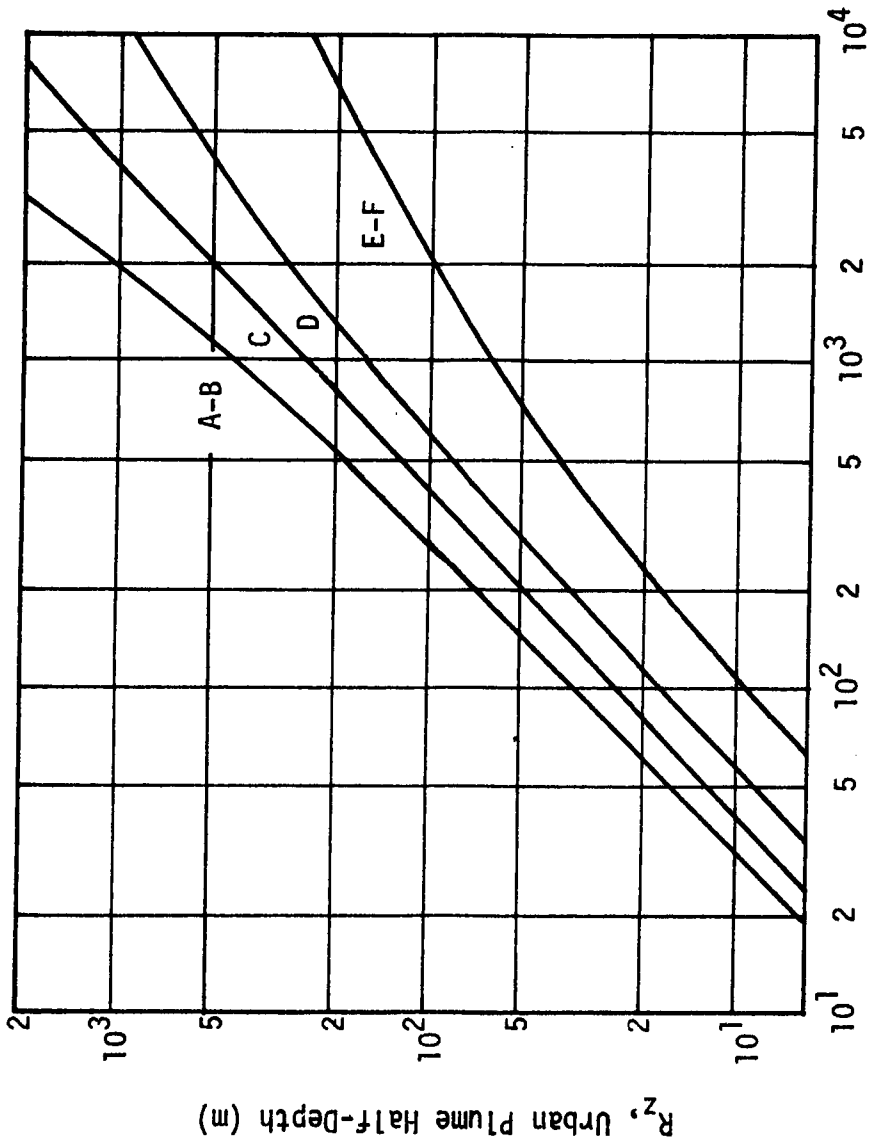

Figure 28. Urban Plume Half-Depth, Rz, vs. Distance Downwind. (From Briggs (38).)

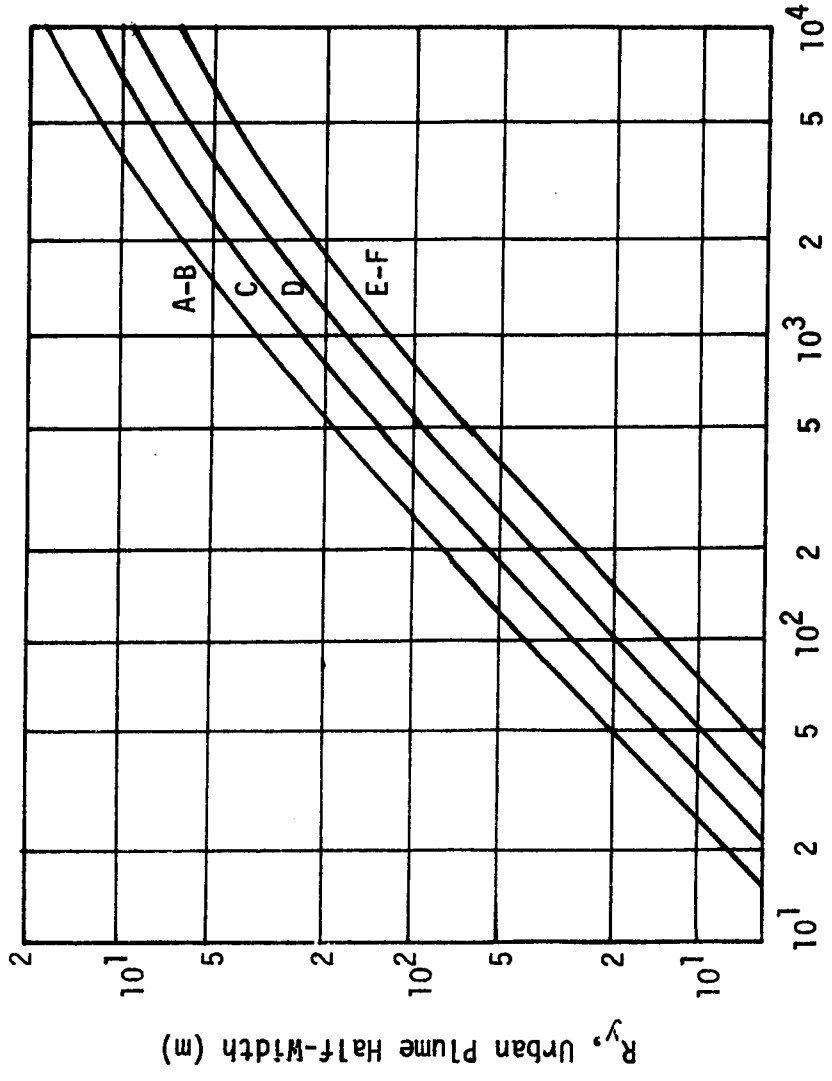

Figure 29. Urban Plume Half-Width, R_y, vs. Distance Downwind. (From Briggs (38).)

of Pasquill's diffusion coefficients may result in as much as an order-of-magnitude underestimation of the axial plume concentration at distances of 10 km according to Islitzer (41). TVA's curves for σ_y and σ_z are shown in Figures 30 and 31.

Line sources. Line source models are used to simulate dispersion from highways where cars are continually emitting pollutants. The form of the Gaussian plume equation used depends on the configuration of the highway and the wind direction. The simplest case is for a ground level "infinite" line source and perpendicular (crosswind) conditions when pollutants are transported in the X direction and dispersed only in the Z direction. Turner (7) suggests the use of the equation:

$$C(x,z) = \frac{2\,Q_L}{(2\pi)^{1/2}\sigma_z\,u} \exp -\frac{1}{2}\left(\frac{z}{\sigma_z}\right)^2 \qquad (17)$$

where

Q_L = emission rate per unit length of highway, ($gm\text{-}sec^{-1}\text{-}m^{-1}$),

x = distance separating road and receptor, and

z = height of receptor above ground.

This equation results in a downwind concentration profile such as illustrated in Figure 32. The condition that the line source be infinite in extent does not introduce large errors as long as the finite road length is greater than 3 σ_y long in both directions from the receptor. If the road is shorter, then the "edge effects" caused by the end of the line source must be accounted for. These edge effects will significantly increase at greater distances from the source. Sutton (42) presented the following equation in 1932 for application to finite line sources:

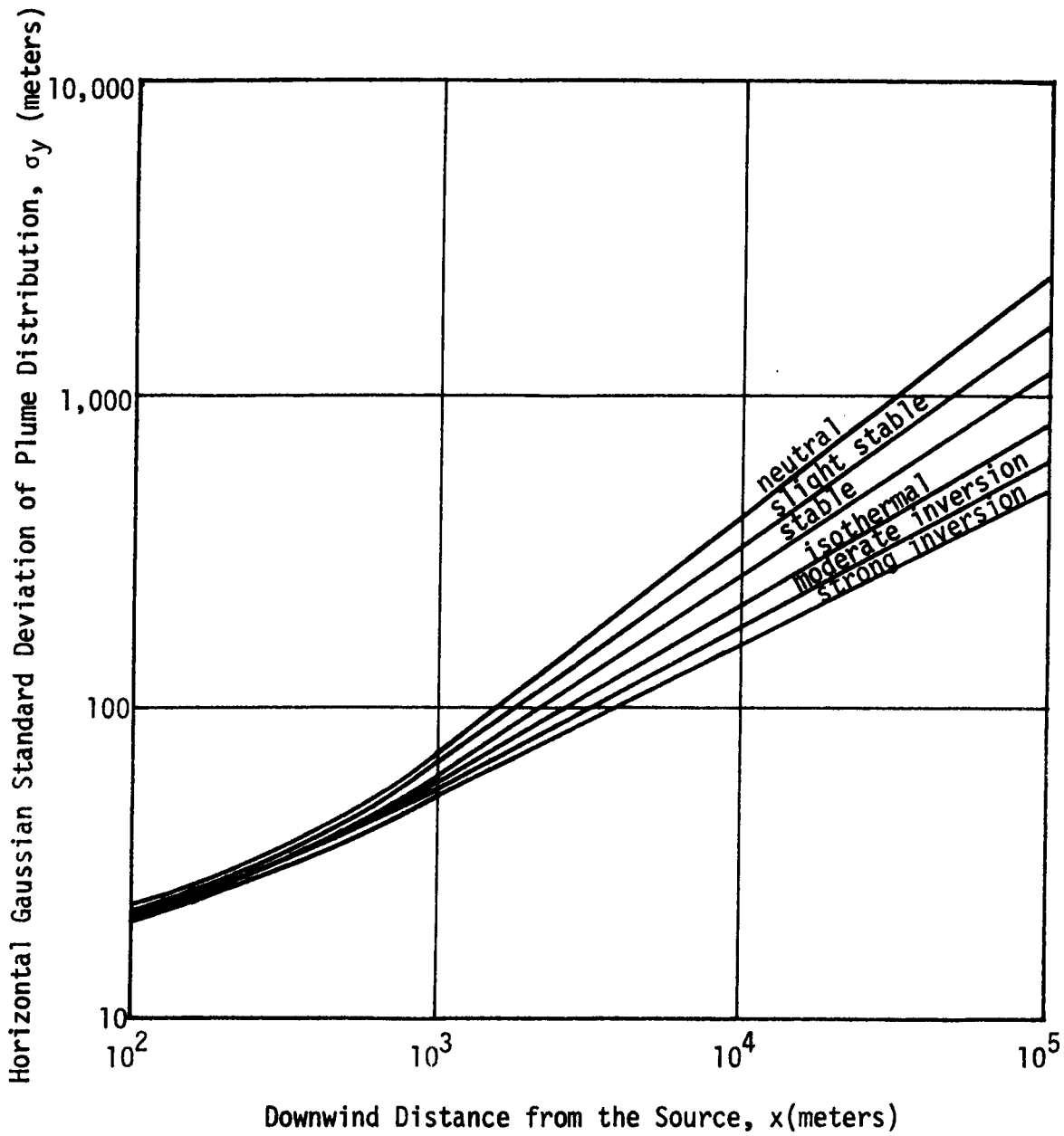

Figure 30. Horizontal Gaussian Standard Deviation of Plume Distribution as a Function of Downwind Distance from the Source. (From TVA (39).)

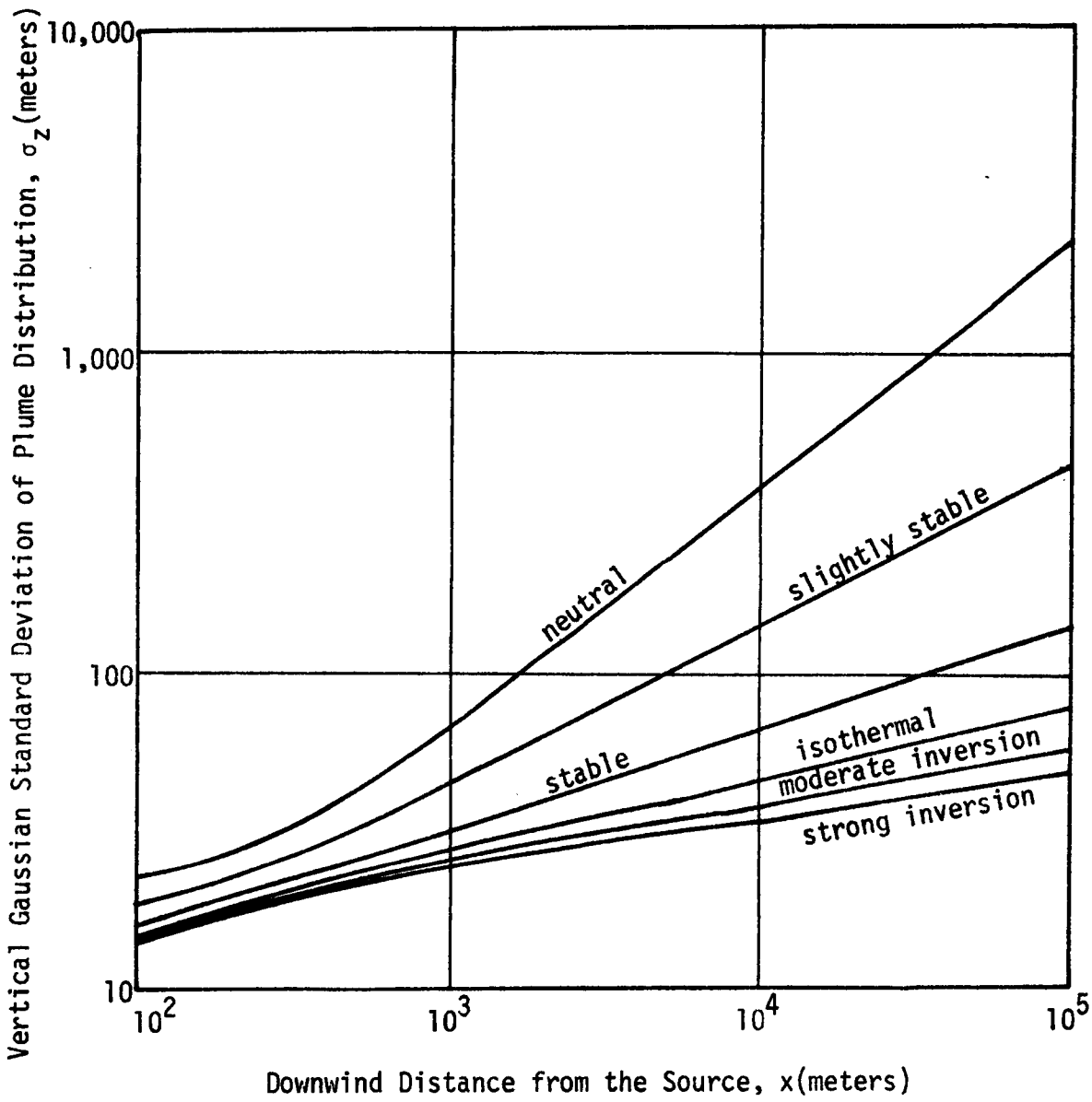

Figure 31. Vertical Gaussian Standard Deviation of Plume Distribution as a Function of Downwind Distance from the Source. (From TVA (39).)

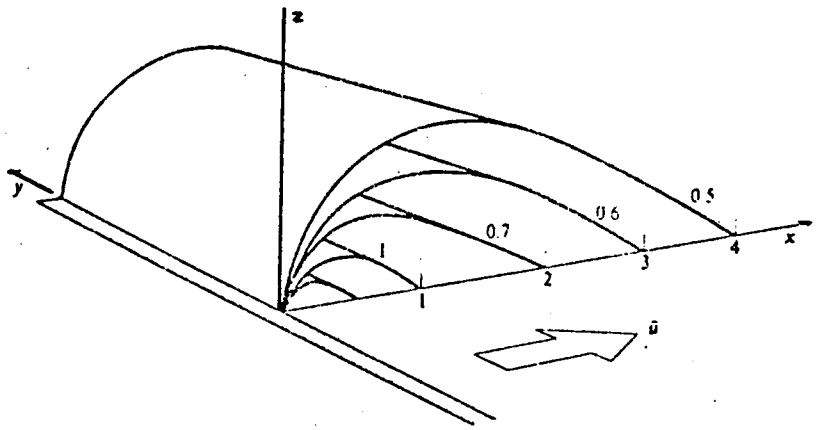

Figure 32. Cross section revealing surface of constant ambient concentration for an infinitely long line source on the y-axis. Only relative concentrations are indicated.

$$C(x,y,0) = \frac{2\,Q_L}{(2\pi)^{1/2}\sigma_z\,\bar{u}} \exp - \left[-\frac{1}{2}\left(\frac{z}{\sigma_z}\right)^2\right] \int_{P_1}^{P_2} \frac{1}{(2\pi)^{1/2}} \exp -\left(\frac{P^2}{2}\right)dp \qquad (18)$$

Where $P_1 = y_1/\sigma_y$ and $P_2 = y_2/\sigma_y$.

In order to account for different wind directions, ϕ (referred to the road), Turner (7) suggests a simple trigonometric correction ($\frac{1}{\sin\,\phi}$ x Equation (17)) which accounts for the decreased wind speed, u, normal to the road. Turner further recommends that this correction be confined to wind angles >45°. It should also be recognized that the distance separating the road and receptor, x, is increased under oblique wind conditions by a similar amount ($\frac{1}{\sin\,\phi}$) such that a different value of $\sigma_z(x)$ is required.

The most difficult case for modeling a line source is under parallel wind conditions when pollutants are transported in the X direction and dispersed in both the y and z directions. In this case a receptor located at point P in Figure 33 will be exposed to pollutant levels which result from the accumulation that occurs as winds pick up and

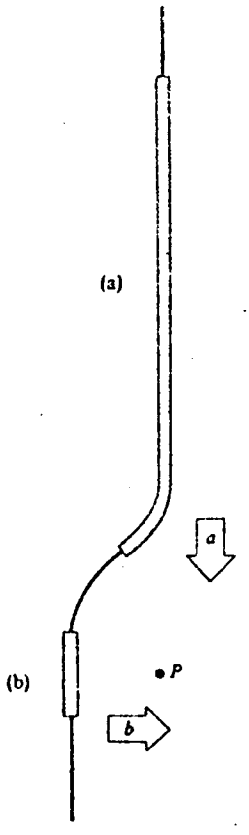

Figure 33. A line source curve around a receptor at P. Wind parallel to the long stretch of road (a) will produce a higher ambient concentration than transverse (b) provided that atmospheric mixing is minimal.

transport pollutants from the long highway section "a" illustrated in the figure. An equation can be derived for the simplest case of ground level source and receptor by integrating the contribution of each incremental length of highway, Δx, from the initial, x_1, and final, x_2, points at which the highway becomes parallel to the wind. This equation is:

$$C(x,o,o,o) = \int_{X_1}^{X_2} \frac{Q_L \, dx}{\pi \, U \, \sigma_z(x) \, \sigma_y(x)} \qquad (19)$$

if the diffusion coefficients $\sigma_z(x)$ and $\sigma_y(x)$ can be expressed in exponential form: $\sigma_z(x) = ax^p$ and $\sigma_y(x) = bx^q$, then the integral can be solved.

$$C(x,o,o,o) = \frac{Q_L}{\pi U} \int_{X_1}^{X_2} \frac{dx}{ab\ x^{(p+q)}} = \frac{Q_L}{ab\ \pi\ U} \frac{x^{1-(p+q)}}{1-(p+q)} \Bigg|_{X_1}^{X_2} \qquad (20)$$

Beaton, et al. (8) have developed an empirical approach to line sources under parallel wind conditions. The equation for a ground level source and receptor is:

$$C(x,y,o,o) = A\left(\frac{Q}{U}\right)\left(\frac{1}{K}\right)\left(\frac{30.5}{W}\right) \exp - \frac{1}{2}\left(\frac{y}{\sigma_y}\right)^2 \qquad (21)$$

where

Q = the emission rate in gm/sec for 100 feet of highway,

K = 4.24,

W = width of road shoulder to shoulder (meters), and

A = an empirical coefficient which accounts for the accumulation of pollutants under parallel wind conditions. A is a function of road length and stability class. (See Figure 34.)

Another approach which is taken by the EPA (9) for modeling line sources (i.e., the EPA "Hiway" model) is to simulate a line source with a number of point sources each with an equal proportion of the total highway pollution emission rate. The sum of the contributions of each point source to air quality at the receptor, P, is equal to the

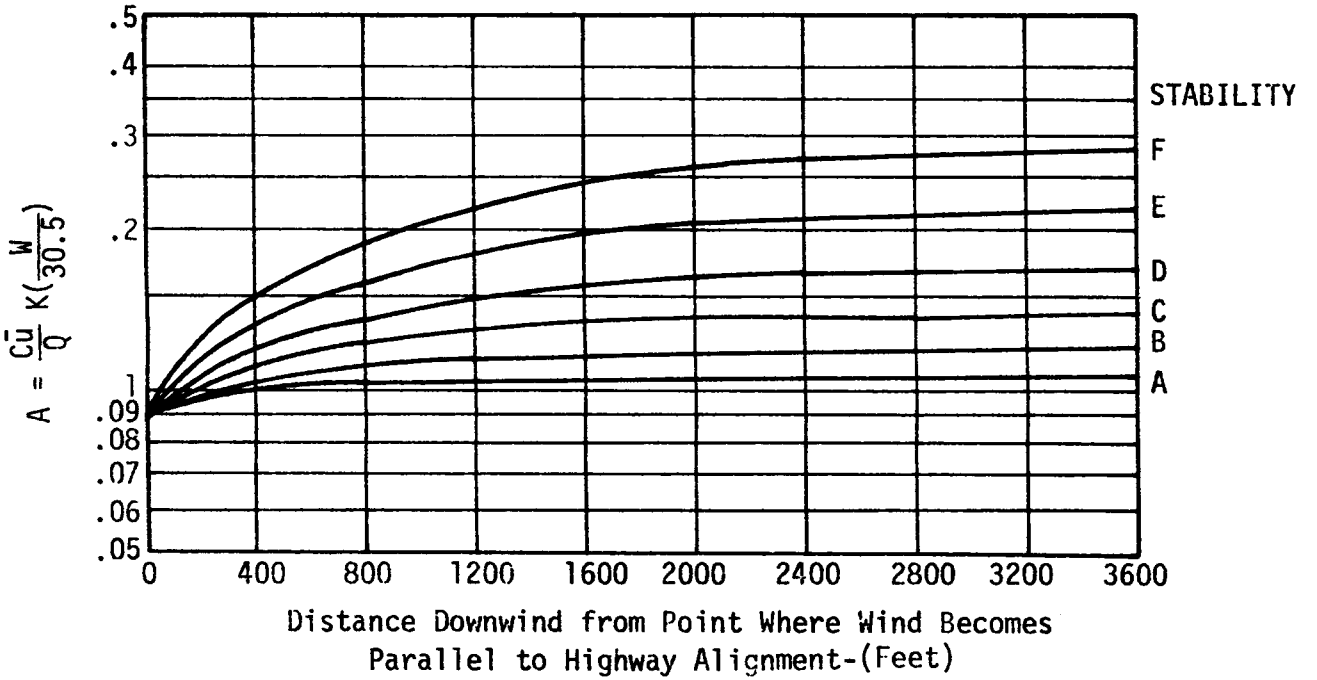

Figure 34. Ground Level Concentration Ratio, A, Downwind from Highway Line Source Parallel Wind At-Grade Section for all Stability Classes (8).

contribution of the line source. (See Figure 35.) The advantage of this method is that the same point source equations can be used regardless of wind direction.

Diffusion coefficients for line sources. As in the case of point sources, the diffusion coefficients for line sources have been determined empirically from field experiments. At present the two sets of diffusion coefficients most widely used are those employed by the California Division of Highways (8) and those used by EPA (9). Figures 36 and 37 show the sigma curves used by California. Gilbert and Davis (43) have compared the σ_z curves used by California and EPA models. Figure 38 illustrates the differences in σ_z between the two models.

Area sources. Area source emissions is the term used in reference to the combined effect of the emissions of large numbers of relatively small sources of pollutant emissions such as residential, commercial, and small industrial fuel burning sources. The distribution of area source emissions is frequently assumed to be uniform over the urban area. The contribution of area sources to the pollutant level measured at an air quality station is a function of the emission density of the area source (ug m^{-2} sec^{-1}) and the upwind extent of the area source. The extent of the area source is defined as the distance from the air monitoring station, to the upwind edge of the area source within which the station is located. Figure 39 illustrates how the extent of the area source may change with direction. In this example the area source has an extent of 1-1/2 km to the east and 5 km to the northwest of the air quality station. The larger the size (or extent) of the area source, the higher the concentration, however, the effect of air quality of

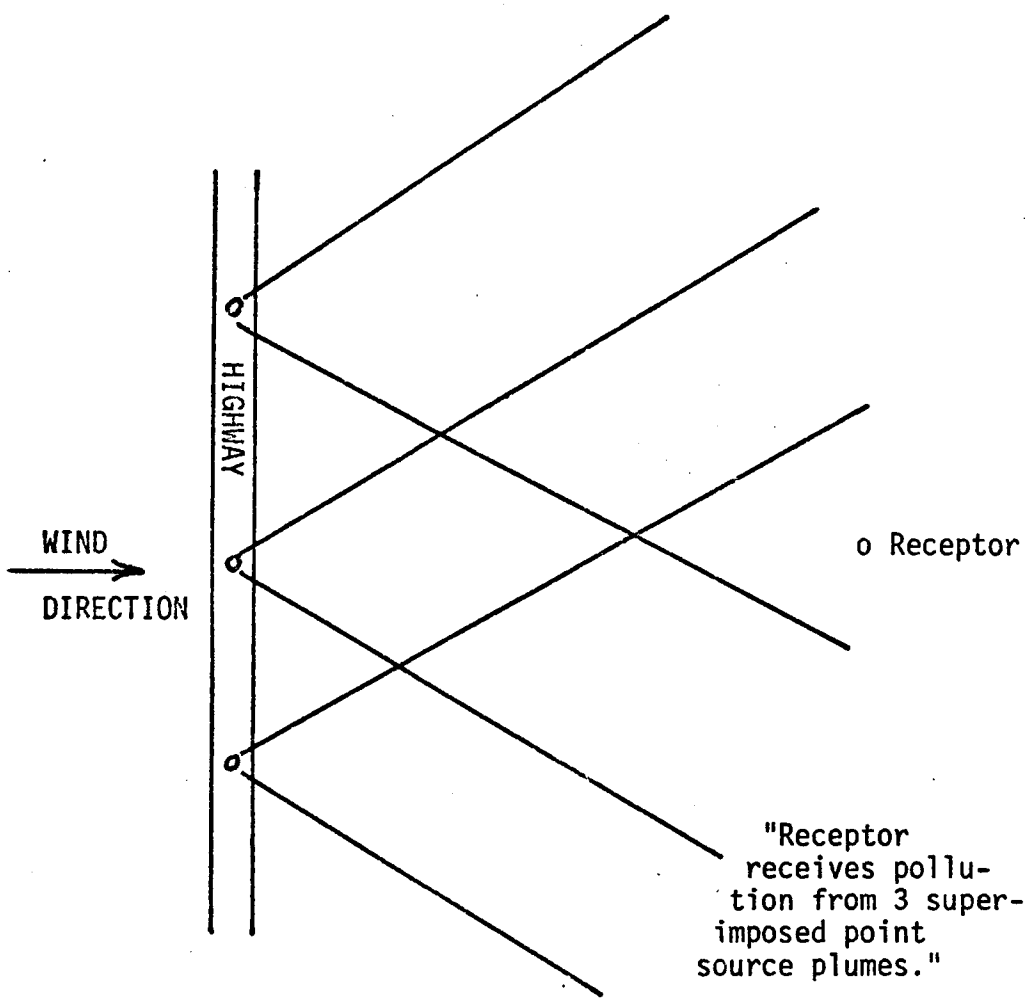

Figure 35. Illustration of how EPA "Hiway" Model Simulates a Line Source with Multiple Point Sources.

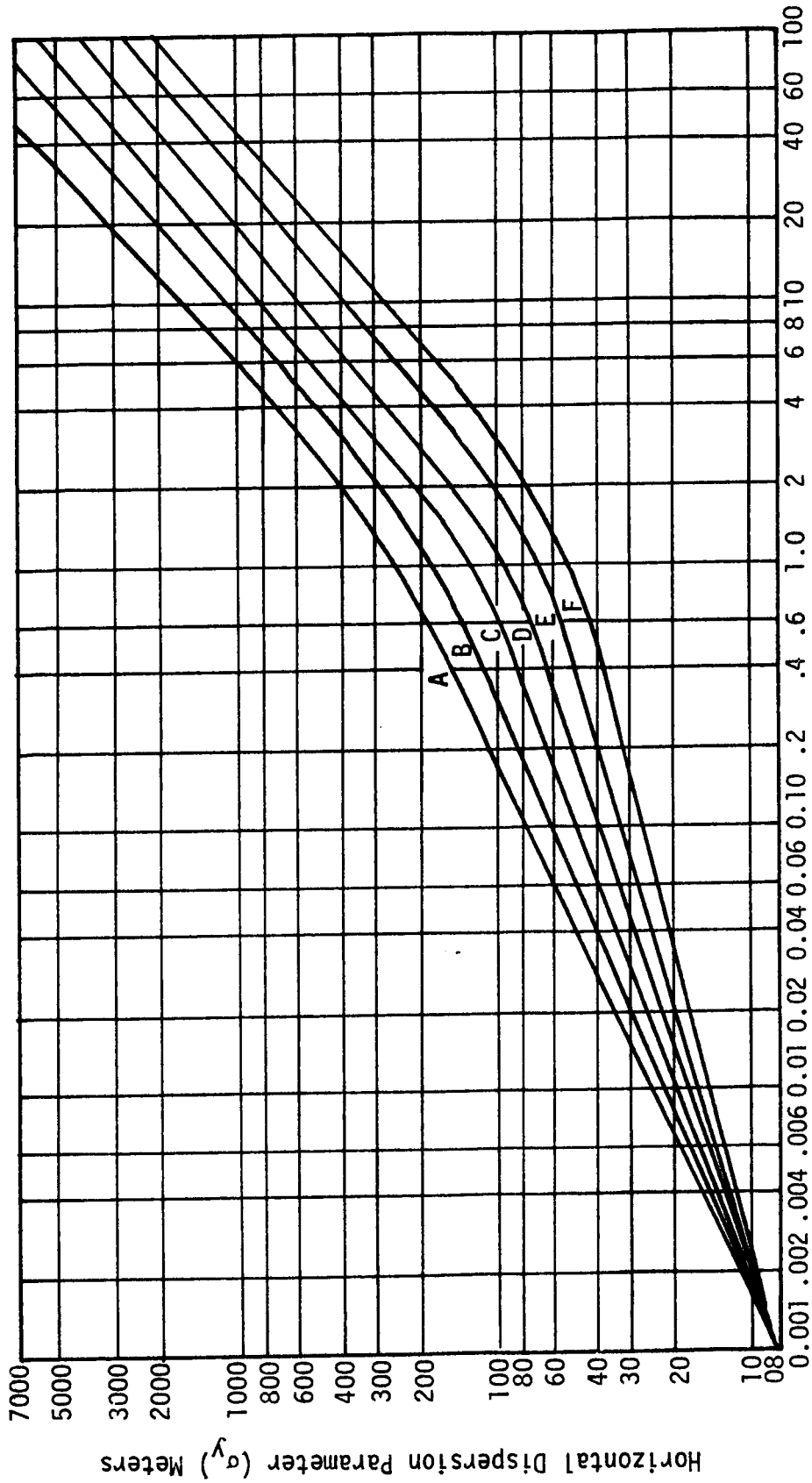

Figure 36. Horizontal Dispersion Parameters. (From California (8).)

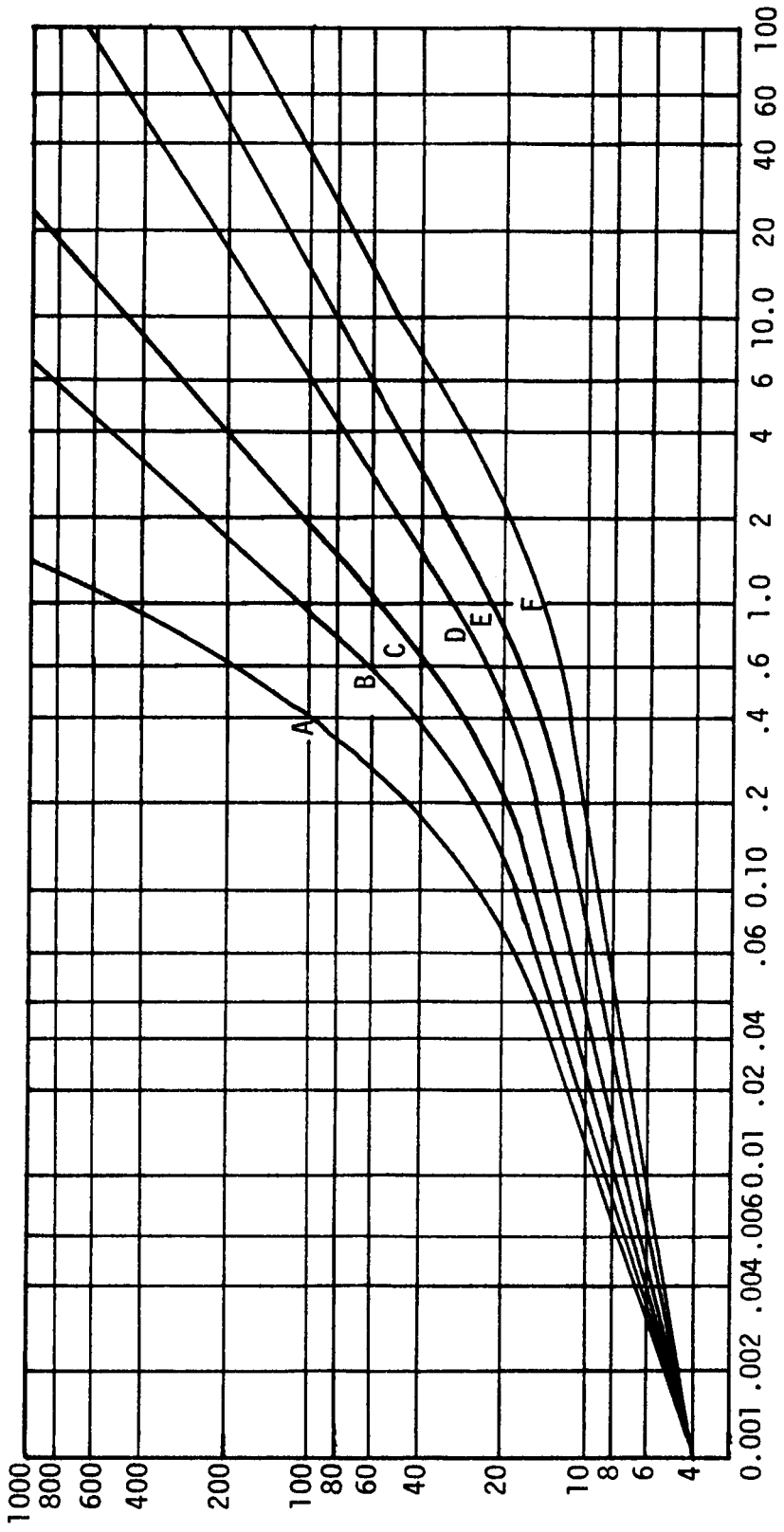

Figure 37. Vertical Dispersion Parameters. (From California (8).)

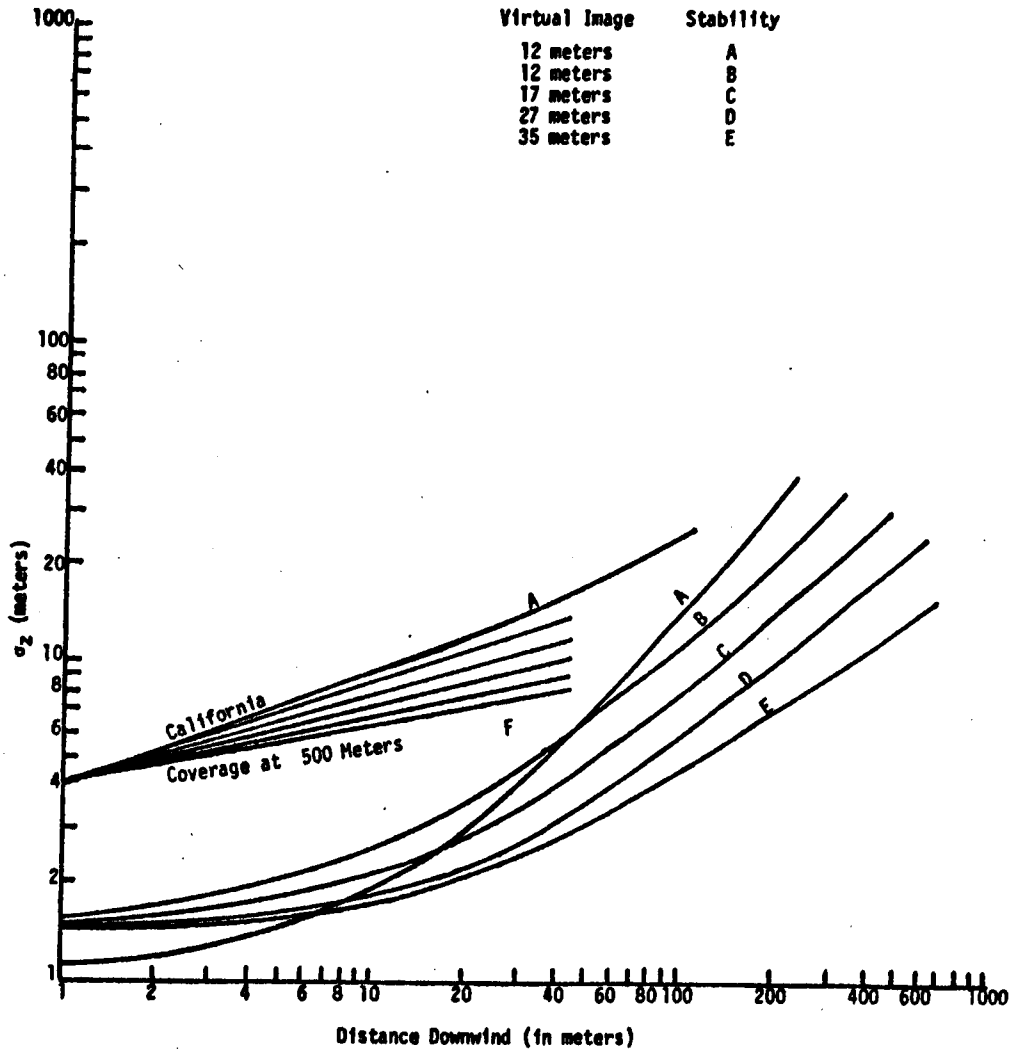

Figure 38. Comparison of σ_z Values Used in the EPA and California Models.

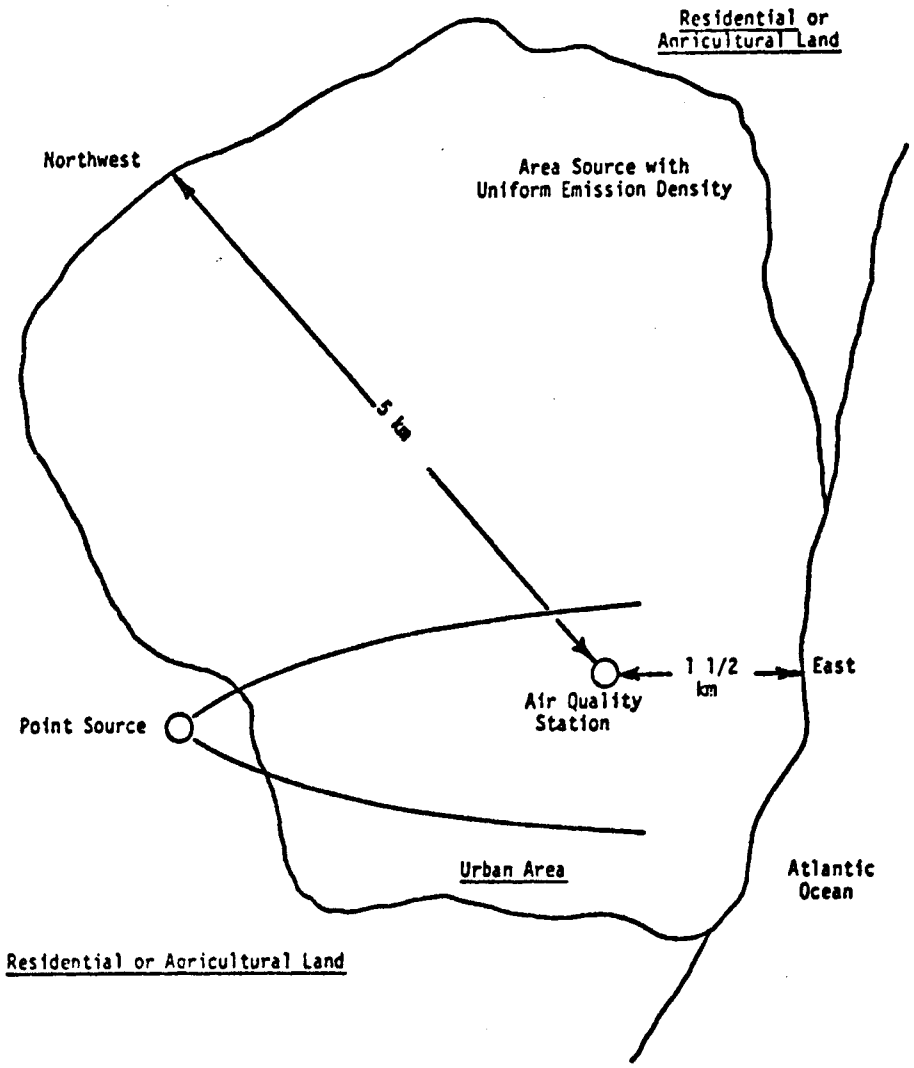

Figure 39. Determining the Extent of the Area Source.

increasing area source size beyond 3 km is fairly small. This effect is illustrated in Figure 40. The technique used to determine the ground level pollutant concentrations resulting from area source emissions is similar to the technique employed by Miller and Holzworth (44).

Figure 40 is the result of the integration of the Gaussian plume equation for a uniform area source extending upwind of a receptor any distance from 100 meters to 10 kilometers. The distance X is located on the abscissa, and the normalized concentration, CU/Q is located on the ordinate axis. The Gaussian equation approximately representing area sources emitting at ground level is:

$$C = \int_{100m}^{x} 2Q\, dx/(2\pi)^{1/2}\, U\, \sigma_z(x) \qquad (22)$$

where

C = concentration at receptor, ug/m^3,

Q = emission density, $ug/m^2.s$,

x = upwind extent of area source from receptor, m,

U = wind speed, m/s, and

$\sigma_z(x)$ = vertical dispersion parameter which is a function of distance from the source and atmospheric stability. In solving Equation 22 a value for $\sigma_z = 0.12\ x^{0.915}$ meters was used as determined by Calder (45). This expression for σ_z assumes that C stability is the most applicable for calculating 24-hour average pollutant concentrations. Stabilities ranging from B to E occur almost every day with durations of minutes to many hours. Stability C

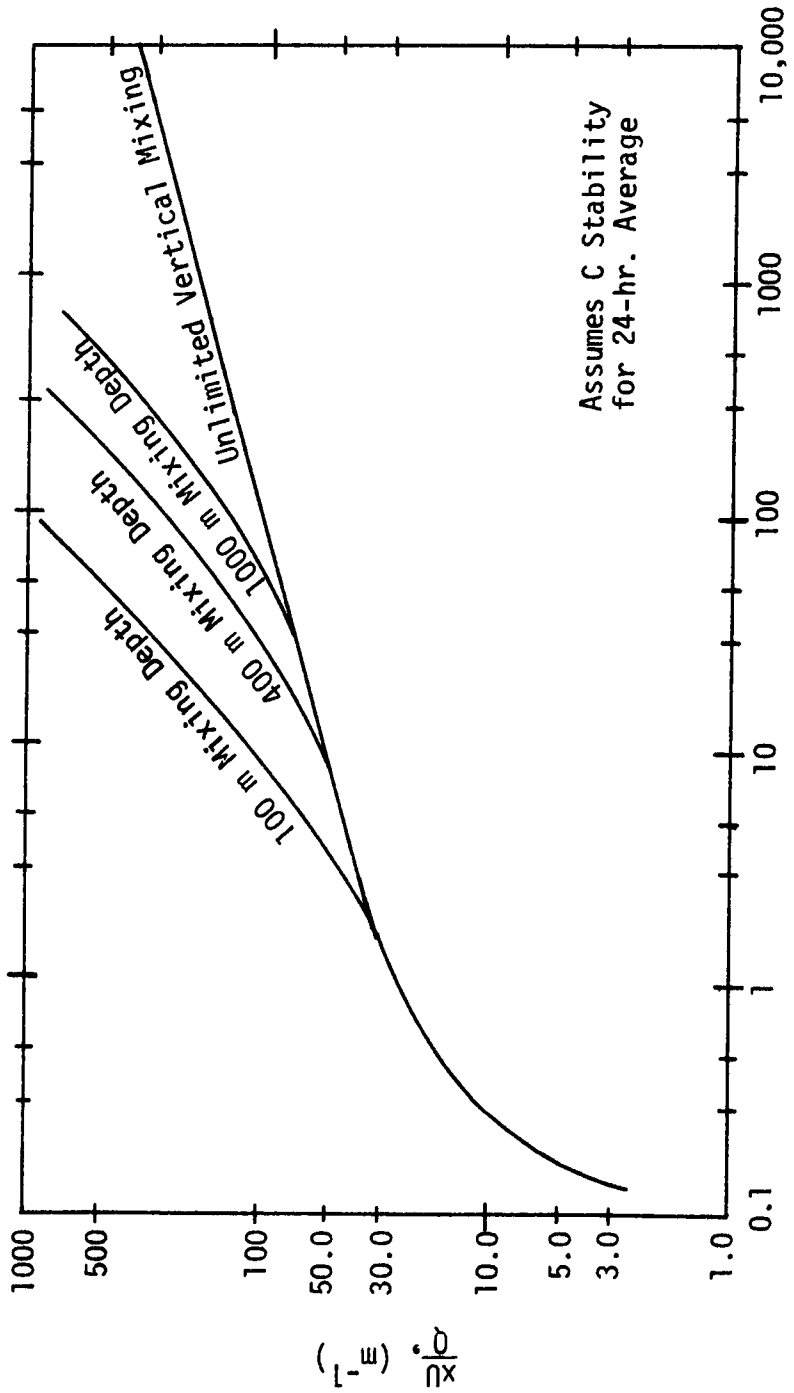

Figure 40. The Effect on Ground Level Pollutant Concentration of Increasing the Size of the Urban Area Source for Various Mixing Depth.

is assumed to average out the effect of much of the early morning and nighttime stable conditions combined with the generally unstable conditions occurring during the middle of the day.

Given the highly approximate model underlying Figure 40, it can be seen that the effect of increasing the extent of the area source from 3 km to 30 km, results in an increase in ground level concentration of a factor of 2. Under conditions of limited vertical mixing, limited by a mixing "lid," the concentration may be increased by a factor of 3 for mixing depths of 400 m and a 100 km area source. In general, varying area source size over a normal range of 3 to 10 kilometers will have a fairly small effect on pollutant concentration under all but the lowest depths.

The Gaussian model for area sources is one of the simplest forms of the Gaussian plume equation, yet urban areas represent one of the most complex sources for which modeling is desired. Hence, the simple calculations described below should not be expected to give precise results due primarily to the simplifying assumptions regarding the homogeneity of source strength throughout the urban area which is common to many area source models. To improve the ability of area source models to resolve more accurately the actual ambient concentrations, some models divide the urban area into grid squares or uniform blocks each having homogeneous source strength within, but different source strengths among the blocks. This type of modeling is exemplified by Gifford and Hanna's (10) simplified models or SRI-APRAC-1A (24) urban area source model.

In the case of SRI's (24) model, a high speed digital computer is needed to perform the many mathematical calculations.

Plume Rise

Introduction

The height to which a plume of flue gases rises into the atmosphere after being emitted from a stack has a significant effect on the resulting ground level pollution concentration downwind. The Gaussian plume equations discussed previously require the effective stack height, H_e, as input information. H_e is equal to the sum of the physical stack height, h_s, and the plume rise, Δh.

$$H_e = h_s + \Delta h \tag{23}$$

Plume rise has been studied by numerous authors (6,35,46-53) each publishing various empirical equations describing their results. Most authors generally recognize that plume rise is dependent on the initial momentum of the gases, the buoyancy of the gases (if at temperatures other than ambient), the vertical temperature structure of the atmosphere and the horizontal wind speed. One of the best consolidations of plume rise results and appropriate equations has been prepared by Briggs (46).

Momentum Sources

Sources at temperatures close to the ambient and with significant exit speeds may be treated as jets in a cross wind. For this case Briggs (46) presents the results of Rupp, et al. (49):

$$\Delta h = 1.5 \left(\frac{V_s}{U}\right) D = 1.5RD \qquad (24)$$

where $R = V_s/U$, V_s is the stack exit velocity, U the average wind speed, and D the stack diameter. Briggs (46) recommends using the constant 3.0 in place of 1.5. Smith (35) gives a similar equation

$$\Delta h = D\left(\frac{V_s}{U}\right)^{1.4}. \qquad (25)$$

Jet rise to its final height is a function of the downwind position x and appears to be $(x/D)^{1/3}$ dependent. An expression for determining Δh as a function of x is given by Briggs (50) as

$$\frac{\Delta h}{D} = 1.89 \left(\frac{R}{1+3/R}\right)^{2/3} \left(\frac{x}{D}\right)^{1/3}. \qquad (26)$$

Buoyant Plumes

In general, the form of the plume rise equation for buoyant plume is

$$\Delta h \propto \left(\frac{F}{US}\right)^{1/3} \qquad (27)$$

where F is the buoyant momentum flux parameter, U is wind speed, and S is an atmospheric stability parameter.

$$F = g\, Vs \left(\frac{D}{2}\right)^2 \left(\frac{T_s - T_a}{T_a}\right) \qquad (28)$$

$$S = \frac{g}{T} \frac{\partial \theta}{\partial z} \qquad (29)$$

where

g = acceleration of gravity,

T_s = stack temperature,

T_a = ambient temperature,

$\frac{\partial \theta}{\partial z}$ = vertical potential temperature gradient, and

T = local potential temperature.

Experimental data have been evaluated and empirical equations for calculating plume rise have been presented by Briggs (46). For transitional rise:

$$\Delta h = 1.6\, F^{1/3}\, u^{-1} x^{2/3}. \tag{30}$$

For final rise under neutral conditions:

$$\Delta h = 1.6\, F^{1/3}\, u^{-1} (10hs)^{2/3} \quad \text{for } h_s > 100m \tag{31}$$

and

$$\Delta h = 1.6\, F^{1/3}\, u^{-1}\, (3.5x^*)^{2/3} \quad \text{for } h_s < 100m \tag{32}$$

(51) where

$$x^* = 0.52\, \left(\frac{sec^{6/5}}{ft^{6/5}}\right)\, F^{2/5}\, h_s^{3/5}. \tag{33}$$

For final rise under stable conditions with wind:

$$\Delta h = 2.9\left(\frac{F}{US}\right)^{1/3}. \tag{34}$$

For final rise under stable and calm conditions:

$$\Delta h = 5.0\ F^{1/4}\ S^{-3/8}. \qquad (35)$$

No reliable methods have thus far been proposed for calculating plume rise under unstable conditions (51).

A Nomographic Solution for Plume Rise

From plume rise experiments TVA (52) has formulated an equation similar to Brigg's Equation (30). TVA's equation is:

$$\Delta h = 114\ C\ U^{-1}\ F^{1/3} \qquad (36)$$

where C is an empirical coefficient equal to

$$C = 1.58 - 0.414\ \frac{\Delta\theta}{\Delta z}. \qquad (37)$$

The number 114 has dimensions ($m^{2/3}$).

Using this equation and mean values of C = 1.58 for neutral conditions and C = 1.10 for stable conditions, TVA (52) has prepared a nomogram which can be used to provide rapid solutions of the plume rise Equation (36). The nomogram is presented in Figure 41.

To use the nomogram, first calculate the parameter, G, where

$$G = V_s\ r^2\ (p_a - p_s)/p_z\ (m^3/sec) \qquad (38)$$

and

V_s = stack gas exit velocity (m/sec),

r = inside radius of stack top (m),

p_a = density of ambient air at stack top (gm/m^3), and

p_s = density of stack gas at stack top (gm/m^3).

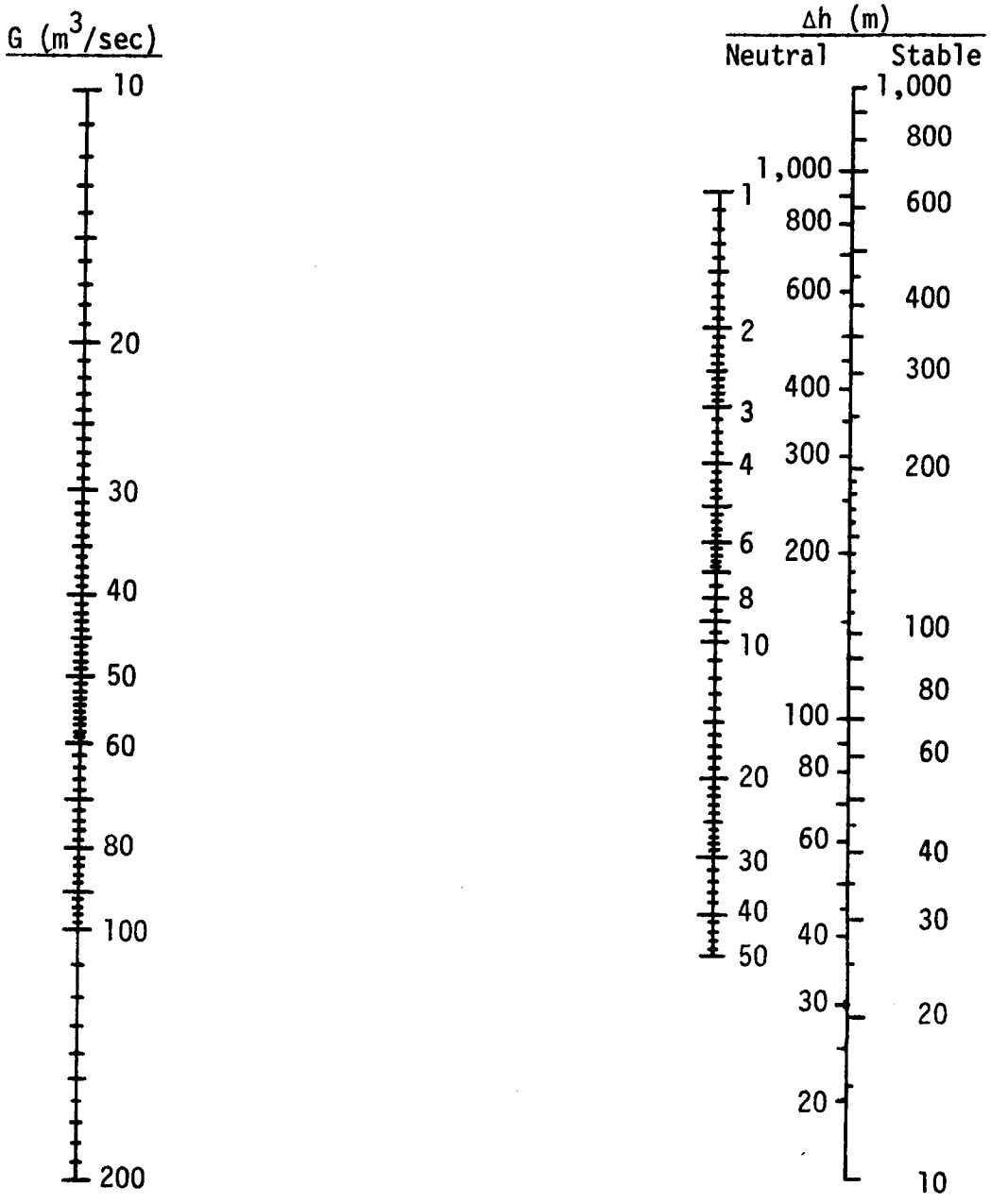

Figure 41. Buoyant Plume Rise, Δh, Versus G and Mean Wind Speed, $\bar{u}$, for neutral and stable atmospheric stability. (From TVA (52).)

Then draw a straight line between the parameter G on the left scale and the mean wind speed at the plume centerline on the center scale. The calculated value for plume rise in either neutral or stable conditions can be read directly off the right hand scale.

General Solutions of Point Source Diffusion Models

Introduction

To gain insight into the nature of the atmospheric diffusion problem it is desirable to obtain general solutions to the models which point out the various relationships among input parameters, and how changes in these parameters affect downwind ground level pollution concentrations. Two different types of solutions are presented in this section: (1) the graphical solutions of Turner (7), and (2) nomographic solutions by TVA (52,54). These solutions are subsequently used for air monitoring site selection. (See Chapter III.)

Graphical Solutions

Turner (7) presents a convenient procedure for determining ground level plume centerline concentrations versus distance downwind from a point source. Turner plots the normalized pollutant concentration, $\chi U/Q$, against distance downwind for various effective stack heights, H, and stability classes (A-F); where χ = pollutant concentration (g/m^3), U = mean wind speed (m/sec), and Q = pollutant emission rate (g/sec). An example of this type of plot is shown in Figure 42 for C stability. Estimates of actual concentrations may be determined by multiplying ordinate values by Q/U.

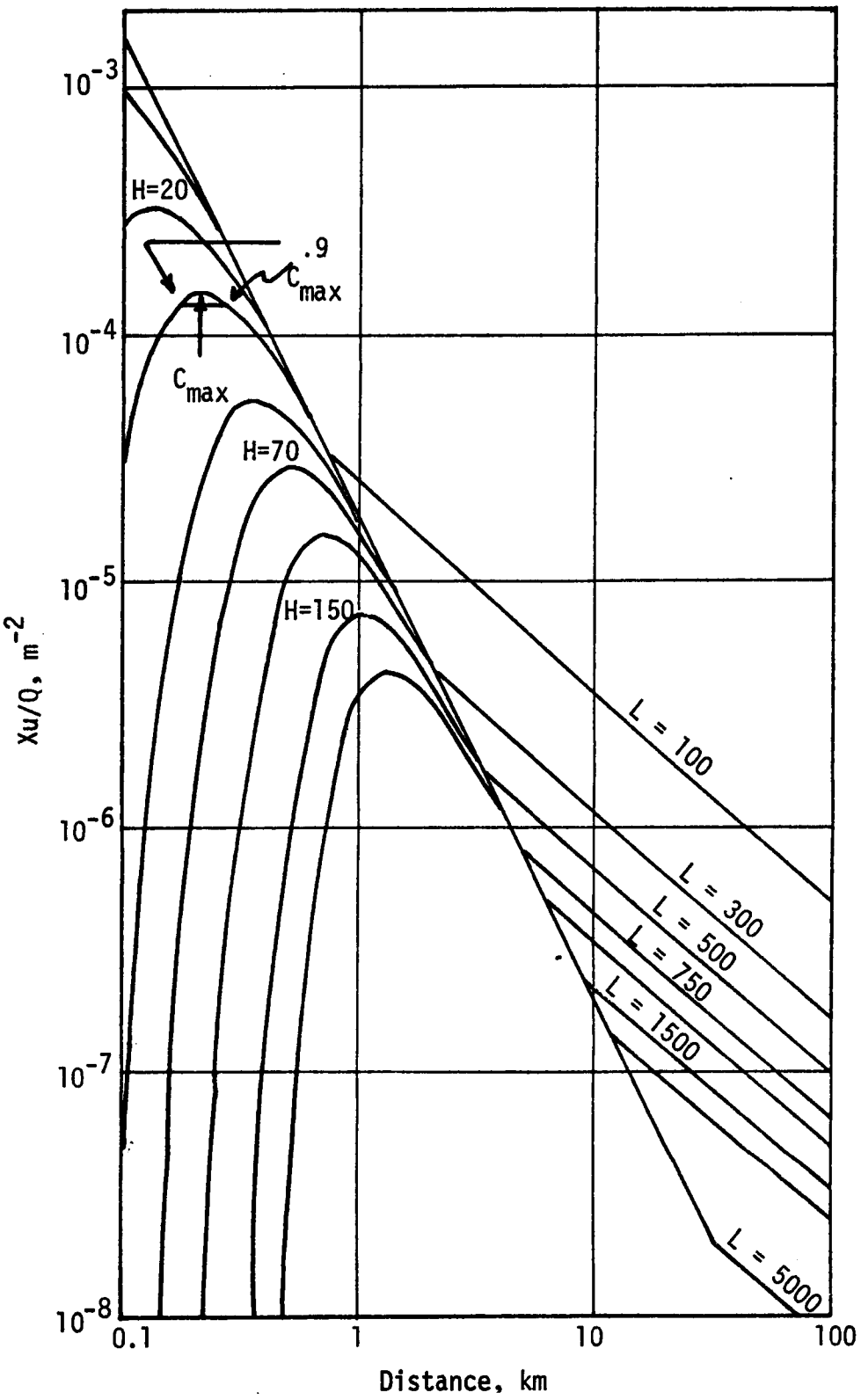

Figure 42. χu/Q With Distance for Various Heights of Emission (H) and Limits to Vertical Dispersion (L), B Stability. (From Turner (7).)

Turner has also plotted normalized ground level concentration isopleths for both ground level sources and elevated sources (i.e., H = 100 meters). Figures 43 and 44 illustrate the theoretical concentrations, $\chi U/Q$, as a function of downwind distance, x, and cross wind distance, y, for C stability. Horizontal concentration gradients in the x and y directions can be inferred from these graphs. (See Turner (7) for plots for stabilities A-F.)

Another graphical solution prepared by Turner shows the location of the maximum normalized ground level concentration, $\chi U/Q$, as a function of effective height of emission, H, and stability class. (See Figure 45.) The maximum concentration can be determined by finding $\chi U/Q$ and multiplying by Q/U. According to Turner (7):

> In using Figure [45], the user must keep in mind that the dispersion at higher levels may differ considerably from that determined by the σ_y's and σ_z's used here. As noted, however, since σ_y generally decreases with height and U increases with height, the product of U $\sigma_y\sigma_z$ will not change appreciably. The greater the effective height, the more likely it is that the stability may not be the same from the ground to this height. With longer travel distances such as the points of maximum concentrations for stable conditions (Types E or F), the stability may change before the plume travels the entire distance.

Nomographic Solutions

TVA (52,54) has presented nomographic methods of solving the Gaussian plume equations for a point source. (See Figures 41, 46, and 47.) These nomograms can be used to calculate the maximum plume centerline concentration for a coning plume, inversion breakup fumigation, and plume trapping conditions. The following is a description of how to use the nomographs taken from the TVA reports (52,54).

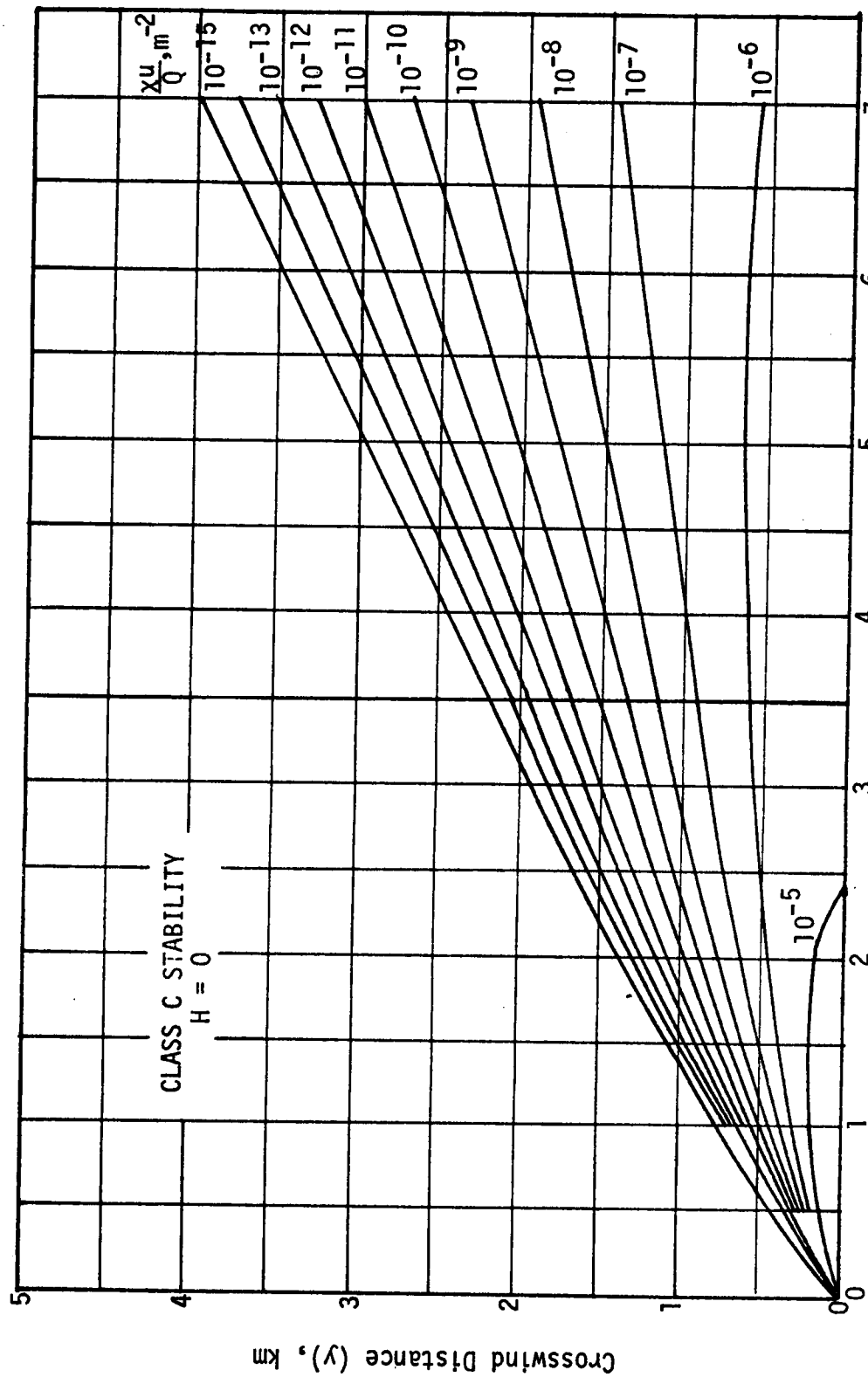

Figure 43. Isopleths of χu/Q for a Ground-Level Source, C Stability. (From Turner (7).)

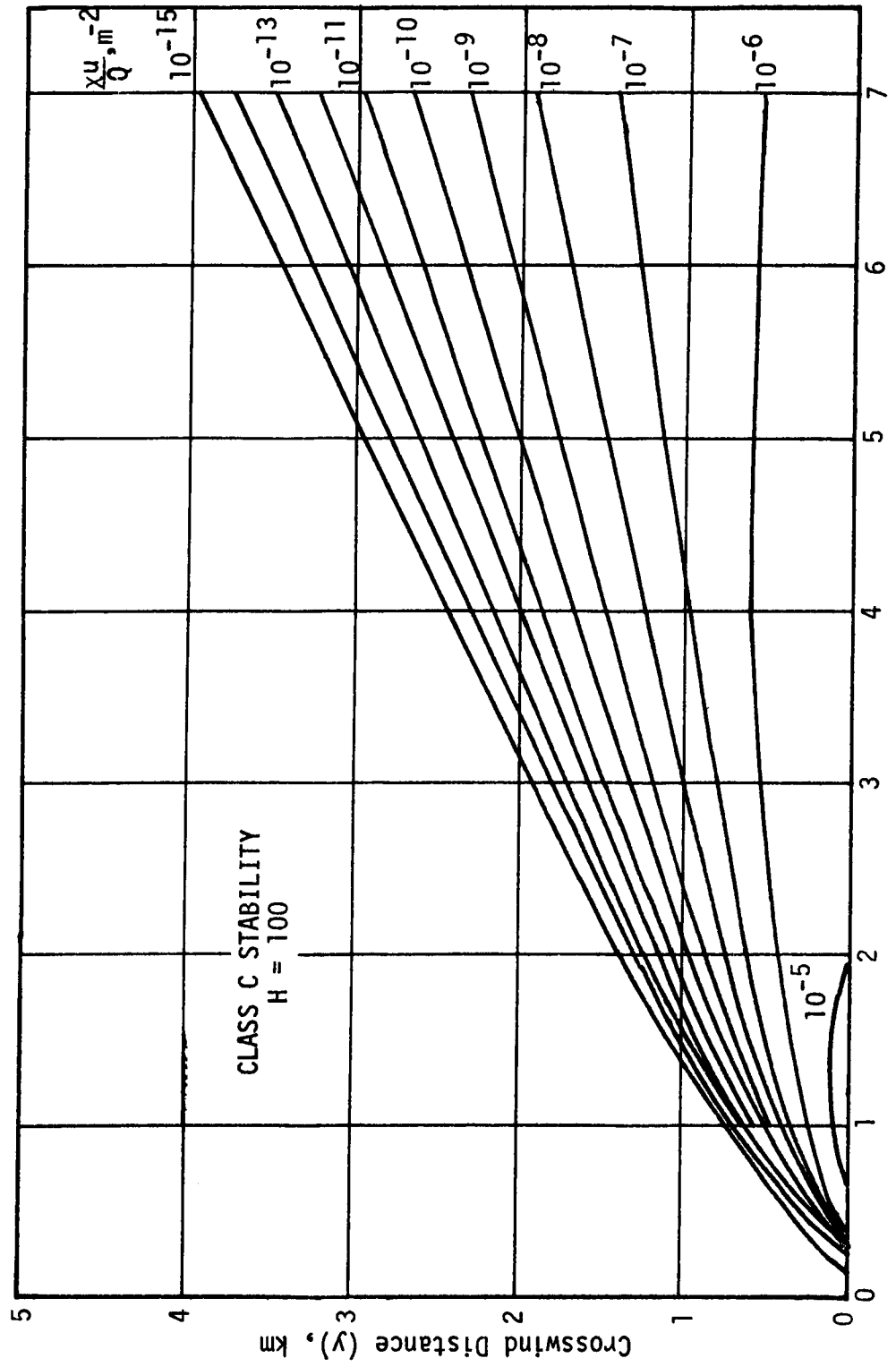

Figure 44. Isopleths of $\chi u/Q$ for a Source 100 Meters High, C Stability. (From Turner (7).)

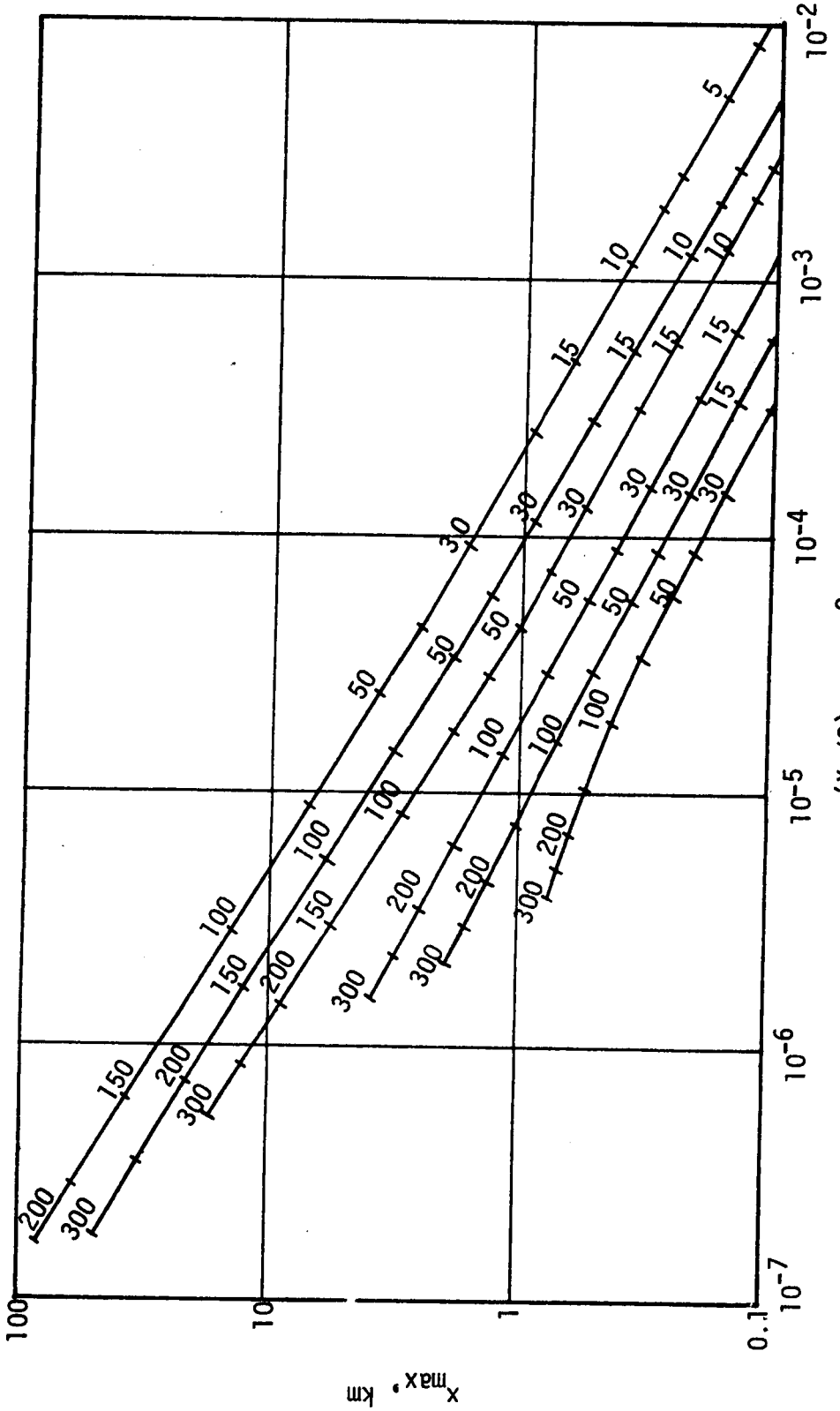

Figure 45. Distance of Maximum Concentration and Maximum χu/Q as a Function of Stability (Curves) and Effective Height (Meters) of Emission (Numbers). (From Turner (7).)

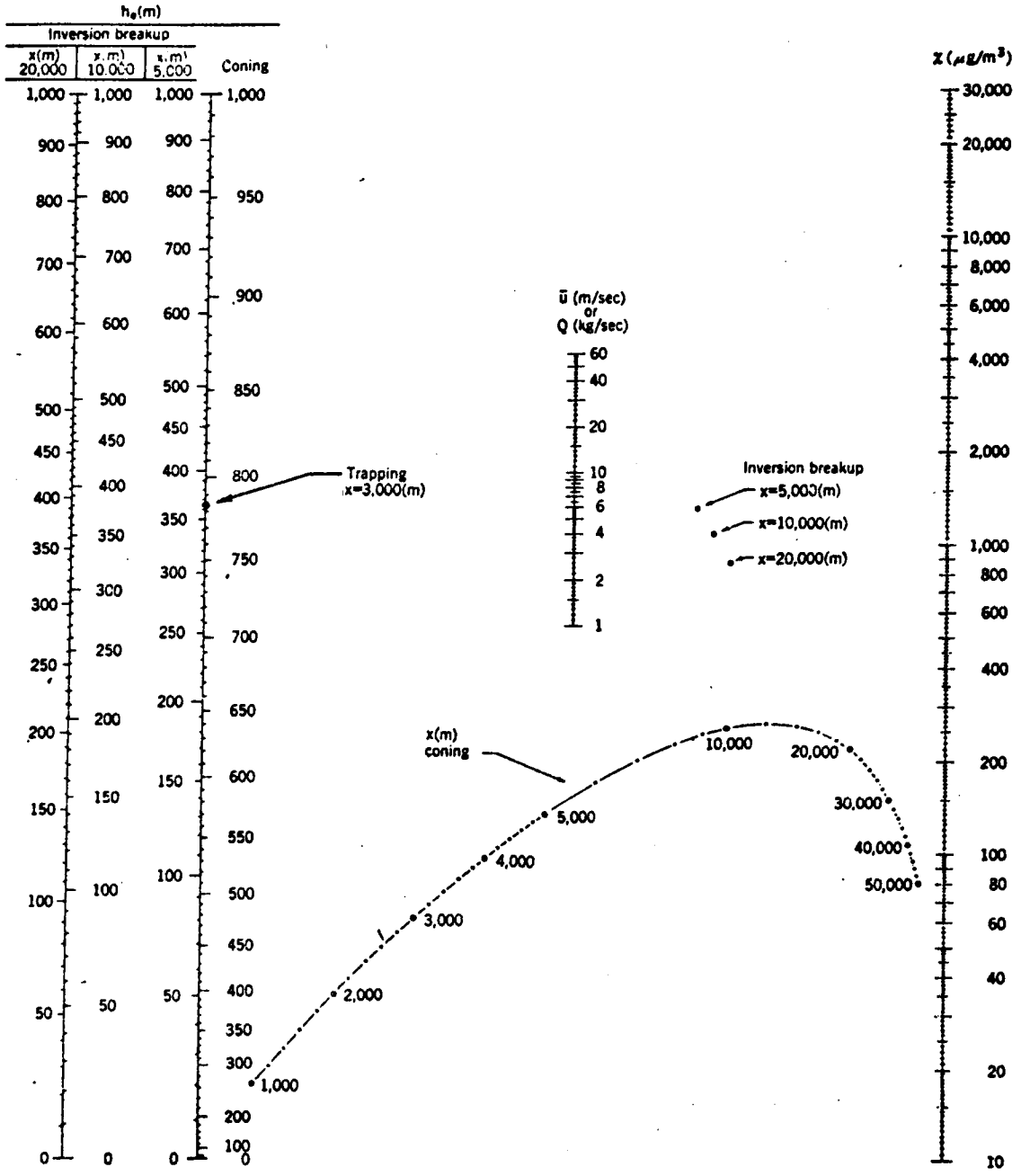

Figure 46. Plume Centerline 1-hr Average Surface Concentration, x, Versus Downwind Distance, r, Effective Stack Height, h_e, Effluent Emission Rate, Q, and Mean Wind Speed, $\bar{u}$.

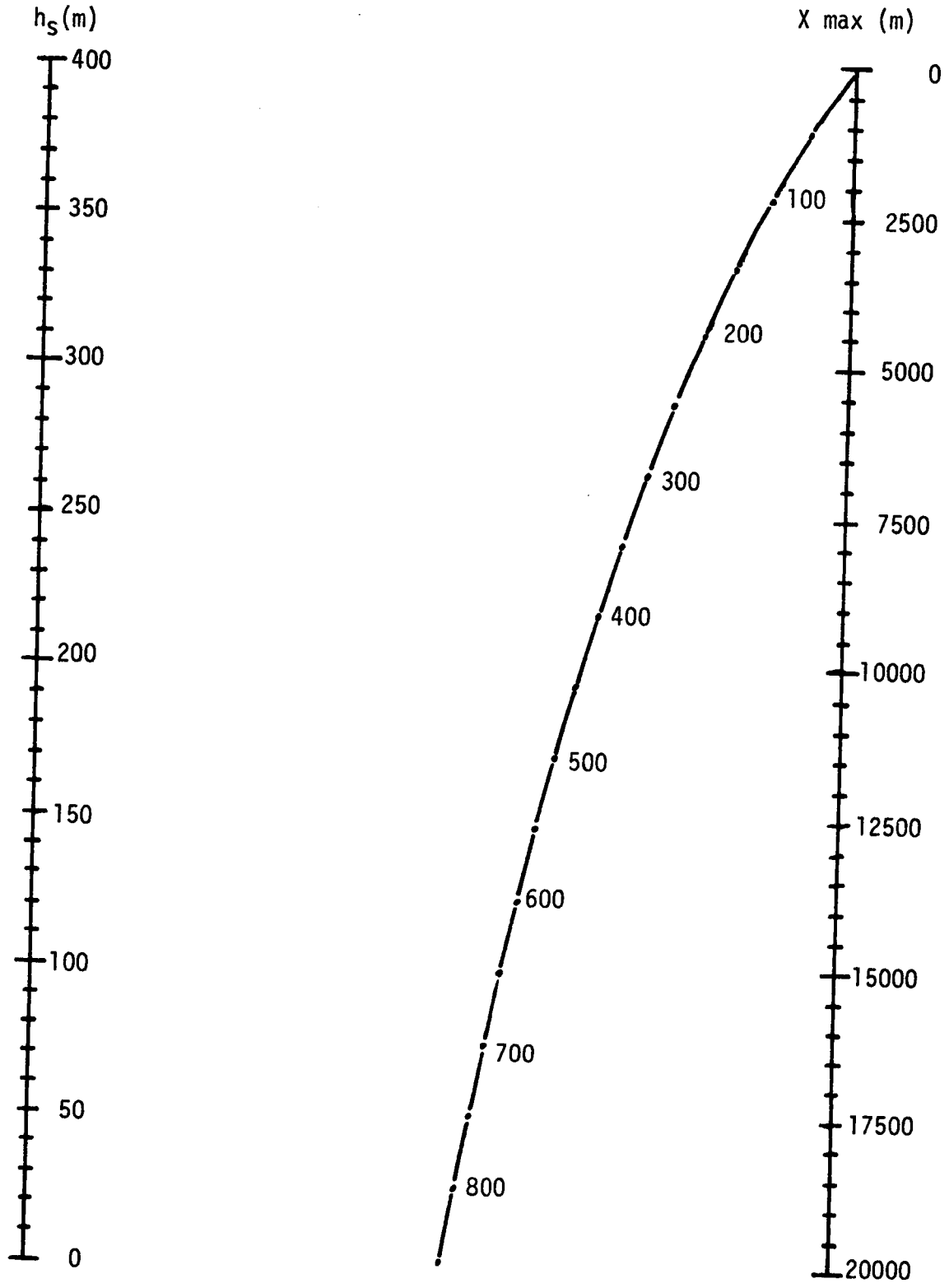

Figure 47. Distance, X_{max}, Versus Stack Height, h_s, and h_d, for Inversion Breakup Dispersion. (From TVA (52).)

Procedure 1 - For Maximum Plume Centerline Surface Concentrations

Coning Dispersion Model:

Step 1 - Project a line from the calculated G value on the left hand G scale of Figure 41 to a value equal to h_s on the right hand neutral Δh scale. Read the $\bar{u}$ value from the center scale. This is the $\bar{u}$ associated with the maximum plume centerline surface concentration, χ_{max}. (Chi, χ, is a symbol denoting 1-hour surface sulfur dioxide concentrations in this guide).

Step 2 - Calculate effective stack height, $h_e = 2h_s$ (m).

Step 3 - Locate this h_e value on the coning h_e scale of Figure 46. Project a line from this point tangent to the curved coning x scale. The point of tangency is the downwind distance where the maximum plume centerline surface concentration is expected to occur. Mark the point where the above projected line intersects the right hand scale. From this point project a line through the $\bar{u}$ value, center scale, obtained previously from Figure 41 to the coning h_e scale. Mark this point of intersection. From this point project a line through the selected Q, center scale, to the right hand scale. Note: if Q < 1 kg/sec, use Q = 1 kg/sec and the appropriate correction factor described later. Intersect value on this right hand scale is the coning maximum 1-hour average plume centerline surface concentration, χ_{max}, in micrograms per cubic meter.

Step 4 - Multiply the result by any correction factors, following the nomograms, that are applicable.

Inversion Breakup Model:

Step 1 - Project a line from the calculated G value on the left hand G scale of Figure 41 through $\bar{u}$ = 3 m/sec to the right hand stable Δh scale. Read Δh in meters from this stable Δh scale. Calculate $h_d = \Delta h + 101$ (m).

Step 2 - Locate h_s on the left hand h_s scale of Figure 47. Locate the h_d value obtained from Step 1 on the center h_d scale. Connecting these two points, project a line to the right hand χ_{max} scale. Intersect point is the distance downwind, χ_{max}, where the maximum inversion breakup surface concentration is expected to occur.

Step 3 - Calculate effective stack height, $h_e = h_s + \Delta h$ (m).

Step 4 - Locate this h_e value on the inversion breakup h_e scale of Figure 46 that represents the x (5,000, 10,000, or 20,000 m) that is most nearly equal to x_{max}. If the x = 10,000 or 20,000 m--h_e scale is utilized, project a horizontal line to the x = 5,000 m--h_e scale and mark the point of intersection on the 5,000 m--h_e scale. If x_{max} is most nearly equal to x = 5,000 m, mark the h_e value obtained from Step 3 on that scale. From the resulting point on the inversion breakup x = 5,000 m--h_e scale project a line through the inversion breakup point, representing the x that is also most nearly equal to x_{max}, to the right hand scale. Mark this point of intersection.

From this point project a line through $\bar{u}$ = 3 m/sec to the coning h_e scale. Mark this point of intersection. From this point project a line through the selected Q, center scale, to the right hand scale. Note: If Q < 1 kg/sec, use Q = 1 kg/sec and the appropriate correction factor described later. Intersect value on this right hand scale is the inversion breakup maximum 1-hour average plume centerline surface concentration, χ_{max}, in micrograms per cubic meter.

Note: the χ_{max} is actually for x = 5,000, 10,000 or 20,000 m which may be significantly different from x_{max}. A more accurate procedure would be to calculate two χ_{max} values, one for $x < x_{max}$ and one for $x > x_{max}$ and then calculate χ_{max} by linear interpolation.

Step 5 - Multiply the result by any correction factors, following the nomograms, that are applicable.

Trapping Model:

Step 1 - Project a line from the trapping, x = 3,000 m dot located on the coning h_e scale of Figure 46 through the appropriate Q, center scale, to the right hand scale. Note: If Q < 1 kg/sec, use Q = 1 kg/sec and the appropriate correction factor described later. Intersect value on this right hand scale is the trapping maximum 1-hour average plume centerline surface concentration, χ_{max}, in micrograms per cubic meter.

Step 2 - Multiply the result by any correction factors, following the nomograms, that are applicable.

Correction Factors:

The following correction factors should be applied, if required, when using the nomograms.

Emission Rate Less Than 1 kg/sec:

For emission rates less than 1 kg/sec, multiply the result from Figure 46 by actual emission rate, Q (kg/sec).

1-Hour to 24-Hour Averaging Time:

Multiply the result from Figure 46 by 1/3 to obtain an estimate of the 24-hour surface concentration, χ, (ug/m^3).

Multiple-Stack Source:

Multiply result from Figure 46 by $N^{4/5}$, where N is the number of stacks of a given height. See Table VI.

Table VI

Correction Factor for Multiple Stack.

Number of Stacks	Correction Factor
N	$N^{4/5}$
2	1.7
3	2.4
4	3.0
5	3.6
6	4.2
7	4.7
8	5.3

If a multiple stack source consists of stacks of approximately one height, and also stacks of a considerably different height, these could be treated as distinct groups of sources and the resulting concentrations from each group added to obtain the total concentration.

CHAPTER III

DESIGNING AIR MONITORING SURVEYS

Introduction

Choosing the "right" location for the "right" monitoring objective requires insight into the nature of air pollution emissions, transport, and dispersion from point, line, and area sources. Criteria for site selection which have been published in the air pollution literature (See Chapter II) consists of general, usually very subjective, recommendations as to the proper choice for a monitoring site. This chapter presents definitive methods for site selection, based on an engineering design approach developed by the author which utilizes available mathematical dispersion models, historical meteorological records, and mathematical solutions from probability and statistics. These tools can be used to provide judgement needed for selecting monitoring sites, setting sampling schedules, and planning the duration of study required to fulfill well defined sampling objectives.

Because many variables must be considered, site selection is one of the most complex and critical elements in the design of an air quality monitoring survey. If the wrong sites are chosen or if a critical site is missed, no amount of accurate data will allow the objective of the study to be fully realized. For this reason, most of this chapter is devoted to site selection. Variables to be considered regarding the proper location of a monitoring site include: the relative locations of pollution sources, physical characteristics of sources (e.g., geometry of source, height of emission, plume rise, etc.) emission rates,

meteorological variables and frequencies of occurrence (i.e., wind speed and direction, atmospheric stability category, vertical temperature structure, etc.), the location of potential receptors, and the monitoring objective proposed for the sampling station.

How to account for these variables in designing air monitoring surveys is the topic of this chapter. The chapter is organized in the following way: A quantitative description of microscale, mesoscale, and macroscale regimes is presented, followed by individual sections on selecting sites near line sources, area sources, and point sources of pollution emissions. Various sections describe methods of determining the numbers of sites needed, when and how long to monitor, sampling schedules, appropriate averaging times for samples, and statistical methods for evaluating the probability of success of a monitoring network.

Defining Micro-, Meso-, and Macroscale Air Pollution Regimes

In analyzing the spatial distribution of pollution concentrations it is important to recognize three separate air pollution regimes, the microscale regime, the mesoscale regime, and the macroscale regime. These regimes were defined qualitatively in Chapter I. This chapter defines the regimes quantitatively according to the magnitudes of the horizontal pollution concentration gradient. To fully understand the nature of each regime both definitions are combined (3,4).

- Macroscale: The macroscale air pollution regime is any air mass exhibiting ground level air pollution concentrations which deviate by less than 20 percent over linear distances greater than 10,000 meters. An example of a macroscale regime is "regional background" air pollution concentrations, which can be fairly homogeneous over linear distances from tens to

hundreds of kilometers. This does not mean, however, that there are not locations within the macroscale regime where ambient air pollution concentrations deviate by more than 20 percent from regional background levels. These deviations can and do occur when mesoscale and microscale air pollution regimes are superimposed upon the regional background air pollution concentration regime.

- Mesoscale: The mesoscale air pollution regime is any air mass exhibiting ground level air pollution concentrations which deviate by less than 20 percent over linear distances between 100 meters and 10,000 meters. The mesoscale regime represents a "community size" air mass exhibiting fairly homogeneous ground level air pollution concentrations-for example, "local background" ambient air pollution concentrations which result, especially within urban areas, from the emission of relatively small quantities of air pollutants from a large number of ground level sources (i.e., automobiles, residential and commercial space heating furnaces, and even numerous small industrial sources). These "local background" concentrations can vary considerably at different locations within an urban area. Concentration gradients greater than 20 percent per 100 meters indicate the presence of a microscale air pollution regime superimposed upon the mesoscale regime.

- Microscale: The microscale air pollution regime is any air mass exhibiting ground level air pollution concentrations which deviate by greater than 20 percent over linear distances up to 100 meters. The microscale air pollution regime represents a relatively small air mass exhibiting large variations in ground level air pollution concentrations. This phenomena usually occurs very near sources of air pollution when the rate of increasing atmospheric dispersion with downwind distance is very great.

From the above definitions it is apparent that ambient concentrations measured near major sources of air pollution consist of three component parts, the microscale concentration (contributed directly by the nearby source), the mesoscale concentration (the local background concentration due to area wide sources of pollutant emissions), and the macroscale concentration (the regional background concentration due to distant pollution sources). Frequently the macroscale pollution concentration is so low that this term can be ignored, leaving only two components to any ground level observation--the local background air

pollution concentration plus the microscale concentration due to a nearby source. Air monitoring sites located outside the microscale regime of highways and other point sources of pollution measure only mesoscale and macroscale concentrations (background).

Since concentrations at one site contain several component parts and because they can vary considerably at different locations within the microscale and the mesoscale regimes, it is important that monitoring sites be carefully selected. The selection of a site requires consideration of the regimes being sampled. This is important for two reasons: first, if the regime being monitored is not known, then on can not know to what sources to attribute high concentration measurements (i.e., close sources or distant sources?); second, the areal extent for which the observed concentration is "representative" will be impossible to determine (i.e., measurements within the microscale regime may be representative of the concentrations occurring only within a few meters of the sampling station, while measurements within the mesoscale regime should be representative of the concentration occurring within hundreds of meters radius of the sampling site).

Locating Monitoring Stations Near Highway Line Sources

Selecting microscale air monitoring sites. In this section, definitive methods for selecting sites are presented, based on the air pollution dispersion models outlined in the California Air Quality Manuals (8) and the quantitative definition of microscale and mesoscale regimes given above. Whenever the physical environment to be monitored violates either of these assumptions, the site selection methods presented may not identify the optimum site.

Figure 48 is a graphical description of the microscale regime near a highway; the regime extends from the upwind edge of the highway downwind where the ambient pollution concentration approaches the local background concentration. The figure shows the mechanical mixing cell, as defined in the California Model (46), where pollutants emitted by automobiles are thoroughly mixed resulting in a region where air pollution concentrations are uniform and relatively high. As the pollutants are transported and dispersed by the wind, the concentrations decrease as the distance from the highway increases. When the concentration approaches the local background concentration the boundary of the microscale regime has been reached.

The microscale regime can also be illustrated graphically by plotting isopleth lines of concentration levels as a function of the concentration in the mixing cell. Figure 49 is an example which shows lines of similar concentration downwind from the edge of a highway source in the horizontal direction, plotted on the abscissa, and the vertical direction, plotted on the ordinate. The family of curves plotted in Figure 49 illustrates the vertical and horizontal locations where the pollution concentration is reduced to 80%, 60%, 40%, 20%, and 10% of the roadside edge levels.

Figure 49 may be used to determine the optimum spacing for microscale monitoring stations used to collect data for validation of the California Line Source Model for the crosswind, C stability, ground level concentration case. Sites should be spaced so that the pollution gradient can be sampled at regular intervals. For a five-down-wind-

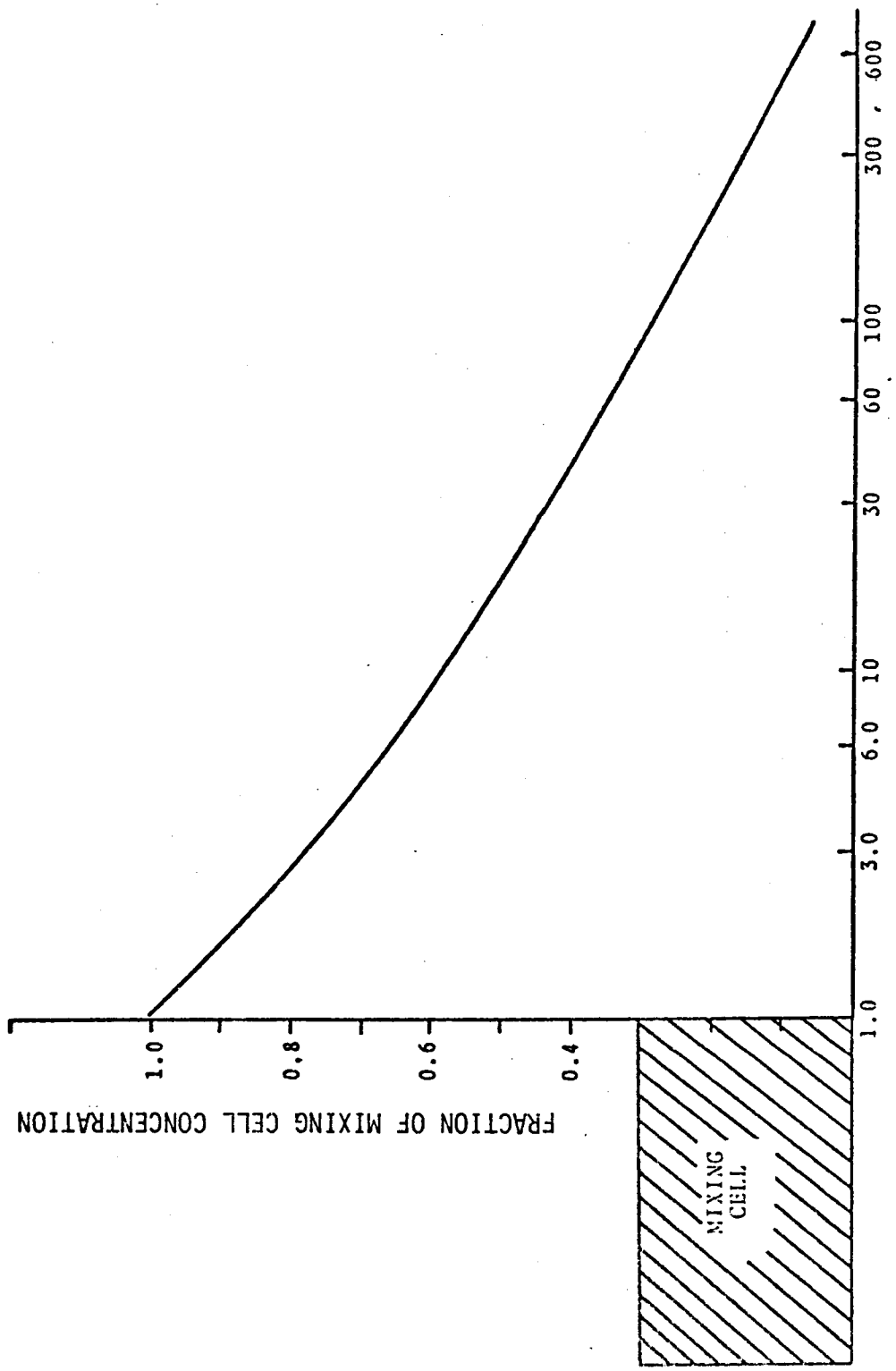

Figure 48. Decrease in Ground Level Ambient Air Pollution Concentration at Increasing Distance Downwind From Highway Edge. (According to California's Model (8)). Assumes C Stability and Zero Background Concentration.

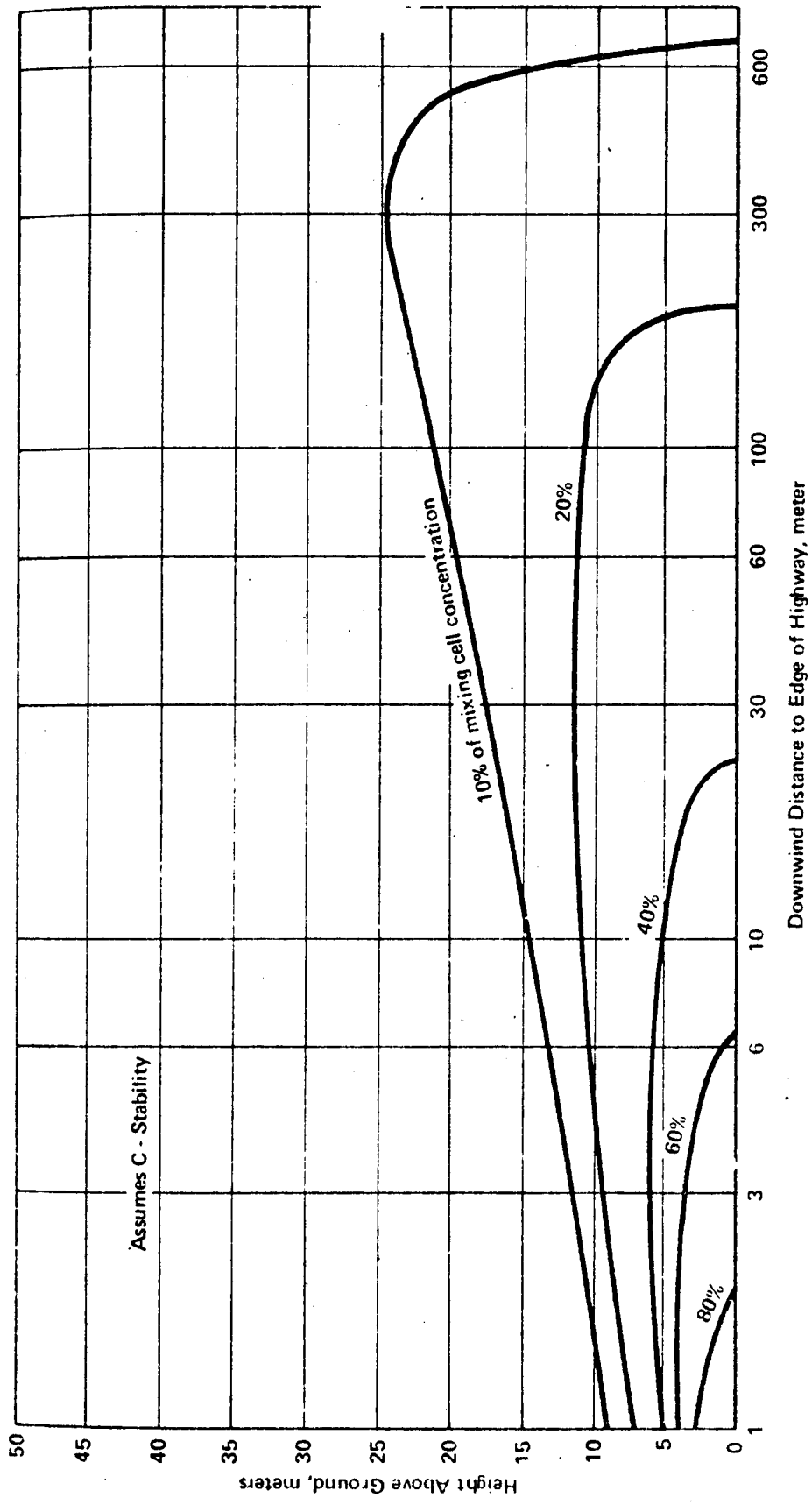

Figure 49. Isopleth Concentration Lines Downwind of a Highway Line Source. (California's Highway Model, At-grade Section (8).)

sampling-site network, sites located at the mixing cell, and at the 80%, 60%, 40%, and 20% isopleths would meet this requirement. The locations would be zero, 2, 7, 23, and 200 meters from the downwind edge of the pavement.

All the curves plotted in Figure 49 were determined using the California Highway Line Source Model (1) for crosswind conditions and C stability. This should provide optimum site spacing for ground level concentrations under C stability and crosswind conditions, but less than optimum for other conditions. In order to design the best possible site spacing pattern, an evaluation should first be performed to determine the full spectrum of events likely to occur downwind of the source. This can be accomplished using historical meteorological data and diffusion models. Figure 50 illustrates the results of such an evaluation, showing the normalized ground level concentration gradient versus normal distance from the road for all possible conditions as described by the California Line Source Model (8). Also given (in parentheses) is the frequency of occurrence of each condition of wind direction and stability taken from historical records for the time period (i.e., season and time of day) during which sampling is proposed.

Since the precise conditions of meteorology that will be encountered in the field cannot be predicted beforehand, the sampling sites should be selected based on optimum spacing for the most probable stability and wind direction condition determined for historical records. Choosing sites using the most probable stability and wind direction should provide the greatest amount of data collected from optimally located sites. If optimum spacing of sites is desired for measurements under a different

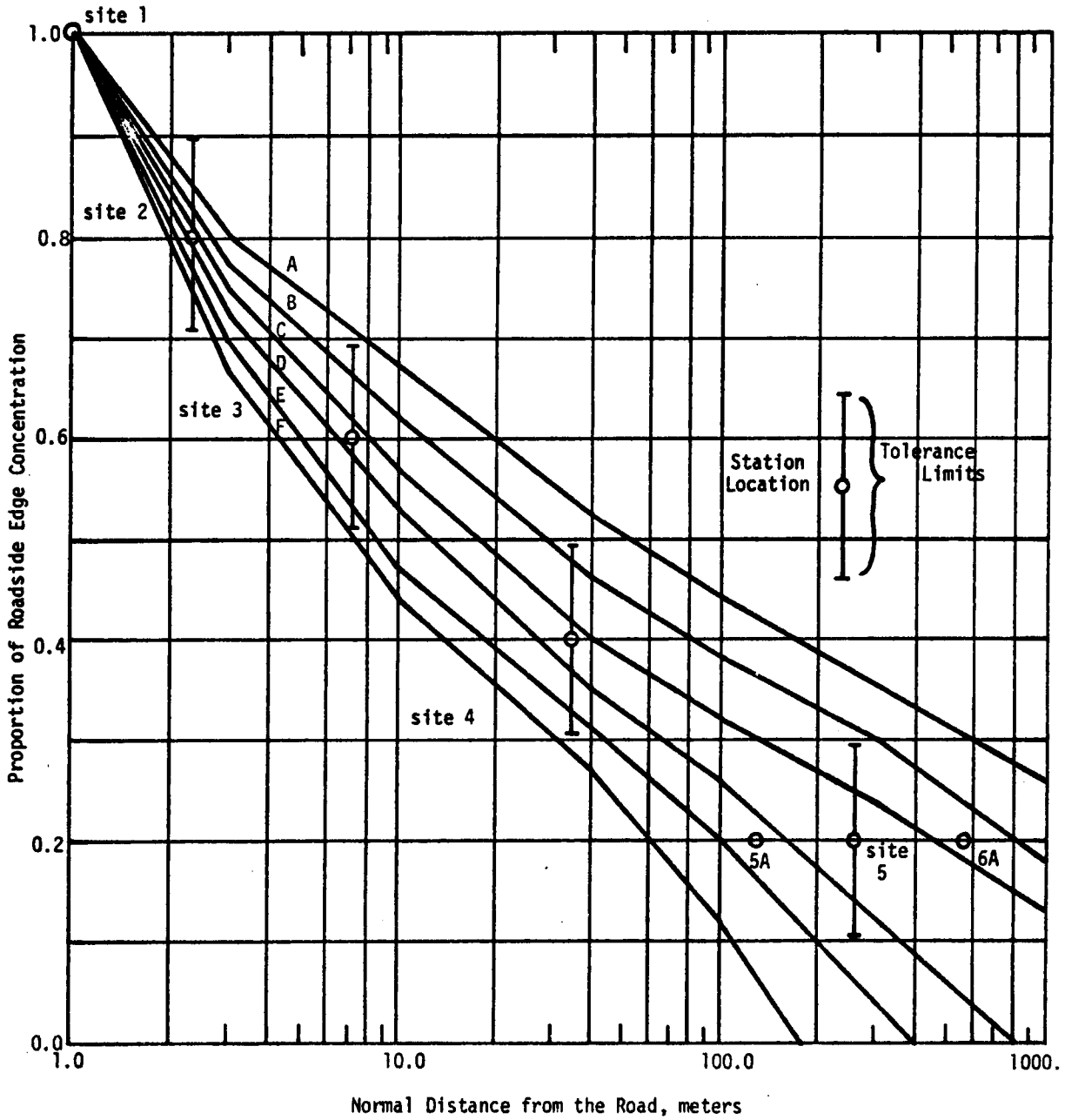

Figure 50. Optimum Locations of Air Sampling Sites Determined for Crosswind Conditions According to the California Model (8).

condition of meteorology, particularly the worst case condition of dispersion, additional sampling sites may be added in order to suppliment the coverage provided by sites already chosen. In this way the sampling array is designed to provide the best data under specific meteorological conditions (e.g., most probable and worst case) while providing less than optimum coverage for other conditions likely to be encountered during the study.

The site selection procedure is best described by use of an example such as Figure 50. The sites shown in Figure 50, located at distances 1, 2.3, 7.2, 33, and 260 meters from the road, were chosen in order to allow sampling during crosswind conditions at regular intervals of 100%, 80%, 60%, 40%, and 20% of the roadside "mixing cell" concentration, C_{mc}, within a tolerance range of $\pm$ 10% of C_{mc}. Using a 10% tolerance range, a site objective of 20% C_{mc}, for example, is considered met whenever the concentration is between 10%-30% C_{mc}. This tolerance range is shown graphically in Figure 50 by a vertical line centered at each site and crossing concentration lines predicted by the model. If the tolerance range crosses a concentration line, then the site can be expected to meet its intended sampling objective within $\pm$ 10%. Figure 51 shows the concentration profile lines predicted for both crosswind and parallel wind conditions and hypothetical frequencies of occurrence of each condition which can be determined from historical meteorological records. By summing the frequency of occurrence of each concentration profile line crossed, the frequency at which the monitoring site will meet its intended sampling objective can be determined. For example, the site locations shown in Figure 51 should meet their intended

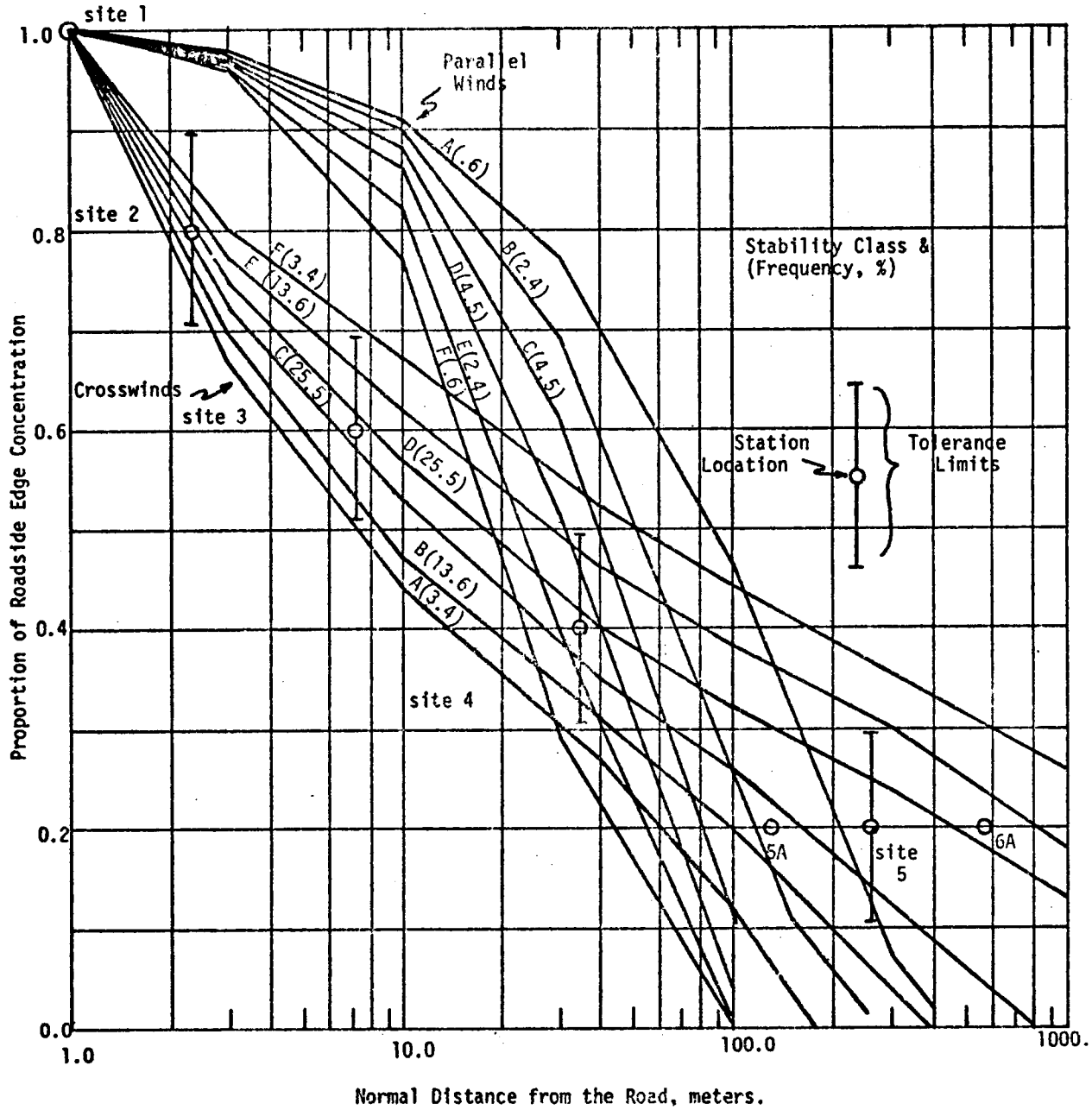

Figure 51. Relative Concentration Versus Normal Distance From an At-Grade Highway for All Wind Directions and Stabilities Calculated From the California Model (8).

objectives 100%, 85%, 81.6%, 78.2%, and 51% of the time for sites #1-5, respectively. However, these sites do not provide uniform coverage at regular intervals for parallel wind conditions, measuring at distances where the ambient concentration is roughly 100%, 97%, 89%, 53%, and <1% of the mixing cell for sites #1-5, respectively. If model validation under parallel winds is desired then additional sites may be needed to measure at distances away from the road where concentrations are reduced to ≈70% and ≈25% of C_{mc}.

The optimum location of each site is the distance from the road where the target concentration (i.e., 40% of mixing cell, etc.) can be measured most frequently (i.e., where the tolerance range crosses concentration profile lines having the greatest frequency of occurrence). In the example given in Figure 51 the poorest coverage is at site #5 which meets its stated objective only 51% of the time. An alternative design which should provide measurements of 20% C_{mc}, 78% of the time would be to move site #5 to 150 meters (site #5A) and add a sixth site at 600 meters (site #6). Site #5A could be used to measure 20 $\pm$ 10% C_{mc} during stabilities B, C, and D, and site #6 could measure 20 $\pm$ 10% C_{mc} during D, E, and F stabilities. This sixth site should allow an additional 27% of the data collected to be within the stated objectives at all sites. The use of a sixth monitoring site may be the most cost effective design, especially if it allows the duration of the study to be shortened because of the improved coverage of the sites.

Selecting mesoscale air monitoring sites. Data from downwind sampling sites describes the concentration of pollution from the project plus the background. For this reason, data from an additional station

located outside the microscale regime, but within the same mesoscale regime is required. This data is required to separate the pollution concentrations into two components, by subtracting the local background from the microscale concentrations measured. The contribution from the project can then be compared to model predictions. Usually a single monitoring station, properly chosen, can be used to establish background levels within the mesoscale regime. Microscale model validation experiments often utilize an array of air samplers located on both sides of the highway. As long as winds do not blow parallel to the roadway, samplers on one side of the highway will provide background data, while samplers on the other side of the highway will measure the highway contribution.

Figures 49 and 50 can also be used to determine a good location for a mesoscale site. The isopleth lines can be used to estimate the theoretical boundary separating the microscale regime of a nearby highway from the mesoscale regime. Once the boundary has been determined, stations designed to sample background concentrations can be located outside the boundary, while stations designed to sample pollutants from the highway plus background can be located within the boundary.

The isopleth which represents the boundary separating the microscale and mesoscale regimes depends on both the concentration within the mixing cell and the background concentration. Figure 52 provides a graphical method for determining which isopleth to use when sampling for carbon monoxide. The equations used in Figure 52 are:

$$\% C_{mc} = \frac{0.5\text{-}BKG}{C_{mc}} \times 100 \text{ for } C_{mc} \leq 2.5\text{ppm CO, or} \qquad (39)$$

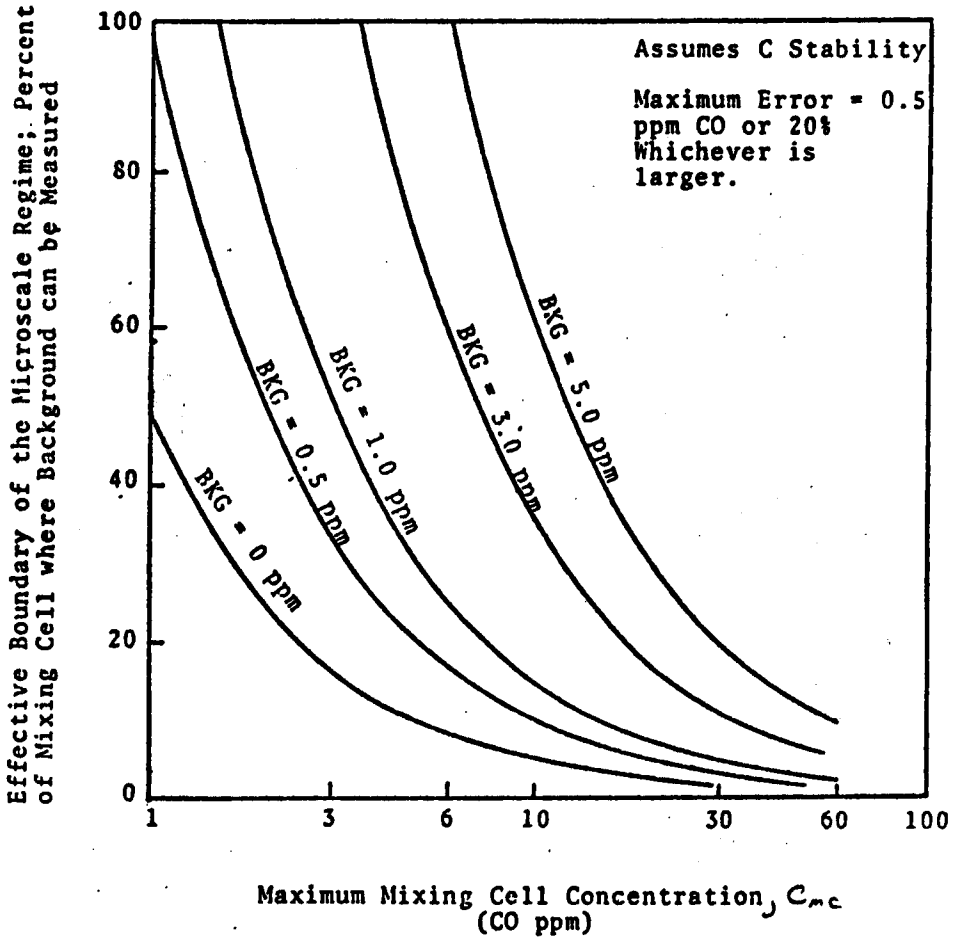

Figure 52. Percentage of Mixing Cell Concentration Where Background Concentrations can Effectively be Measured. (Function of Mixing Cell Concentration and Probable Background Level.)

$$\% C_{mc} = \frac{.2\ C_{mc} - BKG}{C_{mc}} \times 100 \text{ for } C_{mc} \geq 2.5\text{ppm CO.} \qquad (40)$$

This figure can be used to determine what percentage of the mixing cell concentration, $\%C_{mc}$, when added to the background concentration, BKG, will increase the background concentration by 0.5 ppm of CO or 20% (whichever is larger). This means that an air monitoring site located outside the designated isopleth (measured in percent of mixing cell concentration) will measure the local background concentration with an error of up to 20% or 0.5 ppm CO (whichever is larger).

Using Figures 49-52, the project engineer can determine the minimum distance downwind from the highway where a monitoring site should be located for measuring background levels. Mesoscale sites can be located at greater distances downwind or upwind as long as they are outside the microscale regime of the highway. Stations located upwind should also be located at greater distances than the minimum, because the wind direction changes frequently throughout the day and a sampling site that is upwind during one hour may be downwind the next.

There is also a maximum distance within which the sampling site should be located if there is another major source of pollutants nearby. This maximum distance depends on the distance to the source. (See Figure 53.) If a background sampling site is located too far away from the highway corridor for which local background measurements are desired, the measurements taken at the distant site may be significantly different from the local background concentrations which occur at the corridor under study.

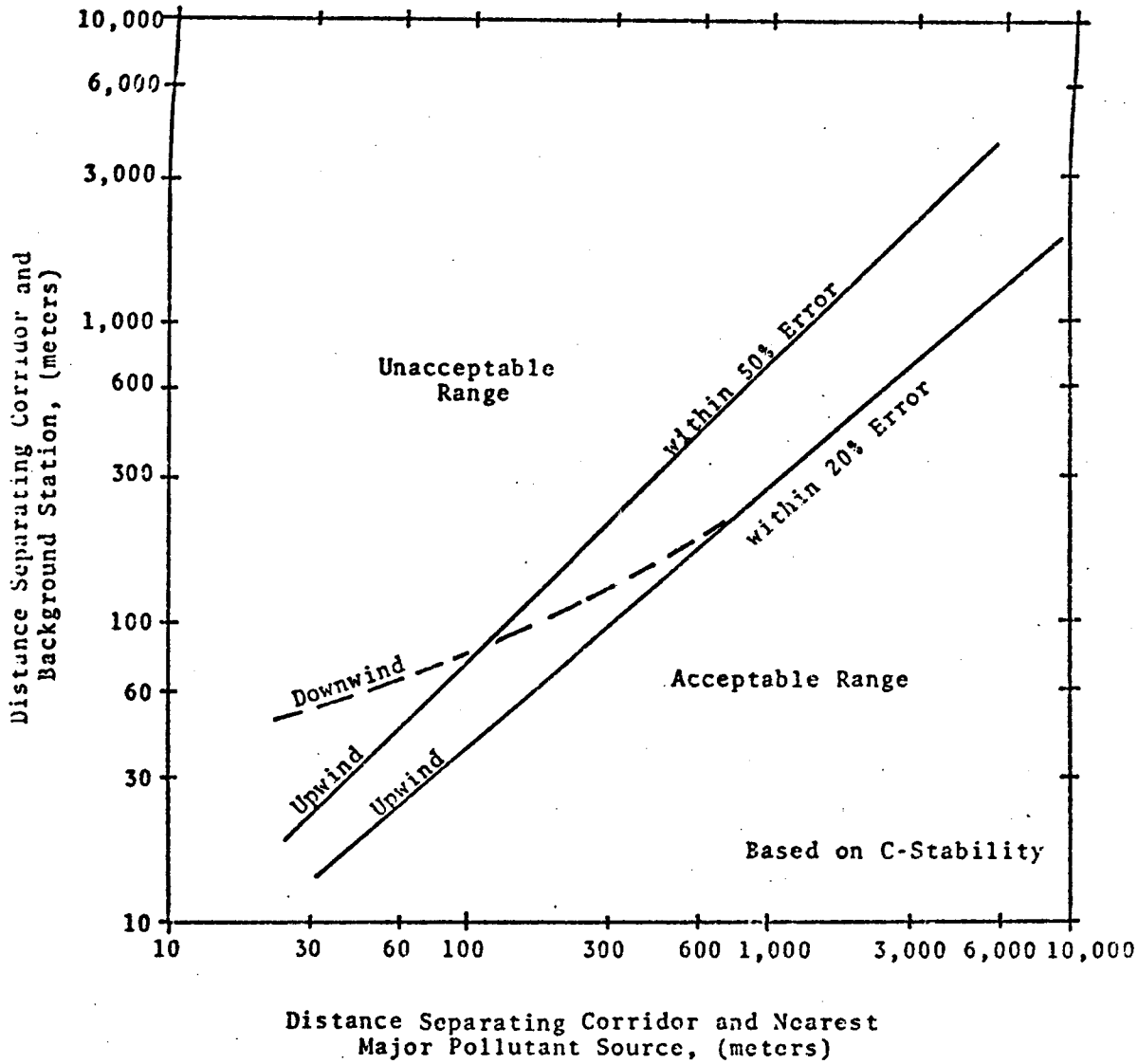

Figure 53. Maximum Distance From Project Corridor that a Mesoscale Background Station Should be Located vs. Distance to Nearest Major Pollution Source.

Figure 53 illustrates the maximum distance that a background site should be located from the highway corridor when other large sources are nearby. The limiting value is based on a maximum error of 20% between the value measured at the distant air sampling site and the expected local background concentration at the highway corridor.

Figure 53 is to be used in selecting a location for a mesoscale site when there is a heavily traveled freeway or arterial within 1,000 meters of the corridor under study. Under these conditions the maximum distance from the corridor and the minimum distance determined using Figures 49-52 may approach similar values. This indicates that the location of the sampling station should be selected precisely in order to obtain accurate results.

Besides the ground level sampling site locations discussed above, local background air pollution concentrations can be measured from air sampling stations located on the top of buildings. Mesoscale sites located on the top of buildings can provide useful and accurate information. However, the buildings must not be too tall or the measurements will not represent the background concentration at ground level. Pollution from nearby sources may contribute significantly to the ground level background concentrations, but not to those measured atop a tall building. For this reason, the height of the sampling site must be limited.

As in the case of the maximum horizontal distance away from a project corridor, the maximum height for a mesoscale monitoring site depends on the distance from the closest major source. Figure 54 illustrates the relationship between distance to a contributing source

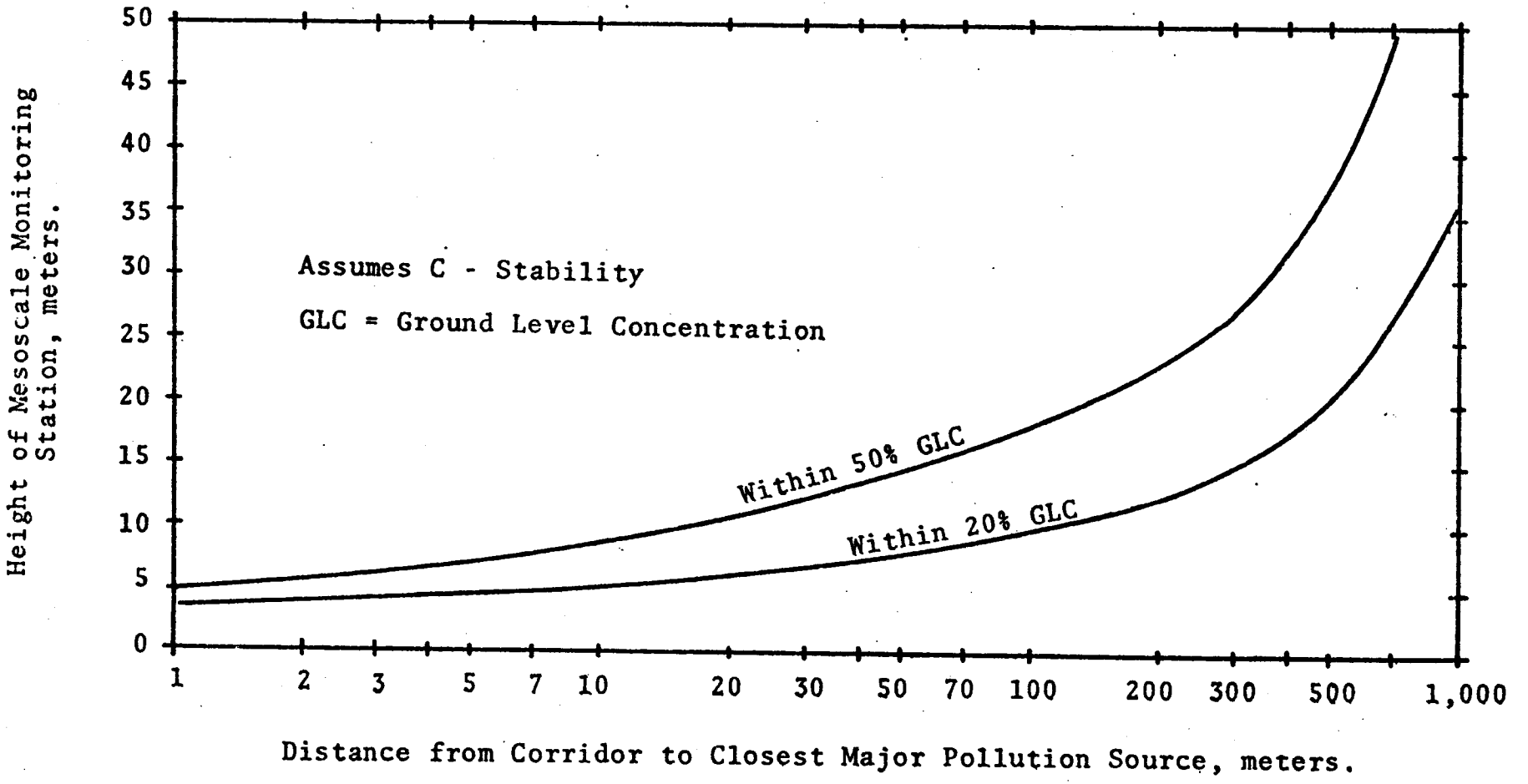

Figure 54. Acceptable Height of a Mesoscale Monitoring Station if Ground Level Concentrations are to be Measured.

and the percent of ground level air pollution concentrations occurring at different heights. With this figure the maximum height at which the local background concentrations can be measured (within an accuracy of 20% of ground level background) can be determined. This error estimate is conservative as it assumes that the closest major source contributes 100% of the ground level concentration and 80% at the indicated height. In practice, no single source would be responsible for all of the local background pollution concentrations, because sources located at greater distances from the sampling site contribute more uniformly to both the concentration at ground level and atop a building. Therefore, in practice, the error between the elevated and ground level measurements will be smaller than 20%.

Figures 49, 53, and 54 were developed using the California Highway Line Source Model for at-grade highway sections, crosswind conditions, and atmospheric stability class C. Stability class C was selected as the stability class most frequently encountered under daytime conditions with urban terrain. Clarke and McElroy (55) have reported measurements of a relatively unstable boundary layer over urban terrain even when adjacent rural environs exhibit very stable (stagnation) conditions near ground level. Clarke and McElroy's results tend to reinforce the use of C stability as the most probable condition encountered within urban environs. If different stability classes are desired, or different models are to be tested, then similar figures can be developed for selecting optimum air monitoring sites.

Where to validate microscale models. To obtain data for validating microscale models for environmental assessment, monitoring sites should

be chosen where:

- the highest concentrations from the project occur (due to large traffic volumes or narrow right-of-way)
- the highway configuration and upwind topography is most representative of the whole project, or
- the basic assumptions of the model are violated (due to highway configuration or topography).

The model may be validated where the highest concentrations occur because that is where the most confidence in the model is needed. Model validation at the most representative location allows the model to be applied generally to the whole project. Validating the model for irregular terrain (hills, valleys, or nearby tall buildings) or complex highway configurations (intersections, elevated or depressed sections, and unusual lane configurations) may be required since models are the least reliable when basic assumptions (i.e., smooth level terrain, uniform wind flow field, and wind speeds greater than 1 m/s) are violated.

Once the sites have been selected, the highway route should be monitored in cross-section sampling at various horizontal or vertical distances from the highway. Special attention should be given to measuring the air pollution concentration at the right-of-way edge. Background concentration measurements should be subtracted from downwind measurements to determine the contribution due to the highway.

Duration of a microscale. The sampling survey should be conducted for a sufficiently long duration so that observations are made under a wide range of source related and meteorology related conditions. The number of replications of each measurement needed for statistically valid results is discussed in Chapter II. Typically, if meteorological conditions are favorable, (i.e., a wide range of wind directions, wind

speeds, and atmospheric stabilities) an intensive air monitoring study lasting from 1-3 weeks is sufficient for microscale model validation. In most cases, air samples should be collected using 15-60 minute averaging times, but sampling for shorter averaging times can be used if traffic and wind data are gathered for comparable intervals. Averaging samples for time periods longer than one hour produces additional errors because changing wind direction has a non-linear effect on the downwind concentration. Whenever the wind direction is not persistent, the short averaging time samples (i.e., 15 minute averages) may be the best.

Air sampling may be conducted either during peak hour traffic or 24 hours a day. For model validation, it is desirable to sample during each hour of the day and night that there is enough traffic to produce measurable pollutant concentrations. In this way, a large amount of data can be collected over a short period of time to allow validation of the model under different meteorological conditions.

The duration of study required can be estimated using historical meteorological data and the statistical methods given in Chapter III. By way of model calculations, the average and range of concentrations expected to be measured at each station can be determined. The range divided by about six can be used to estimate the standard deviation. Dividing the range by six assumes that the extreme values calculated approximate the highest and lowest 0.1% of all possible concentrations. Using the nomograph in Figure 15, page 61, the number of samples needed can be estimated. The duration of study required can then be determined by dividing the number of samples required, n, by the frequency of

occurrence of a particular condition of meteorology expressed as a percentage, f, times the number of samples, S, collected at each site per day or hour.

$$\text{length of study required} = \frac{n}{f(S)} \qquad (41)$$

Typically, values of n range from 30-100 samples and S might be from 1-4 per hour. For unusual events occurring less than 5% of the time and if 40 samples were needed and S = 4 per hour, then the duration of study required would be 200 hours. At 12 hours a day of sampling, this would require more than two weeks of sampling. For frequently occurring conditions, sufficient data might be obtained in a few days.

Selecting Sites for Monitoring Area Wide Background Concentrations

Introduction. The methods presented in this chapter for selecting monitoring sites for area sources are designed primarily for use in determining background concentrations near major point and line source projects. Site selection is then constrained to determining the maximum concentrations due to area sources within the major impact area of the point or line source under study. Worst case air quality levels most likely occur where high background concentrations are added to high project concentrations. (See Chapter I.)

Where to monitor. The number and location of sites where background air pollution levels should be monitored will depend on the variety of homogeneous areas within the overall study area. Homogeneous areas can be selected on the basis of land use patterns, common meteorological regimes, types of highway design, and sensitive receptor areas, as outlined in Chapter I.

These features should be considered and may be plotted on a map of the area. Ideally, samples should be taken within each of the different homogeneous sections. However, if manpower and/or equipment limitations restrict the number of sampling sites, the sites to be air monitored should be selected on a priority basis. Three locations have particular priority for environmental assessment: (See Figure 1, page 6.)

- where the maximum project concentrations, C_{max}, is expected,
- where maximum background, C_{Bmax}, is expected, and
- where high air pollution concentrations are expected at sensitive receptors.

Determining where maximum project concentrations, C_{max}, occur can be accomplished by use of an appropriate line or point source dispersion model. In the case of surveillance of a single major source (point or line) the location of C_{Pmax} and the spatial distribution of air pollutants is primarily dependent on meteorology. For area sources, with ground level emissions, the spatial distribution of conservative air pollutants (i.e., not photochemical) is primarily dominated by the distribution of sources because the effects of meteorology are the same for all sources. The one exception is the accumulation of pollutants in the downwind direction, (See Figure 40, page 97) where C_{max} occurs downwind of the greatest continuous area source extent.

Where maximum background concentrations are expected can also be determined using a mesoscale air pollution dispersion model. Otherwise, the best procedure may be to use a grid method of identifying where pollution emissions are high and subsequently concentrations will probably be high. The procedure for using the grid method is to:

1. Locate the project area on a topographic map.
2. Identify probable homogeneous meteorological regimes based on uniformity of topography.
3. Divide each meteorological regime into areas of homogeneous land use.
4. Divide each land use area into uniform grid squares. (See example for a proposed highway corridor, Figure 55.)
5. Calculate the hourly or daily average ground level air pollution emission flux (in $ug\text{-}m^{-2}\text{-}sec^{-1}$) for the grid squares from available emission inventories or traffic data.
6. Use the emission flux values as an indication of where monitoring stations may be appropriate.

Homogeneous meteorological regimes are assumed to prevail except where ground surface features affect the wind flow field. Surface features such as mountains, ridges, valleys, coastlines or large lakes, and divergent urban and rural land forms should be noted as possible boundaries separating homogeneous meteorological regimes. Within each meteorological regime, areas of homogeneous land use can be divided into uniform grid squares. (Figure 55.) The size of the grid square can vary; however, grid squares smaller than one square kilometer are not recommended. As shown in the figure, areas with low, uniform emission rates can be represented with larger grid squares. Areas where emission rates are relatively high and variable, as in downtown areas, may be better represented by small ones.

After the grid squares have been labeled according to emission flux (See Figure 56), the general locations where high and low concentrations

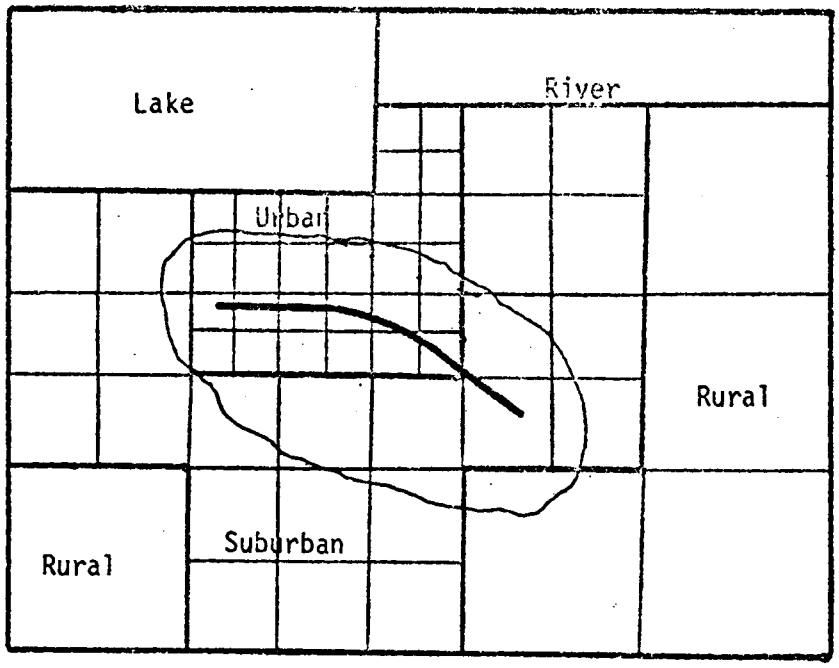

Figure 55. Study Area Divided into Grid Squares According to Land Use.

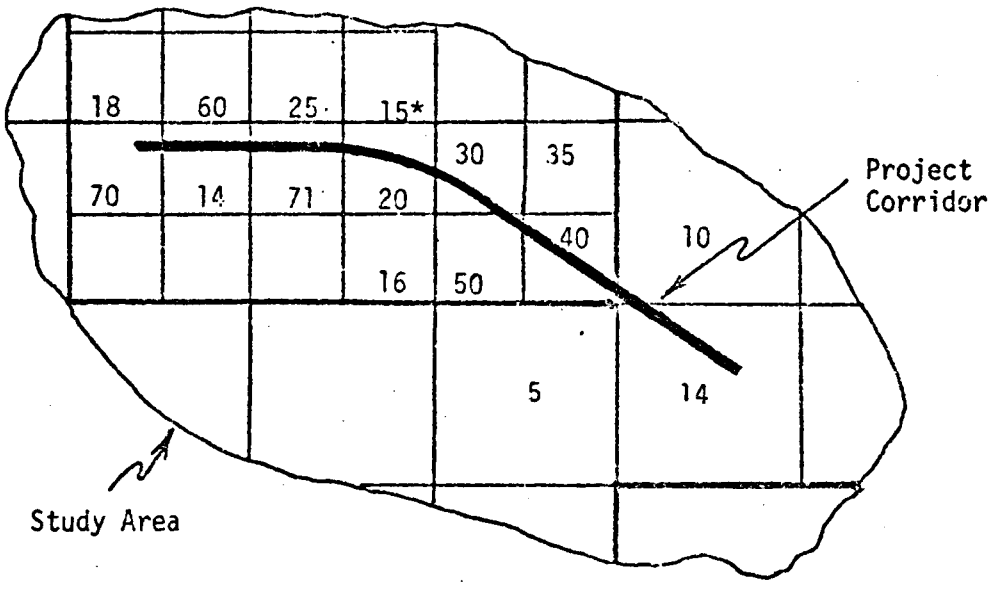

Figure 56. Average Emission Flux Values for Each Grid Square near Project Corridor.

*Numbers represent average area source emission densities of CO in ug/m^2-sec.

occur can be inferred. Gifford and Hanna (10) have developed a simplified urban air pollution model employing uniform grid squares. They consider the accumulation of pollutants as the wind passes over a city to be a "weak function of city size." For quite large grid areas, 5 x 5 km or more, where the emission flux varies little from grid to grid, the grid square containing the receptor point is "as a rule the dominant one." For this reason, Gifford and Hanna (10) conclude that it may be unnecessary to include the influence of remote upwind source areas.

Grid squares labeled according to emission flux can be used to determine where the highest pollution concentrations are likely to occur. Using grid blocks such as shown in Figure 56, it is possible to estimate the location of the maximum background concentration, C_{Bmax}. A monitoring station near the center of the maximum grid square should provide reasonable results. The highest concentrations will occur within the highest grid probably toward the downwind side. An additional station near a downwind edge of the grid may be desirable. When good spatial resolution of background is needed stations should also be located within grid squares having moderate and low emission fluxes.

Locating monitoring stations near sensitive receptors is as important as measuring the maximum background concentration. Maximum background is needed for "full disclosure" in environmental impact statement, however, the impact at sensitive receptors must also be documented. Some data is needed to assure that levels at sensitive receptors will be lower than levels at maximum background sites, especially if levels are expected to be near the NAAQS (National Ambient Air Quality Standards),

or if controversy is anticipated. Whenever possible, some amount of monitoring should be conducted at each sensitive receptor site along the project corridor. Sensitive receptors may, of course, be selected for physiological or political reasons.

Once the general locations for mesoscale monitoring sites have been selected, the specific location of each site should be determined using the information presented in Figures 49-54 to insure that the site is within the appropriate mesoscale regime and outside any micro-scale regimes. Care should be taken to insure that each sampling site meets the additional criteria of:

- area wide "representative exposure"
- accessibility for personnel
- availability of electrical facilities (if needed)
- provisions of some degree of equipment security (storm damage and vandalism).

Number of mesoscale sites required. A survey designed to provide good spatial resolution for background levels within the mesoscale regime must have the "right" number of stations, at the "right" location. The number of sites needed will depend on the diversity of land use, the meteorology, the number of sensitive receptors, and the degree of spatial resolution desired. Figure 5, page 25 illustrates the relationship between the number of stations, the level of equipment and sophistication employed at each station, and the expected quality of the resulting study in terms of the ability to provide spatial resolution. The three zones designated as "poor," "acceptable," and "good" estimate the spatial resolution expected for the experiment. Use of only a

few stations will provide "poor" spatial resolution, because the locations where minimum, maximum, and average concentrations occur cannot be clearly separated and identified. A study achieving "good" spatial resolution requires simultaneous measurements from many locations to establish the area wide mean concentration while identifying locations where the minimum and maximum concentration occur. "Acceptable" spatial resolution requires several carefully selected stations, which provide sufficient evidence that the location where the highest concentrations occur has been identified and monitored, and that the levels everywhere else within the study area exhibit lower pollution concentrations. Under conditions of moderately diverse land use, a survey designed to provide an "acceptable" level of spatial resolution may require from 5 to 15 sites. If land use patterns are very diverse, more sites may be needed.

Averaging times for the air samples and duration. An air quality study should provide adequate temporal, as well as spatial, resolution of air pollution concentrations. An air sampling survey designed to provide good temporal resolution within the mesoscale regime must: (1) include samples having a short enough averaging time to compare to one hour air quality standards; and (2) last long enough for the effects resulting from all possible combinations of source strength and meteorological phenomena to be observed or at least reliably estimated using statistical techniques. Obtaining samples averaged over a short interval requires either continuous sampling, or grab samples collected over one hour intervals. This eliminates several methods of air sampling which collect samples averaged over much longer time periods. Monitoring

long enough to sample all variations of source strength and meteorology may require as long as a year.

Continuous monitoring for one year assures that samples are taken during all seasons of the year, on all days, and during all hours. Such sampling would provide the best data describing the temporal distribution of pollution concentrations. However, the high cost of maintaining and operating such a station, as well as the long lag time between the initiation of the survey and the final results are unreasonable. Therefore, most surveys must compromise the best available methodology by using a sampling schedule designed to include only the periods when the highest pollution concentrations are expected to occur. In this way the "worst case" pollution levels can be determined while the temporal distribution of low concentrations will be less accurate. Such a sampling program would tend to report "conservatively higher" results. This compromised survey would be a "worst case" analysis, and usually would represent an acceptable approach for assessing environmental impact.

In order to conduct a "worst case" analysis, periods of high pollution concentration must be predictable. When designing sampling schedules, one must know when the highest concentrations are likely to occur and schedule accordingly. In most urban areas, these time periods are regular and reproducible. Some air pollutants exhibit "worst case seasons" during the year, "worst case days" during the week and "worst case hours" during the day. For example, the worst case season for ozone might be summer; the worst case days might be weekdays; and the worst case hours might be from 12 noon to 7 p.m. A survey designed to provide a "worst case" analysis for ozone at such a station would only require

monitoring between 12 noon to 7 p.m. each weekday during the summer months. Compared to a full year study, this is a considerable reduction in the amount of monitoring required. Figure 57 illustrates hypothetical temporal profiles of ambient CO and O_3 air pollutant concentrations with typical seasonal, daily, and diurnal air pollution trends. Specific profiles can be developed with historic data available from CAMP stations or state and local air pollution control agencies.

Seasonal, daily, and diurnal pollution profiles vary for different pollutants, different geographical areas (macroscale variations), and at different locations within a study area (mesoscale variations). This is due to variations in source strength and meteorology. The most reliable method for predicting the worst case periods is to use historical air pollution measurements from an air monitoring station operated by the local Air Pollution Control Department (APCD) and located within or near the study area. The highest pollution concentrations should correspond to the periods of peak concentrations measured at the APCD stations. This is true only when the APCD station is located within the same mesoscale regime as the study area. If the APCD station measures pollutants within a microscale regime or is located very distant from the study area, there can be large differences in the occurrence of maximum concentrations. Similar temporal profiles in ambient pollution level cannot necessarily be inferred. For example, if the APCD station is located near the south edge of an urban area and the study site is near the north edge, maximum background concentrations at the APCD will occur when winds blow from the north; conversely, maximum concentrations at the study site will occur when winds blow

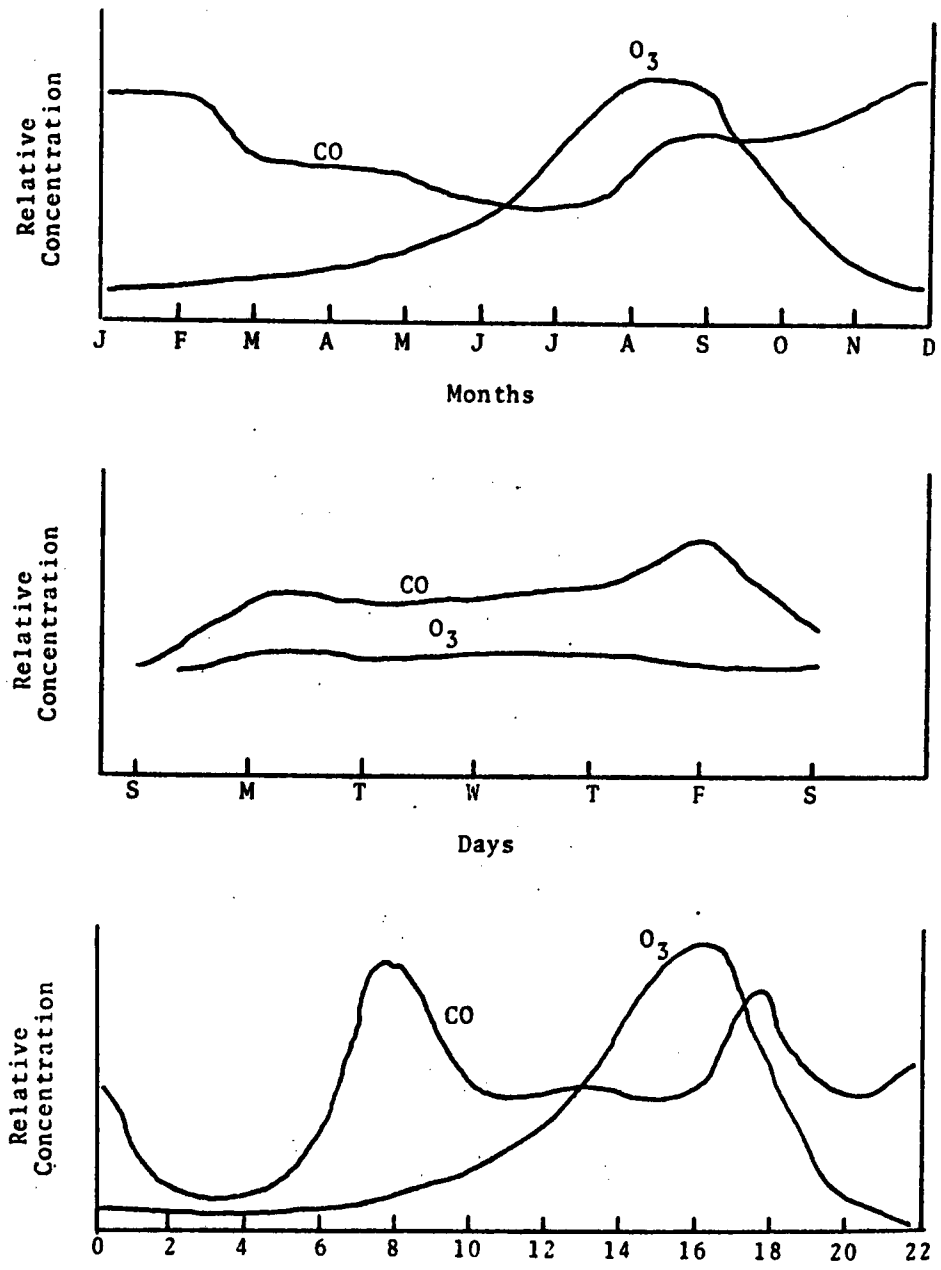

Figure 57. Hypothetic Profiles of Typical Seasonal, Daily, and Hourly Fluctuations in CO and O_3 Concentrations.

from the south. In this example, the "worst case season" for APCD station might be during the winter when the prevailing winds are out of the north, while the "worst case season" for the study site might occur during the season of the year when the prevailing winds are southerly.

Peak concentrations can also be "out of phase" with APCD peak measurements when the study site is located several kilometers from the APCD station. For example, in an urban area photochemical oxidant concentrations may peak at midafternoon, this same air mass might then be carried over rural terrain. The ground level oxidant concentration in the rural area would peak several hours later in the afternoon.

These examples illustrate that historical data can be misused for predicting worst case time periods. Historical data should be used, but judiciously taking into account the effects of wind speed, wind direction, and relative location of the APCD station and the study site.

Sampling schedules. Once the most probable worst case periods have been estimated, a sampling schedule can be prepared which includes all these worst case time periods. The duration of the sampling survey should be increased by 35-50% to assure that worst case conditions are observed. This additional sampling should be conducted half before and half after the expected worst case time period. For example, when the worst case season is estimated between mid-December and the end of January, an additional ten days of sampling during the first weeks of December and the first weeks of February would provide a safety factor to assure that worst case concentrations are included. Typically,

background carbon monoxide studies should be conducted for one to six months including the worst case season of the year.

When employing a sampling network consisting of primary and secondary sampling stations, sampling schedules for secondary stations may require sampling only on some of the days that the primary station is operated. Choosing which days can be done systematically (i.e., every other day, or every third day), or randomly (i.e., using a random number table). An unbiased sampling schedule should be prepared at the beginning of the sampling program and followed to its conclusion. The primary stations should be sampled at least every third day to assure that no major meteorological phenomena, such as high pressure related subsidence inversions or stagnations, are entirely missed.

The number of days that sampling is required can be estimated using Figures 15-18, pages 61, 62, 65, and 66. For example, if the predicted standard geometric deviation of daily average SO_2 concentrations is between 2.0 and 3.0 and the worst case season can be predicted within 90 days, the number of days which require sampling in order to determine the daily mean SO_2 concentration within $\pm$ 20% with 95% confidence is from 34 to 56 days (derived from Figure 18, page 66). The sampling days should be evenly distributed over the 90 day period. The specific days can be chosen on either a systematic or a random basis.

Applying Diffusion Models to Selecting Air Monitoring Sites Near Point Sources

The following sections describe a general methodology for selecting air monitoring sites near point sources. The objective of monitoring a point source is assumed to be to determine the maximum impact of the

source on air quality in the immediate area. Most important are the maximum ground level concentrations which occur for various averaging times (i.e., 1-hour, 3-hours, 1-day, and 1-year). The basic approach taken here is to determine where the maximum concentrations are expected to occur using point source atmospheric diffusion models, then locate monitoring sites in these areas. Measured concentrations can then be compared to NAAQS.

The methodology recommended includes six major steps: (1) an evaluation of historical meteorological records, (2) setting precisely defined monitoring objectives, (3) running models to determine C_{max} and where it most likely occurs, (4) determining the size of the representative sampling area which can be covered by a single station (coverage ratio), (5) determining the minimum number of sites needed to insure a desired number of observations of C_{max} (a statistical approach), and (6) the optimum number of location of stations required to meet monitoring objectives with a high probability of success.

Evaluate historical data. It is very important before choosing a monitoring site to evaluate the type and frequency of meteorological conditions likely to occur, especially conditions adverse to the dispersion of air pollutants. This includes wind speeds, wind directions, atmospheric stability conditions, mixing heights, vertical temperature gradients and any other available data pertinent to atmospheric diffusion. Ground level pollution concentrations near point sources are highly dependent on meteorological conditions which affect plume rise and the rates of transport and diffusion of pollutants.

There are a number of meteorological phenomena which produce especially high ground level pollutant concentrations. Some of the most important conditions are inversion breakup fumigation, plume trapping by an elevated inversion, and coning under critical wind speeds. These conditions usually produce the highest concentrations but occur infrequently. Other equally important conditions are those which produce near maximum concentrations and occur much more frequently (such as, stable and unstable conditions with low wind speeds). It is also valuable to determine the meteorological conditions which occur most frequently (i.e., annual mean wind speed and neutral conditions) since these conditions may affect long term average concentrations. Before selecting air monitoring sites the meteorological conditions for which monitoring data is desired must be specifically delineated. Locations where the maximum concentrations occur under these conditions can then be determined using diffusion models.

Using model results to delineate potential zones for monitoring. When selecting air monitoring sites near a point source it is highly desirable to have a good idea where these maximum concentrations are likely to occur so that the monitoring station can be so located. At the present time the best method of determining where the maximum concentrations occur is to use point source diffusion models. The diffusion of air pollutants from point sources is quite complex due to the number of variables interacting to affect nearby ground level concentrations (i.e., wind speed, wind direction, atmospheric stability, inversion heights, plus emission rates, plume rise, and topographic effects). Therefore, the meteorological conditions which produce

maximum pollution levels are not always easy to determine. However, an organized step-by-step approach can be used to determine the locations where maximum levels occur and the likelihood that an air monitoring station located at these points would in fact measure the maximum values.

Because sampling objectives may include monitoring under many meteorological conditions, a large number of sites may be required. A good method of selecting potential zones for monitoring is to display the results of diffusion calculations as shown in Figure 58. This figure shows graphically the range of distances downwind from the source where maximum concentration occur under each range of meteorological conditions. This figure can then be used to select potential sampling sites. For example, a site located in zone (1) would be needed to monitor during low wind speed and unstable conditions; zone (2) is required for monitoring during both trapping and inversion breakup conditions; zone (3) could monitor during conning at critical wind speeds and mean wind speeds under neutral conditions; zone (4) could monitor both mean wind speed-neutral conditions and low wind speed-stable conditions; in some cases sites in zone (5) may be desirable to document that ambient levels are less outside the major impact area described by the inner zones.

Figure 58 becomes even more valuable when calculated values of maximum concentration, C_{mc}, are recorded in each box as well as the probable frequency of occurrence of various wind speed, stabilities, mixing heights, and wind directions which can be obtained in summary form from the National Weather Service (27). This data can then be used to establish priorities in choosing monitoring sites. Monitoring

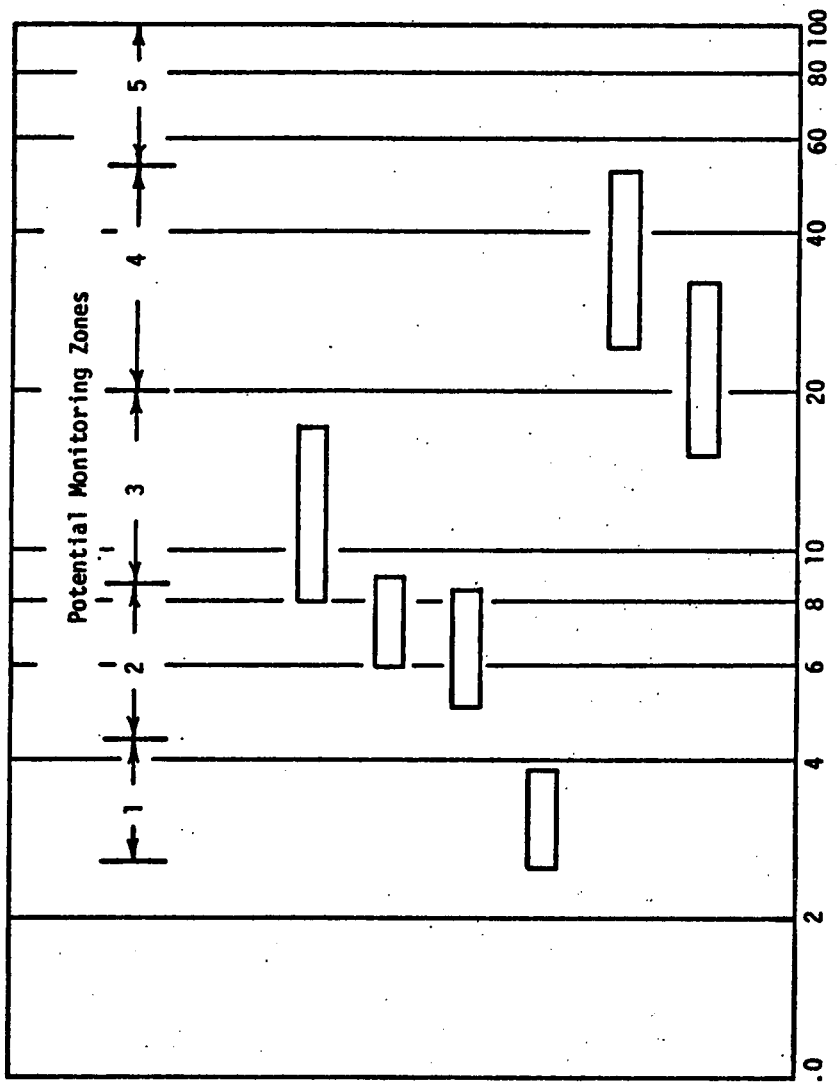

Figure 58. Identifying Potential Zones Where C_{max} May Occur.

locations where maximum concentrations occur very frequently should probably receive a higher priority than locations where C_{max} occurs infrequently.

Calculating C_{max} and X_{max} using models. When using diffusion models to assist in air monitoring site selection, the most important result obtained is where the maximum ground level concentrations, C_{max}, occur. For a point source C_{max} occurs along the plume centerline at a distance, X_{max}, from the source. Several methods are presented to determine C_{max} and its location downwind X_{max}.

The first step in point source modeling is to calculate the plume rise. This can be done using TVA's nomograph presented in Chapter II, Figure 41, page 103. Using Figure 41, the plume rise under either neutral or stable conditions can be estimated for various wind speeds. This value for plume rise, Δh, plus stack height, h_s, equals the effective stack height, h_e, used in diffusion calculations. Other methods of calculating the expected plume rise have been presented by Briggs (46) and Fay (47) which can be used in place of Figure 41 if preferred. Most authors agree that estimating plume rise under unstable conditions is questionable at best due to the lack of data and uncertainties in defining air motions under unstable conditions. For this reason a conservative solution is recommended, that is, to underestimate plume rise by using TVA's (52) nomogram for neutral conditions and wind speeds = 3 m/sec. (3 m/sec is TVA's reasonable minimum $\bar{u}$ at stack top.)

The next step is to determine the distance downwind where the maximum concentrations occur under each meteorological condition of interest. This can be determined for the coning plume, trapped plume,

and inversion breakup fumigation by using nomograms prepared by TVA shown in Figures 46-47, pages 110 and 111. Another method, which is especially appropriate for short to moderately tall stacks where inversion breakup fumigation and plume trapping are not problems, employs a figure prepared by Turner (7). (See Figure 45, page 109.) By first using Figure 41, page 103, to determine the plume rise, Figure 45 can then be used to determine the distance downwind where the maximum concentration occurs. This figure is based on the Pasquill-Gifford (36) curves for σ_y and σ_z. This figure is also convenient for calculating C_{max}.

Each of the methods described for locating potential monitoring sites give precise results implying that the best location is at exactly the distance calculated by the models. In fact, diffusion calculations as recommended above do not predict accurately the precise location where maximum concentrations occur. A more realistic solution to the models is to calculate where maximum concentrations occur for a narrow range of conditions rather than a precise point. For example, rather than determine where the maximum concentration occurs for neutral stability at the mean wind speed, U = 5.7 m/sec, it would be more realistic to determine X_{max} for wind speeds for say 4-7 m/sec. X_{max} would occur at different locations for U = 4 m/sec due to the difference in plume rise. The frequency of occurrence of wind speeds between 4-7 m/sec could be determined from historical meteorological summaries such as STAR (56). When calculating X_{max} locations for each meteorological condition of interest it is recommended that wind speed ranges of at least $\pm$ 1 m/sec be used in place of precise values, so that a range of distances of X_{max} and frequencies of occurrence can be determined.

Determining the optimum number and location for sites. When air monitoring near point sources the number of sites needed to confidently determine the total impact of the source can be quite large. As shown in Figure 58, four or five zones may require data in a single direction downwind. If this number is multiplied by the number of directions from which the wind can blow, then a very large number of monitoring sites seems necessary. In practice, such a large number of sites is usually out of the question so that the survey objectives must be compromised by monitoring in only a few selected downwind directions. Which downwind directions should be monitored can be determined from an examination of historical wind direction/frequency data; and a consideration for the potential receptors in each direction.

Realistically, maximum ambient air pollution concentrations can never be measured precisely because of the extremely large number of sampling locations it would require to define the entire concentration profile and identify the maximum. Even when diffusion models are used, they predict that maximum concentrations, C_{max}, occur at a single point on the ground; however, by using a tolerance range about C_{max} an area can be defined within which the ambient concentration is equal to C_{max} minus the tolerance range. Monitoring locations can then be chosen within this defined area for the purpose of measuring maximum concentrations within some tolerance (i.e., within 10% of C_{max} or within 20% of C_{max}, etc.). The acceptable tolerance range will have an effect on the number and location of stations for air monitoring; the greater the tolerance, the fewer stations will be required. An acceptable tolerance range should be based on analysis of the maximum expected levels compared to air

quality standards. If maximum levels are expected to be near standards then the tolerance should be small. Conversely, low concentrations need not be resolved as accurately as high concentrations, so that a greater tolerance range may be acceptable. The example calculations and figures presented in this paper assume a tolerance range of 10%. Similar figures can be prepared for other tolerance values.

Before selecting specific sites for air monitoring within each zone it is necessary that some general solutions of Gaussian point source dispersion models be carefully looked at. From these general solutions conclusions may be drawn regarding the proper location and spacing of sampling sites.

Representative sampling area. One of the most important determinations which can be made using the models is the size, shape, and extent of the representative sampling area about a monitoring station. Representative areas can be defined using a tolerance range in the same manner as the areas about the point where C_{max} occurs were defined. Knowing the size and shape of the representative area allows guidelines for minimum spacing between stations, and assists greatly in determining the number of stations required.

From Turner's (7) curves (See Figure 42, page 105) of normalized concentration, x U/Q, versus distance downwind, x, it is apparent that the point where the maximum ground level concentration occurs is also where the rate of change in the concentration with respect to downwind distance is at a minimum. This means that concentrations are fairly uniform where C_{max} occurs. Turner's curves can be used to determine

the distance toward and away from the source within which the concentrations deviate from C_{max} only by some minimum amount (such as 10%). Figure 59, determined graphically from Turner's curves, shows the radial distance from the source, X_{10}, within which concentrations are within 10% of C_{max} when the peak occurs at X for two stability classes.

Besides being used to determine the extent of the "representative area" in the radial direction, Figure 59 also provides at least an upper limit to the number of monitoring sites needed in this direction. Even if sites are to be located to provide complete coverage so that at least one station monitors concentrations within 10% of C_{max}, the maximum number of stations required can be determined graphically as shown in Figure 60. Figure 60 illustrates the same boundaries shown in Figure 59 except that each "step" represents the area which can be covered by a single monitoring site. For example, if all C_{max} values are expected to occur within 1-10 km, then, from Figure 60, the maximum number of downwind stations needed in one direction is 4-5. Note that under unstable atmospheric conditions the boundaries in Figure 59 are narrower such that more "steps" are required to cover the same distance shown in Figure 60.

In addition to the downwind extent of the "representative area," it is also important to know the crosswind extent. The distance, Y_{10}, within which concentrations are within 10% of C_{max} can be calculated from the equation,

$$(1-0.10) = \exp -\frac{1}{2}\left(\frac{Y_{10}^2}{\sigma_y^2}\right) \qquad (42)$$

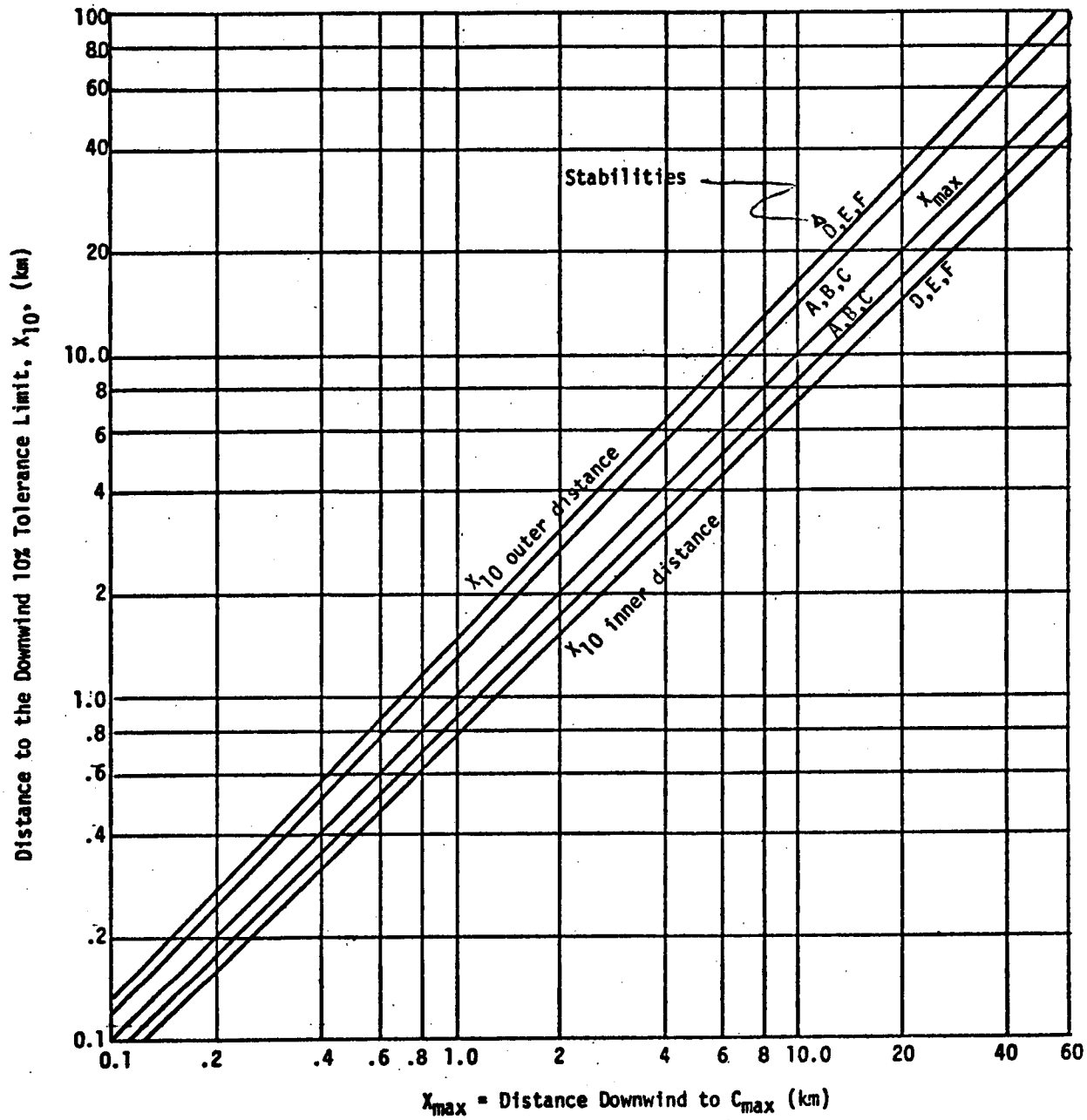

Figure 59. Graphical Method for Determining X_{10} Versus Distance Downwind to X_{max}. (X_{10} = distance from the Source to 0.9 C_{max} = $|X-X_{max}|$).

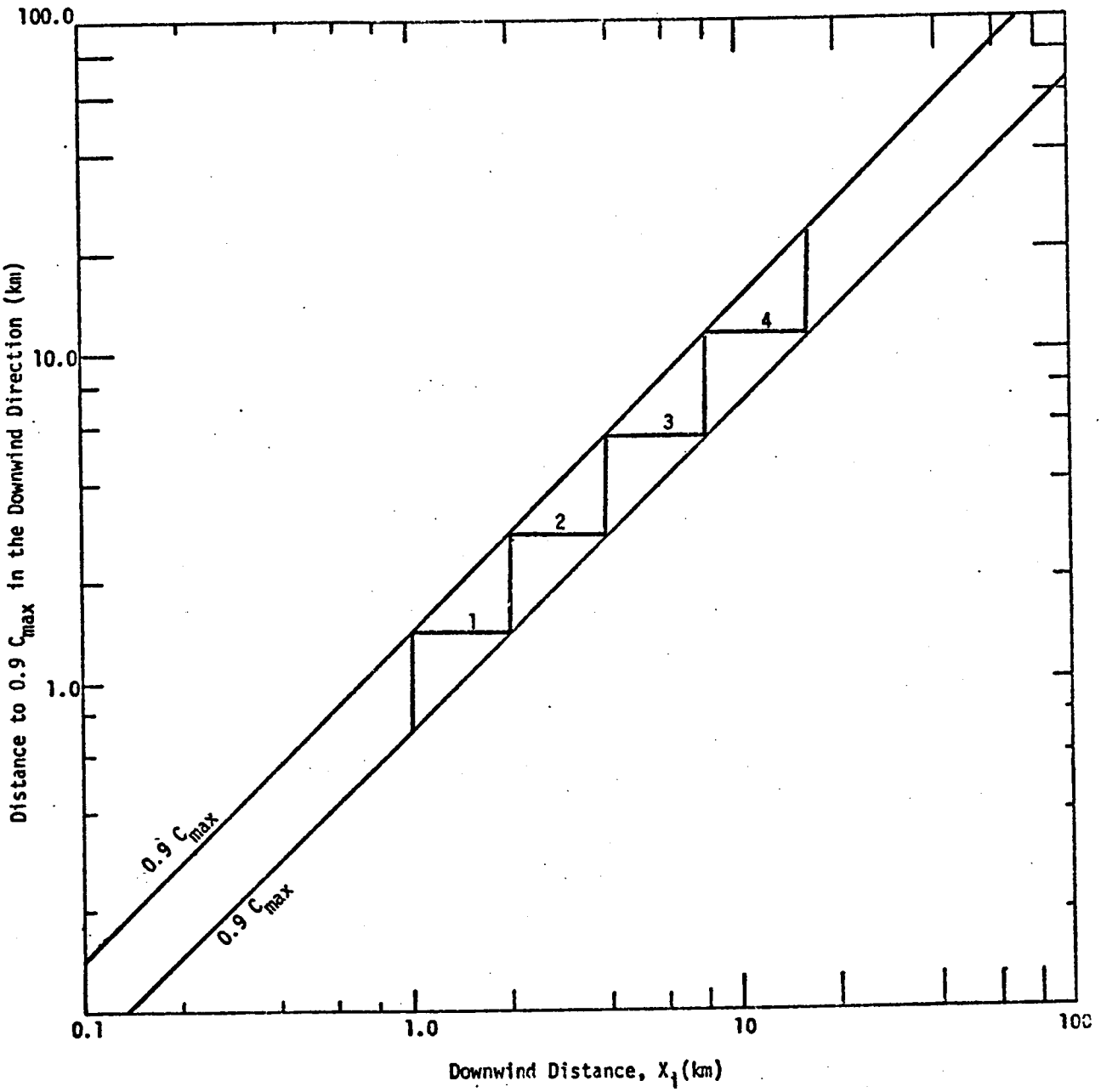

Figure 60. Illustrating the Number of Sites Needed to Maximize Coverage Between 1-10 km for D Stability.

which is derived from the general Gaussian plume Equation (14). This reduces simply to,

$$Y_{10} = 0.92\ \sigma_y(x). \qquad (43)$$

Values of Y_{10} for various distances downwind, and stability classes are plotted in Figure 61 (σ_y's are Pasquill-Gifford values).

Values of X_{10} and Y_{10} can now be calculated to determine the size and shape of the "representative area" under C_{max} conditions. As is apparent from a comparison of Figures 60 and 61, values of X_{10} tend to exceed Y_{10} by an order to magnitude for most stabilities. This results in an impact area which is ellipical in shape, (an ellipse is used here to approximate what is actually a "teardrop" shape) with a long major axis in the radial direction from the source and a relatively short minor axis in the crosswind direction. An example of an impact area an arbitrary distance from a source is illustrated in Figure 62. This configuration of the impact area under C_{max} conditions should be taken into account when proposing air monitoring sites.

The best method for determining the optimum number and location of monitoring sites is to take into account the size of the "representative area" under C_{max} conditions, the size of the potential zone requiring monitoring (from Figure 58), and the frequency of occurrence of meteorological conditions causing C_{max} values in each zone. A statistical approach is the most appropriate. The first step is to determine the ratio of the representative area of a monitoring station located in the center of a potential zone to the area encompassed by the zone (the zone is "donut" shaped if wind direction is not accounted.

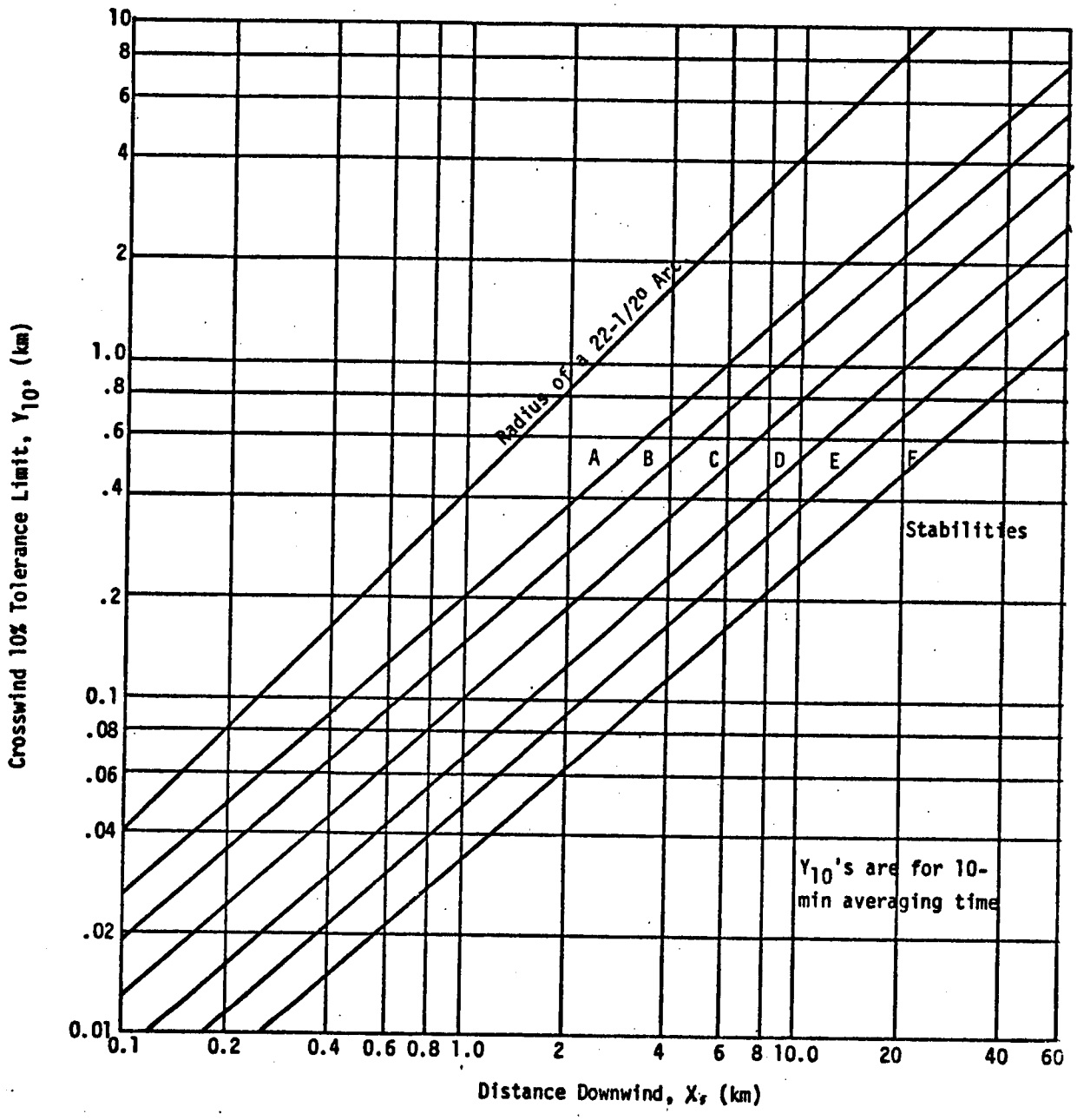

Figure 61. Y_{10} Versus Distance Downwind for Six Stabilities.

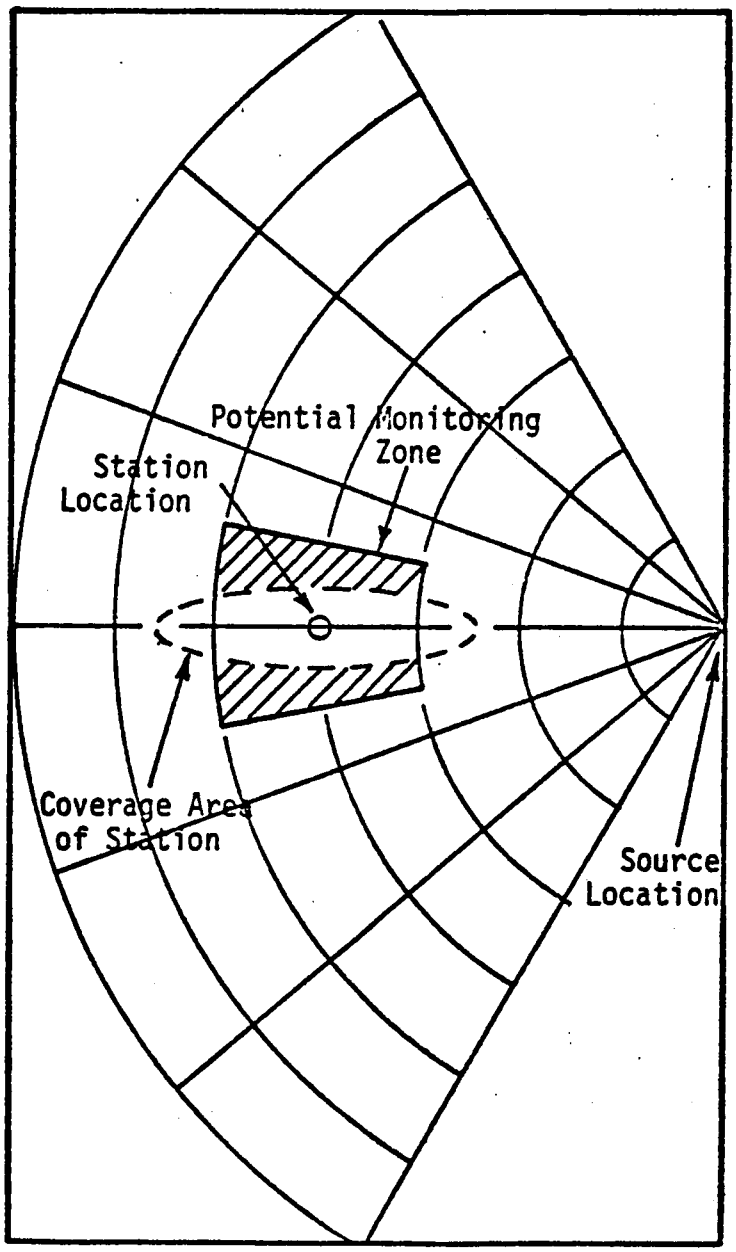

Figure 62. Illustration of the Coverage Area of a Single Station Downwind of a Point Source. (Shaded area represents the area within the potential monitoring zone not covered by the station. The ratio of the coverage area to the total area of the potential zone equals the coverage ratio.)

for). If X_{10} <(radial dimension of the zone), then the proportion of the zone covered by a single monitoring station can be calculated from,

$$CR_S = \frac{\text{Area of Ellipse}}{\text{Area of Sector}} = \frac{\pi\left(\frac{X_{10}+Y_{10}}{4}\right)^2}{\pi(X_{z_0}-X_{z_1})^2} \qquad (44)$$

where

CR_S = the coverage ratio for one station (without regard for wind direction)

X_{z_1} = inside radius of circular zone, and

X_{z_0} = outside radius of circular zone.

Figure 62 depicts the representative area, a potential zone, and the coverage ratio, CR, graphically. Coverage ratios, CR, can be calculated for a single station, CR_S, or for all stations combined. The sum of all station coverage ratios equals the total coverage ratio, CR_T, for the network. To calculate coverage ratio for a single wind direction, multiply the CR from Equation (44) by the number of wind sectors the "donut" shaped zone is divided into.

The area where the maximum concentration, C_{max}, will occur divided by the area where it could occur is equal to the coverage ratio for a single station and the probability, P, that one station located anywhere within the areas where C_{max} could occur will actually measure C_{max}. To calculate the probability that one station will measure the maximum concentration n times when the meteorological conditions causing C_{max} occur N times per year can be calculated using the binomical distribution function (56).

$$P = \frac{N!}{n!(N-n)!} C.R.^{n}(1-C.R.)^{N-n} \quad (45)$$

For large values of N, the probability, P, or coverage ratio, CR, is best determined by using the normal approximation to the binomial distribution and solving for the statistic, Z. The probability associated with various Z values can be determined from the statistical table given in Table VII. Z is calculated using the equation

$$Z = \frac{n-NP}{(NP(1-P))^{1/2}} \quad (46)$$

The analysis of the Gaussian plume previously discussed indicates that the area where maximum ground level concentrations occur is very narrow in the Y-direction and quite long in the X-direction (See Figure 62). For this reason, the likelihood that a monitoring station will successfully observe maximum levels is highly dependent on its circumferential location about the source. For this reason, simplified estimates of CR for $X_{10} > (X_{z_o}-X_{z_i})$ are sufficient in most cases. CR is then determined by dividing $Y_{10}(x)$ by either the circumference of a circle, for all wind directions, or a single arc about the point source for one wind direction, having a radius equal to the downwind distance, x. The circumference can be calculated using the equation,

$$\text{Circumference} = 2 \pi x. \quad (47)$$

Using this simplified method of estimating the coverage ratio of a station, CR_S, Figure 63 was prepared which gives coverage ratios for one station located within a single $22\text{-}1/2^{o}$ wind sector plotted against

Table VII

Table of Probabilities Associated with Values as Extreme as Observed Values of z in the Normal Distribution.

z	.00	.01	.02	.03	.04	.05	.06	.07	.08	.09
.0	.5000	.4960	.4920	.4880	.4840	.4801	.4761	.4721	.4681	.4641
.1	.4602	.4562	.4522	.4483	.4443	.4404	.4364	.4325	.4286	.4247
.2	.4207	.4168	.4129	.4090	.4052	.4013	.3974	.3936	.3897	.3859
.3	.3821	.3783	.3745	.3707	.3669	.3632	.3594	.3557	.3520	.3483
.4	.3446	.3409	.3372	.3336	.3300	.3264	.3228	.3192	.3156	.3121
.5	.3085	.3050	.3015	.2981	.2946	.2912	.2877	.2843	.2810	.2776
.6	.2743	.2709	.2676	.2643	.2611	.2578	.2546	.2514	.2483	.2451
.7	.2420	.2389	2358	.2327	.2296	.2266	.2236	.2206	.2177	.2148
.8	.2119	.2090	.2061	.2033	.2005	.1977	.1949	.1922	.1894	.1867
.9	.1841	.1814	.1788	.1762	.1736	.1711	.1685	.1660	.1635	.1611
1.0	.1587	.1562	.1539	.1515	.1492	.1469	.1446	.1423	.1401	.1379
1.1	.1357	.1335	.1314	.1292	.1271	.1251	.1230	.1210	.1190	.1170
1.2	.1151	.1131	.1112	.1093	.1075	.1056	.1038	.1020	.1003	.0985
1.3	.0968	.0951	.0934	.0918	.0901	.0885	.0869	.0853	.0838	.0823
1.4	.0808	.0793	.0778	.0764	.0749	.0735	.0721	.0708	.0694	.0681
1.5	.0668	.0655	.0643	.0630	.0618	.0606	.0594	.0582	.0571	.0559
1.6	.0548	.0537	.0526	.0516	.0505	.0495	.0485	.0475	.0465	.0455
1.7	.0446	.0436	.0427	.0418	.0409	.0401	.0392	.0384	.0375	.0367
1.8	.0359	.0351	.0344	.0336	.0329	.0322	.0314	.0307	.0301	.0294
1.9	.0287	.0281	.0274	.0268	.0262	.0256	.0250	.0244	.0239	.0233
2.0	.0228	.0222	.0217	.0212	.0207	.0202	.0197	.0192	.0188	.0183
2.1	.0179	.0174	.0170	.0166	.0162	.0158	.0154	.0150	.0146	.0143
2.2	.0139	.0136	.0132	.0129	.0125	.0122	.0119	.0116	.0113	.0110
2.3	.0107	.0104	.0102	0099	.0096	.0094	.0091	.0089	.0087	.0084
2.4	.0082	.0080	.0078	.0075	.0073	.0071	.0069	.0068	.0066	.0064
2.5	.0062	.0060	.0059	.0057	.0055	.0054	.0052	.0051	.0049	.0048
2.6	.0047	.0045	.0044	.0043	.0041	.0040	.0039	.0038	.0037	.0036
2.7	.0035	.0034	.0033	.0032	.0031	.0030	.0029	.0028	.0027	.0026
2.8	.0026	.0025	.0024	.0023	.0023	.0022	.0021	.0021	.0020	.0019
2.9	.0019	.0018	.0018	.0017	.0016	.0016	.0015	.0015	.0014	.0014
3.0	.0013	.0013	.0013	.0012	.0012	.0011	.0011	.0011	.0010	.0010
3.1	.0010	.0009	.0009	.0009	.0008	.0008	.0008	.0008	.0007	.0007
3.2	.0007									
3.3	.0005									
3.4	.0003									
3.5	.00023									
3.6	.00016									
3.7	.00011									
3.8	.00007									
3.9	.00005									
4.0	.00003									

The body of the table gives one-tailed probabilities under H_0 of z. The left-hand marginal column gives various of z to one decimal place. The top row gives various values to the second decimal place. Thus, for example, the one-tailed p of $z \geq .11$ or $z \leq -.11$ is p - .4562.

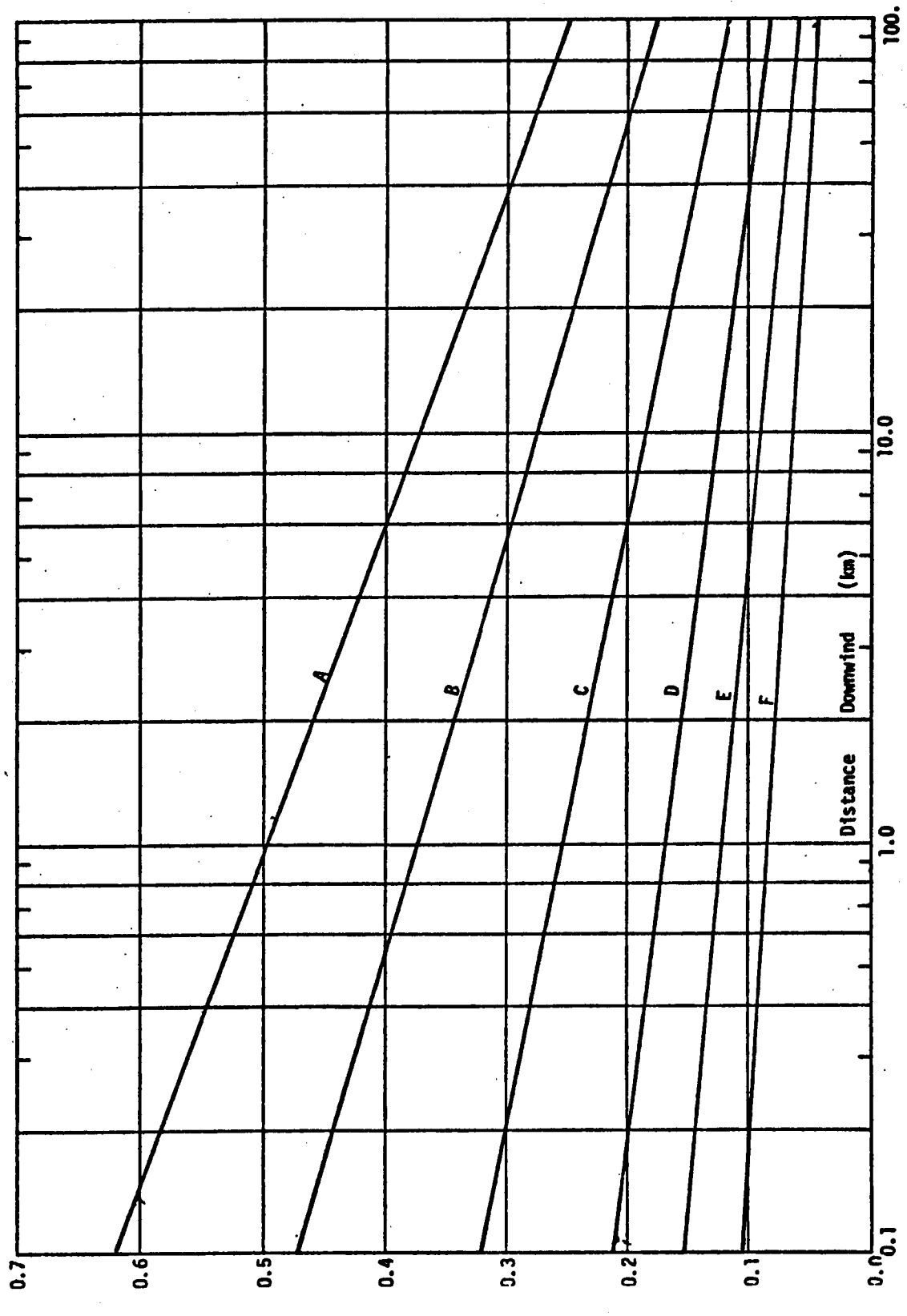

Figure 63. Single Station Coverage Ratios, CR_S, Versus Distance Downwind for Six Stability Classes. (CR_S values are for 10 min. averaging times.)

downwind distance, x, for various stabilities. Using this figure coverage ratios for single stations can be determined assuming they are properly located in the downwind direction, x.

The calculated value for CR, plus the probable number of occurrences of the meteorological conditions producing C_{max} in a given zone can then be used to determine the probability of n successful measurements of C_{max} using Equation (46); or if the number of desired successes is fixed, then the probability or coverage ratio required to assure at least n successes within a desired level of confidence can be calculated. General solutions of Equation (46) are given in Figure 64. This figure can be used to determine the total coverage ratio, CR_T, required to allow n successful measurements of C_{max} with 99% confidence given the frequency of occurrence, N, each year of the meteorological event producing C_{max}.

After solving the total coverage ratio required, the number of stations needed in the crosswind direction can be calculated.

$$N_S = \frac{CR_T}{CR_S} \tag{48}$$

where

N_S = number of stations needed,

CR_S = coverage ratio of each station, and

CR_T = total coverage ratio required to achieve desired results.

The effect of averaging time on coverage ratio. Coverage ratios are highly dependent on the extent of the representative sampling area in the Y-direction, which is in turn dependent on the averaging time of the sample. Several authors (i.e., Hino (58), Turner (7), et al.)

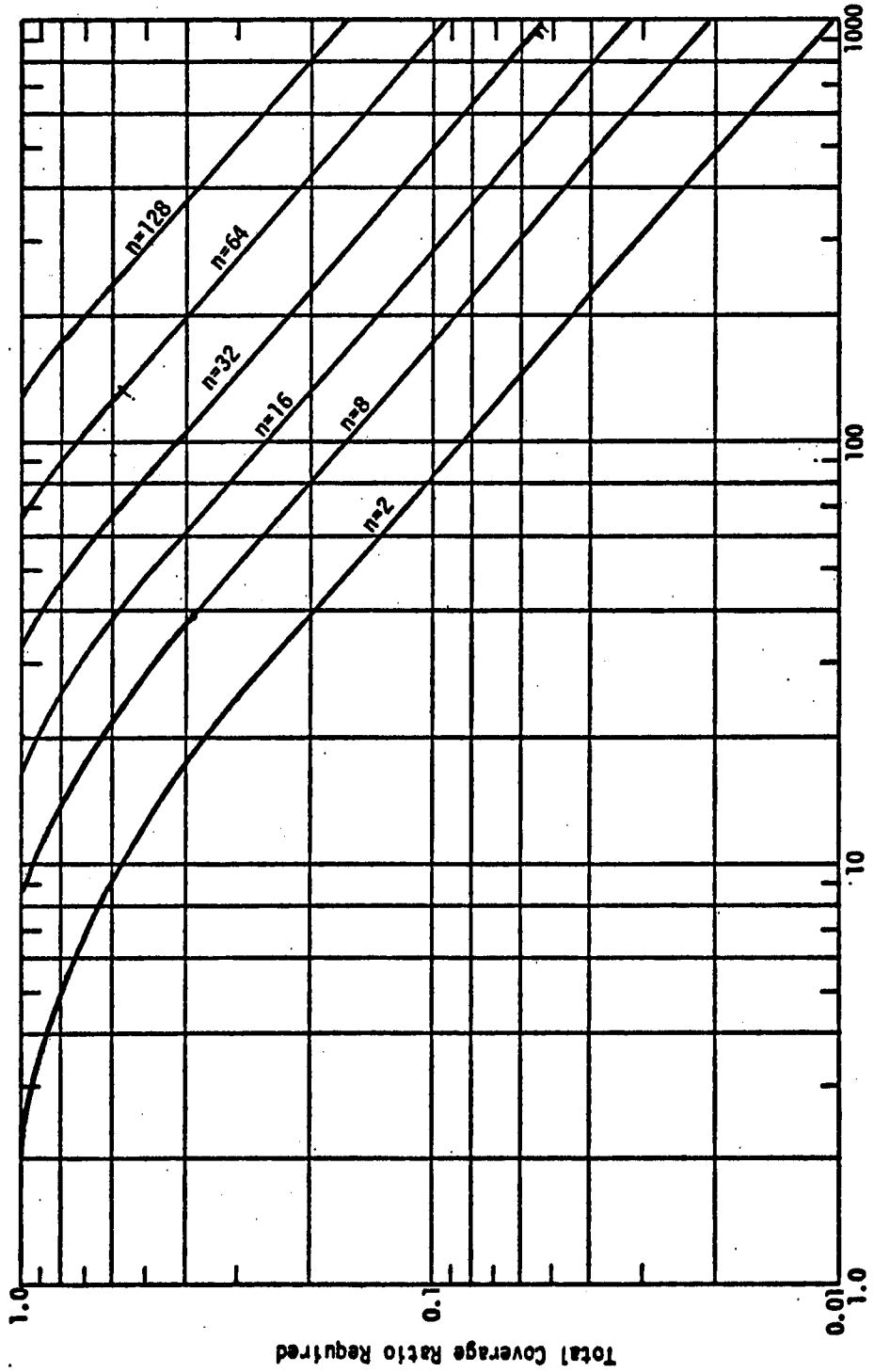

Figure 64. Coverage Ratio Required to Observe C_{max}, n times, with 99% Confidence, versus the Number of Occurrences, N, of Meteorological Phenomena Causing C_{max}.

have pointed out the relationship between σ_y and sample averaging time, usually expressed as the exponential relationship,

$$\sigma_y \propto (t)^{-0.5} \tag{49}$$

where t = averaging time in minutes. (Also see Figure 65.) The physical cause of increasing σ_y with averaging time is due to the effects of meandering wind direction.

Because $CR \propto Y_{10} = .92\ \sigma_y(x)$, the coverage ratio varies with averaging time. The values of Y_{10} given in Figure 61 are for 10 minute average concentrations. For longer averaging times the effect of meandering wind direction is to increase Y_{10}. Correction factors, CF, which can be used to increase Y_{10} and subsequently CR_S to account for averaging times different from 10 minutes can be calculated from the equation:

$$CF = \frac{(10)^{-0.5}}{(t)^{-0.5}} = .316t^{0.5} \tag{50}$$

Typical values are:

1-hr	2.4
3-hr	4.2
10-hr	7.7
24-hr	12.0

Can one station observe C_{max} twice? The number of stations required to observe C_{max} at least twice can be determined using Figure 64, however, what is the likelihood that C_{max} will be observed twice by the same station (appropriately applicable to checking compliance with NAAQS)? This probability is solely dependent on the coverage ratio of each station and not affected by the number of stations used. Figure 66 can

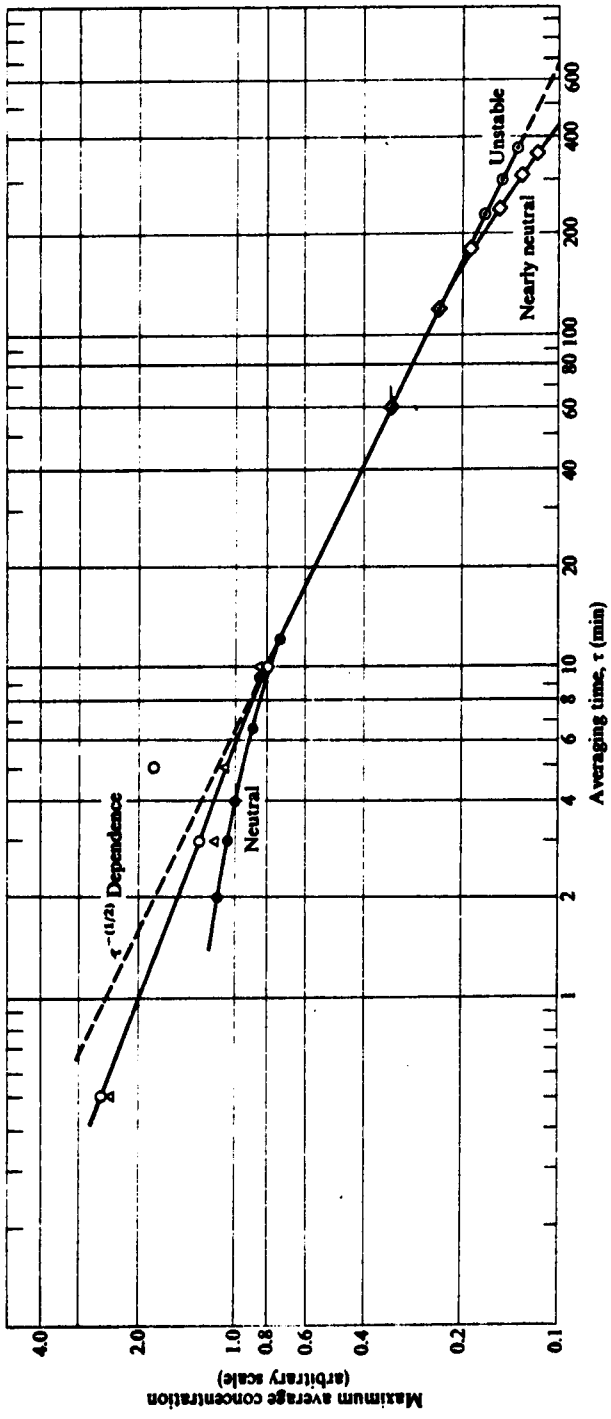

Figure 65. Dependence of the Maximum Concentration on Averaging Time. (From Hino (58).)

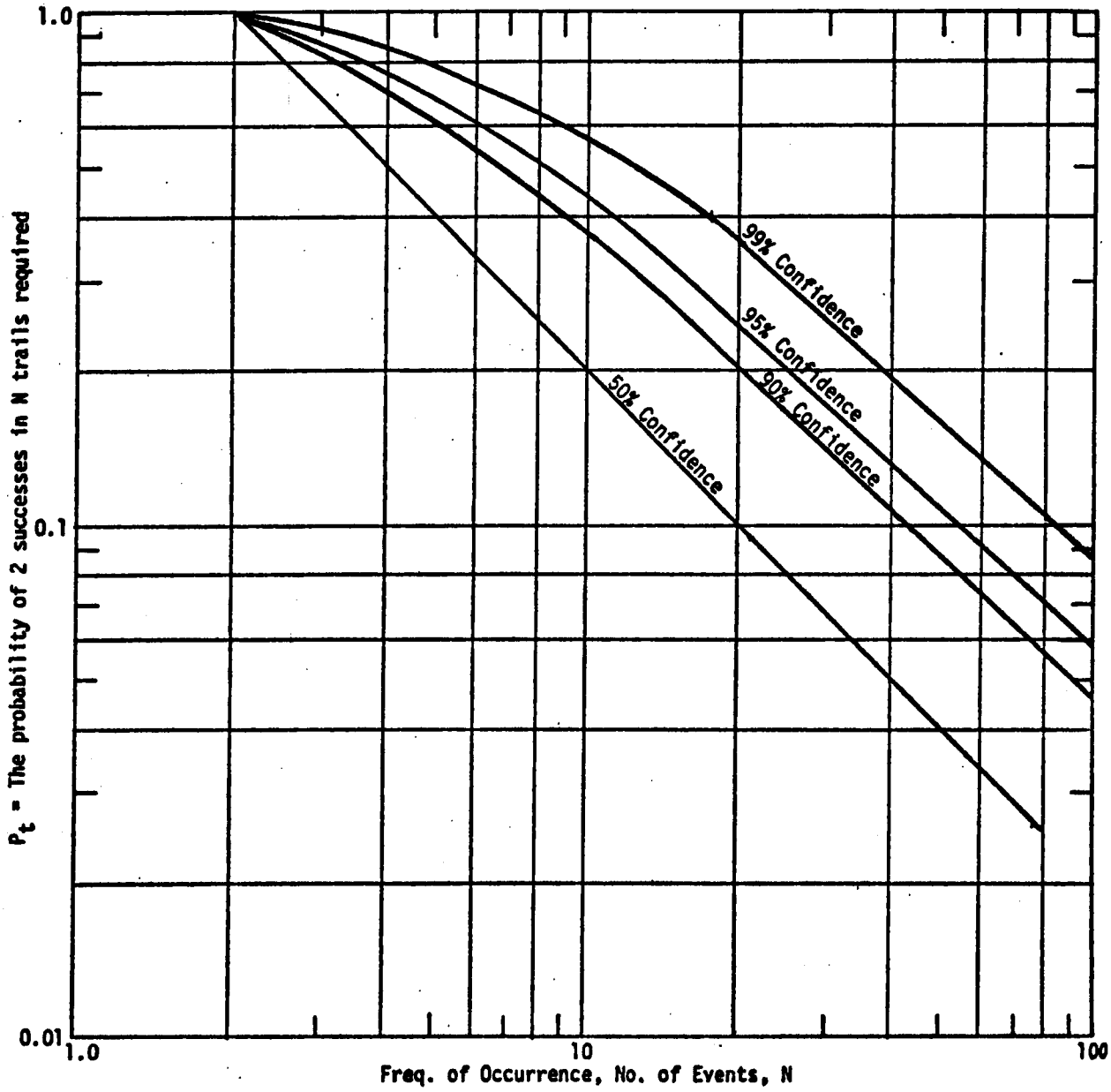

Figure 66. The Probability Required to Successfully Monitor C_{max} Twice if the Appropriate Meteorological Event Occurs N Times. (for various confidence levels.)

be used to determine the coverage ratio required by one station to insure that C_{max} is observed at least twice, given the number of times the meteorological event causing C_{max} occurs, N, and the desired confidence level. The results can be used to indicate if monitoring some meteorological phenomena should be attempted at all. For example, if the coverage ratio of a monitoring site is equal to 0.2 and the expected number of occurrences of meteorology causing C_{max}, N = 10, then the probability, or confidence level, that C_{max} will be measured at least twice is only 50%. Hence, there is only a 50:50 chance that any monitoring station will observe two occurrences of C_{max} even though it occurs 10 times. In such a case, it is probably inadvisable to attempt to monitor C_{max} under this condition at all. In light of the expense of air monitoring, sites should not be chosen to monitor C_{max} when the probability of success is low. Figure 66 shows how many times a meteorological event should occur in order to be 90% certain that C_{max} will be observed twice at one site for a range of values of CR_S. For example, for CR_S = .2 the meteorological event should occur at least 20 times each year to be 90% certain; for CR_S = 0.1 the same event must occur 43 times per year.

Selecting specific monitoring sites. Techniques for evaluating the number and location of air monitoring sites needed to monitor values of C_{max} have now been presented. The various techniques must now be integrated into a systematic approach to site selection. The steps are outlined below:

1. Evaluate historical meteorological data to determine prevailing meteorology and the frequency of occurrence of adverse condition for air pollution dispersion. Choose ranges of meteorological conditions under which air monitoring may be desirable and directions from the source where conditions occur most frequently.
2. Using point source models (computer models, nomographs, or general solutions presented herein) determine C_{max} and X_{max} under each range of meteorological conditions. From X_{max} identify potential zones where air monitoring stations may be needed.
3. Locate potential sites in the downwind directions where C_{max} values occur most frequently. Note that different C_{max} values occur under different types of meteorology all of which may not occur most frequently in the same direction. Hence, this step does not simply mean to locate sites downwind of the prevailing wind direction.
4. Using Figures 58-66 determine the proper spacing and number of sites needed in the X direction to provide adequate coverage of each monitoring zone.
5. Determine the single station coverage ratio, CR_S, for the distances downwind and stability classes chosen in steps 1-3.
6. Calculate the total coverage ratio, CR_T, required by the network for each meteorological condition of interest and desired number of observations, n. Divide CR_T by CR_S to determine number of stations needed in the crosswind direction.

7. Finally calculate the probability of successful observations of C_{max} for each station, and if this probability is very low then some stations may be eliminated.

It is important to remember that the figures given are based on a tolerance range for C_{max} of 10%. If a different tolerance range is desired, then new curves should be prepared from the basic equations presented in the text. The steps in the site selection process remain the same.

The site selection procedure presented herein is designed for locating sites having the highest probability of successfully measuring maximum ground level pollutant concentrations occurring near point sources. In practice other objectives may be equally important such as monitoring pollutant levels near sensitive receptors. Therefore, the sites identified using the procedures presented here should also be evaluated to see if certain site locations can be altered in order that multiple objectives might be served by the same site or if additional sites are needed.

CHAPTER IV

A SURVEY DESIGN FOR LINE SOURCE MODEL VALIDATION

Introduction

Determination of the changes in air quality near proposed highway projects often involves the use of mathematical diffusion models (9,8). These models are based on idealized consideration of air flow and terrain and provide theoretical estimates of the likely air pollution concentration levels and their temporal and spatial variation for present and proposed conditions. Air monitoring data collected near a highway can be utilized to validate or calibrate the idealized models and account for localized conditions which may vary from the basic assumptions on which the models are based (3,4).

This chapter describes an air monitoring survey designed for this purpose and presents the model validation results. Both correlation and regression analyses were used to compare predicted to measured CO concentrations. The models tested include EPA Highway (9); California Line Source (8) and two Empirical Models.

Field measurements were made of traffic, meteorological conditions and air quality levels. The meteorological and source strength data were used as model input information. The air quality data was used to compare to model predictions (59).

General Description of Models

EPA Model

The EPA HIWAY model estimates nonreactive air pollutant concentrations downwind from a highway line source of finite length. Concentration is calculated by the approximation of a line source by a finite number of evenly spaced continuous point sources of strength equal to the total line source strength divided by the number of sources used to simulate the line.

Because of the physical significance of mechanical mixing above the roadway, some initial values of the vertical and horizontal dispersion parameters are assumed. To accomplish this, the point source is displaced by a virtual distance upwind such that σ_z and σ_y have initial values at roadside.

California Model (8)

The California model also estimates nonreactive air pollutant concentrations near a highway corridor. The mathematical model, which is based on the Gaussian infinite line source diffusion equation, calculates concentrations of pollutants within a turbulent mixing cell above the highway as well as the receptor points downwind.

In the crosswind case, the mixing cell concentration is determined by the wind speed and pollutant emission rate of the vehicles. Dispersion downwind is dependent on the atmospheric stability classification. In the parallel wind case, the California model accumulates pollutants within the mixing cell to account for downwind buildup. Pollutants are then dispersed laterally at a rate dominated by stability class.

Major Differences in the Models

The major differences in the two models are outlined below (59):

1. California uses a Gaussian line source equation while EPA uses an integrated point source equation. As a result, the California model requires separate equations for predicting under crosswind and parallel wind conditions while EPA's model needs only one equation.

2. EPA's model requires separate traffic and emission data for each lane of the highway. Downwind concentrations are calculated by superimposing the separate pollutant contributions of each traffic lane. California's model uses the total traffic volume and emission rate for all lanes combined, assuming that all emissions are initially dispersed from a uniform "mixing cell" extending from road shoulder to shoulder (for medians < 30 ft.).

3. Initial dispersion of pollutants at the roadside edge is handled differently in the two models. The EPA model uses a virtual source correction providing an initial σ_z = 1.5 meters. The California model assumes a "mixing cell" with initial σ_z = 4 meters. (Figure [67].)

4. In both models downwind dispersion is described by the empirical dispersion coefficients, σ_y and σ_z. The models use different dispersion coefficients. (Figure [68].)

Model Assumptions

The following basic assumptions are common to both models (59):

1. The mass of pollutants is conserved throughout the downwind length of the plume. No material is lost by reaction or by sedimentation.

2. The ground surface, when encountered, is a perfect plume reflector.

3. There exists no wind shear in the vertical direction. The wind velocity used should be representative of the average wind velocity between $\pm \sigma_z$ from the plume centerline in the vertical sense.

4. Dispersion occurs only by turbulent diffusion which varys according to Pasquill's atmospheric stability categories (36).

5. Atmospheric stability is constant within the mixing layer containing both sources and receptor.

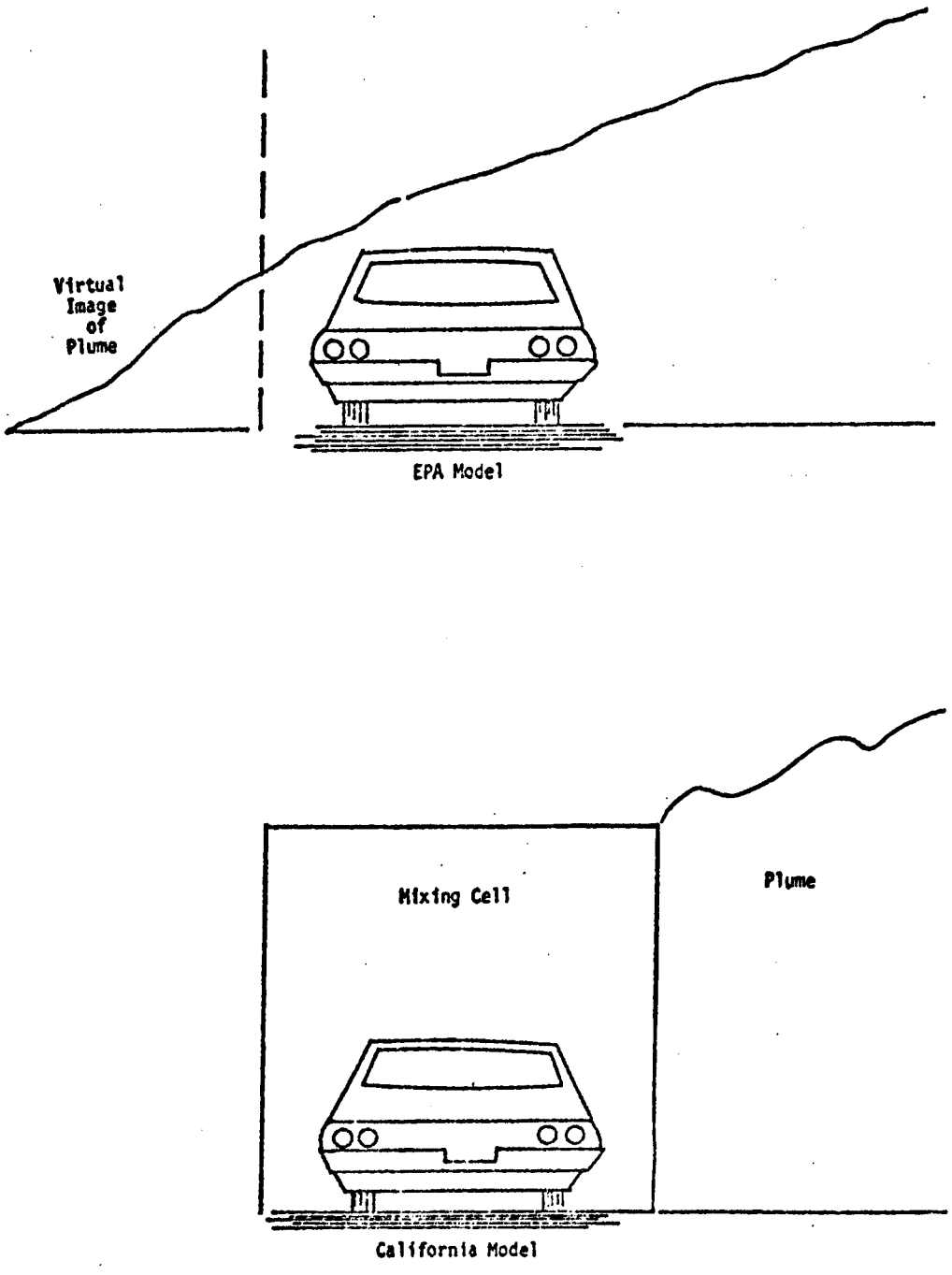

Figure 67. Dispersion From Virtual Image (EPA Model) and Mixing Cell (California Model).

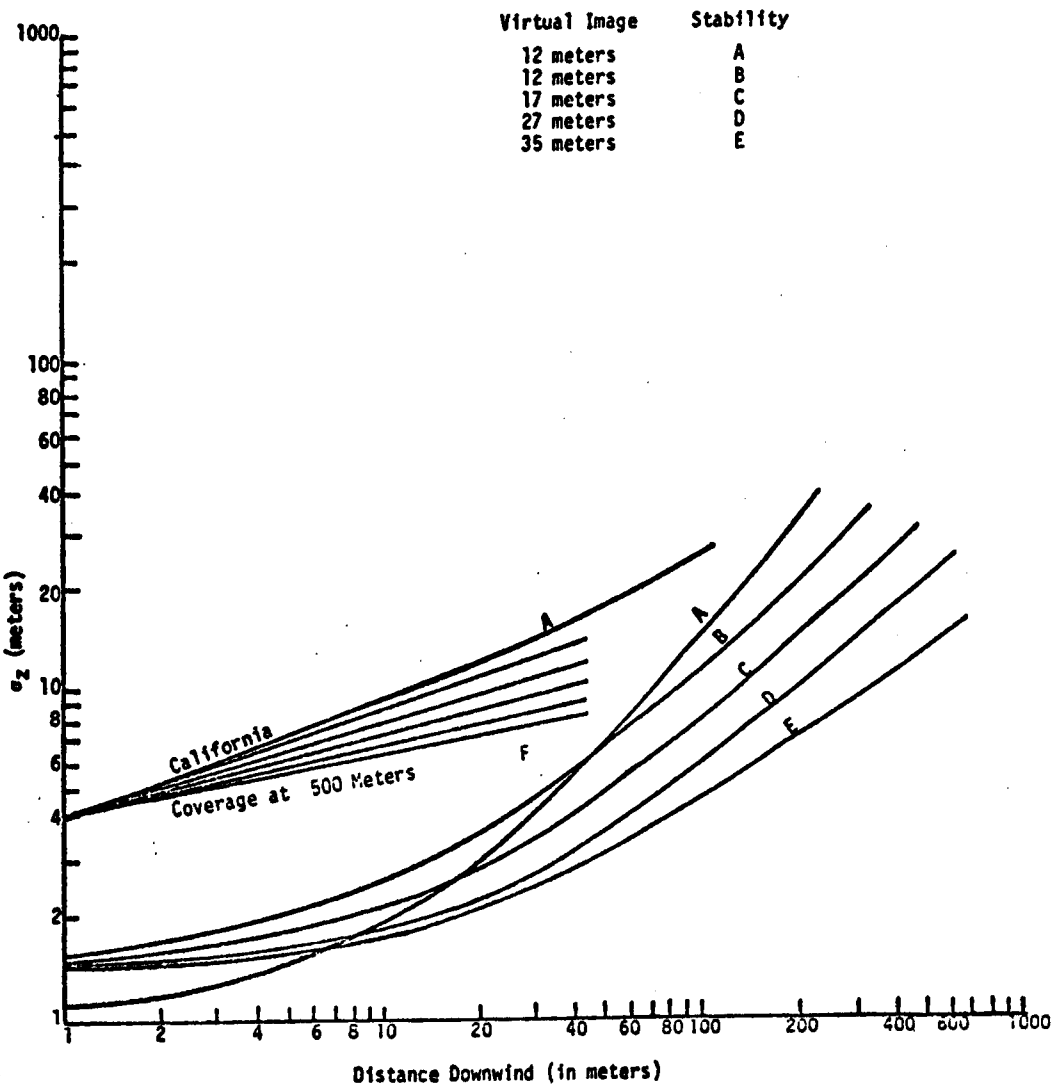

Figure 68. Comparison of σ_z Values Used in the EPA and California Models.

6. There exists no mixing of material in the x axis (i.e., longitudinal mixing).

7. Emissions are from continuous sources.

8. The dispersion parameters σ_y and σ_z are good for modeling atmospheric dispersion over flat, grassy terrain with no significant aerodynamic roughness nor any artificial vertical instability induced by heat island effects associated with urban areas.

Model Input Parameters

The input parameters required for the models are (59):

1. Geometry of the highway (i.e., road length, road angle with respect to north and road elevation either at grade, elevated or depressed).

2. Receptor location in both the horizontal and vertical directions with respect to the road.

3. Meteorology including wind speed, wind direction with respect to the road and Pasquill's atmospheric stability category.

4. Pollutant emission rate from vehicles based on traffic volume, traffic speed, vehicle age mix, and heavy duty vehicle mix.

Field measurements were made for all the above input parameters so that measured pollution concentrations could be compared to model predicted concentrations under identical conditions. In order to compare only the dispersion characteristics of the two models, identical emission factors were used based on an average light duty vehicle emission factor of 24.7 grams of CO per vehicle mile for cars traveling greater than 30 mph; and 77 grams of CO per heavy duty vehicle mile traveled. The light duty vehicle emission factor was determined from data presented in EPA's vehicle emission rate study conducted in six cities (60) for vehicles operating under steady-state conditions. The Six Cities Study was performed on vehicles representative of a 1972 model year mix. The age mix correction factor is equal to the ratio of:

$$\frac{\text{1973 1/2 AP-42 CO emission factor}}{\text{1972 AP-42 CO emission factor}} = \frac{59}{58} = 0.87 \qquad (51)$$

This factor was multiplied times the average emission rate for vehicle speeds greater than 30 mph taken from the Six Cities Study = 28.4 grams/vehicle mile (determined graphically from reference 61).

The heavy duty vehicle emission factor used assumes that one-half of the trucks were diesel powered and half were powered by gasoline engines. An average emission factor of 134 grams per mile per gasoline powered truck and 20.4 grams CO per mile per diesel truck were used to calculate an overall average HDV emission rate of 77 grams per mile (61).

EPA and California Model Equations

EPA Model

The EPA HIWAY model simulates a highway with a finite number of point sources and calculates the downwind concentration from each point using the Gaussian point source diffusion equation. The total contribution of all points is calculated by a numerical integration of the Gaussian point source equation over a finite length. The concentration, χ from the line source of length L, incremental length of $d\ell$, and incremental emission rate of, $q\ell$, is given by:

$$\chi = \frac{q_\ell}{u} \int_0^L f \, d\ell \qquad (52)$$

where for stable conditions or if the mixing height is greater or equal to 5000 meters:

$$f = \frac{1}{2\pi\sigma_y\sigma_z} \exp\left[-\frac{1}{2}\left(\frac{y}{\sigma_y}\right)^2\right]\left[\exp\left[-\frac{1}{2}\left(\frac{z-H}{\sigma_z}\right)^2\right] + \exp\left[-\frac{1}{2}\left(\frac{z+H}{\sigma_z}\right)^2\right]\right] \quad (53)$$

where

H = height of the road above ground level, m

z = height of the receptor above ground level, m

σ_y & σ_z = horizontal and vertical dispersion parameters, respectively, m.

The value of the integral (Equation 52) is approximated by use of the trapezoidal rule. Let $\Delta\ell = L/N$. Then the trapezoidal approximation gives:

$$\chi = \frac{q\Delta\ell}{u}\left[\frac{1}{2}(f_o + f_N) + \sum_{i=1}^{N-1} f_i\right] \quad (54)$$

where f_i is evaluated from Equation 53 for $\ell + i\Delta\ell$.

The above evaluation of the integral is repeated for each lane of traffic and the resulting concentrations summed to represent the total concentration from the highway segment.

California Model

The California model uses separate equations for calculating pollutant concentrations under crosswind and parallel wind conditions. The most general form of the crosswind equation has the form of the Gaussian line source equation:

$$C = \frac{4.24\ Q}{2\ K\ \sigma_z\ U \sin\ \phi}\left[\exp\left[-\frac{1}{2}\left(\frac{z+H}{\sigma_z}\right)^2\right] + \exp\left[-\frac{1}{2}\left(\frac{z-H}{\sigma_z}\right)^2\right]\right] \quad (55)$$

where

C = concentration of pollutant, in gm/m^3

Q = emission source, in gm/sec-m

$\bar{U}$ = wind speed, in m/sec (1 mph = 0.449 m/sec)

K = empirical coefficient = 4.24

ϕ = angle of wind with respect to highway alignment, in degrees

σ_z = vertical dispersion parameter, in meters

H = height of highway above surrounding terrain, in meters

z = height of receptor above surrounding ground surface, in meters.

For the parallel wind case, the California model allows for a buildup of pollution concentration within the mixing cell. The estimated concentrations within the mechanical mixing cell for parallel winds, where the ratio of 30.5/W is less than or equal to one, can be determined from the following equation:

$$C = A \frac{Q}{\bar{U}} \frac{1}{K} \frac{30.5}{W} \qquad (56)$$

where

C = concentration of pollutant (gm/m^3) within the mechanical mixing cell

$\bar{U}$ = wind speed (m/sec)

K = empirical coefficient = 4.24

W = width of roadway from edge of shoulder to edge of shoulder, in meters

A = downwind concentration ratio for parallel winds (accumulation term) is defined as $\frac{C\bar{U}K}{Q} \frac{W}{30.5}$ and determined from curves in Figures 79-85 of Volume V of the Air Quality Manuals (8).

30.5 = the initial width (meters) of the highway used for the finite element of area in developing the model for parallel winds

Q = source emission strength (gm/sec).

For parallel winds, the source emission strength (Q) is calculated using the following equation:

$$Q = [\text{emission factor}] \times [\text{vehicles/hour}] \times [5.26 \times 10^{-6}] \qquad (57)$$

Where the numerical constant is a factor to convert units of the products (vph)(gm/mi) to gm/sec for a length of highway of 100 feet.

To estimate the ground level pollutant concentration at a distance away from the highway (when the wind is parallel to the alignment) the following equation is used:

$$C = ppm_{mc} \exp -\frac{1}{2}\left(\frac{Y}{\sigma_y}\right)^2 \times \frac{1}{2}\left[\exp -\frac{1}{2}\left(\frac{z+H}{\sigma_z}\right)^2 + \exp -\frac{1}{2}\left(\frac{z-H}{\sigma_z}\right)^2\right] \qquad (58)$$

where

ppm_{mc} = concentration of CO at the highway within the mechanical mixing cell

Y = normal distance in meters from receptor to near edge of highway shoulder

σ_y, σ_z = horizontal and vertical dispersion parameters in meters. These values are obtained from empirical data depending on the receptor's normal distance (Y) from the highway and on the stability class.

Experimental Procedure

Air pollution, meteorological, and traffic measurements were made near a major arterial in Nashville, Tennessee for the period July 16-20, and August 17-24, 1973. This was an at-grade site and was selected to minimize terrain effects (Figure 69). A 250 foot flat, grass covered area extended north from the road. A small hill (70 feet high) with a gradual slope was located 2,200 feet southwest.

Wind speed and direction were measured continuously, 24 hours a day, throughout the duration of the field investigation. During the first monitoring period, a single MRI wind instrument was mounted 12 feet above the ground and 30 feet from the road's edge. During the second monitoring period, an additional wind instrument was mounted at a height of 30 feet and located about 20 feet northwest of the first.

Carbon monoxide concentrations were measured at the roadside edge, downwind of the highway and upwind of the highway (background). Concentrations were measured at various distances by using a sampling array of five probes along a horizontal profile perpendicular to the highway. Each of the probes were at a height of five feet. Air samples were pumped continuously through tubing to a sampling manifold located at the mobile air monitoring trailer and analyzed with an NDIR-CO instrument. Background concentrations were collected with an ECO-lyzer CO analyzer which was positioned about 400 feet upwind (southside) of Gallatin Road.

During the second field monitoring period there were large variations in wind direction. Because of this, CO concentration dispersed

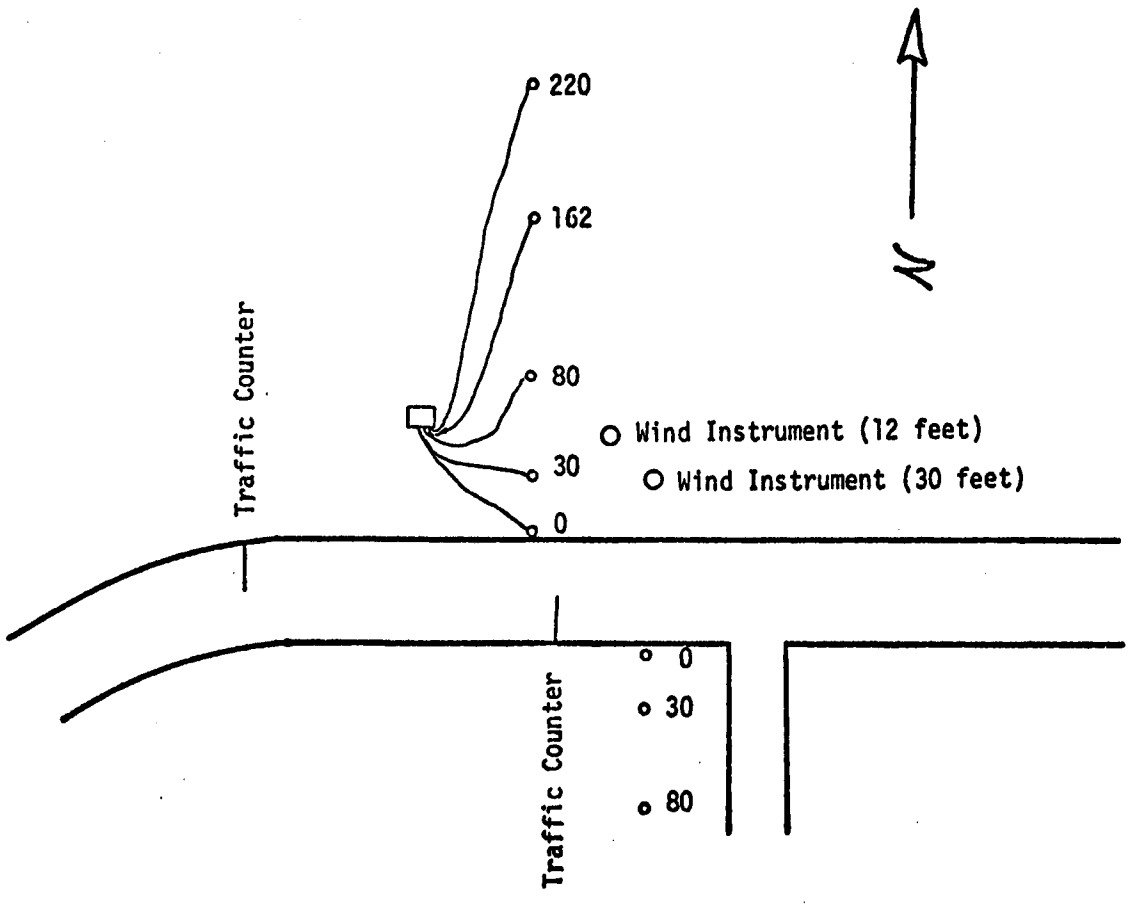

Figure 69. Gallatin Road Location Site 10.

from the highway source were measured by both sides of the highway. A bag sampling network was used on the south side of the road (62).

To insure accuracy in pollutant concentration measurements, the analyzers were calibrated before and after each peak traffic sampling period. A two point calibration procedure was employed using a zero and an upscale span gas. Before field use, instrument linearity was checked in the laboratory using span gases of different concentrations (63). Two different procedures of calibration were employed in the field: direct injection of span gas from a compressed gas cylinder through a vented mixing chamber, and by use of sampling bags. Calibration using sampling bags allowed a dynamic calibration through both the sampling lines and instrument. This allowed the integrity of the entire sampling train to be checked.

Fifteen minute traffic counts were made continuously by the use of pneumatic counter/recorders. A separate counter was used for inbound and outbound traffic volumes. Average vehicle speed was measured by timing vehicles over a known distance. The time averaging method utilizes an observer who times a vehicle, chosen at random, between two easily recognizable end points. Adequate course lengths (>500 ft) and a stop watch provide necessary accuracy in the measurement. Heavy duty vehicle (HDV) mix was obtained by manual counts.

Atmospheric stability measurements were based on surface wind speed, insolation (strong, moderate, slight), percent cloud cover, and time of day (angle of sun). A hygrothermograph was used in the field to determine temperature changes. Stabilities were classified according to one of the

six Pasquill stability classes of A, B, C, D, E, and F, which range from extremely unstable to extremely stable (36).

Data Presentation

EPA and California Models

Table VIII and IX present the results of correlation and regression analysis comparing measured ambient carbon monoxide concentrations to concentrations predicted by the EPA and California models. The raw data used for statistical analysis consisted of 568 data sets of CO concentrations measured downwind of the highway, background concentrations measured upwind of the highway and the concentration predicted by the models. Measured versus predicted concentrations have been evaluated according to wind angle, receptor distance, and stability of the following criteria:

1. Wind angle group. Wind angles with respect to the road alignment were separated into three categories, parallel 0-15°, oblique 15-60°, and perpendicular 60-90°.

2. Receptor distance. The distance from the sampling probe to the center of the road is the receptor distance. The data was separated only according to those receptors at the edge of the road shoulder or "mixing cell" (roadside receptor) and those located at the farther distances downwind.

3. Stability category. Pasquill's six stability categories (A-F) were used to separate data subsets.

Table VIII and IX utilize the following code:

1. A coded description of the data set using three digits in the following order: wind angle - stability - receptor distance. Where (1) wind angle 11 = parallel winds, 12 = oblique, and 13 = perpendicular winds referred to the road; (2) stability category 1 = A, 2 = B, 3 = C, 4 = D, 5 = E, and 6 = F; and (3) receptor distance 1 = roadside receptor, and 2 = downwind receptors (out to 300 feet from center of road).

Table VIII

Statistical Data Summary: EPA Model - Site 10

(Measured Background Subtracted)

Data Set	N	Mean	σ	CV%	Prob>F	r	m	b
0-0-0	538	1.60	1.34	73	0.0001	0.492	0.331	1.13
0-0-1	177	2.62	1.56	52	0.0001	0.505	0.272	2.08
0-0-2	361	1.10	0.839	71	0.0001	0.393	0.263	0.796
11-0-0	19	2.21	2.21	55	0.0001	0.847	0.236	0.590
12-0-0	224	1.43	1.24	65	0.0001	0.665	0.755	0.444
13-0-0	295	1.69	1.32	58	0.0001	0.669	1.33	0.150
0-1-0	6	1.55	1.36	29	0.003	0.954	2.03	-0.447
0-2-0	207	1.56	1.16	51	0.0001	0.726	1.90	-0.124
0-3-0	273	1.60	1.40	65	0.0001	0.668	0.796	0.491
0-4-0	20	1.63	1.01	31	0.0001	0.874	1.60	-1.40
0-5-0	26	2.17	1.97	64	0.0001	0.722	0.210	0.958
0-6-0	6	0.270	0.170	29	0.011	0.911	2.63	-2.56
11-0-1	5	5.23	1.61	28	0.277	0.607	0.104	3.61
11-0-2	14	1.13	1.11	60	0.001	0.807	0.194	0.399
12-0-1	69	2.36	1.49	35	0.0001	0.833	0.959	0.705
12-0-2	155	1.01	0.823	73	0.0001	0.437	0.387	0.582
13-0-1	103	2.67	1.50	42	0.0001	0.666	1.34	0.667
13-0-2	192	1.16	0.829	61	0.0001	0.518	0.800	0.381
11-3-0	10	1.76	2.24	29	0.0001	0.977	0.590	-0.514
11-5-0	9	2.71	2.20	31	0.0002	0.934	0.203	0.635
12-1-0	6	1.55	1.36	29	0.003	0.954	2.03	-0.447
12-2-0	88	1.36	0.909	54	0.0001	0.592	1.22	0.337
12-3-0	110	1.43	1.35	57	0.0001	0.794	1.09	-0.054
12-5-0	17	1.89	1.84	58	0.0001	0.822	0.909	-1.21
12-6-0	3	0.270	0.190	19	0.121	0.982	3.05	-2.96
13-2-0	119	1.71	1.30	45	0.0001	0.804	2.35	-0.464
13-3-0	153	1.71	1.37	57	0.0001	0.710	1.32	0.057
13-4-0	20	1.63	1.01	31	0.0001	0.874	1.60	-1.40
13-6-0	3	0.270	0.190	19	0.121	0.982	3.05	-3.08
11-3-2	8	0.849	1.17	60	0.002	0.914	0.507	-0.346
11-5-1	3	5.12	1.97	27	0.334	0.865	0.156	2.08
11-5-2	6	1.51	0.993	23	0.004	0.950	0.146	0.680
12-1-2	4	0.750	0.560	17	0.017	0.983	1.52	-0.180
12-2-1	34	1.69	0.983	47	0.0001	0.616	1.25	0.342
12-2-2	54	1.15	0.801	62	0.001	0.459	1.11	0.395
12-3-1	27	3.05	1.46	24	0.0001	0.875	0.983	0.883
12-3-2	83	0.909	0.779	72	0.0001	0.558	0.642	0.202
12-5-1	5	3.26	2.55	30	0.016	0.944	1.01	-0.460
12-5-2	12	1.31	1.16	51	0.001	0.834	0.698	-0.985
13-2-1	41	2.90	1.30	29	0.0001	0.768	2.12	0.229
13-2-2	78	1.09	0.761	55	0.0001	0.630	1.52	-0.051
13-3-1	53	2.62	1.65	41	0.0001	0.770	1.46	0.283
13-3-2	100	1.23	0.885	62	0.0001	0.511	0.779	0.398
13-4-1	8	2.15	1.17	31	0.008	0.846	1.82	-1.76
13-4-2	12	1.28	0.757	29	0.0001	0.883	1.31	-0.974

Table IX

Statistical Data Summary: California Model - Site 10

(Measured Background Subtracted)

Data Set	N	Mean	σ	CV%	Prob>F	r	m	b
0-0-0	568	1.62	1.33	70	0.0001	0.513	0.382	1.10
0-0-1	198	2.56	1.55	51	0.0001	0.553	0.380	1.78
0-0-2	370	1.12	0.834	72	0.0001	0.269	0.168	0.950
11-0-0	44	1.81	1.76	55	0.0001	0.827	0.348	0.108
12-0-0	226	1.47	1.24	64	0.0001	0.652	0.686	0.622
13-0-0	298	1.70	1.31	52	0.0001	0.735	1.46	0.350
0-1-0	6	1.55	1.36	29	0.003	0.957	1.25	-0.331
0-2-0	223	1.53	1.16	61	0.0001	0.592	1.26	0.452
0-3-0	281	1.64	1.38	72	0.0001	0.511	0.429	1.05
0-4-0	26	1.91	1.24	45	0.0001	0.740	0.380	1.04
0-5-0	26	2.17	1.97	66	0.0001	0.696	0.313	0.742
0-6-0	6	0.270	0.170	20	0.003	0.959	0.885	-0.336
11-0-1	14	3.39	2.02	24	0.0001	0.919	0.347	0.961
11-0-2	30	1.07	1.00	68	0.0001	0.702	0.222	0.204
12-0-1	75	2.35	1.47	48	0.0001	0.644	0.602	1.15
12-0-2	151	1.04	0.813	73	0.0001	0.378	0.463	0.637
13-0-1	109	2.60	1.51	43	0.0001	0.675	1.33	0.646
13-0-2	189	1.18	0.821	61	0.0001	0.480	1.28	0.392
11-2-0	13	0.897	0.637	67	0.149	0.424	0.585	0.075
11-3-0	16	1.65	1.87	60	0.0001	0.860	0.474	-0.964
11-4-0	6	2.86	1.56	30	0.025	0.867	0.419	0.492
11-5-0	9	2.71	2.20	45	0.003	0.854	0.335	-0.067
12-1-0	6	1.55	1.36	29	0.003	0.957	1.25	-0.331
12-2-0	91	1.39	0.956	61	0.0001	0.475	0.788	0.705
12-3-0	109	1.51	1.33	65	0.0001	0.675	0.666	0.613
12-5-0	17	1.89	1.84	48	0.0001	0.882	1.11	-0.985
12-6-0	3	0.270	0.190	27	0.175	0.963	0.903	-0.338
13-2-0	119	1.71	1.30	42	0.0001	0.839	2.20	-0.031
13-3-0	156	1.73	1.36	54	0.0001	0.728	1.30	0.437
13-4-0	20	1.63	1.01	39	0.0001	0.795	1.35	-0.115
13-6-0	3	0.270	0.190	28	0.179	0.961	0.877	-0.341
11-2-1	5	1.55	0.526	39	0.904	0.076	0.111	1.35
11-2-2	8	0.491	0.222	45	0.361	-0.374	-0.199	0.731
11-3-1	4	3.73	2.15	30	0.092	0.908	0.393	0.335
11-3-2	12	0.959	1.19	96	0.016	0.676	0.389	-0.784
11-4-2	4	1.91	0.652	24	0.175	0.825	0.190	1.13
11-5-1	3	5.12	1.97	32	0.404	0.806	0.312	1.23
11-5-2	6	1.51	0.993	25	0.005	0.941	0.189	0.332
12-1-2	4	0.750	0.560	15	0.013	0.987	1.76	-0.745
12-2-1	37	1.74	1.06	56	0.011	0.414	0.703	0.842
12-2-2	54	1.15	0.801	66	0.009	0.352	0.880	0.632
12-3-1	30	2.95	1.43	42	0.003	0.525	0.391	1.93
12-3-2	79	0.961	0.762	73	0.0002	0.408	0.573	0.466
12-5-1	5	3.26	2.55	28	0.013	0.950	1.07	-0.338
12-5-2	12	1.31	1.16	65	0.009	0.718	0.901	-0.721
13-2-1	41	2.90	1.30	29	0.0001	0.766	2.01	0.273
13-2-2	78	1.09	0.761	59	0.0001	0.555	2.15	-0.038
13-3-1	59	2.49	1.65	46	0.0001	0.726	1.31	0.482
13-3-2	97	1.27	0.868	62	0.0001	0.438	1.07	0.560
13-4-1	8	2.15	1.17	34	0.015	0.811	1.99	-1.54
13-4-2	12	1.28	0.757	33	0.001	0.847	2.22	-0.749

2. N, the number of data points in the data set.

3. Mean, the mean measured CO concentration.

4. σ, the standard deviation of the measured concentration.

5. CV%, the coefficient of variation, equal to the ratio of the standard error of y from the regression line divided by the mean measured concentration.

6. Prob>F, the probability that the critical F-test (64) statistic has not been exceeded; equal to the probability that the calculated regression line is based on random numbers.

7. r, the correlation coefficient.

8. m, the slope of the calculated least squares regression line.

9. b, the intercept of the regression line.

In addition to the tables, statistical data summary diagrams were prepared which contain the correlation coefficient, r, the ratio of the mean predicted concentration divided by the mean measured concentration, k, and the number of data points in each data set, n (Figures 70 and 71).

Empirical Models

Two empirical models were developed and calibrated using the measured data on source strength, meteorology, and carbon monoxide concentrations. The first empirical model, called EMP-1, was derived from dimensional analysis and has the form

$$C \alpha \frac{k Q}{U (X/\sin \phi)^a} \qquad (59)$$

where

C = concentration at ground level from an at-grade highway, ug/m^3

Q = pollutant emission rate, ug/m-sec

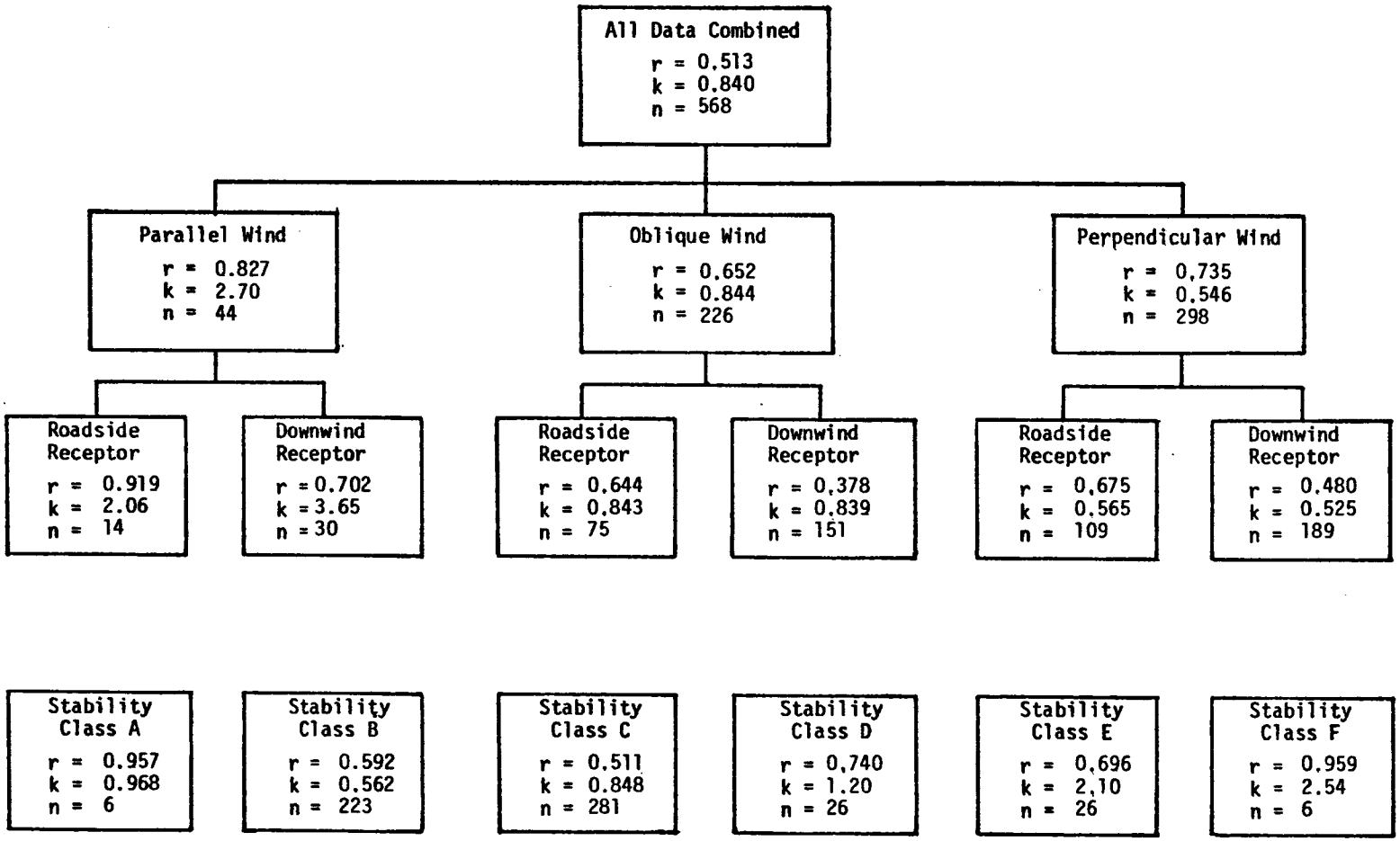

Figure 70. Statistical Data Summary Diagram, California Site 10. (Measured Concentration minus Background.)

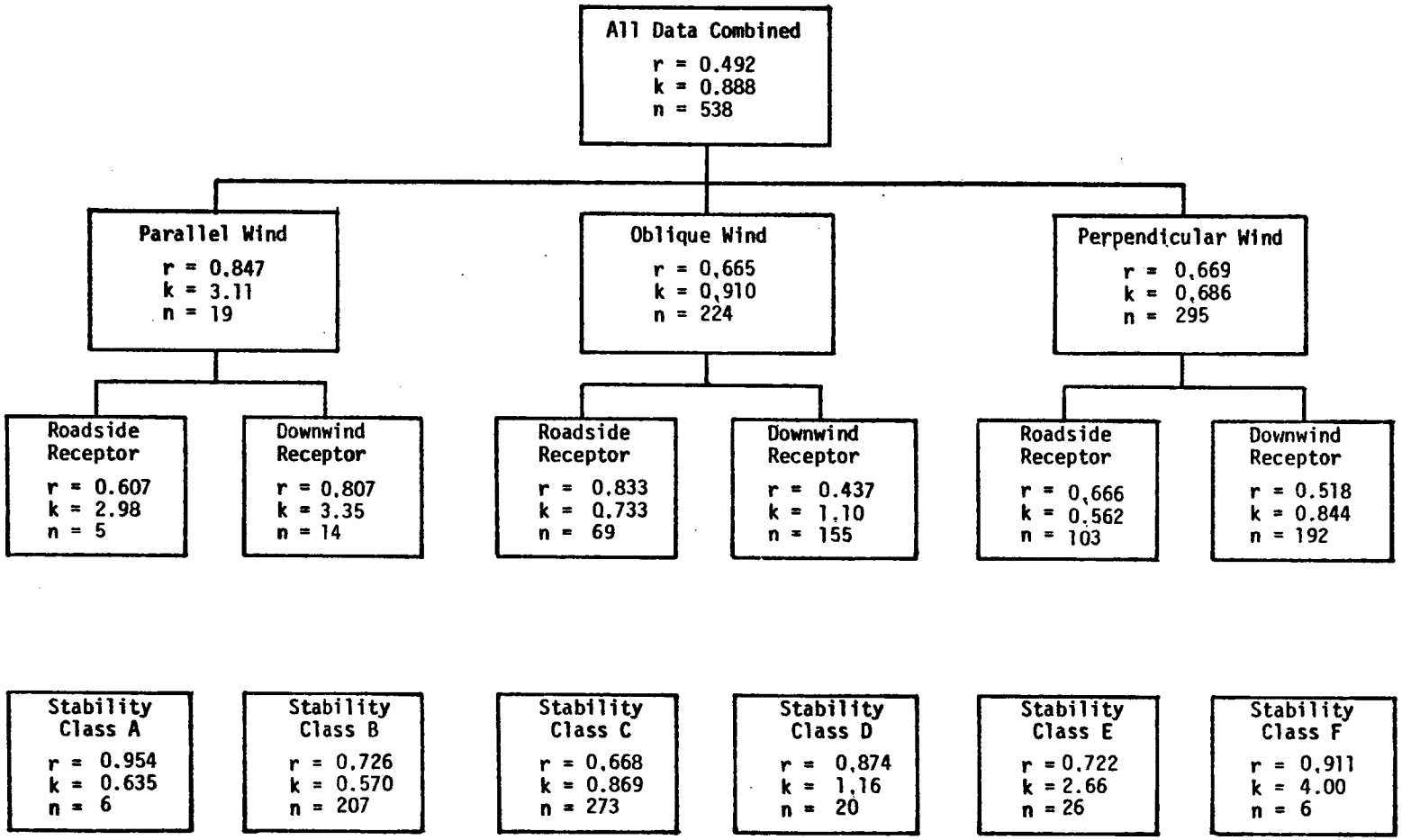

Figure 71. Statistical Data Summary Diagram, EPA Site 10. (Measured Concentration minus Background.)

U = mean wind speed normal to the road, m/sec

X = distance from center of the road to the receptor

θ = the angle of the wind with respect to the road, degrees,

k & a = empirical coefficients.

A regression analysis was performed on ln(CU/Q) versus ln(X/sin θ) using 524 measurements during perpendicular and oblique wind conditions. The values obtained for the slope of the regression line a = -1.106 and the intercept k = 8.18 were used to calibrate the model. The final equation for EMP-1 was

$$C_1 = \frac{8.18\ Q}{U\ (X/\sin\theta)^{1.106}} \qquad \text{(EMP-1)}$$

Another empirical model, EMP-2, was derived having a basic form first suggested by Briggs (65). The initial dispersion of pollutants within the microscale regime of highways is assumed to be dominated by the turbulent wake induced by moving vehicles. Downwind of the highway pollutant are dispersed as the turbulent wake grows and is transported by the wind. Initial dispersion is related to the magnitude of the turbulent momentum flux, Fm, generated by the cars, while downwind dispersion is related to the growth of the wake which may be expected to follow a 2/3's power law function with time. The basic form of the equation used is

$$C \propto \frac{k_1\ Q}{(Fm)^{1/3}(\frac{X}{U})^{2/3}\ U} \qquad (60)$$

where

$Fm = (C_D A_F V^2)$

C_D = drag coefficient for cars in air ≈ 0.4

A_F = frontal area of vehicles 22 ft^2 = 2.05 m^2

V = velocity of vehicles, m/sec

k_1 = an empirical coefficient.

A regression analysis was performed on measured concentrations versus EMP-2 using 524 measurements during perpendicular and oblique wind conditions. The value obtained for the slope of the regression line k_1 = 13.7 was used to calibrate the model. The final equation was

$$C_2 = \frac{13.7\ Q}{(.4A_F V^2)^{1/3}\ (X/U)^{2/3}\ U} \qquad \text{(EMP-2)}$$

The results of the statistical analysis of measured CO concentrations versus CO concentrations predicted by EMP-1 and EMP-2 are presented in Figures 72 and 73.

Discussion of Results

Introduction

The output of the regression analysis can be used to indicate the precision and accuracy of mathematical model predictions when compared to measure pollutant concentrations. The method of analysis uses the correlation coefficient, r, as an index of the precision of the association between predicted and measured concentrations. Whenever the correlation coefficient is high, the model performs well under the conditions included within the data set.

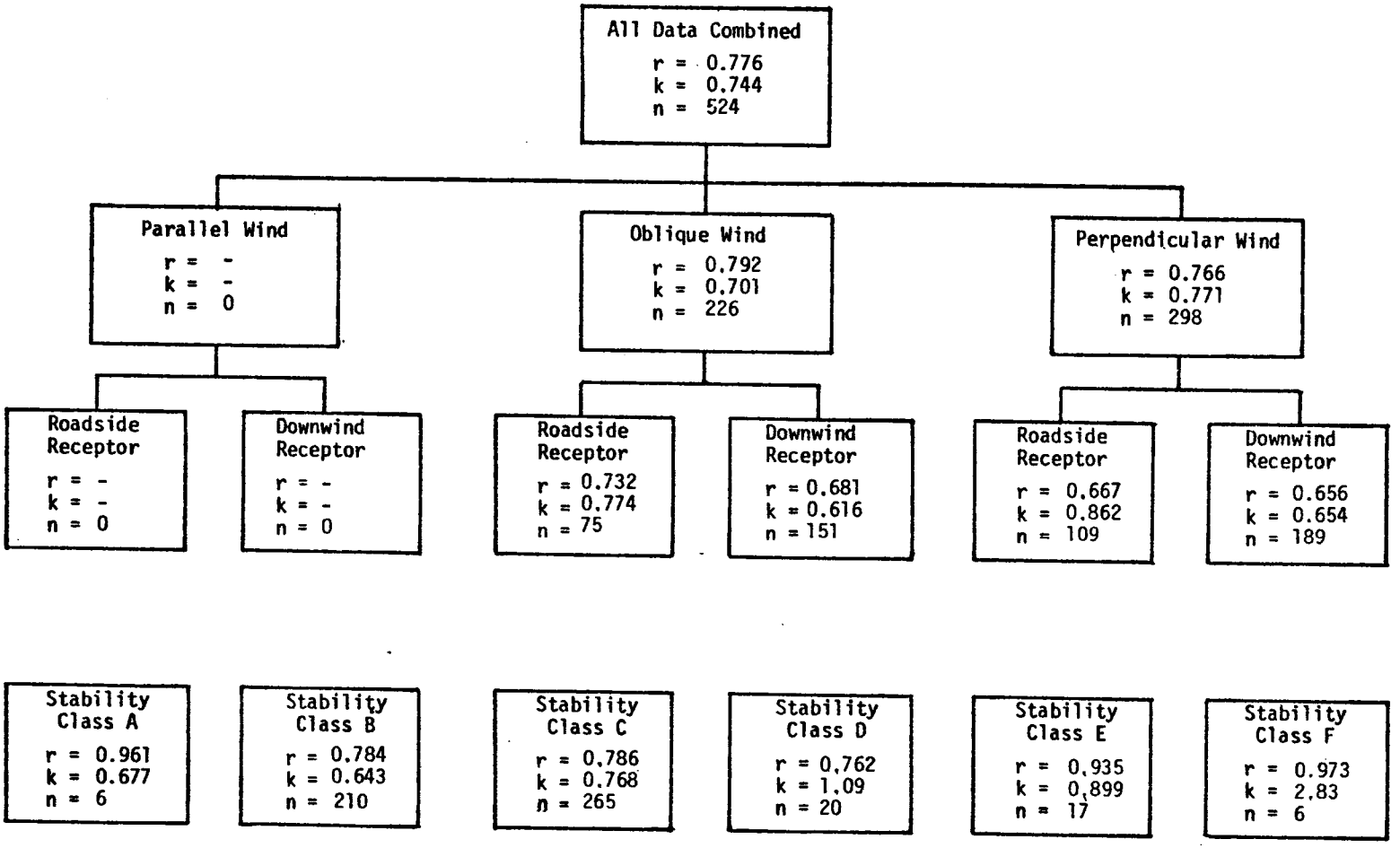

Figure 72. Statistical Data Summary Diagram, EMP-1 Site 10. (Measured Concentration minus Background.)

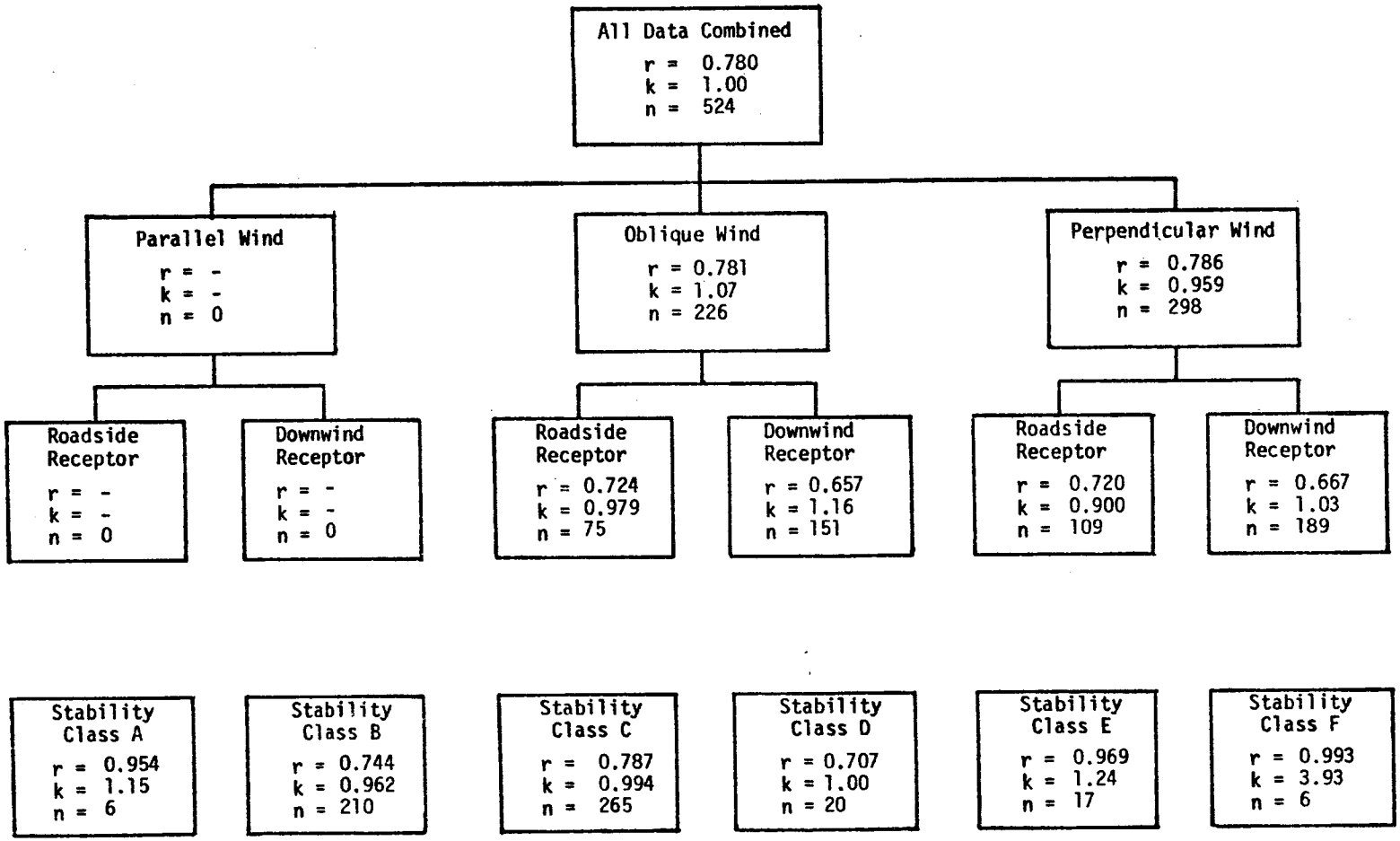

Figure 73. Statistical Data Summary Diagram, EMP-2 Site 10.
(Measured Concentration minus Background.)

A second parameter, k, equal to the ratio of the average predicted concentration divided by the average measured concentration, is used as an indication of the relative "accuracy" of the model. Values of k greater than one indicate that, on the average, the model tends to overpredict the measured concentration; k values less than one indicate underprediction. The size of the data set, n, is also important and must be considered when evaluating the significance of r and k values. Also, it is important to note that model accuracy is dependent on precision, such that k values tend to be meaningless when correlation coefficients are quite low.

Experimental Error

Variability in the comparision of measured and predicted concentrations results from two sources, (1) inadequacies of the model to predict accurately under the range of conditions contained within a data set and (2) experimental error. An estimate of experimental error can be made by comparing the expected accuracy of CO measurements to the concentrations typically observed in the field. The sensitivity of CO analyzers as reported by the manufacturers is 0.5 ppm. More than half of the field measurements of CO were less than 2.0 ppm. Therefore, errors of a magnitude equal to (0.5/2.0) x 100% = 25% or greater probably occur frequently in the data. Background concentrations averaged less than 1 ppm, therefore, errors of 50% and greater probably occur for this data due to analyzer sensitivity. Additional errors occurred because of the use of different analyzers.

Performance of the EPA and California Models

Using the Statistical Data Summary of Figures 70 and 71, some general conclusions can be drawn regarding the performance of the EPA and California models at this site. The EPA model is considered first.

The overall precision of the EPA model is reflected in a correlation coefficient, $r = 0.49$. Correlation coefficients are significantly improved when data is separated by wind angle ($r = .85$ for parallel and $r = .67$ for perpendicular and oblique winds). The EPA model tends to overestimate for parallel winds and underestimate for crosswind conditions. The parallel case overpredicts by $\simeq 3$. The average accuracy of perpendicular and oblique wind predictions ranges from 44% under- to 10% overprediction. Model precision tends to be better for roadside receptors, but accuracy is better for downwind receptors. The relative accuracy of downwind receptor predictions compared to roadside edge receptor predictions is approximately 40% for perpendicular and oblique conditions.

Regarding atmospheric stability categories, the EPA model tends to overestimate for stable conditions and underestimate during unstable conditions. The error ranges from 43% underprediction for B-stability to 166% overprediction for E-stability.

The California model performs similarly to the EPA model. The overall correlation coefficient, $r = 0.51$, is improved when the data is separated by wind direction, where $r = .83$ for parallel, $r = .65$ for oblique, and $r = .74$ for crosswind conditions. The model tends to overpredict for parallel winds by a factor of from 2 to 3.6; and underpredict for crosswind and oblique wind conditions (i.e., 16% for oblique and 45%

for crosswind). While the precision of the California Model is generally less than EPA, the accuracy of roadside receptor prediction is comparible to downwind receptor predictions for both crosswind and oblique wind conditions indicating that the model tends to predict the rate of downwind dispersion rather well.

Figures 74, 75, and 76 illustrate the rate of dispersion of pollutants downwind of a highway as predicted by the models compared to the results obtained from field measurements. The figures show the non-dimensionalized horizontal concentration profile from roadside edge to 100 meters downwind as predicted for B and E stabilities by the EPA and California models for perpendicular, oblique and parallel winds, respectively. Also shown are the average measured relative concentrations for all stabilities combined.

Figure 74 indicates that under perpendicular wind conditions the measured concentrations fall off more rapidly than predicted by the California model. The EPA model predicts that concentrations will fall off more slowly than indicated by the data. Under oblique wind conditions (See Figure 75) a similar trend occurs.

Figure 76, for parallel wind conditions, shows that the field data falls between the predicted values from the two models. The EPA model predicts concentrations to fall off more rapidly, while California predicts a slower decrease in concentration with distance downwind than observed.

Performance of the Empirical Model

In general, the correlation coefficients for both Empirical models tend to be the same or higher than for the EPA or California models

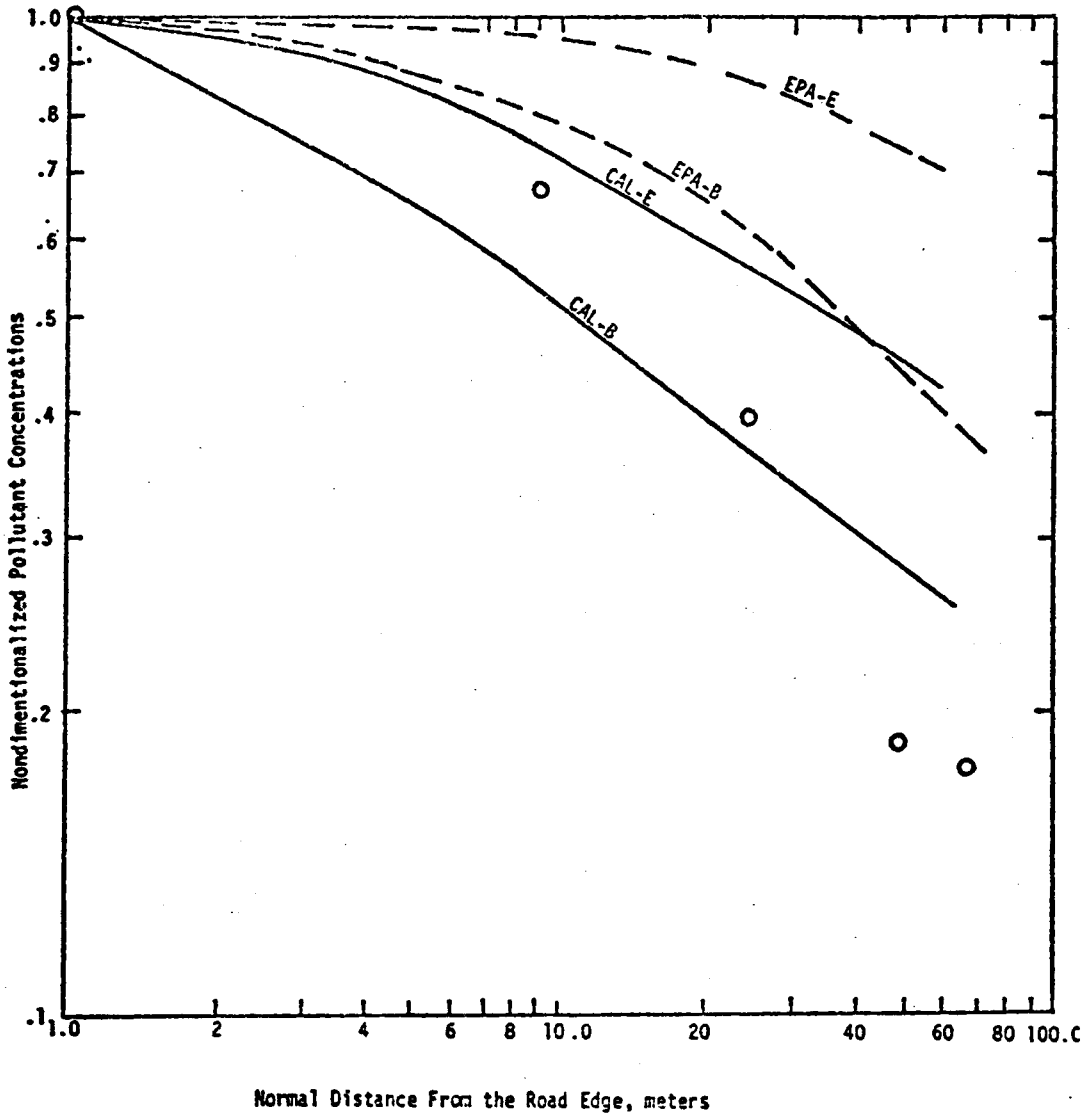

Figure 74. Nondimensionalized Pollutant Concentration Versus Normal Distance Downwind of the Road as Calculated Using EPA and California Models for Stabilities B & E Under Perpendicular Wind Conditions. Also Plotted is the Average Value Measured at Site 10 for all Stabilities Combined.

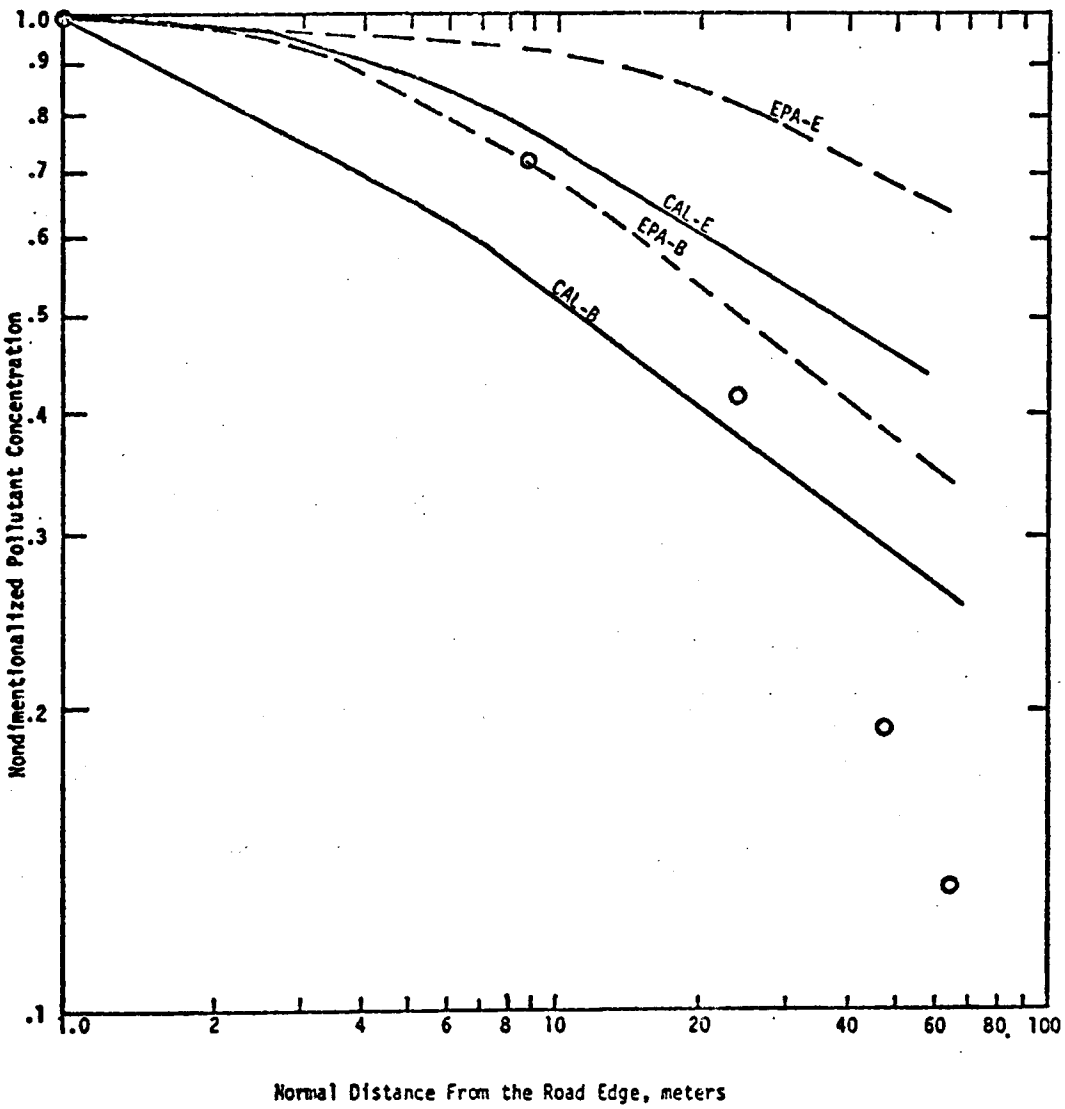

Figure 75. Nondimensionalized Pollutant Concentrations Versus Normal Distance From the Road Edge as Calculated Using the EPA and California Models for Stabilities B & E Under Oblique (45°) Wind Conditions. Also Plotted is the Average Value Measured at Site 10 for all Stabilities Combined.

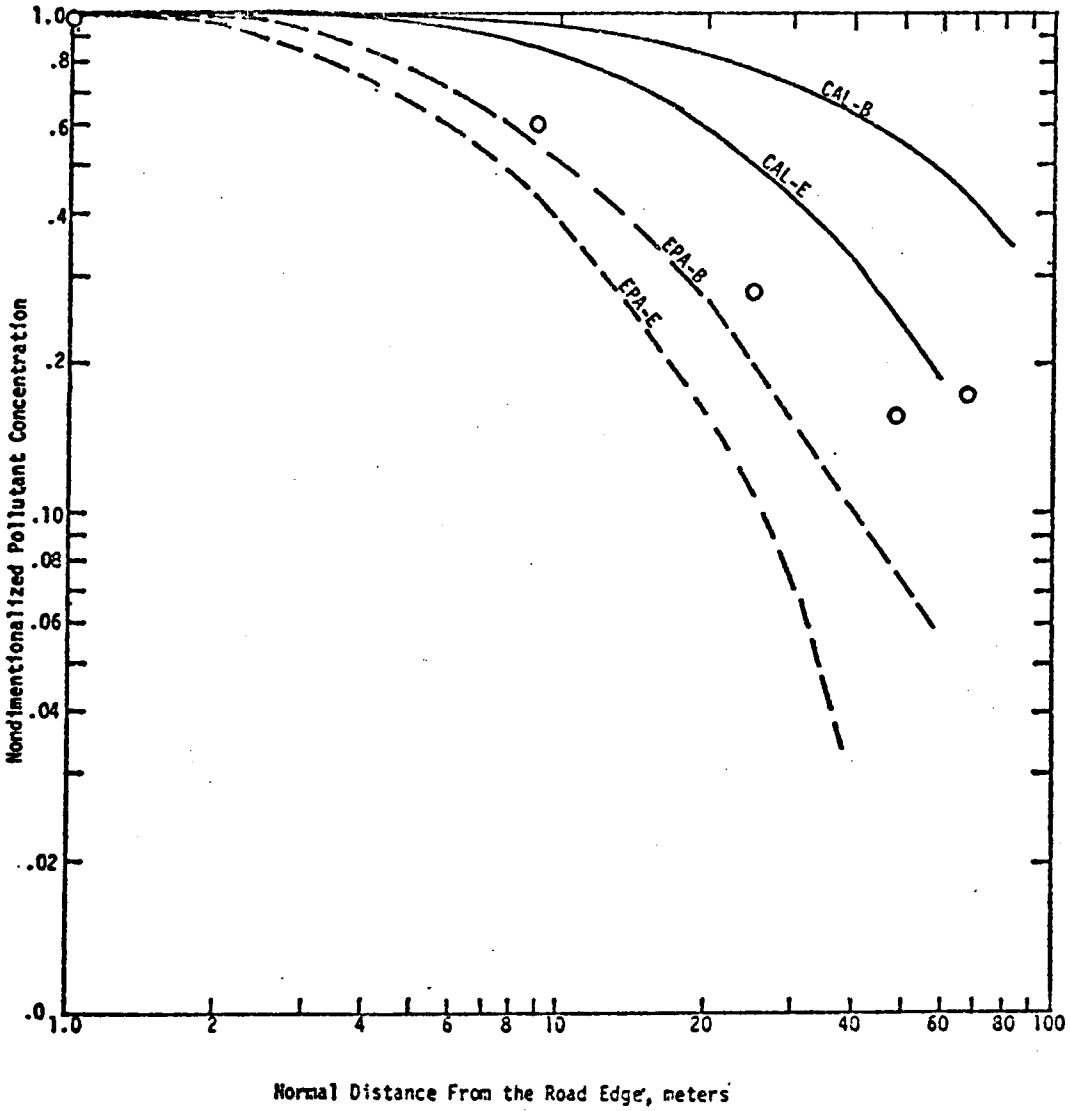

Figure 76. Nondimensionalized Pollutant Concentration Versus Normal Distance for the Road as Calculated Using the EPA and California Models for Stabilities B & E. Under Parallel Wind Conditions. Also Plotted is the Average Value Measured at Site 10 for all Stabilities Combined.

under similar conditions. The greatest improvement in precision is for downwind receptor concentrations where EPA and California range from $r = .38$ to $r = .52$ while EMP-1 and EMP-2 range from $r = .66$ to $r = .68$. The correlation coefficients used are for calibrated EPA, California, and Empirical models. This is because correlation coefficients measure only the degree of association between the models and data, and are independent of the mathematical relationship between mean measure and predicted values.

It appears that the EPA and California models both overcompensate for the effects of atmospheric stability class, and that a calibrated empirical model which does not account for any change in stability class may provide more precise results. The EMP-2 model fits data within an average error of 4% for stability classes B, C, and D, and within 30% between B and E stabilities. The range of the error between similar stability classes for EMP-1 is 45%. This compares to a range of $\simeq$ 200% for the EPA and California models.

Conclusions

A comparison of predicted and measured concentrations near an at-grade road has shown that the idealized diffusion models tend to overestimate concentrations under parallel wind conditions and underestimate concentrations for perpendicular and oblique wind conditions. Two Empirical models were developed which were independent of atmospheric stability conditions. These models show promise as predictive models and should be tested at other sites.

LIST OF REFERENCES

LIST OF REFERENCES

1. Clean Air Act (42 U.S.C. 1857 et seq.) includes the Clean Air Act of 1963 (P.L. 88-206) and amendments made by the "Motor Vehicle Air Pollution Control Act" - P.L. 89-272 (October 20, 1965), the "Clean Air Act Amendments of 1966 - P.L. 89-675 (October 15, 1966), the "Air Quality Act of 1967" - P.L. 90-148 (November 21, 1967), and the "Clean Air Amendments of 1970" - P.L. 91-604 - (December 31, 1970).

2. National Environmental Policy Act, U.S.C., Public Law No. 91-190 (1970).

3. Noll, Kenneth E. and Miller, Terry L., "Design of Highway Air Monitoring Surveys - Vol. I, Publication of the Federal Highway Administration, March 1975. Implementation Package No. 75-1.

4. Miller, Terry L. and Noll, Kenneth E., Highway Air Quality Monitoring Manual, Publication of the Federal Highway Administration, March 1975. Implementation Package No. 75-2.

5. "National Primary and Secondary Air Quality Standards," Federal Register, Vol. 36, No. 84, Friday, April 30, 1971.

6. Slade, David H., editor, Meteorology and Atomic Energy - 1968, U. S. Atomic Energy Commission, Office of Information Services, Oak Ridge, TN, July 1968.

7. Turner, D. Bruce, Workbook of Atmospheric Dispersion Estimates, U. S. EPA Publication No. AP-26 (1970).

8. Beaton, J. L., Ranzieri, A. J., Shirley, E. C., and Skog, J. B., Air Quality Manual - Vol. IV, Mathematical Approach to Estimating Highway Impact of Air Quality, California Department of Public Works, Division of Highways, Sacramento, CA, April 1972.

9. U. S. Environmental Protection Agency, "A User's Guide for Hiway," National Environmental Research Center, Meteorology Lab, Research Triangle Park, NC 27711, November 1974.

10. Gifford, F. A. and Hanna, S. R., "Modeling Urban Air Pollution," Atmos. Envir., No. 7, 131-136 (1973).

11. Instrumentation for Environmental Monitoring - Air, Lawrence Berkeley Laboratory, University of California, Berkeley, Dec. 1973.

12. U. S. Environmental Protection Agency, Designation of Unacceptable Analytical Methods of Measurements for Criteria Pollutants, EPA Publication No. OAQPS 1.2-018, May 1974.

13. Guidelines: A/Q Surveillance Networks, AP-98, May 1971.

14. Pooler, Francis, "Network Requirements for the St. Louis Regional Air Pollution Study," APCA, March 1974.

15. Harrison, Paul R., "Considerations for Siting A/Q Monitors in Urban Areas," Presented at 65th APCA Meeting, June 1972.

16. Highways and Air Quality, Special Report 141, Highway Research Board, 1973.

17. Ott, Wayne and Eliassen, Rolf, "A Survey Technique for Determining the Representativeness of Urban Air Monitoring Stations With Respect to Carbon Monoxide," APCA, Aug. 1973.

18. Ott, Wayne R., "Development of Criteria for Siting Air Monitoring Stations," Presented 68th APCA Meeting, June 1975.

19. Montgomery, T. L., et al., "Controlling Ambient SO_2," Journal of Metals, June 1973.

20. Federal Register (Implementation Plans) (36FR15486).

21. Hougland, Erik S. and Stephens, Thomas N., "Air Pollutant Monitor Siting by Analytical Techniques," Presented 67th APCA Meeting, June 1974.

22. Seinfield, John H., "Optimal Location of Pollutant Monitoring Stations in an Airsled," Atmospheric Environment, Vol. 6, pp. 847-858, 1972.

23. Beaton, J. L., Ranzieri, A. J., and Skog, J. B., Air Quality Manual Vol. I, Calif. Dept. of Public Works, Division of Highways, Sacramento, Calif., Report No. FHWA-RD-72-33, April 1972.

24. Mancuso, R. L., and Ludwig, F. L., User's Manual for the APRAC-1A Urban Diffusion Model Computer Program, Contract No. CAPA-3-68 (1-69), Stanford Research Insti., Menlo Park, Calif., Proj. No. 8563, Sept. 1972.

25. Proceedings of Symposium on Multiple-Source Urban Diffusion Models, U.S.E.P.A. Pub. No. AP-86.

26. Duncan, J. R. and Miller, T. L., Air Resources Management in Knox County, Technical Report #3, Knox Co. Dept. of Air Pollution Control, April 1972.

27. Selective Guide to Climatic Data Sources, Envr. Data Service, U.S. Dept. of Commerce, ESSA, Pub. No. KMRD No. 4.11.

28. Hale, Wayne E., "Sample Size Determination for the Lognormal Distribution," Atmos. Environ., Vol. 6, No. 6, June 1972, pp. 419-422.

29. Hunt, W. F. Jr., "The Precision Associated with the Sampling Frequency of Lognormally Distributed Air Pollution Measurements," Journal of Air Pollution Control Assoc., Vol. 22, No. 9, Sept. 1972, pp. 687-691.

30. Saltzman, B. E., "Simplified Methods for Statistical Interpretation of Monitoring Data," Journal of Air Pollution Control Assoc., Vol. 22, No. 2, Feb. 1972, pp. 90-95.

31. Bibbero, Robert J. and Young, Irvin, G., Systems Approach to Air Pollution Control, John Wiley & Sons, New York, 1974.

32. Treybal, Robert E., Mass-Transfer Operations, 2nd Edition McGraw-Hill, 1968, p. 17.

33. Hanna, Steve, Lecture Notes for Diffusion Meteorology, Course No. 5760, University of Tennessee, 1973.

34. Somers, E. V., in W. Strauss, Ed. Air Pollution Control, Pt. 1 Wiley: New York, 1971, p. 6.

35. Smith, M. (ed.), Recommended Guide for the Production of the Dispersion of Airborne Effluent, Am. Soc. Mech. Eng., 1968.

36. Pasquill, F., Atmospheric Diffusion, Van Nostrand: New York, 1969.

37. Smith, M. E. and Singer, I. A., An Improved Method of Estimating Concentrations and Related Phenomena from a Point Source Emission, USAEC Report BNL-9700, Brookhaven National Laboratory, 1965.

38. Briggs, Gary A., Diffusion Estimation for Small Emissions, A.T.D.L., Oak Ridge, TN, (Draft Report), May 1973.

39. TVA, "Summary of Tennessee Valley Authority Atmospheric Dispersion Modeling," presented by the Conf. on the TVA Experience of Intnat'l Institute for Applied Systems Analysis, Schloss, Laxenburg, Austria, Oct. 1974.

40. Hilst, G. R. and Simpson C. L., Observations of Vertical Diffusion Rates in Stable Atmospheres, J. Meteorol., 15(1):125-126.

41. Islitzer, David, (same as ref. 36); p. 133.

42. Sutton, O. G., 1932, A Theory of Eddy Diffusion in the Atmosphere," Proc. Roy. Soc. London, A, 135, 143-165.

43. Gilbert, Jeffrey and Davis, Wayne T., "A Comparison of EPA and California Line Source Diffusion Models," Unpublished paper, Department of Environmental Engineering, University of Tennessee, 1974.

44. Miller, Marvin E. and Holzworth, George, C., "An Atmospheric Diffusion Model for Metropolitan Areas,: J. APCA, Vol. 17, No. 1, Jan. 1967, pp. 46-50.

45. Calder, K. L., "A Climatological Model for Multiple Source Urban Air Pollution," Proceedings of the 2nd Meeting of the Expert Panel on Air Pollution Modeling, N.A.T.O. Committee on the Challenges of Modern Society, Paris, France, July 26-27, 1971.

50. Briggs, Gary A., "Some Recent Analyses of Plume Rise Observations," Proc. 2nd Intern. Clean Air Conf., Washington, D.C., 1970, Academic Press, New York.

51. Briggs, Gary A., Class Notes from Course Taught at Univ. of Tenn., Knoxville, TN, May 1975.

52. Montogomery, T. L., et al., "A Simplified Technique Use to Evaluate Atmospheric Dispersion of Emissions from Large Power Plants," J.A.P.C.A., May 1973, Vol. 23, No. 5, p. 388-394.

53. Montgomery, Thomas L., et al., "Results of Recent TVA Investigations of Plume Rise," APCA Vol. 22, No. 10, Oct. 1972.

54. Engineering Guide for Evaluating Dispersion of Sulfur Dioxide Emission, internal document of the Tennessee Valley Authority, 1971.

55. Clarke, John F. and McElroy, James L., "Effects of Ambient Meteorology and Urban Morphological Features on the Vertical Temperature Structure Over Cities,: Presented at the 67th Annual Meeting of the Air Pollution Control Assoc., Denver, Colorado, June 9-13, 1974, Paper No. 74-73.

56. STAR Program: Seasonal and Annual Wind Distribution by Pasquill Stability Classes (6), Available: National Climatic Center, Federal Bldg., Asheville, NC.

57. Miller, Irwin and Freund, John F., Probability and Statistics for Engineers, Prectic-Hall, Inc., Englewood Cliffs, NJ, 1965.

58. Hino, Mikio, "Maximum Ground-Level Concentration and Sampling Time," Atmos. Environ., Vol. 2, 1968, p. 149-165.

59. Noll, Kenneth E., et al., Air Monitoring Program to Determine the Impact of Highways on Ambient Air Quality, Final Report Tennessee Department of Transportation, Department of Civil Engineering, University of Tennessee, Knoxville, July 1975.

60. Study of the Emission from Light Duty Vehicles in Six Cities, APTD-1497, U. S. Environmental Protection Agency, Ann Arbor, Michigan, March 1973.

61. Compilation of Air Pollution Emission Factor, Second Edition, U. S. Environmental Protection Agency, AP-42, Research Triangle Park, North Carolina, April 1973.

62. Noll, K. E., Burdick, J. C., III, Miller, T. L., Gilbert, J., Rainey, R. G. Jr., and Jones, K., Highway Air Monitoring Data Summary and General Solution to the Highway Line Source Model, Department of Civil Engineering, The University of Tennessee, December 1974.

63. Noll, K. E., Walling, J. O., and Arnold, B. L., Calibration Procedures for Continuous Air Monitoring Instruments, Vol. I, Department of Civil Engineering, The University of Tennessee, September 1972.

64. SAS (Statistical Analysis System) designed by Anthony BArr and James Goodnight, Dept. of Statistics, North Carolina State University, User Manual Published by Student Supply Stores, NCSU, Raleigh, NC, August 1972.

VITA

Terron (Terry) Lee Miller was born in Spartanburg, South Carolina, on April 5, 1948. In 1956 he moved to Knoxville, Tennessee. He attended elementary schools in that city and was graduated from Bearden High School in 1966. The following September he entered The University of Tennessee, and in June 1972, he received a Bachelor of Science degree in Engineering Science.

He entered the Graduate School at The University of Tennessee in September 1972, and received a Master's degree in Environmental Engineering in August 1973. In December 1975, he received the Doctor of Philosophy degree with a major in Civil Engineering. He is a member of the Air Pollution Control Association and president of Enviro-Measure, Inc.

He is married to the former Rebecca Joyce Gass of Knoxville, Tennessee.